

## General Disclaimer

### One or more of the Following Statements may affect this Document

- This document has been reproduced from the best copy furnished by the organizational source. It is being released in the interest of making available as much information as possible.
- This document may contain data, which exceeds the sheet parameters. It was furnished in this condition by the organizational source and is the best copy available.
- This document may contain tone-on-tone or color graphs, charts and/or pictures, which have been reproduced in black and white.
- This document is paginated as submitted by the original source.
- Portions of this document are not fully legible due to the historical nature of some of the material. However, it is the best reproduction available from the original submission.

(NASA-TM-X-73208-Vol-2) AEROX: COMPUTER  
PROGRAM FOR TRANSONIC AIRCRAFT AERODYNAMICS  
TO HIGH ANGLES OF ATTACK. VOLUME 2:  
COMPARISONS OF TEST CASES WITH EXPERIMENT  
(NASA) 140 p HC A07/MF A01

N77-20023

Unclas  
22810

CSSL 01A G3/02

**NASA TECHNICAL  
MEMORANDUM**

**NASA TM X-73,208**

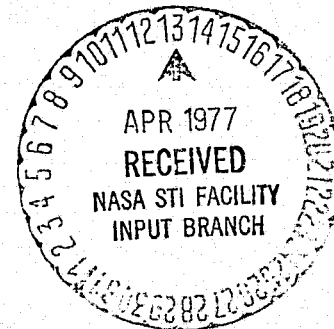
NASA TM X-73,208

**AEROX - COMPUTER PROGRAM FOR TRANSONIC AIRCRAFT  
AERODYNAMICS TO HIGH ANGLES OF ATTACK**

**VOLUME II - COMPARISONS OF TEST CASES WITH EXPERIMENT**

**John A. Axelson**

**Ames Research Center  
Moffett Field, Calif. 94035**



**February 1977**

1. Report No. TM X-73,208	2. Government Accession No.	3. Recipient's Catalog No.	
4. Title and Subtitle AEROX — COMPUTER PROGRAM FOR TRANSONIC AIRCRAFT AERODYNAMICS TO HIGH ANGLES OF ATTACK VOLUME II — COMPARISONS OF TEST CASES WITH EXPERIMENT		5. Report Date	
		6. Performing Organization Code	
7. Author(s) John A. Axelson		8. Performing Organization Report No. A-6927	
		10. Work Unit No. 505-06-19	
9. Performing Organization Name and Address Ames Research Center Moffett Field, Calif. 94035		11. Contract or Grant No.	
		13. Type of Report and Period Covered Technical Memorandum	
12. Sponsoring Agency Name and Address National Aeronautics and Space Administration Washington, D. C. 20546		14. Sponsoring Agency Code	
		15. Supplementary Notes	
16. Abstract <p>The theory, users' guide, test cases, and program listing are presented in the three volumes. The AEROX program estimates lift, induced-drag and pitching moments to high angles of attack (typ. 60°) for wings and for wing-body combinations with or without an aft horizontal tail. Minimum drag coefficients are not estimated, but may be input for inclusion in the total aerodynamic parameters which are output in listed and plotted formats.</p>			
17. Key Words (Suggested by Author(s)) Aerodynamics Computer programming and software		18. Distribution Statement Unlimited STAR Categories — 02.	
19. Security Classif. (of this report) Unclassified	20. Security Classif. (of this page) Unclassified	21. No. of Pages 140	22. Price* \$5.75

TABLE OF CONTENTS — VOLUME II

SUMMARY . . . . .	1
Test Cases . . . . .	2
Data Presentation . . . . .	2
DISCUSSION . . . . .	2
Accuracy . . . . .	2
Applicability . . . . .	4
CONCLUSION . . . . .	4
NOMENCLATURE . . . . .	5
REFERENCES . . . . .	8
TABLES I-IX. INPUTS FOR TEST CASES . . . . .	9-17
FIGURES	
Figure 1.- Flow zones, and models indicated for test cases . . .	18-20
Figure 2.- F-4 aerodynamic estimates and data . . . . .	21-25
Figure 3.- F-5         "         "         "         " . . . . .	26-32
Figure 4.- Model L         "         "         "         " . . . . .	33-41
Figure 5.- Model A-1         "         "         "         " . . . . .	42-56
Figure 6.- Model A-2         "         "         "         " . . . . .	57-71
Figure 7.- Model A-3         "         "         "         " . . . . .	72-86
Figure 8.- Model A-4         "         "         "         " . . . . .	87-101
Figure 9.- Model A-5         "         "         "         " . . . . .	102-116
Figure 10.- Shuttle Orbiter . . . . .	117-137



- A E R O X -

COMPUTER PROGRAM FOR TRANSONIC AIRCRAFT AERODYNAMICS  
TO HIGH ANGLES OF ATTACK

VOLUME II

COMPARISONS OF TEST CASES WITH EXPERIMENT

John A. Axelson  
Ames Research Center

Summary

The present Volume II presents comparisons of the estimated and experimental aerodynamics for nine aircraft configurations over a wide range of angles of attack and Mach numbers. The aerodynamic theory formulated for the AEROX program is documented in Volume I. Program operators should consult pages 15 through 19 of Volume I. A program listing and sample output tables and plots are shown in Volume III.

AEROX provides estimates of the lift, induced-drag and pitching-moment coefficients for wings, bodies, and for wing-body combinations with or without an aft horizontal tail. Both trimmed and untrimmed characteristics are estimated. Zero-lift drag coefficients (including friction, wave and propulsion-system additive drags) are not evaluated in AEROX, but may be input for inclusion in the output values of total drag coefficient and lift/drag ratio. The method is based on new, explicit aerodynamic formulations accounting for compressibility, transonic flow with strong shock waves and separation, and supersonic flow with detached leading-edge shock waves. The transonic airfoil mathematical model incorporates the Laitone limit Mach number criterion, with the chordwise location of the shock as an input parameter rather than an extracted solution. A new lift equation derived from the integration of downwash momentum is used for nonpotential flow regimes. The directness of this new, overall approach and the rapid execution time of the corresponding AEROX program are ideally suited for use in computerized aircraft preliminary designs and optimizations, and in activities dealing with aerodynamic instruction and research.

## Test Cases

Validation of the AEROX program is presented in the form of comparisons of the estimated and experimental longitudinal aerodynamics for nine different aircraft configurations over the broad flight envelope shown in figure 1(a). Sketches of each configuration appear in figures 1(b) through 1(j), and the dimensional inputs are summarized in Tables I through IX. The test cases include the F4; the F5; a light-weight fighter configuration designated Model L; five related research models identified as A-1 through A-5; and the shuttle orbiter.

## Data Presentation

The experimental results presented in figures 2 through 10 consist of static aerodynamic coefficients measured in wind tunnels and reported in references 1 through 7. Shown in the figures are lift curves ( $C_L$  versus  $\alpha$ ), drag polars ( $C_L$  versus  $C_D$ ), and pitching-moment coefficients ( $C_m$  versus  $\alpha$  or  $C_L$ ). The AEROX program includes the option for estimating trimmed characteristics (ITRIM=1) up to  $25^\circ$  angle of attack. Comparisons of the AEROX trimmed estimates with the limited amount of available, trimmed-flight data indicate the same good agreement as displayed here with the estimated and measured static aerodynamics. The small numbers appearing on the plots identify the flow regime (fig. 1(a)) and the particular equations (vol. I) used in the estimation. Two sets of symbols for the same model identify different test conditions or model supports.

## DISCUSSION

### Accuracy

The formulations in the AEROX program constitute the only known analytical method for estimating transonic aircraft aerodynamics to maximum lift. No estimates are included for the effects of the propulsion system, such as the inlets, nacelles, nozzles or power-induced effects. Approximations are included for the contributions of the nose, afterbody, horizontal tail and wing leading-edge

chord extensions or strakes. In view of the complexity of the problem, and in light of the simplifications required in arriving at a rapid, practicable computer program, the goal for accuracy is realistically set at  $\pm 5$  percent of the maximum values of lift and drag coefficient, and  $\pm 5$  percent CBARW in the aerodynamic center location used in evaluation of the pitching-moment coefficients. Over 90 percent of the 117 pages of data comparisons presented here meet the goal. There is generally good agreement at all angles of attack.

Test points which differ from the estimates by greater than  $\pm 5$  percent do not necessarily infer errors in the program, but rather these differences can often be attributed to test procedure or model contours not appropriate to the present analysis. For example, the reduced lift measured for model L at the higher angles of attack at a Mach number of 1.8, (fig. 4(d)) is believed to stem in part from the relatively large model (1.5 ft. span) in the 4-foot supersonic wind tunnel.

Subsonic experimental lift coefficients which are well below the estimates are shown in figures 6(a,c), 7(a,c), and 8(a,c) for the related models A-2, A-3 and A-4. These lower experimental lift coefficients above  $10^\circ$  angle of attack can be attributed to the poor subsonic characteristics normally associated with the type of airfoil used on these models. For simplicity of construction, the sections were double beveled, flat airfoils with four essentially sharp ridge lines, which would tend to promote separation at subsonic speeds (but not at supersonic speeds). Note that in the case of model A-3, tail off, (fig. 7(a)), the flow apparently re-established itself above  $30^\circ$  angle of attack, and good agreement with estimate resulted. There was agreement at all angles of attack for models A-1 and A-5 at 0.6 Mach number (figs. 5(a), 9(a)). These models had the highest sweep angles for the leading edges and the ridge lines and experienced relatively little separation.

Because of the sharp ridge lines and almost sharp leading edges on the wings of models A-1 through A-5, the airfoil designator was set at ALELJ=1 for subsonic speeds. The small bluntness of the leading edges would promote detached bow shocks at supersonic speeds, so the value of ALELJ used was 5 for the supersonic estimates. The leading-edge radius has strong influence at transonic

speeds, but at supersonic conditions with detached bow shocks, it exerts no direct influence on lift in the present program. The leading-edge radius at these conditions (i.e.,  $Z=6$ ) continues to influence the wave drag and the  $C_{D0}$  values entered on the input sheets (Tables I - IX).

### Applicability

The AEROX program provides estimates of longitudinal aerodynamics through maximum lift at all Mach numbers above those where low-speed, viscous stall predominates. The separate or combined characteristics of wings, bodies and tails are estimated. The program should also prove useful for augmenting, correlating, and validating limited or questionable samples of experimental data. Because of the low cost and versatility of the AEROX program and its parameterization capability, it constitutes a valuable aid for design, instruction and research activities.

### CONCLUSION

The AEROX computer program provides estimates of lift and induced drag coefficients for aircraft (including maximum lift) at transonic and supersonic speeds with an accuracy generally within  $\pm 5$  percent of the maximum values. The accuracy for the estimated pitching-moment coefficients is generally within  $\pm 5$  percent of the wing mean aerodynamic chord for the aerodynamic center location. The AEROX program provides a valuable tool for estimating, correlating, augmenting and validating aerodynamic characteristics and is ideally suited to computerized design, instruction and research activities.

## Nomenclature

The symbols appearing on the input and output listings of AEROX and on the enclosed figures are defined as follows:

ALJLJ,J	Input integer identifying type of airfoil ( $1 \leq J \leq 5$ ). See AXE listing.
ALFTR	trimmed angle of attack (ITRIM=1), deg.
ALPHA,	angle of attack of wing reference plane, deg.
ALTV	input altitude, ft.
APLAN	plan area of nose, sq. ft.
ARH	input aspect ratio of horizontal tail
ARW	input aspect ratio of wing
ASECT	nose maximum cross-sectional area, sq. ft.
BDMAX	input body diameter, ft.
CBARW	wing mean aerodynamic chord, ft.
CDHOR	horizontal tail induced drag coefficient (ref. to wing area)
CDN	nose or body induced drag coefficient (ref. to wing area)
CD0	input wing minimum drag coefficient
CDOB	input additive drag coefficient (body, tail, propulsion system)
CDSEP	wing separation drag coefficient (Z=4)
CDTOT,CD	total drag coefficient
CDW	wing induced drag coefficient
CLHOR	horizontal tail lift coefficient (ref. to wing area)
CLN	nose or body lift coefficient (ref. to wing area)
CLO	input wing lift coefficient at zero angle of attack (subsonic)
CLOB	input additive lift coefficient (body, propulsion system)
CLTOT,CL	total lift coefficient
CLW	wing lift coefficient
CLWL	lift coefficient for wing lower surface
CLWU	lift coefficient for wing upper surface
CM,C <sub>m</sub>	pitching-moment coefficient
CMO	input wing pitching-moment coefficient at zero angle of attack
CMOB	input additive pitching-moment coefficient (body, propulsion)
CROOT	wing root ( $C_r$ ) chord, ft.
CTIP	wing tip chord, ft.
DALTR	increment of angle of attack to maintain $C_L$ during trim, deg.

DELH increment of tail deflection to trim, deg.  
 DLWING wing lift-curve slope, per rad.  
 DWASH downwash angle at horizontal tail, deg.  
 FTOTL multiplying factor to change lift coefficient reference area  
 FTOTD " " " " drag " " "  
 FCM " " " " pitching-moment coefficient reference  
 area or length  
 ICDO input control integer for minimum drag; 0, CDO omitted; 1, input wing  
 CDO included.  
 IFLEX input control integer for strake bluntness; 0, sharp; 1, blunt.  
 ITRIM input control integer for trim; 0, untrimmed; 1, trimmed ( $\alpha \pm 25^\circ$ )  
 IT input horizontal tail incidence, deg.  
 IXCD input control integer for limit shock position; 0, constant X/C;  
 1, limit shock sweep angle SHK specified from XCD at airplane  
 centerline.  
 J,ALELJ input integer identifying airfoil. See AXE listing.  
 L/D lift/drag ratio when ICDO=1.  
 LE tail length from moment center or center of gravity, ft.  
 LT tail length from C<sub>BARW</sub>/4, ft.  
 M,SMN Mach number  
 RNLOC Reynolds number per foot.  
 ROC input leading-edge radius-to-chord ratio for J=5 airfoils.  
 SEXT input area of forward wing-chord extensions (strakes), sq. ft.  
 SHK input sweep angle of limit shock when IXCD=1), deg.  
 SHOR input horizontal tail area, sq. ft.  
 SMN,M Mach number  
 SPANW wing span, ft.  
 SQH input sweep angle of horizontal tail C/4 line, deg.  
 SQW input sweep angle of wing C/4 line, deg.  
 SWING input wing reference area, sq. ft.  
 SWPWLE sweep angle of wing leading edge, rad.  
 TCRW input thickness-to-chord ratio of wing root ( $C_r$ ) chord  
 TCTW input thickness-to-chord ratio of wing tip chord.  
 TRW input wing taper ratio,  
 XCD input designated chordwise location of limit shock, Z=4.  
 XCG input longitudinal station of moment center or center-of-gravity, ft.  
 XEXT input longitudinal station of centroid of wing chord extension SEXT, ft.

XLB       input body length, ft.  
XLN       input nose length, ft.  
XQHOR     input longitudinal station of horizontal tail C/4, ft.  
XQMAC     input longitudinal station of wing CBARW/4, ft.  
YHOR       input horizontal tail height from wing chord plane, positive for  
           high tail, ft.  
Z         integer identifying flow zone.

## References

1. Woods, A. R., "Performance Data and Substantiation" McDonnell Aircraft Corporation, Dec. 1973.
2. Ackerman, N. G., and Warren, B. L., "F-5 Basic Aerodynamic Drag Data", Norair Report NOR 64-2, Northrop Corporation, January, 1964.
3. Levin, A. D., and Petroff, D. N., "An Experimental Investigation of Single and Double-Hinged Leading-Edge Flaps on a Model of an F-5A Aircraft at Transonic Mach Numbers", TMX-62,095, Jan. 1972, NASA.
4. Dollyhigh, S. M., "Subsonic and Supersonic Stability and Control Characteristics of an Aft-Tail Fighter Configuration with Cambered and Uncambered Wings and Uncambered Fuselage", NASA TMX-3078, 1974.
5. Jorgensen, L. H., and Nelson, E. R., "Experimental Aerodynamic Characteristics for Slender Bodies with Thin Wings and Tail at Angles of Attack from 0° to 58° and Mach Numbers from 0.6 to 2.0", TMX-3310, March 1976, NASA.
6. Esparza, V., and Embury, W. R., "Results of Investigations on an 0.015-Scale 140 A/B Configuration Space Shuttle Vehicle Orbiter Model (49-0) in the LTV 4- by 4-Foot High-Speed Wing Tunnel", NASA Contract NAS9-13247, DMS-DR-2037, NASA CR-134,405, August 1974.
7. Gillins, R. L., "Results of Investigations (OA77 and OA78) on an 0.015-Scale 140 A/B Configuration Space Shuttle Vehicle Orbiter Model 49-0 in the AEDC VKF B and C Wind Tunnels", NASA Contract NAS9-13247, DMS-DR-2134, NASA CR-134,429, January 1975.



TABLE I

INPUT FOR F4 TEST CASE (Fig. 2a-e)

(TITLE UP TO 56 CHARACTERS LONG) ← F4 TEST CASE (OVERPRINT)

&ARRAYS

NSMN = 6

SHN = 0.40 , 0.90 , 1.00 , 1.20 , 1.60 , 1.95 ,

ICDD = 1

CDD = .0190 , .0200 , .0310 , .0420 , .0415 , .0410 ,

CHD = 6.\*0. ,

CLOB = 6.\*0. ,

COOB = 6.\*0. ,

CHOB = 6.\*0. ,

ITRIM = 0 ,

&END

&WINGIN

ALELJ = 3

MNARW = 2.82 , MXARW = 2.82 , INARW = 1.0 ,

MNTRW = 0.167 , MXTRW = 0.167 , INTRW = 1.0 ,

MNSOW = 45.0 , MXSOW = 45.0 , INSOW = 1.0 , CLD = 0.0 ,

SWING = 530.0 , SPANW = 38.41 , CROOT = 23.5 , CTIP = 3.17 ,

TCBW = 0.064 , TCTW = 0.030 , XOMAC = 25.763 , CBARW = 16.442 ,

ROC = 0 , SEXT = 0 , XEXT = 0 , IPLEX = 0 ,

&END

&NOSEIN

BDMAX = 5.7 , XLN = 20.0 , XLB = 44.0 , XCG = 26.565 ,

&END

&TAILIN

SHOR = 96.23 , XOHOR = 50.13 , ARH = 3.23 , SQH = 35.5 ,

YHOR = 1.75 , IT = 0 ,

&END

&FLOWIN

MNALF = 2 , MXALF = 40 , INALF = 2 ,

MNXCD = 0.35 , HXXCD = 1.0 , INXCD = 0.325 ,

IXCD = 0 , SHK = 0 ,

ALTV = 35000 ,

&END

&FACTOR

PTOTL = 1.0 , PTOTD = 1.0 , FCM = 1.0 ,

&END

&OUTPUT

IDATA = 1 , ITABL = 1 ,

IPLOT = 1 , PPLOT = 1 ,

LDISP = 1 , 1 , 1 , 1 , 1 ,

DDISP = 1 , 1 , 1 , 1 ,

&END

TABLE II  
 INPUT FOR F5 TEST CASE (Fig. 3a-g)

(TITLE UP TO 56 CHARACTERS LONG) ← F5 TEST CASE

BARAYS

NSMN = 5  
 SHN = 0.6 , 0.9 , 1.1 , 1.2 , 1.4 ,  
 ICDD = 1  
 CDD = 0.0212 , 0.0225 , 0.0470 , 0.0485 , 0.0490 ,  
 CMD = 5.\*0. ,  
 CLOP = 5.\*0. ,  
 CDOB = 5.\*0. ,  
 CMOB = 5.\*0. ,  
 ITRIM = 0  
 SEND

SWINGIN

ALEJ = 1  
 MNARW = 3.75 , MXARW = 3.75 , INARW = 1.0 ,  
 MNTRW = 0.2 , MXTRW = 0.2 , INTRW = 1.0 ,  
 MNSOM = 24.0 , MXSOM = 24.0 , INSOM = 1.0 , CLO = 0.0 ,  
 SWING = 170. , SPANW = 25.25 , CRODT = 11.221 , CTIP = 2.244 ,  
 TCRW = 0.048 , TCTW = 0.045 , XOMAC = 25.99 , CBARW = 7.73 ,  
 ROC = 0. , SEXT = 0. , XEXT = 0. , IFLEX = 0 ,  
 SEND

ENDSEIN

BDMAX = 4.3 , XLN = 22.5 , XLB = 44.0 , XCG = 25.14 ,  
 SEND

STATLIN

SHOR = 59.0 , XOMOR = 38.96 , ARH = 2.88 , SQH = 25.0 ,  
 YHOR = 0.0 , IT = 0.0 ,  
 SEND

BFLOWIN

MNALF = 2.0 , MXALF = 40.0 , INALF = 2.0 ,  
 MNXCD = 0.35 , MXXCD = 0.675 , INXCD = 0.325 ,  
 IXCD = 0 , SHK = 0. ,  
 ALTV = 35000. ,  
 SEND

FACTOR

PTOTL = 1.0 , PTOTD = 1.0 , FCM = 1.0 ,  
 SEND

OUTPUT

IDATA = 1 , ITABL = 1 ,  
 IPLOY = 1 , PPLOY = 1 ,  
 LDISP = 1 , 1 , 1 , 1 , 1 , 1 ,  
 DDISP = 1 , 1 , 1 , 1 ,  
 SEND

TABLE III  
 INPUT FOR MODEL L TEST CASE (Fig. 4a-i)

(TITLE UP TO 56 CHARACTERS LONG) ← MODEL L

```

BARRAYS
NSMN  4
SRN   0.5 , 0.8 , 1.2 , 1.8 ,
ICDD  1
CDD   0.0210 , 0.0200 , 0.0360 , 0.0210
CHO   4.*0.
CLOB  4.*0.
CDOB  4.*0.
CHOB  4.*0.
ITRIM 0
SEND

EMINGIN
ALELJ 3
MNARW 2.75 , MXARW = 2.75 , INARW = 1.0
MNTRW 0.2 , MXTRW = 0.2 , INTRW = 1.0
MNSOM 43.53 , MXSOM = 43.53 , INSOM = 1.0 , CLO = 0.0
SWING 752.398 , SPANW = 45.552 , CRODT = 27.5 , CTIP = 5.504
TCRW  0.045 , TCTW = 0.045 , XOMAC = 38.2 , CBARW = 19.185
ROC   0. , SEXT = 0. , XEXT = 0. , IFLEX = 0
SEND

EMOSEIN
EDMAX 5.8 , XLN = 25.0 , XLB = 67.07 , XCG = 37.4
SEND

KYATLIN
SHOR  256.4 , XOMOR = 12.8 , ARH = 2.912 , SQH = 37.5
YHOR  -2.286 , IT = 0.
SEND

EFLOWIN
MNALF 2.0 , MXALF = 40.0 , INALF = 3.0
MNXCD 0.35 , MXXCD = 0.675 , INXCD = 0.325
IKCD  0 , SHK = 0.
ALTY  35000.
SEND

EFACTOR
PTOTL 1. , PTOTD = 1. , FCM = 1.
SEND

EOUTPUT
IDATA 1 , ITABL = 1
IPLOT 1 , PPLOT = 1
LDISP 1 , 1 , 1 , 1 , 1
DDISP 1 , 1 , 1
SEND
  
```

**TABLE IV**  
**INPUT FOR MODEL A-1 (Fig. 5a-0)**

(TITLE UP TO 56 CHARACTERS LONG) ← MODEL A-1

**PARAMETERS**

NSMN • 5 ,  
SMN • 0.6 , 0.9 , 1.2 , 1.5 , 2.0 ,  
ICDD • 1  
† CDD • 0.0180 , 0.0200 , 0.050 , 0.0400 , 0.0340 ,  
CDO • 5.\*0. ,  
CLO • 5.\*0. ,  
CDB • 5.\*0. ,  
CHOB • -0.01 , 0.0 , 0.0 , 0.0 , 0.0 ,  
ITRM • 0  
END

**SWINGIN**

\* ALEJ • 1;5 ,  
ANRW • 4.0 , MXRW = 4.0 , INRW = 1.0 ,  
NTRW • 0.0 , MXTRW = 0.0 , INTRW = 1.0 ,  
NNSW • 36.87 , MXSW = 36.87 , INSW = 1.0 , CLO = 0.0 ,  
SWNG • 108.16 , SPANW = 20.80 , CROD = 10.4 , CTIP = 0.0 ,  
TCBW • 0.0138 , TCTW = 0.100 , XOMAC = 13.0 , CBRW = 6.933 ,  
\* ROC • 0. ; 0.002 , SEXT = 0. , XEXT = 0. , IFLEX = 0 ,  
END

**ENDSEIN**

BDMAX • 2.6 , XLN = 9.1 , XLB • 26.0 OFF  
21.58 , XCG • 13.0 ,  
END

**BTATLIN**

SHOR • 42.25 , XOMOR = 22.4 , ARH • 4.0 , SQH • 22.5 ,  
VHOR • 0.0 , IT = 0.0 ,  
END

**BFLOWIN**

MNALF • 2.0 , MXALF = 40.0 , INALF = 2.0 ,  
MNXCD • 0.3 , MXCD = 0.9 , INXCD = 0.3 ,  
IXCD • 0 , SHK = 0. ,  
ALTV • 30000. ,  
END

**EFACOR**

PTOTL • 1. , PTOTD = 1. , FCM • 1. ,  
END

**OUTPUT**

IDATA • 1. , ITABL • 1. ,  
IPLOT • 1 , PPLLOT • 1 ,  
LDISP • 1 , 1 , 1 , 1 , 1 , 1 ,  
DDISP • 1 , 1 , 1 , 1 ,  
END

4 DATA SETS CALCULATED (2 JS for tail on & Tail off) FOR MODELS A-1 THRU A-5

\* For J=1 ROC = 0  
J=5 ROC = .002

† TAIL ON CDD VALUE 2 SHOWN ABOVE. TAIL OFF CDD = .012 , .014 , .024 , .023 , .022.  
SHOR = 0.

TABLE V  
INPUT FOR MODEL A-2 (Fig. 6a-0)

TITLE UP TO 56 CHARACTERS LONG ← MODEL A-2

BARARRAYS

MSMN = 5  
 SHN = 0.6, 0.9, 1.2, 1.5, 2.0  
 ICDO = 1  
 CDO = 0.018, 0.022, 0.050, 0.042, 0.040  
 CMO = 5. \* 0.  
 CLOP = 5. \* 0.  
 CDOB = 5. \* 0.  
 ITRIM = 0  
 BEND

EWINGIN

ALELJ = 1, 5  
 MNARW = 4.0, MXARW = 4.0, INARW = 1.0  
 MNTRW = 0.25, MXTRW = 0.25, INTRW = 1.0  
 MNSOW = 24.23, MXSOW = 24.23, INSOW = 1.0, CLO = 0.0  
 SWING = 108.16, SPANW = 20.80, CRODT = 8.32, CTIP = 2.28  
 TCRW = 0.0172, TCTW = 0.0688, XOMAC = 13.732, CBARW = 5.827  
 ROC = 0.0; 0.002, SEXT = 0, XEXT = 0, IFLEX = 0  
 BEND

KNOSEIN

BDMAX = 2.6, XLN = 10.65, XLB = 21.57, XCG = 12.832  
 BEND

LYTAILIN

SHOR = 42.25, XOHOR = 23.4, ARH = 4.0, SQH = 22.5  
 YHOR = 0, IT = 0  
 BEND

BFLOWIN

MNALF = 2.0, MXALF = 40.0, INALF = 2.0  
 MNXCD = 0.3, MXXCD = 0.9, INXCD = 0.3  
 IXCD = 0, SHK = 0  
 ALTV = 30000  
 BEND

BFACTOR

PTOTL = 1, FTOTD = 1, FCM = 1  
 BEND

BOUTPUT

IDATA = 1, ITABL = 1  
 IPLOT = 1, PPLDT =  
 LDISP = 1, 1, 1, 1, 1, 1  
 DDISP = 1, 1, 1, 1  
 BEND

TAIL OFF CDO = .012, .012, .027, .024, .025  
 SHK = 0.

**TABLE VI**  
**INPUT FOR MODEL A-3 (Fig. 7a-0)**

**TITLE UP TO 56 CHARACTERS LONG ← MODEL A-3**

**&ARRAYS**

MSMN = 5.  
 SHN = 0.6 , 0.9 , 1.2 , 1.5 , 2.0 ,  
 ICDO = 1  
 CDO = 0.019 , 0.022 , 0.050 , 0.042 , 0.040 ,  
 CHO = 5.\*0.  
 CLOB = 5.\*0.  
 CDOB = 5.\*0.  
 CHOB = 5.\*0.  
 ITRIM = 0  
**END**

**&WINGIN**

ALELJ = 1 , 5  
 MNARW = 4.0 , MXARW = 4.0 , INARW = 1.0  
 MNTRW = 0.5 , MXTRW = 0.5 , INTRW = 1.0  
 MNSOW = 14.03 , MXSOW = 14.03 , INSOW = 1.0 , CLO = 0.0  
 SWING = 102.16 , SPANW = 20.80 , CROOT = 6.93 , CTIP = 3.467  
 TCRW = 0.0206 , TCTW = 0.0414 , XOMAC = 14.157 , CBARW = 5.311  
 ROC = 0 , 0.002 , SEXT = 0 , XEXT = 0 , IFLEX = 0  
**END**

**&NOSEIN**

BDMAX = 2.6 , XLN = 11.7 , XLB = 26.0 OFF  
 21.58 IN , XCG = 14.157  
**END**

**&TAILIN**

SHOR = 42.25 , XOHOR = 23.4 , ARH = 4.0 , SQH = 22.5  
 YHOR = 0 , IT = 0  
**END**

**&FLOWIN**

MNALF = 2.0 , MXALF = 40.0 , INALF = 2.0  
 MNXCD = 0.3 , MXXCD = 0.9 , INXCD = 0.3  
 IXCD = 0 , SHK = 0  
 ALTV = 30.000  
**END**

**&FACTOR**

PTOTL = 1 , PTOTD = 1 , FCM = 1  
**END**

**&OUTPUT**

IDATA = 1 , ITABL = 1  
 IPLOY = 1 , PPLOY = 1  
 LDISP = 1 , 1 , 1 , 1 , 1 , 1  
 DDISP = 1 , 1 , 1 , 1  
**END**

TAIL OFF CDO = 0.013 , 0.016 , 0.033 , 0.035 , 0.028 ,  
 SHOR = 0

TABLE VII  
INPUT FOR MODEL A-4 (Fig. 8a-0)

TITLE UP TO 56 CHARACTERS LONG ← MODEL A-4

**PARAMETERS**

NSMN = 5  
 SRN = 0.6 , 0.9 , 1.2 , 1.5 , 2.0 ,  
 ICDD = 1  
 CDD = 0.018 , 0.024 , 0.05 , 0.042 , 0.040 ,  
 CHD = 5 \* 0 ,  
 CLOS = 5 \* 0 ,  
 CDOB = 5 \* 0 ,  
 CHOB = 5 \* 0 ,  
 ITRIM = 0  
**END**

**SWINGIN**

ALELJ = 1; 5  
 MNARM = 5.0 , MXARM = 5.0 , INARM = 1.0 ,  
 MNTRW = 0.25 , MXTRW = 0.25 , INTRW = 1.0 ,  
 MNSON = 19.8 , MXSON = 19.8 , INSON = 1.0 , CLO = 0.0 ,  
 SWING = 108.16 , SPANW = 23.26 , CRODT = 7.14 , CTIP = 1.86 ,  
 TCBW = 0.0192 , TCTH = 0.077 , XOMAC = 14.294 , CBARW = 5.208 ,  
 ROC = 0; 0.002 , SEXT = 0 , XEXT = 0 , IFLEX = 0 ,  
**END**

**BNOSKIN**

BDMAX = 2.6 , XLN = 11.38 , XLB = 26.7<sup>FL</sup> / 21.58<sup>SP</sup> , XCG = 14.51 ,  
**END**

**STATLIN**

SMOR = 42.25 , XOHOR = 23.4 , ARH = 4.0 , SQH = 22.5 ,  
 YHOR = , IT = ,  
**END**

**FLOWIN**

MNALF = 2.0 , MXALF = 40.0 , INALF = 2.0 ,  
 MNXCD = 0.3 , MXXCD = 0.9 , INXCD = 0.3 ,  
 IXCD = 0 , SHK = 0 ,  
 ALTV = 30000 ,  
**END**

**FACTOR**

PTOTL = 1 , PTOTD = 1 , FCM = 1 ,  
**END**

**OUTPUT**

IDATA = 1 , ITABL = 1 ,  
 IPLOY = 1 , PPLOY = 1 ,  
 LDISP = 1 , 1 , 1 , 1 , 1 , 1 ,  
 DDISP = 1 , 1 , 1 , 1 ,  
**END**

TAIL OFF CDD = 0.13 , 0.16 , 0.034 , 0.036 , 0.028  
 SHOR = 0

TABLE VIII  
INPUT FOR MODEL A-5 (Fig. 9a-0)

TITLE UP TO 56 CHARACTERS LONG ← MODEL A-5

BARARRAYS

NSMN = 5  
 SHN = 0.6 , 0.9 , 1.2 , 1.5 , 2.0 ,  
 ICDD = 1  
 CDD = 0.016 , 0.018 , 0.050 , 0.040 , 0.035 ,  
 CHD = 5 \* 0 ,  
 CLOS = 5 \* 0 ,  
 COOR = 5 \* 0 ,  
 CHOB = 5 \* 0 ,  
 ITRIM = 0  
 BEND

SWINGIN

ALEJ = 1 ; 5  
 MNARW = 3.0 , MXARW = 3.0 , INARW = 1.0 ,  
 MNTRW = 0.25 , MXTRW = 0.25 , INTRW = 1.0 ,  
 MNROW = 31.0 , MXROW = 31.0 , INROW = 1.0 , CLD = 0.0 ,  
 SWING = 108.16 , SPANW = 18.0 , CRODT = 9.6 , CTIP = 2.4 ,  
 TCBW = .0149 , TCTW = .0595 , XOMAC = 13.16 , CBARW = 6.72 ,  
 ROC = 0 ; 0.002 , SEXT = 0 , XEXT = 0 , IFLEX = 0 ,  
 BEND

KNOWSETN

BDMAX = 2.6 , XLN = 9.63 , XLB = 26.0 OFF ON 21.58 , XCG = 13.16 ,  
 BEND

STATLIN

SHOR = 42.25 , XOMOR = 23.4 , ARH = 4.0 , SOM = 22.5 ,  
 YHOR = 0 , IT = 0 ,  
 BEND

FLOWIN

MNALF = 2.0 , MXALF = 40.0 , INALF = 2.0 ,  
 MNXCD = 0.3 , MXXCD = 0.9 , INXCD = 0.3 ,  
 IXCD = 0 , SHK = 0 ,  
 ALTV = 30000 ,  
 BEND

FACTOR

PTOTL = 1 , PTOTD = 1 , FCM = 1 ,  
 BEND

OUTPUT

IDATA = 1 , ITABL = 1 ,  
 IPLOT = 1 , PPLOT = 1 ,  
 LDISP = 1 , 1 , 1 , 1 , 1 ,  
 DDISP = 1 , 1 , 1 ,  
 BEND

TAIL OFF CDD = .010 , .012 , .025 , .025 , .022 ,  
 SHOR = 0 .



TABLE IX  
INPUT FOR SHUTTLE (Fig. 10a-u)

TITLE UP TO 56 CHARACTERS LONG ← SHUTTLE ORBITER

BARARRAYS

NSMN = 7,

SMN = 0.6, 0.9, 1.2, 1.6, 2.0, 4.0, 7.0,

ICDD = 1

CDD = 0.064, 0.086, 0.176, 0.160, 0.143, 0.093, 0.065,

CHD = 7 \* 0.

CLOS = -0.1, -0.1, -0.06, -0.04, -0.06, -0.07, 0.0,

CDOR = 7 \* 0.

CHOB = 0.06, 0.08, 0.08, 0.04, 0.02, -0.01, 0.0,

ITRIM = 0

END

EWINGIN

ALELJ = 2

MNARW = 2.26, MXARW = 2.26, INARW = 1.

MNTRW = 0.2, MXTRW = 0.2, INTRW = 1.

MNSOW = 35.2, MXSOW = 35.2, INSOW = 1, CLO = 0.0,

SWING = 87.16, SPANW = 14.05, CROOT = 10.327, CTIP = 2.062,

TCTW = 0.11, TCTW = 0.11, XOMAC = 13.49, CBARW = 7.2,

ROC = 0, SEXT = 37.7, XEXT = 6.5, IFLEX = 1

END

ENHSEIN

BDMAX = 3.0, XLN = 0, XLB = 0, XCG = 12.58,

END

KYATLIN

SHOR = 0.0, XOMOR = 19.0, ARH = 0, SQH = 0,

YHOR = 0, IT = 0

END

EFLWIN

MNALF = 2.0, MXALF = 40.0, INALF = 2.0

MNXCD = 0.5, HXXCD = 1.0, INXCD = 0.25

IXCD = 0, SHK = 0

ALTY = 50000

END

EFACOR

PTOTL = 1, PTOTD = 1, FCM = 1

END

EOUPUT

IDATA = 1, ITABL = 1

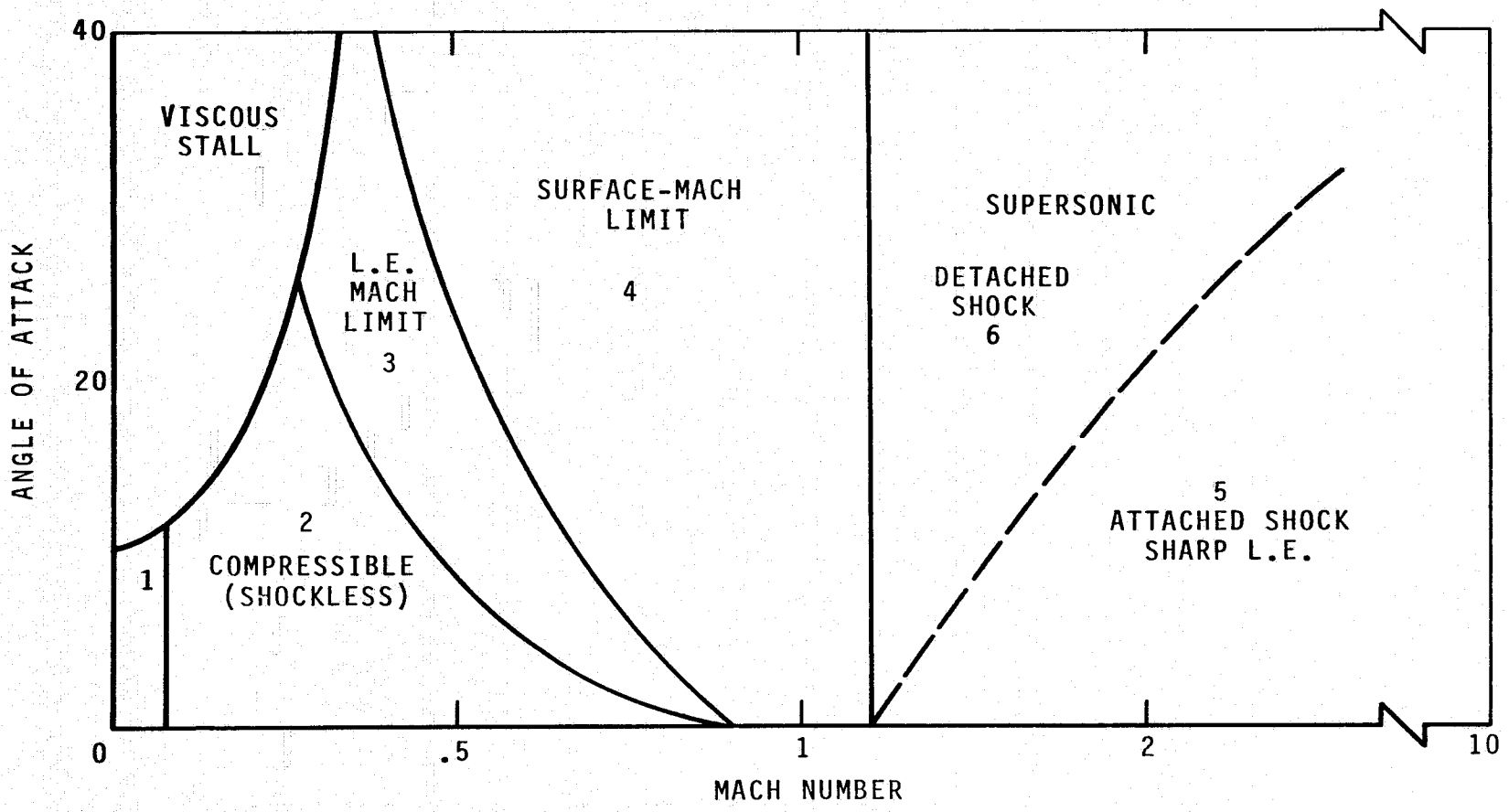
IPLOT = 1, PFPLOT = 1

LDISP = 1, 1, 1, 1, 1, 1

DDISP = 1, 1, 1, 1

END

ORIGINAL PAGE IS  
OF POOR QUALITY



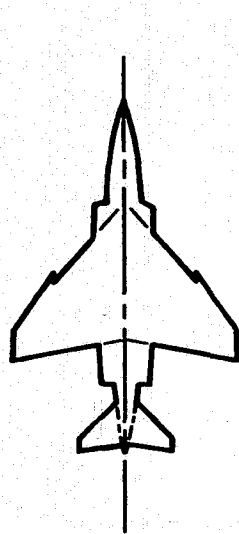
(a) FLOW ZONES.

FIGURE 1.- FLOW ZONES AND MODELS INDICATED FOR TEST CASES.

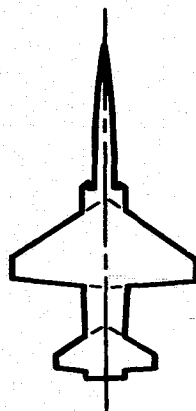
MODEL	F4	F5	L	A1	A2	A3	A4	A5	SHUTTLE
REFERENCE	1	2, 3	4	← 5 →					6, 7
INPUT TABLE	I	II	III	IV	V	VI	VII	VIII	IX
DATA FIGURE	2(a-e)	3(a-g)	4(a-i)	5(a-o)	6(a-o)	7(a-o)	8(a-o)	9(a-o)	10(a-u)
WING ASPECT RATIO	2.82	3.75	2.75	4.00	4.00	4.00	5.00	3.00	2.26
WING TAPER RATIO	0.17	0.20	0.20	0.00	0.25	0.50	0.25	0.25	0.20
NOMINAL $\alpha$ - RANGE	0° to 32°	0° to 22°	0° to 20°	← 0° to 60° →					0° to 33°
MACH NUMBERS	0.9, 1.2	0.6, 0.9, 1.1, 1.2	0.5, 0.8, 1.2, 1.8	← 0.6, 0.9, 1.2, 1.5, 2.0 →					0.6, 0.9, 1.2, 1.6, 2.0, 4.0, 8.0

(b) TEST CASE SUMMARY.

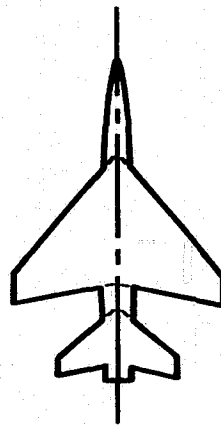
FIGURE 1.- CONTINUED.



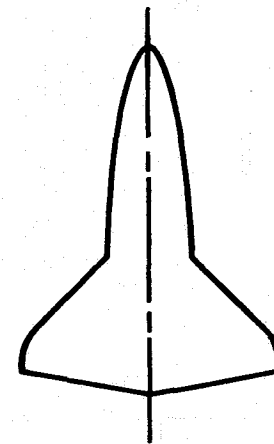
F4



F5

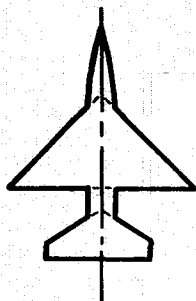


L

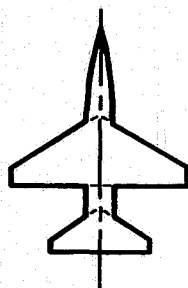


SHUTTLE

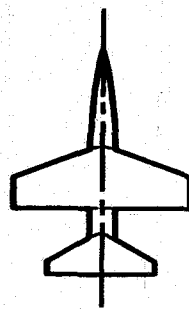
20



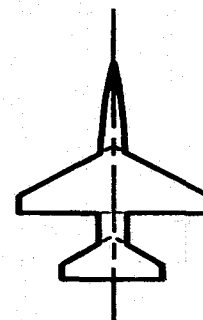
A1



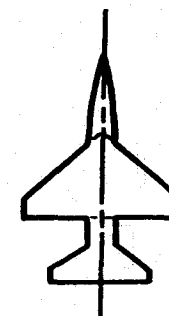
A2



A3



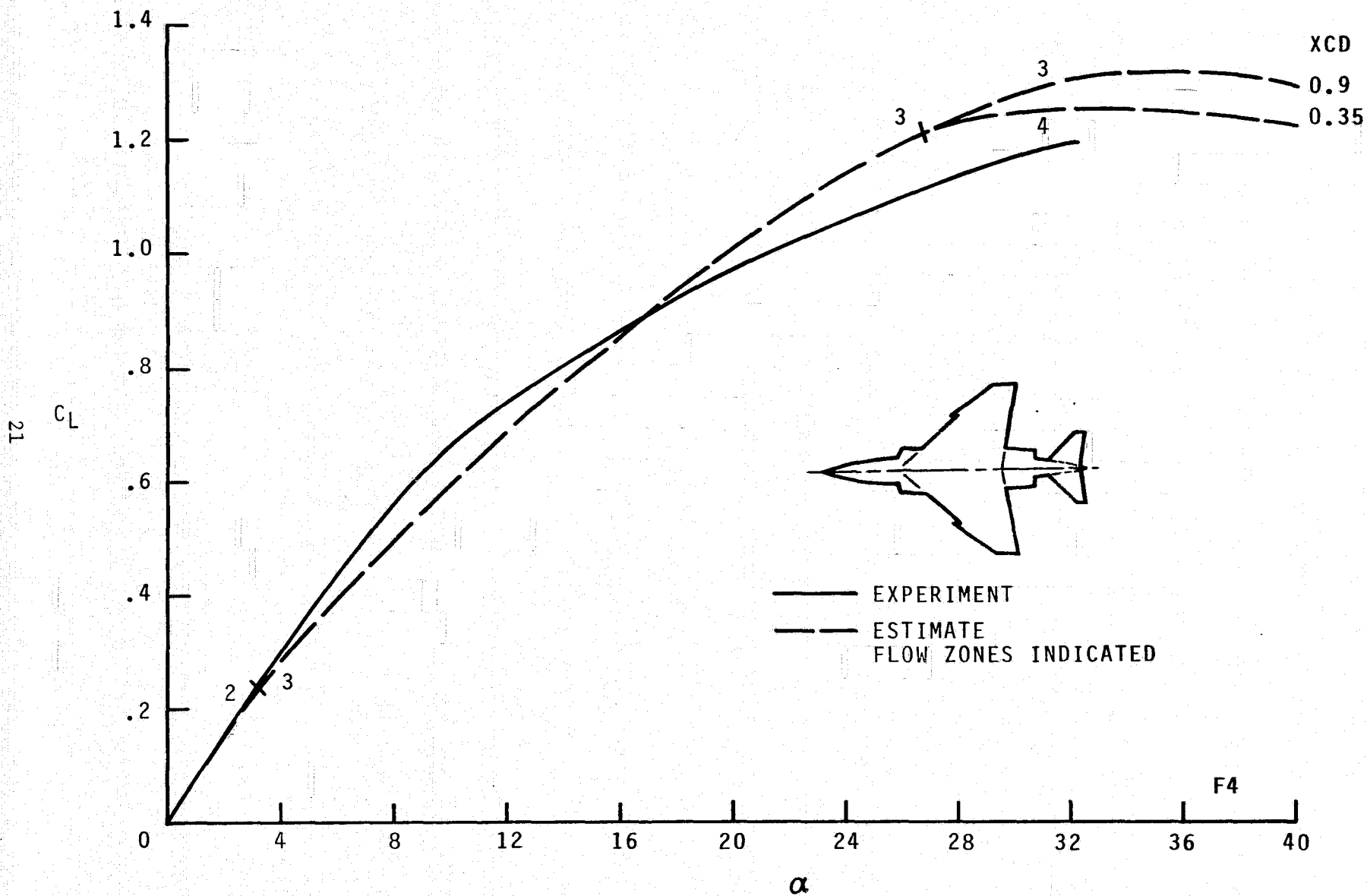
A4



A5

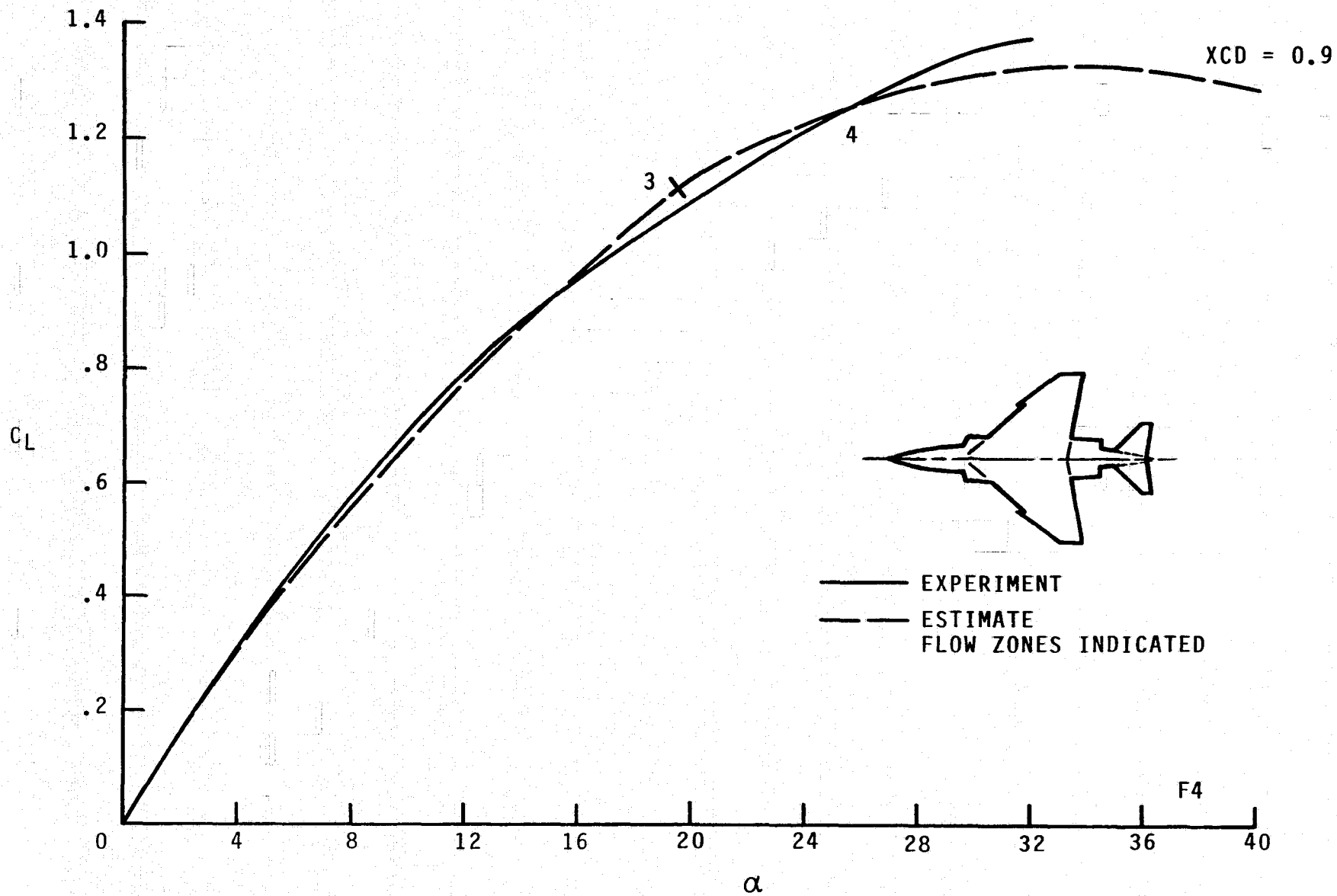
(c) MODEL SKETCHES.

FIGURE 1.- CONCLUDED.



(a)  $C_L$  VERSUS  $\alpha$ ;  $M = 0.9$ .

FIGURE 2.- AERODYNAMICS FOR THE F4;  $J = 3$ .



(b)  $C_L$  VERSUS  $\alpha$ ;  $M = 1.2$ .

FIGURE 2.- CONTINUED.

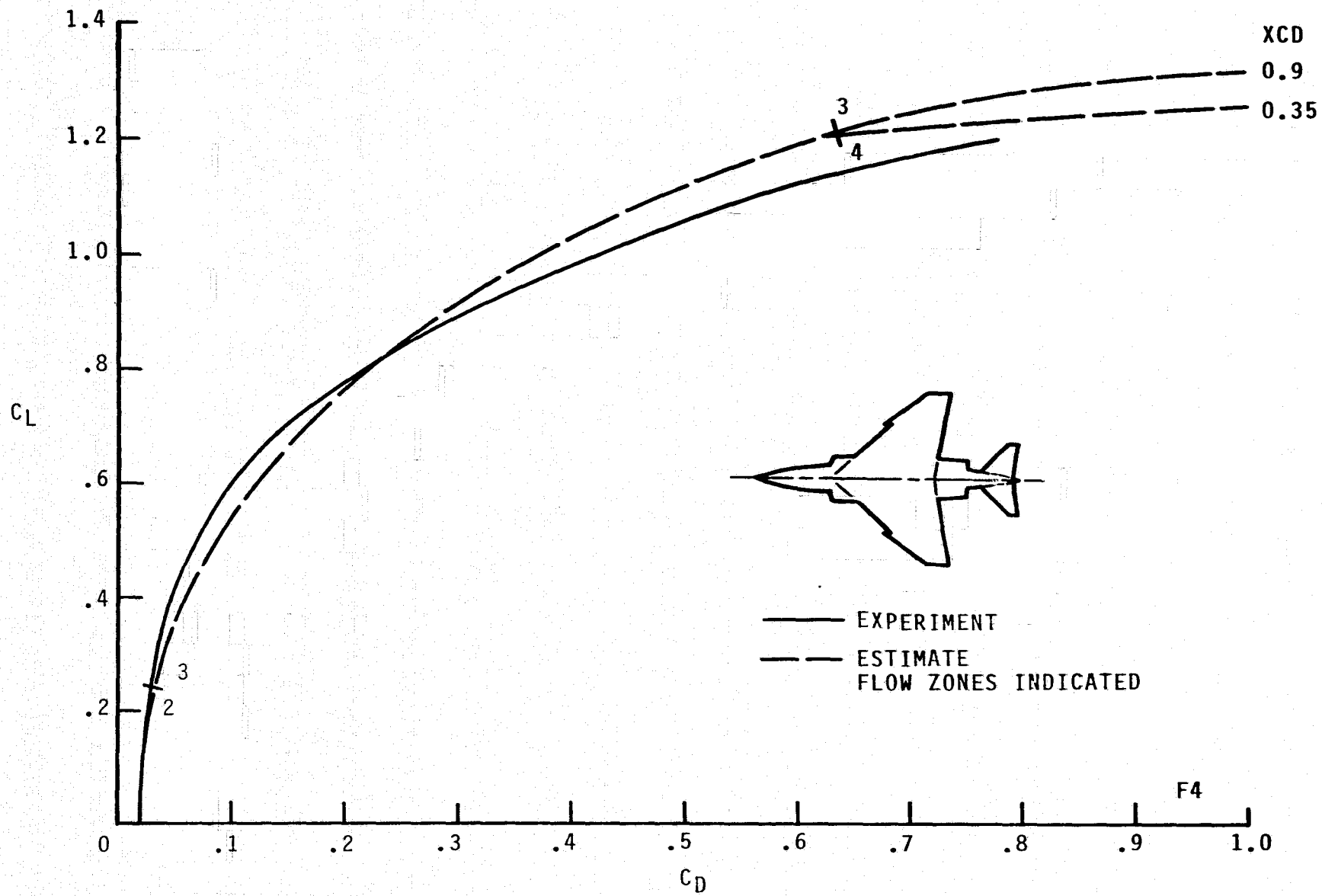
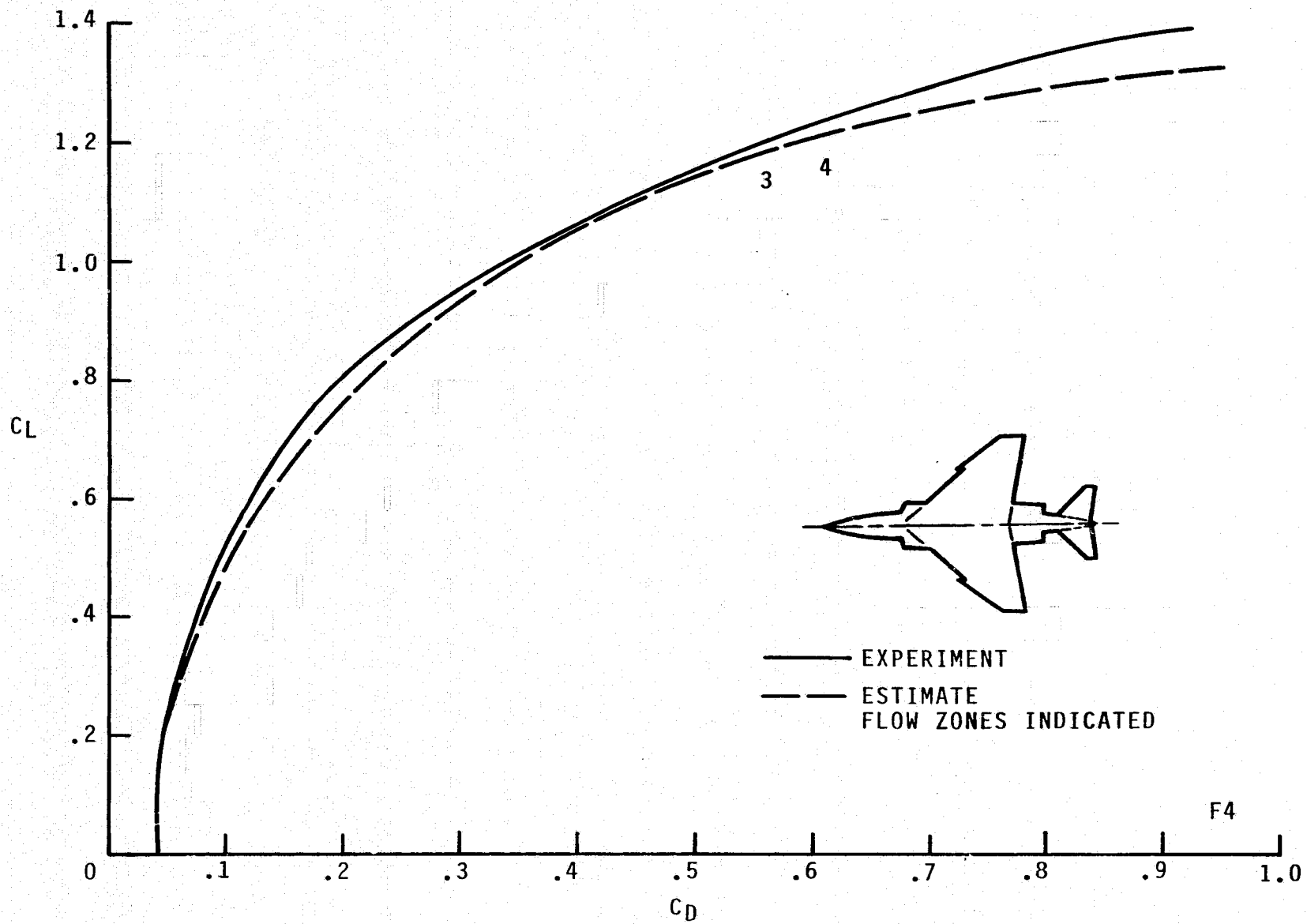
(c)  $C_L$  VERSUS  $C_D$ ;  $M = 0.9$ .

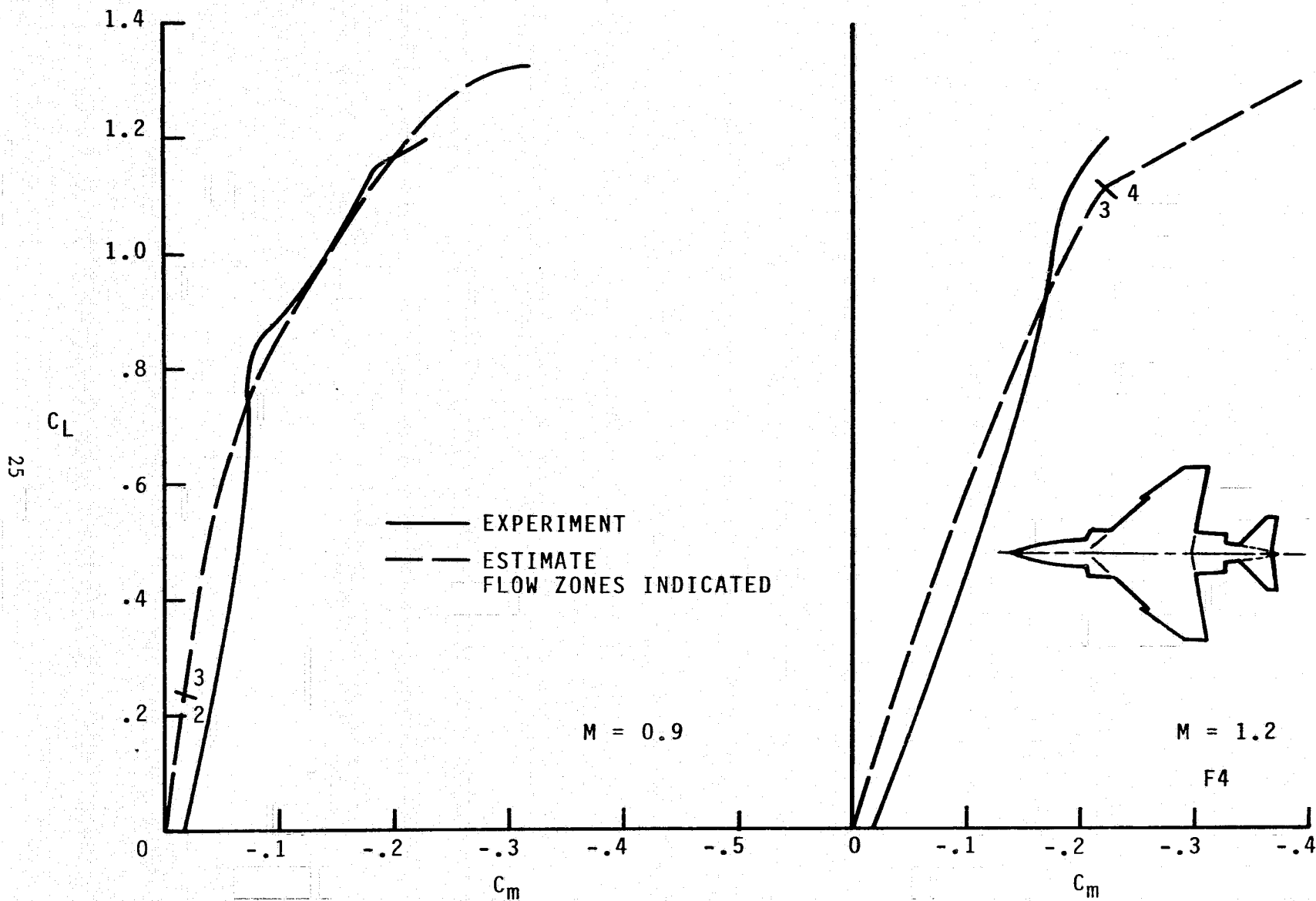
FIGURE 2.- CONTINUED.



(d)  $C_L$  VERSUS  $C_D$ ;  $M = 1.2$ .

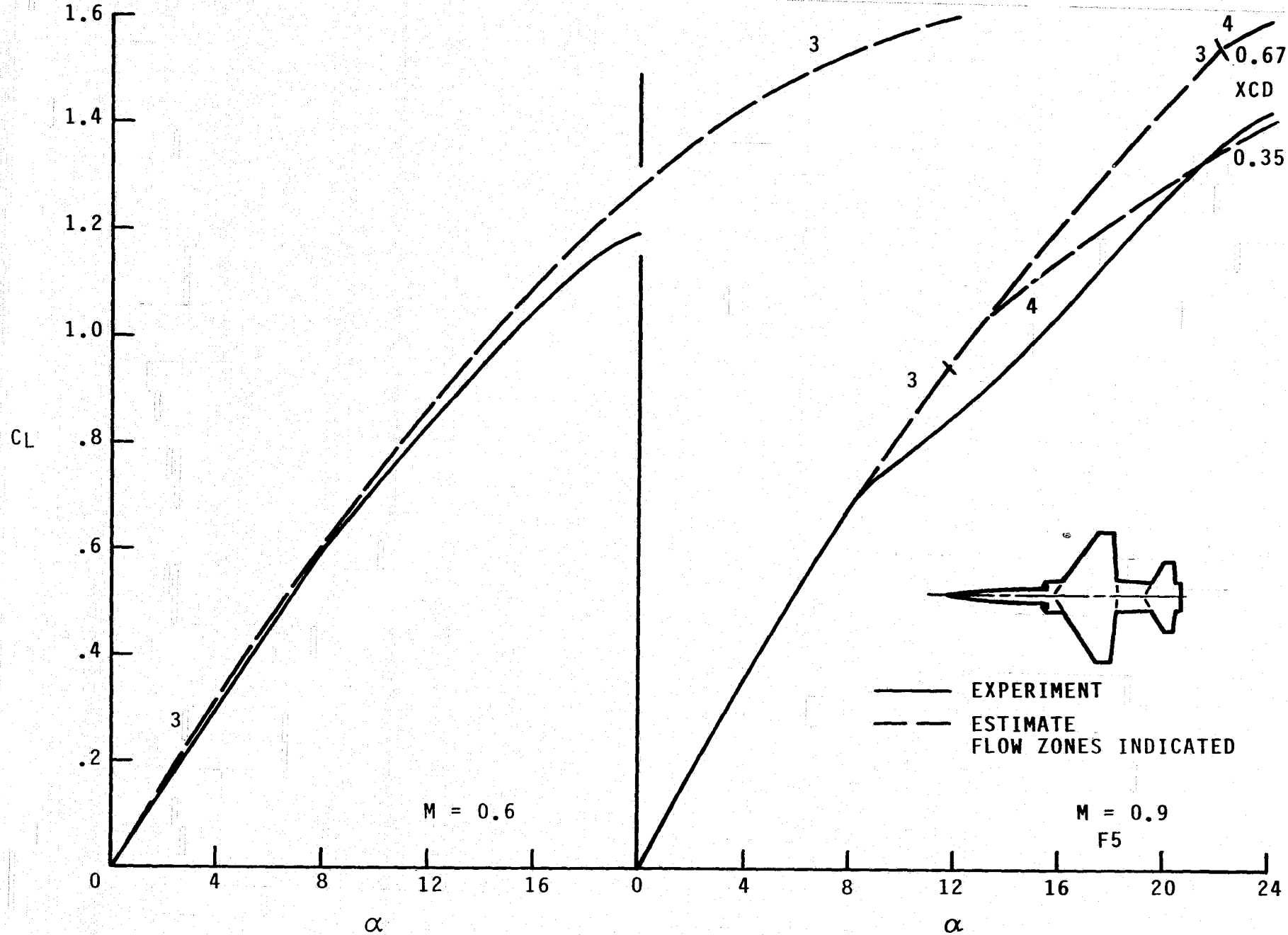
FIGURE 2.- CONTINUED.





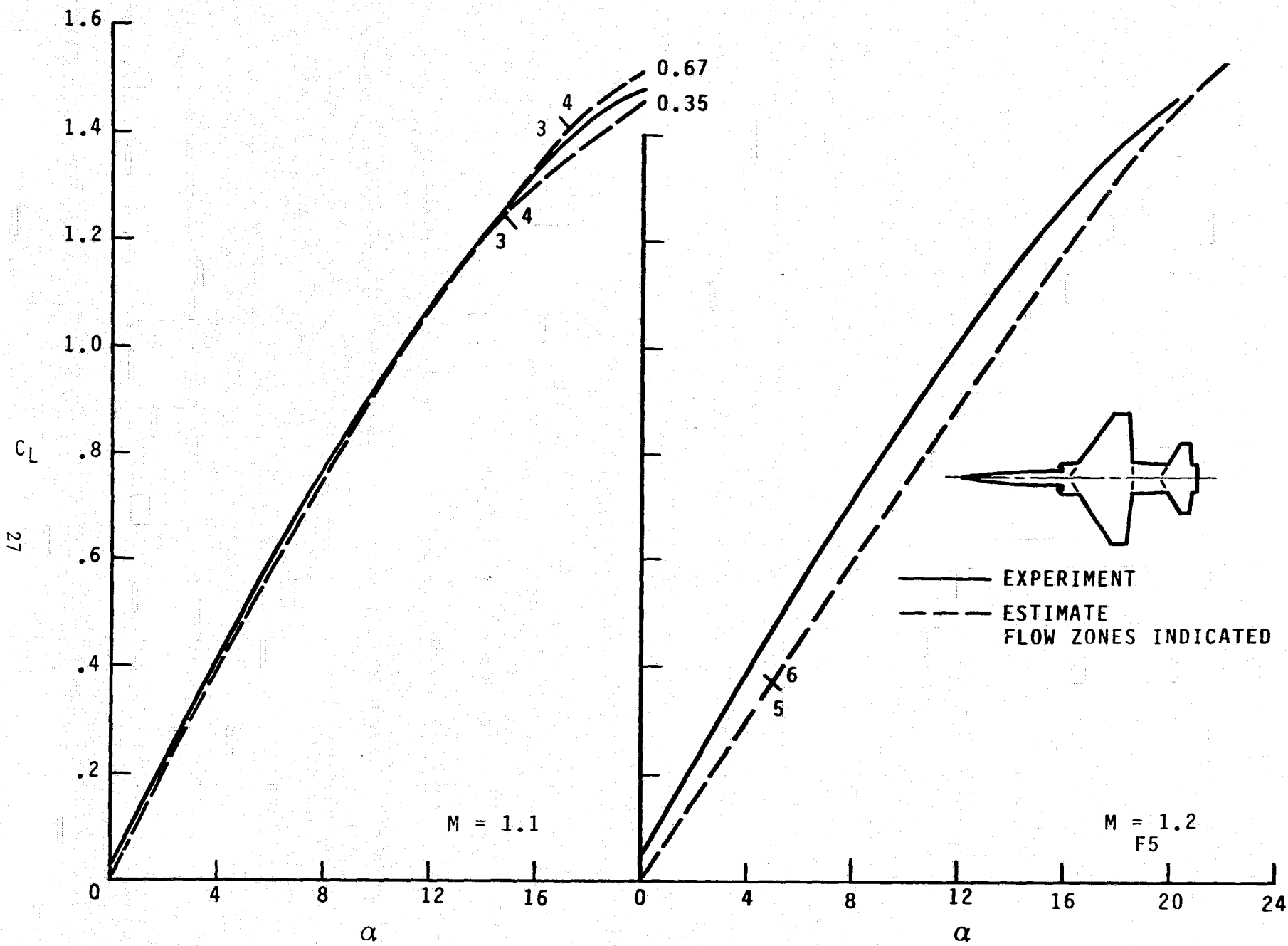
(e)  $C_L$  VERSUS  $C_m$ ; M = 0.9, 1.2.

FIGURE 2.- CONCLUDED.



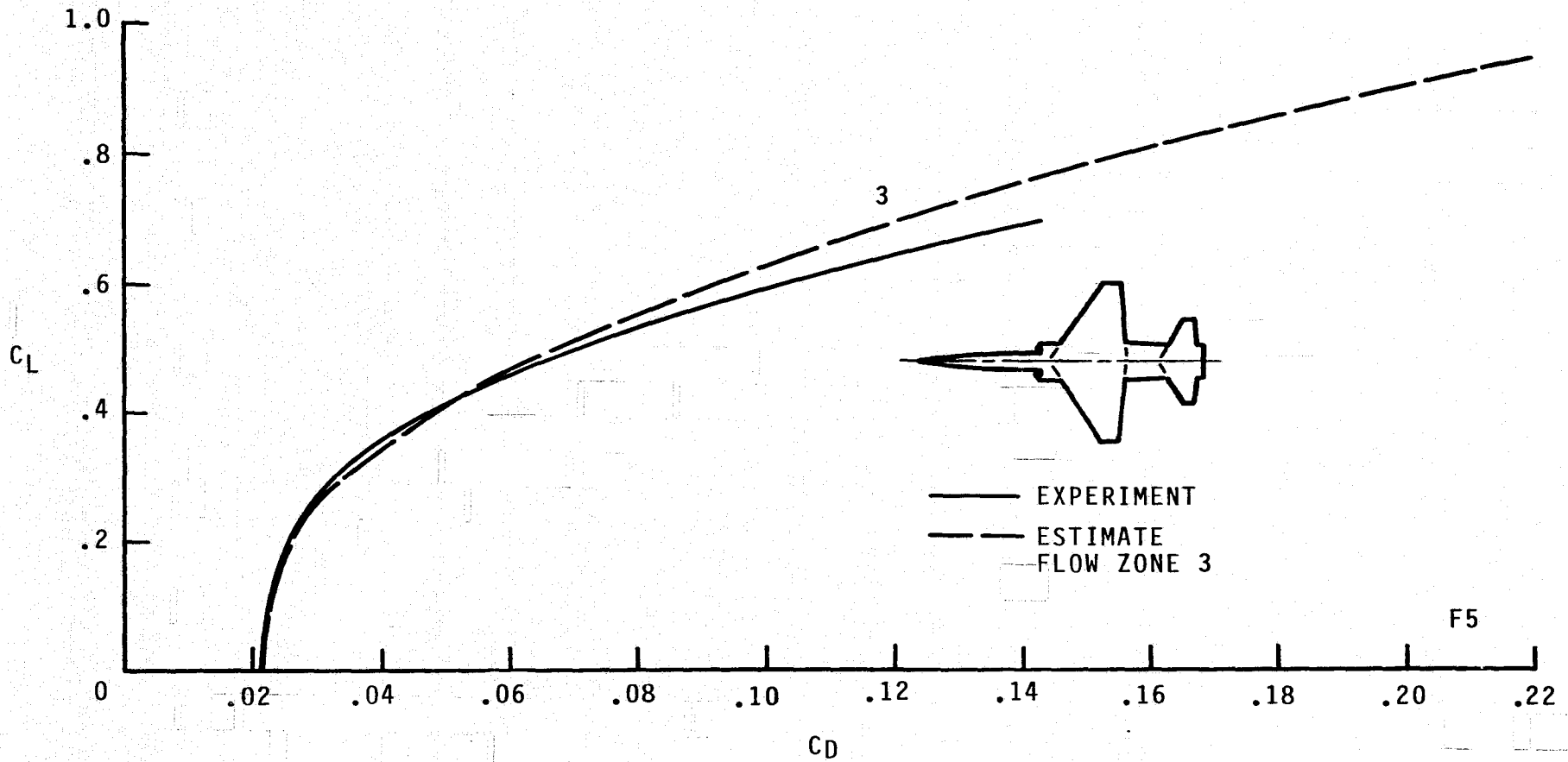
(a)  $C_L$  VERSUS  $\alpha$ ;  $M = 0.6, 0.9$ .

FIGURE 3.- AERODYNAMICS FOR THE F5,  $J = 1$ .



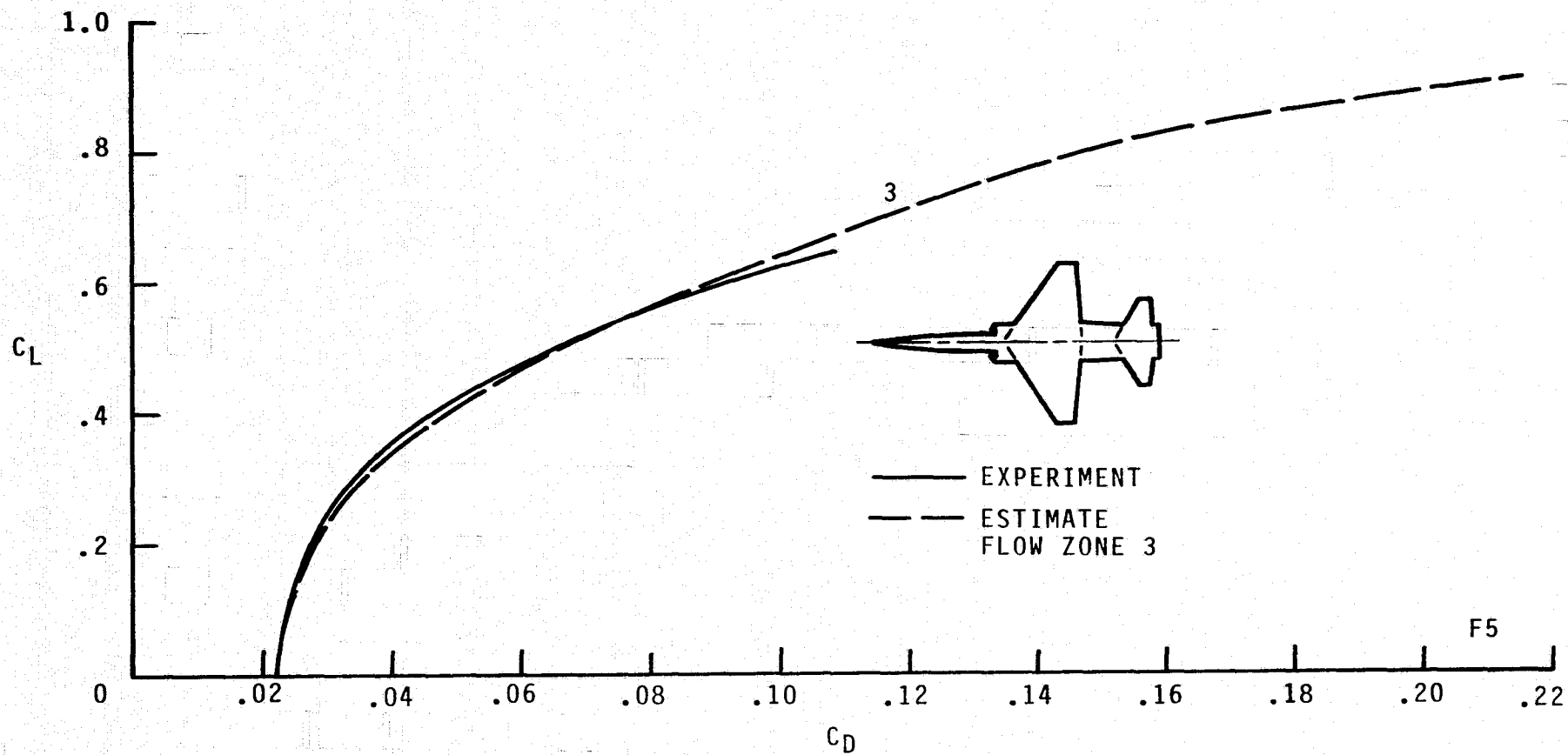
(b)  $C_L$  VERSUS  $\alpha$ ;  $M = 1.1, 1.2$ .

FIGURE 3.- CONTINUED.



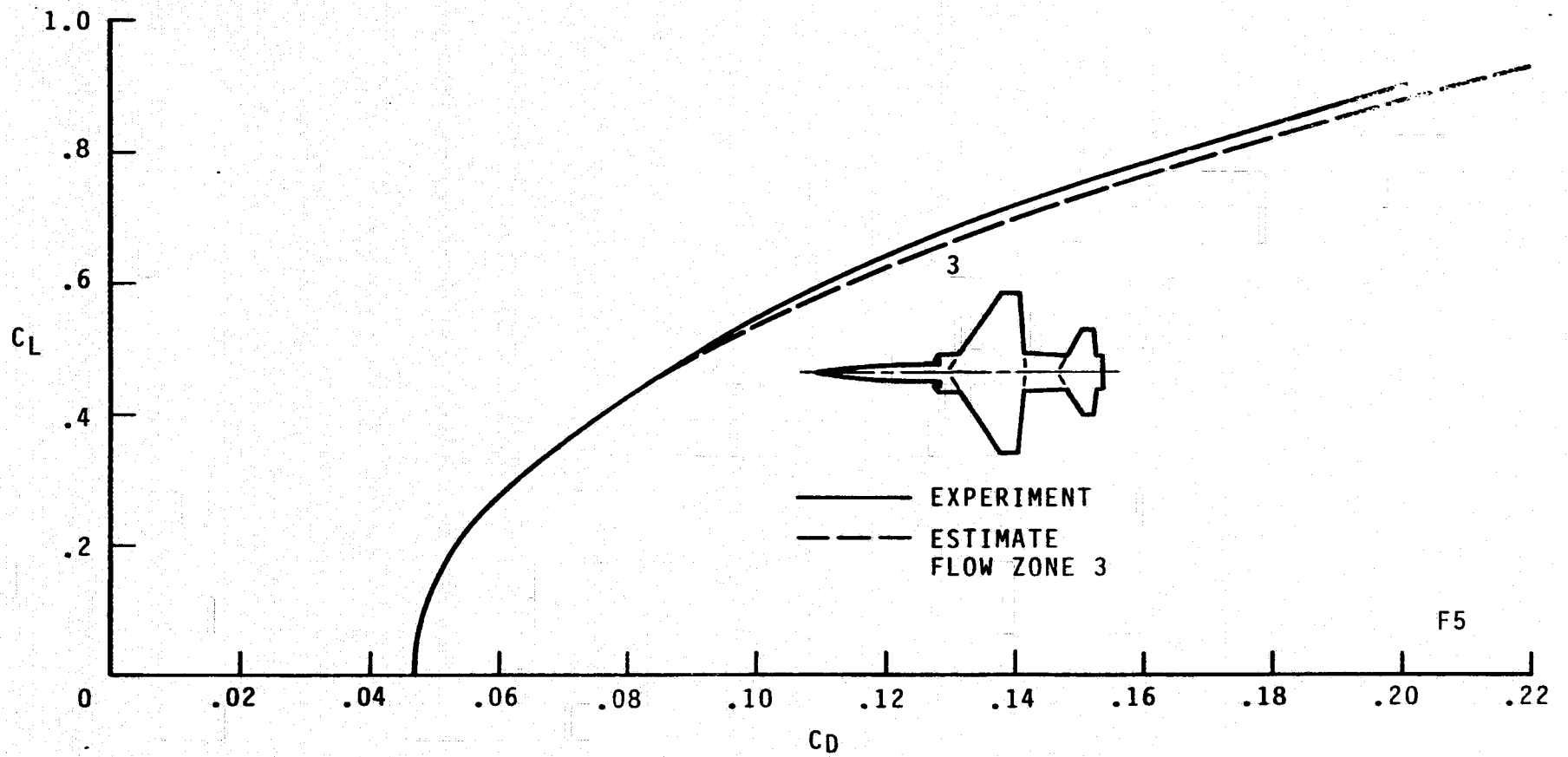
(c)  $C_L$  VERSUS  $C_D$ ;  $M = 0.6$ .

FIGURE 3.- CONTINUED.



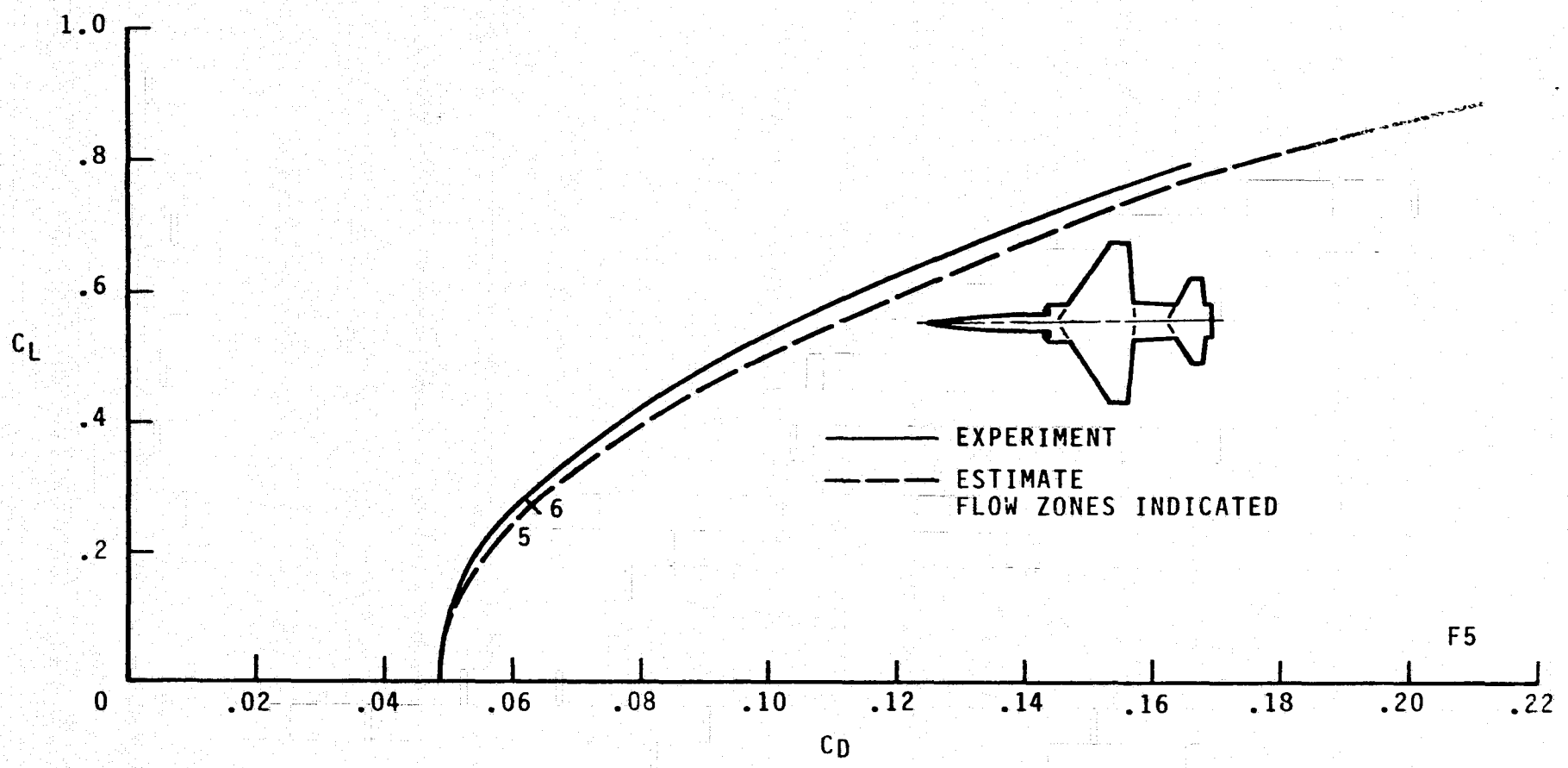
(d)  $C_L$  VERSUS  $C_D$ ;  $M = 0.9$ .

FIGURE 3.- CONTINUED.



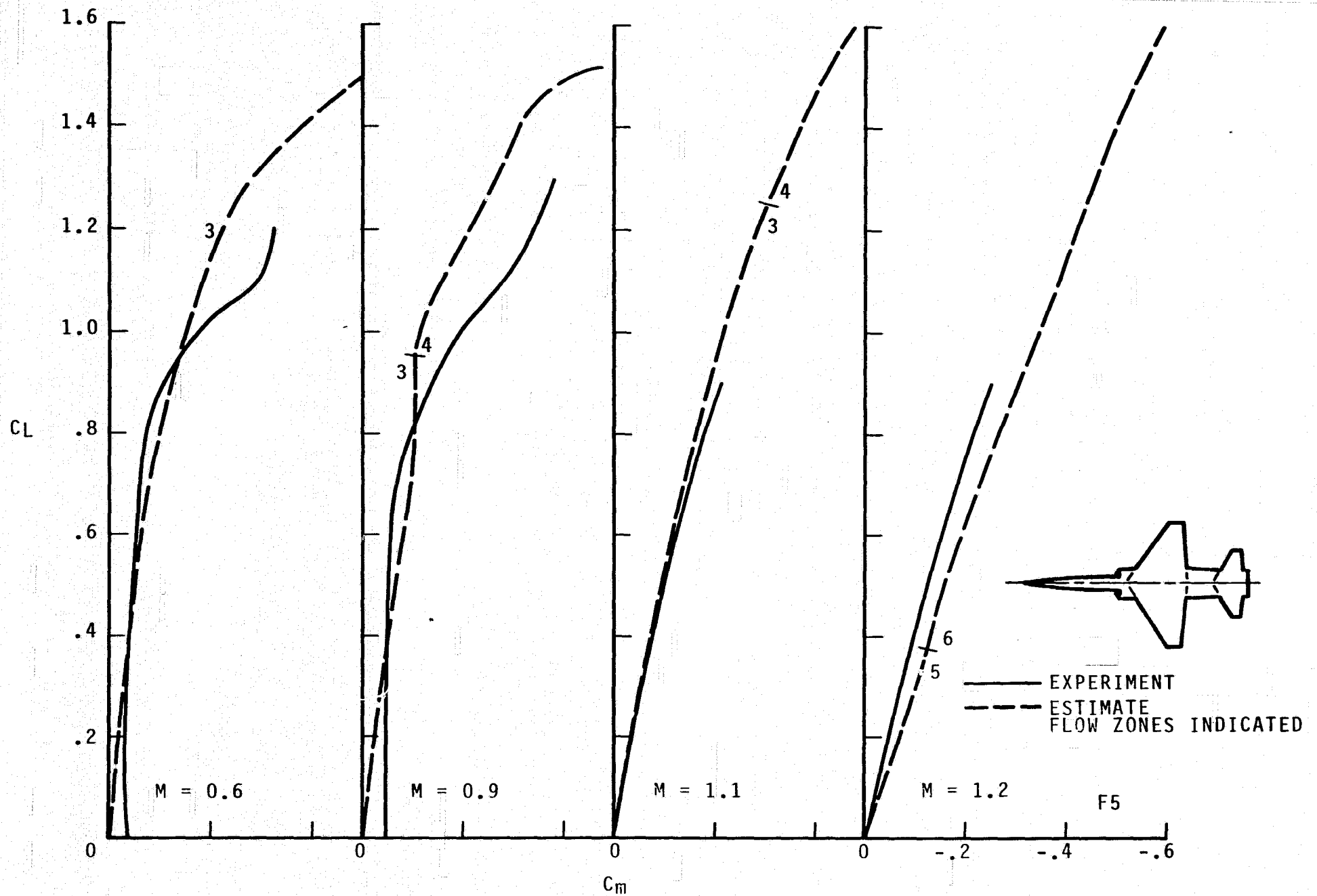
(e)  $C_L$  VERSUS  $C_D$ ;  $M = 1.1$ .

FIGURE 3.- CONTINUED.



(f)  $C_L$  VERSUS  $C_D$ ;  $M = 1.2$ .

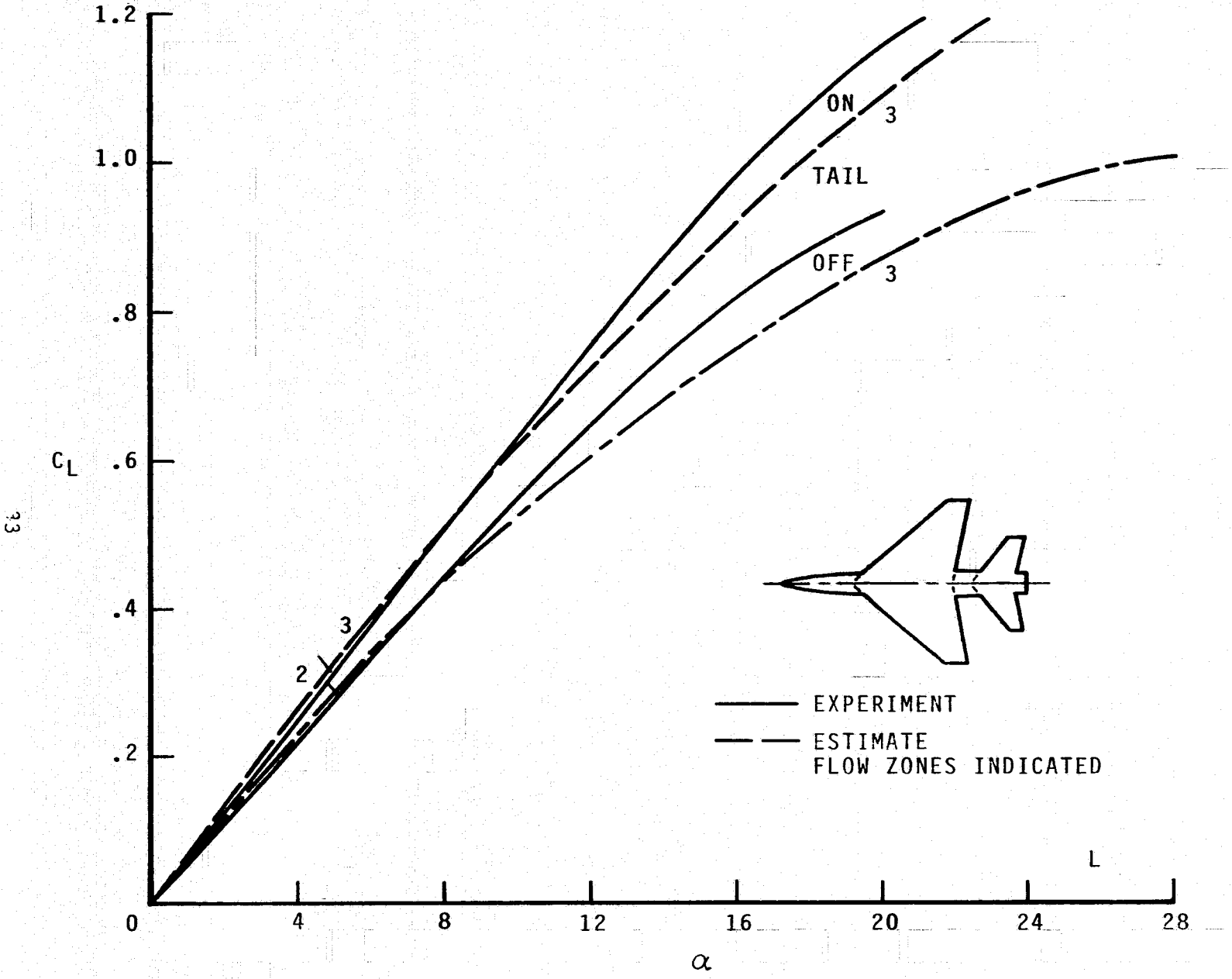
FIGURE 3.- CONTINUED.



(g)  $C_L$  VERSUS  $C_m$ ;  $M = 0.6, 0.9, 1.1, 1.2$ .

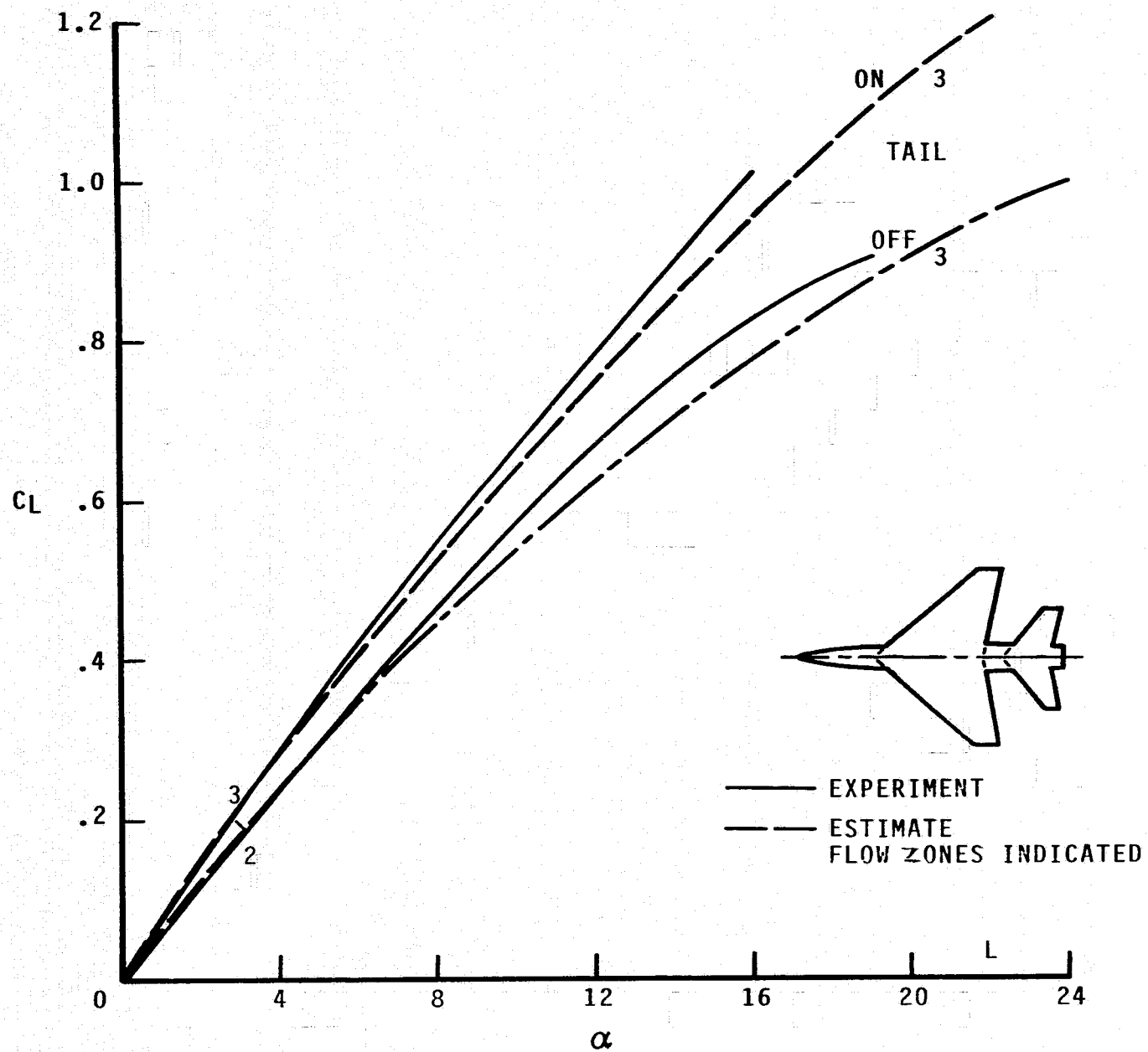
FIGURE 3.- CONCLUDED.





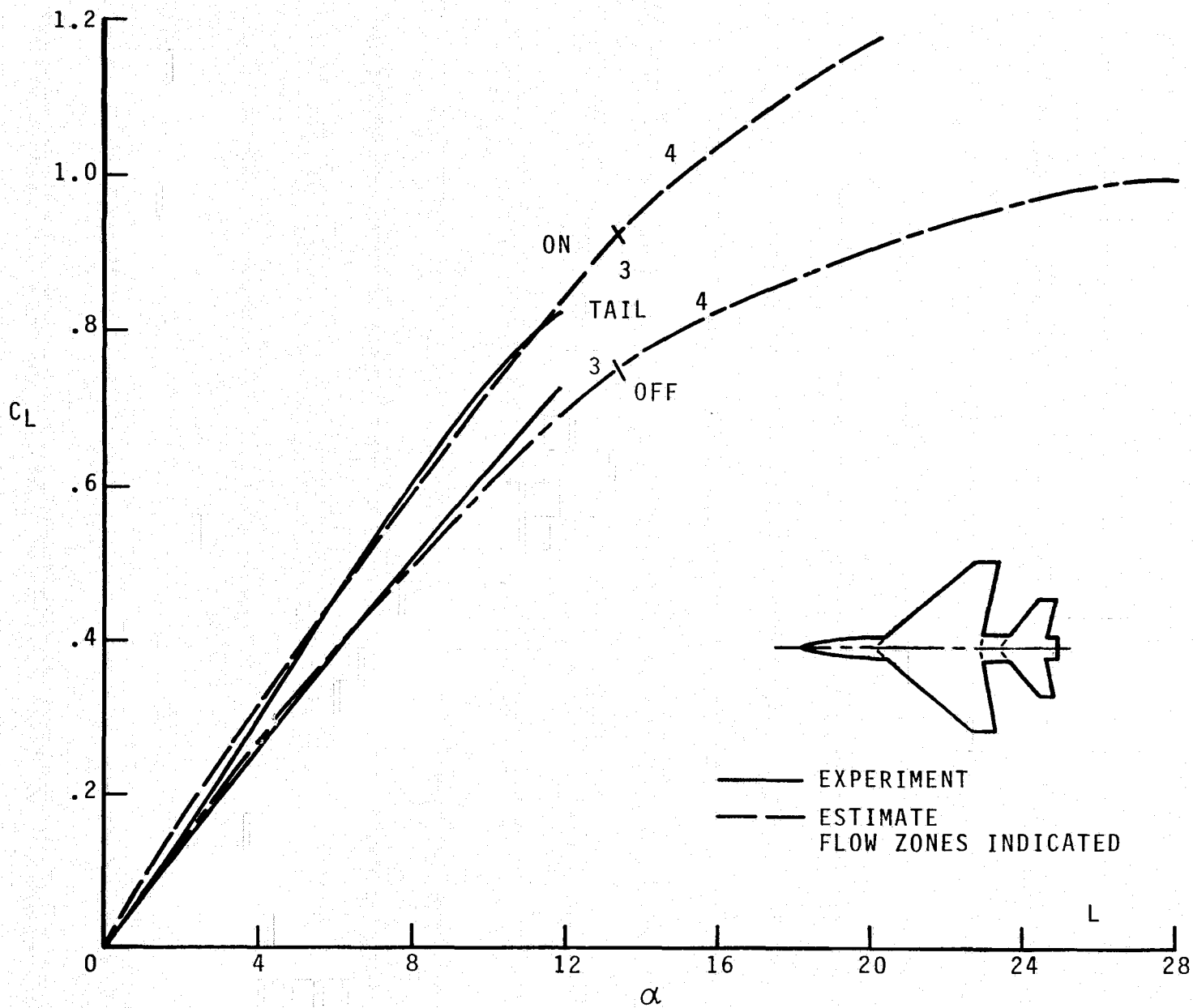
(a)  $C_L$  VERSUS  $\alpha$ ;  $M = 0.5$ .

FIGURE 4.- AERODYNAMICS FOR MODEL L;  $J = 3$ .



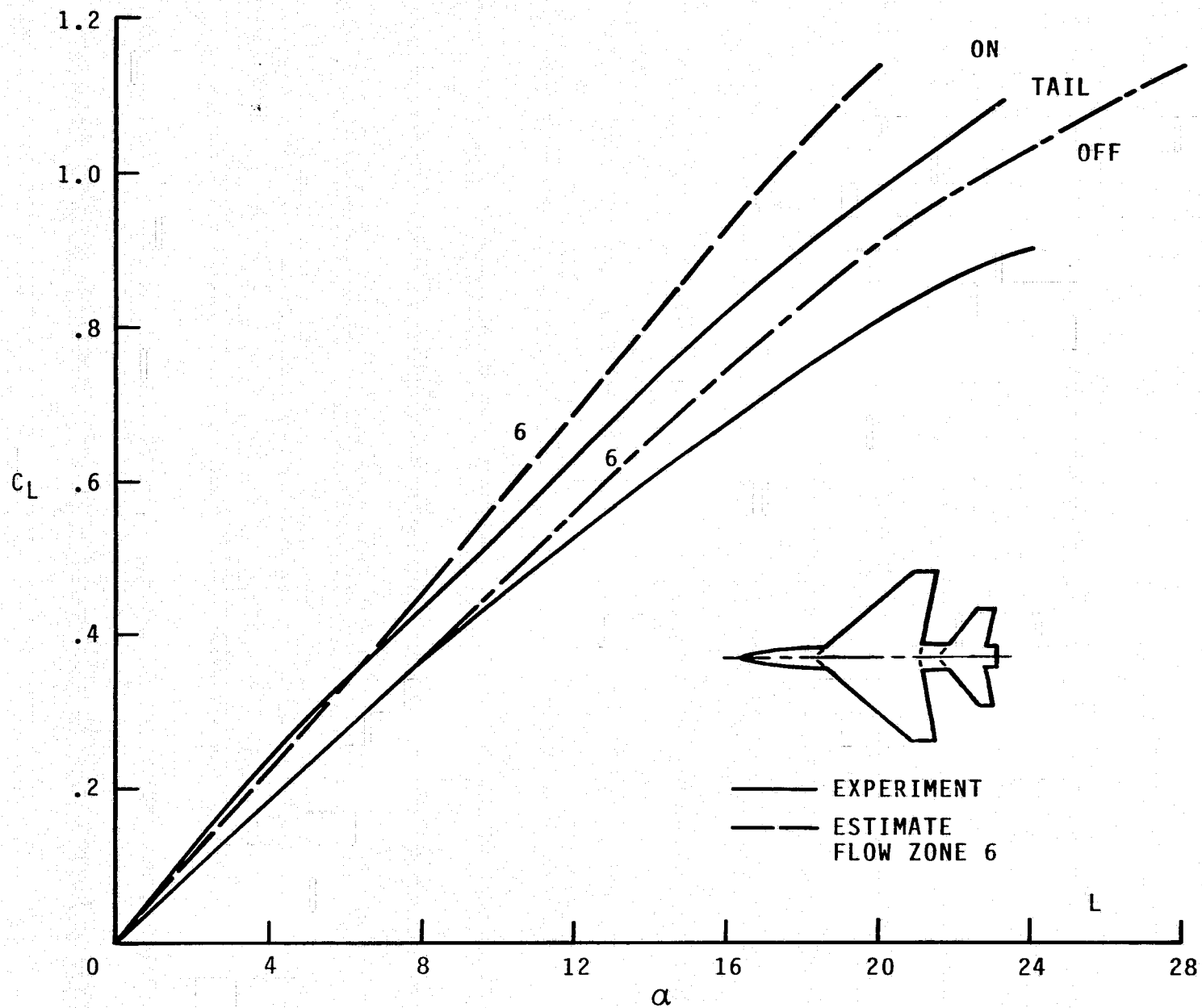
(b)  $C_L$  VERSUS  $\alpha$ ;  $M = 0.8$ .

FIGURE 4.- CONTINUED.



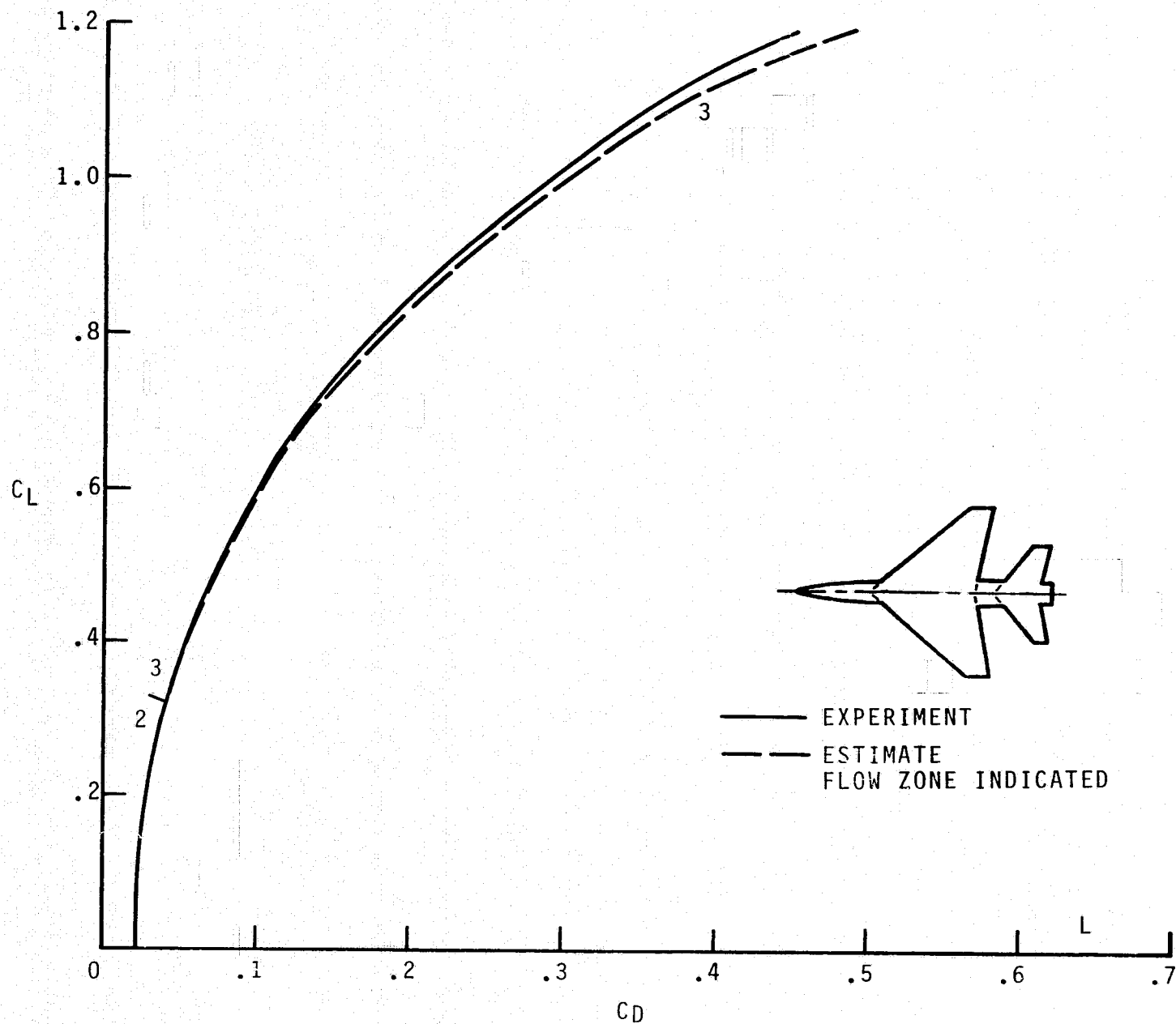
(c)  $C_L$  VERSUS  $\alpha$ ;  $M = 1.2$ .

FIGURE 4.- CONTINUED



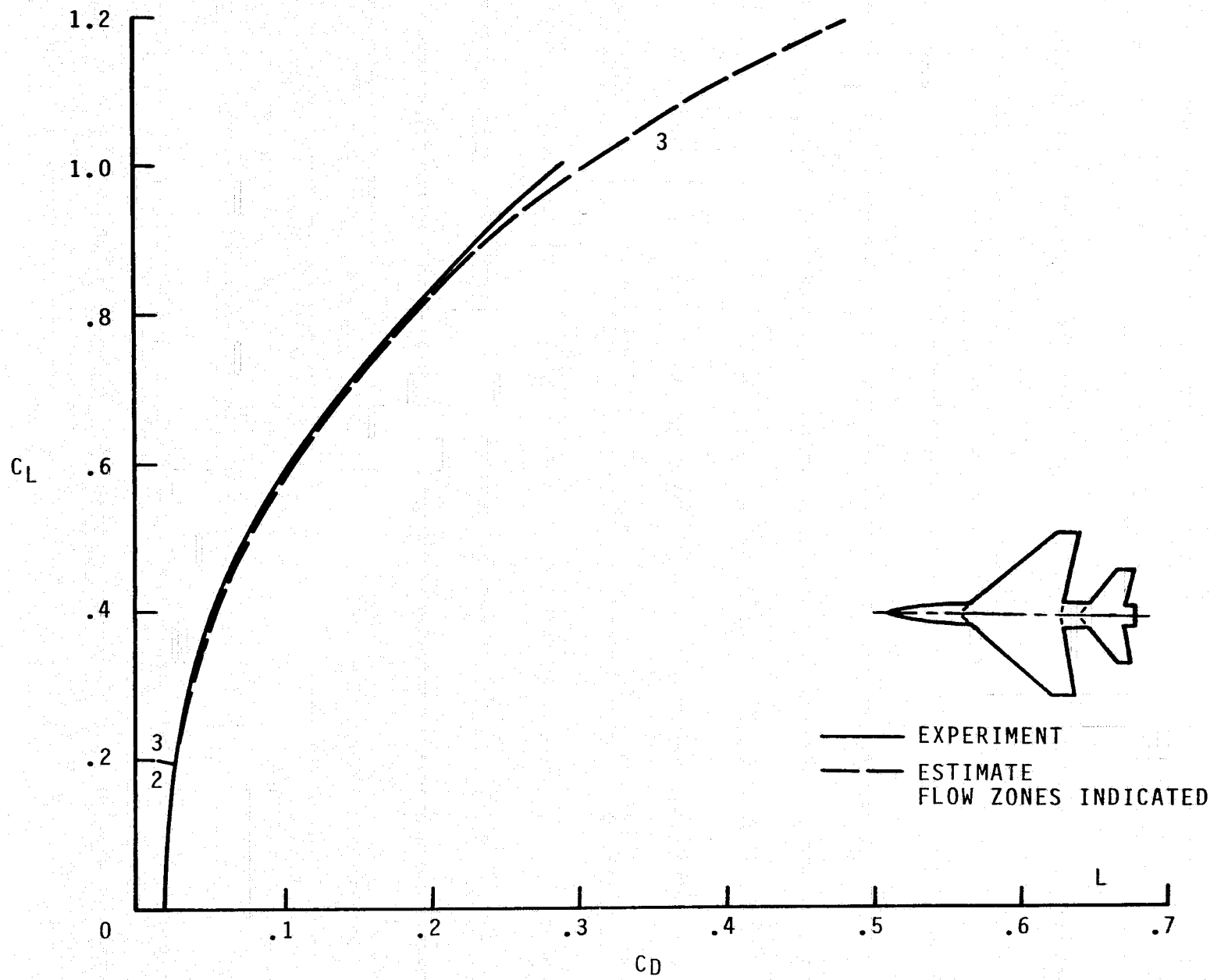
(d)  $C_L$  VERSUS  $\alpha$ ;  $M = 1.8$ .

FIGURE 4.- CONTINUED.



(e)  $C_L$  VERSUS  $C_D$ ;  $M = 0.5$ .

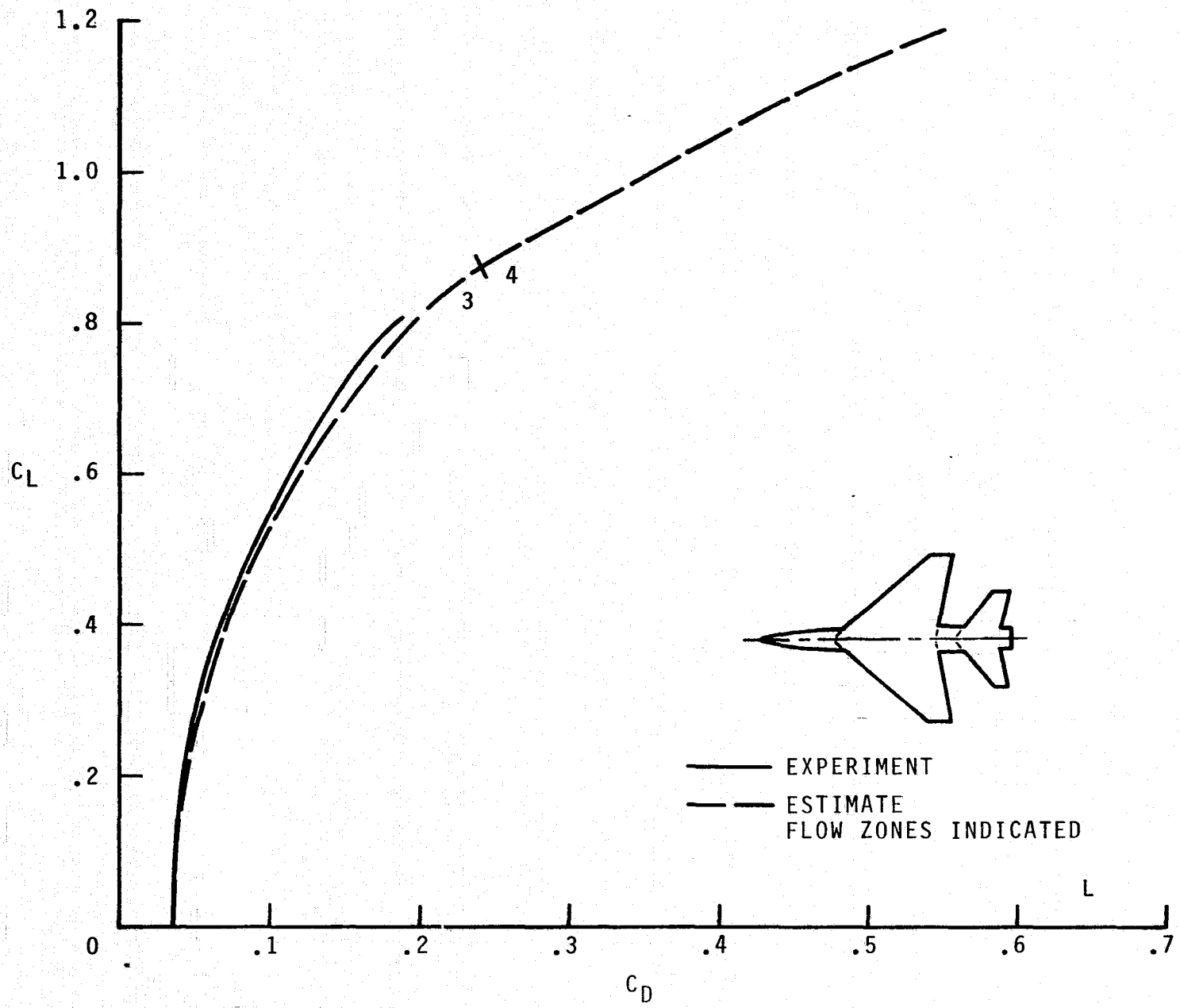
FIGURE 4.- CONTINUED.



(f)  $C_L$  VERSUS  $C_D$ ;  $M = 0.8$ .

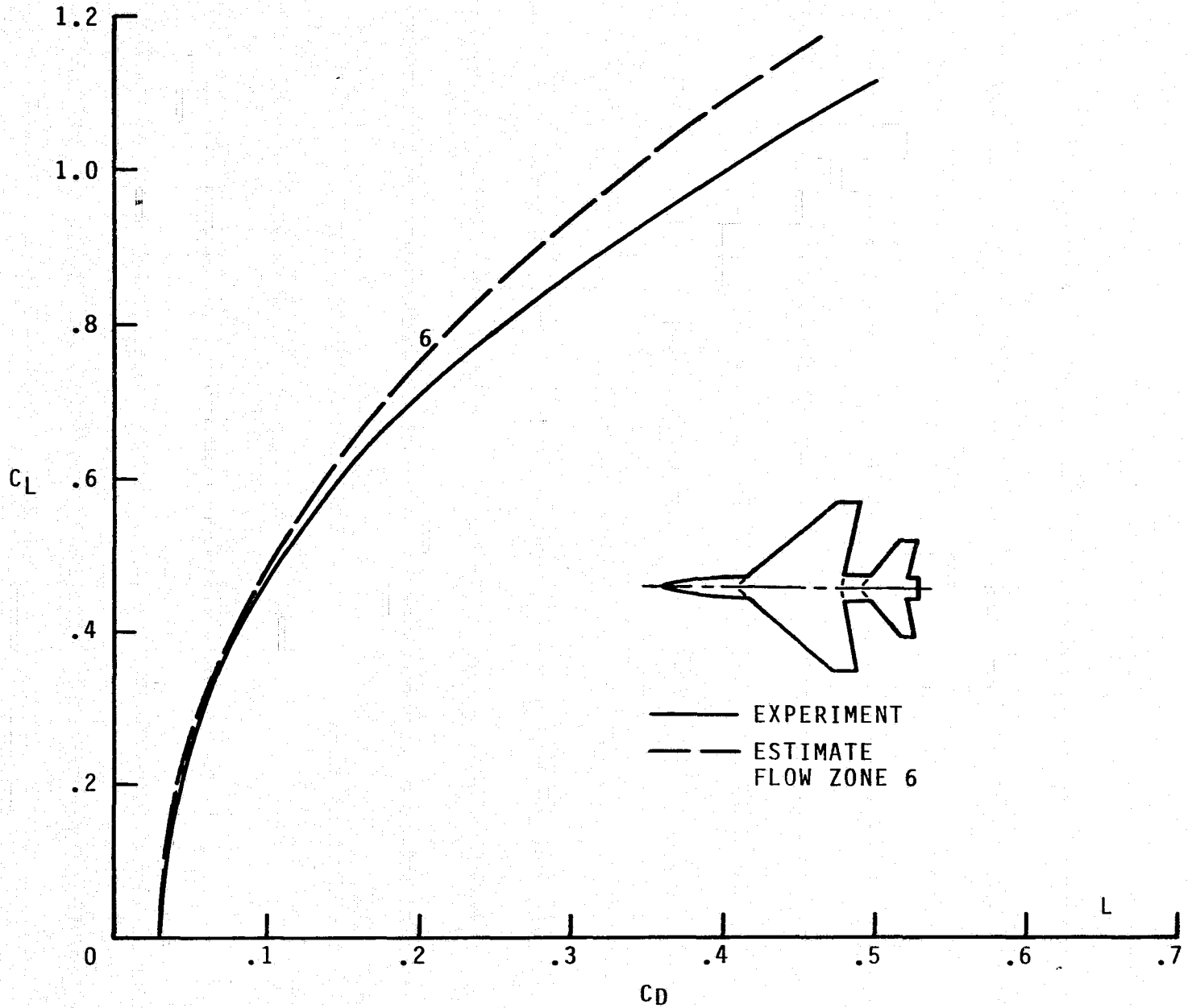
FIGURE 4.- CONTINUED.

39



(g)  $C_L$  VERSUS  $C_D$ ;  $M = 1.2$ .

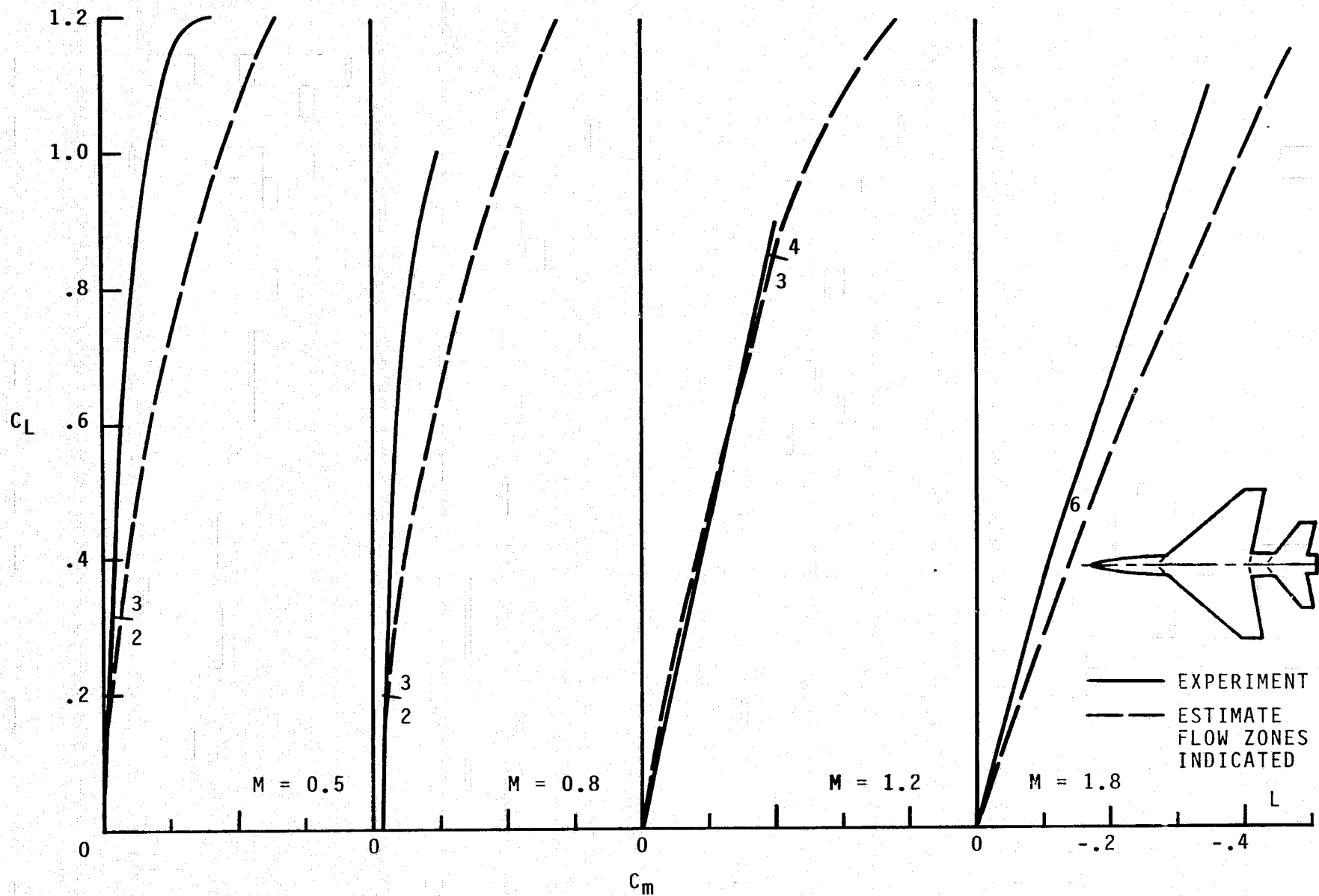
FIGURE 4.- CONTINUED.



(h)  $C_L$  VERSUS  $C_D$ ;  $M = 1.8$ .

FIGURE 4.- CONTINUED.



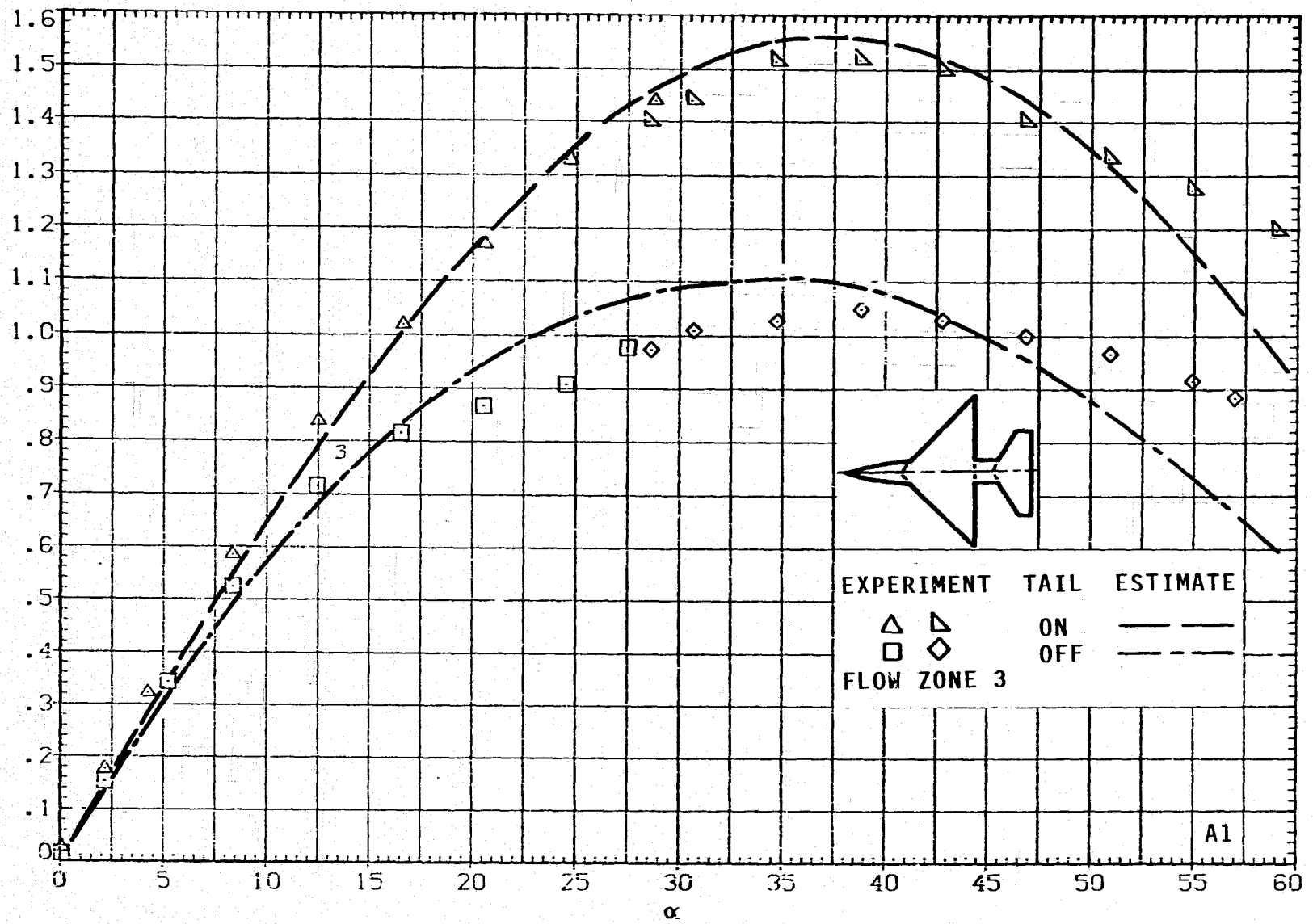


(i)  $C_L$  VERSUS  $C_m$  ;  $M = 0.5, 0.8, 1.2, 1.8$ .

FIGURE 4.- CONCLUDED.

42

$C_L$



(a)  $C_L$  VERSUS  $\alpha$ ;  $M = 0.6$ ,  $J = 1$ .

FIGURE 5.- AERODYNAMICS FOR MODEL A1;  $ARW = 4$ ,  $TRW = 0$ .

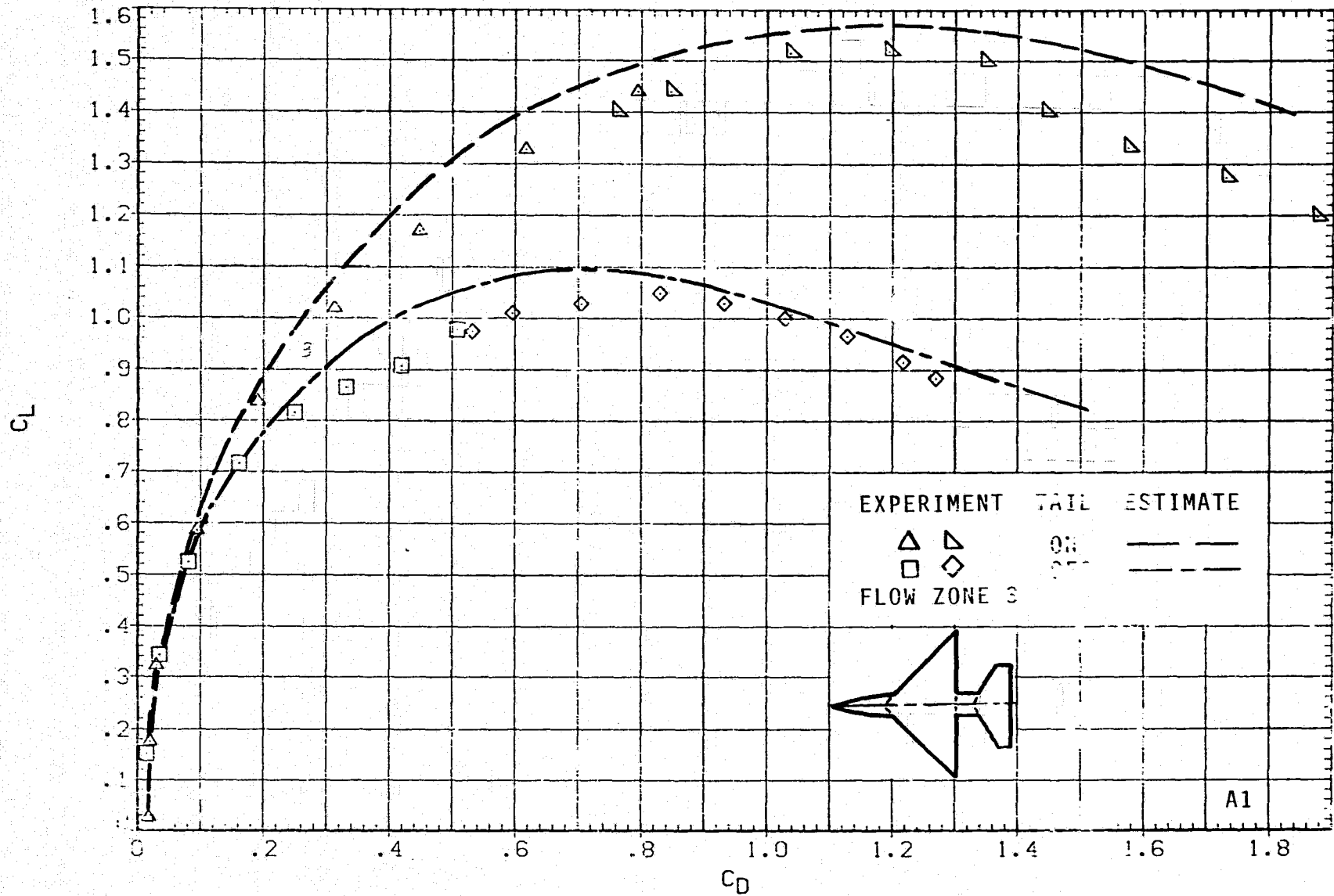
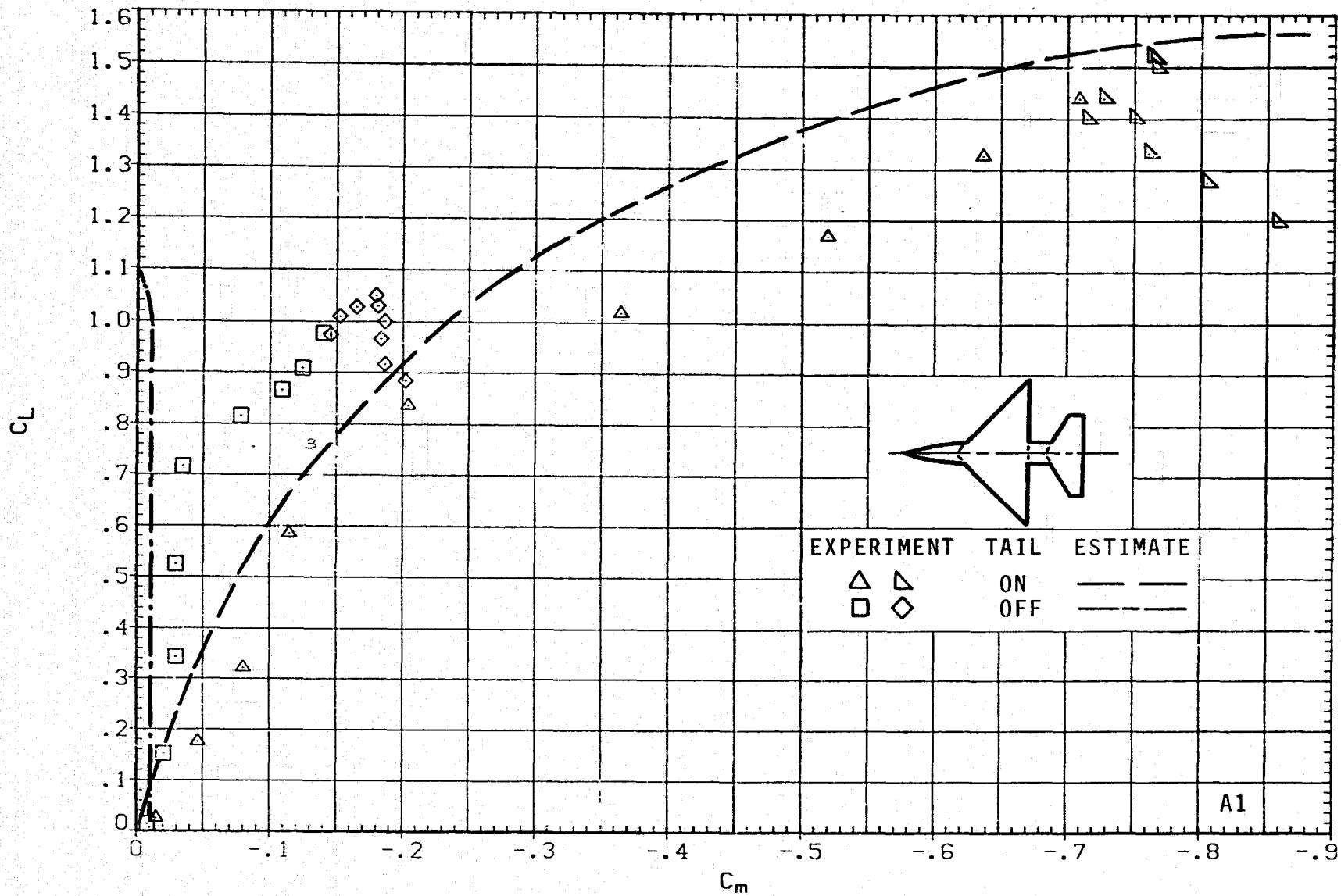
(b)  $C_L$  VERSUS  $C_D$ ;  $M = 0.6$ ,  $J = 1$ .

FIGURE 5.- CONTINUED.



(c)  $C_L$  VERSUS  $C_m$ ;  $M = 0.6$ ,  $J = 1$ .

FIGURE 5.- CONTINUED.

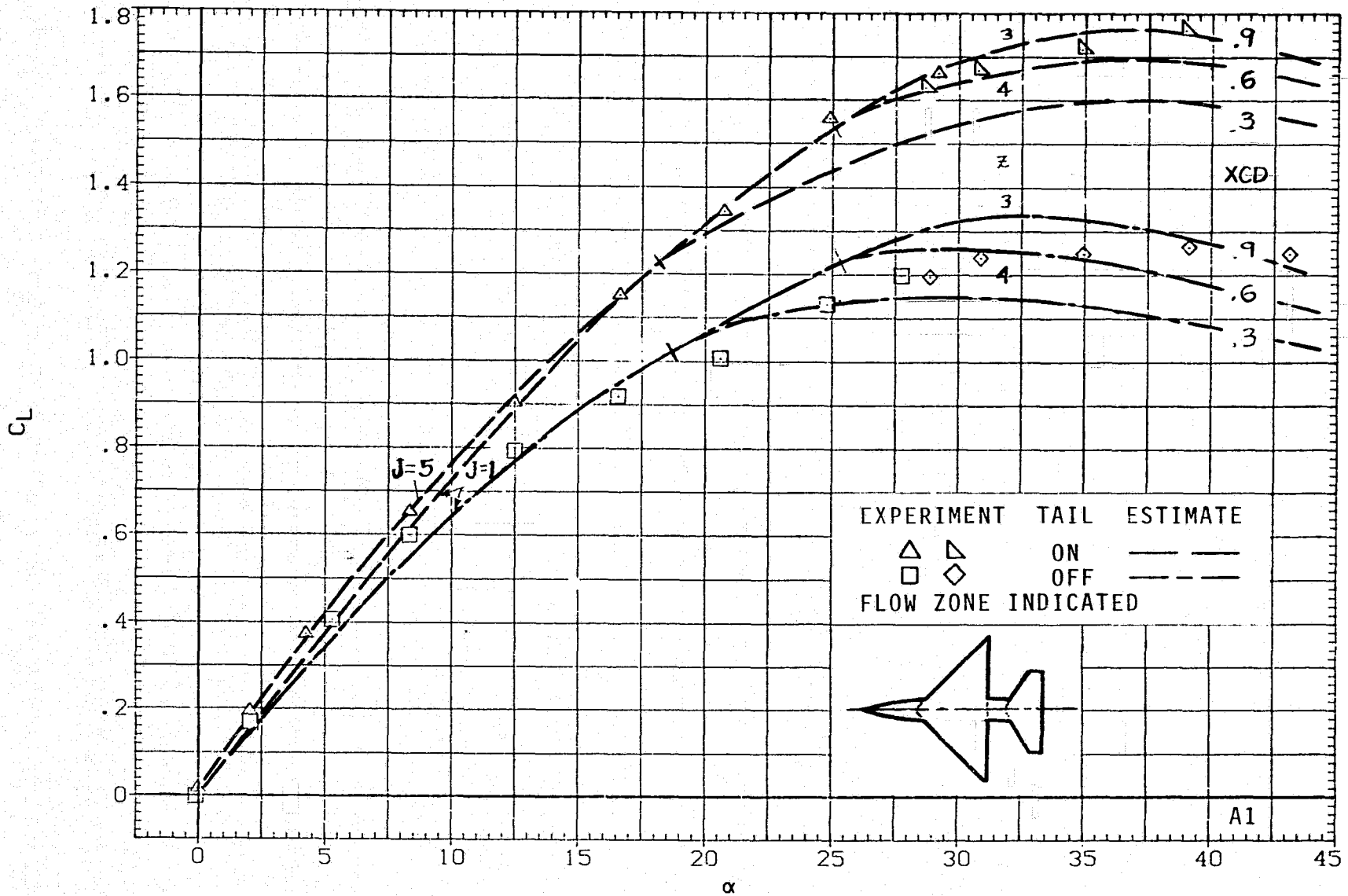
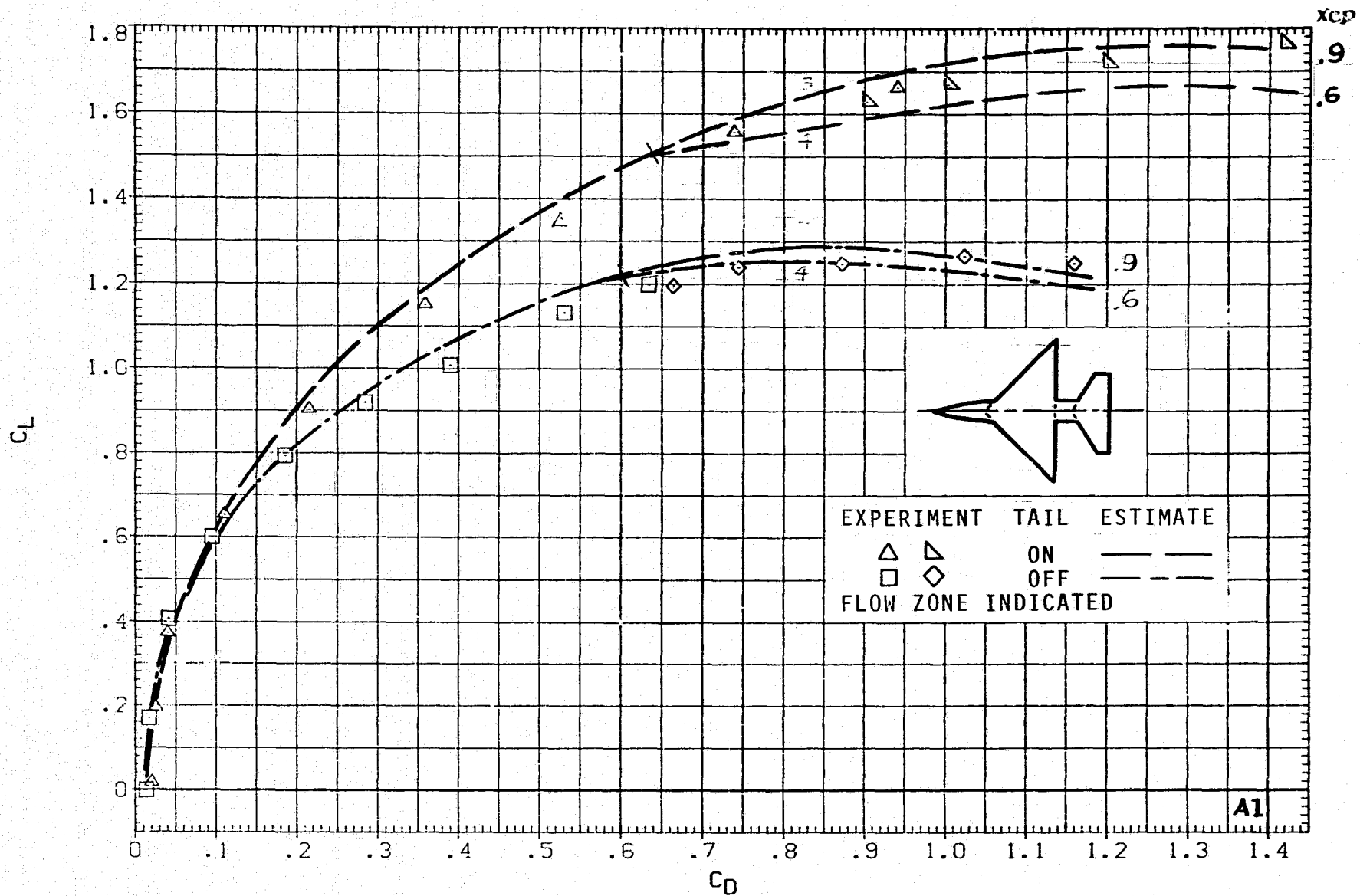
(d)  $C_L$  VERSUS  $\alpha$ ;  $M = 0.9$ ,  $J = 1$ .

FIGURE 5.- CONTINUED.



(e)  $C_L$  VERSUS  $C_D$ ;  $M = 0.9$ ,  $J = 1$ .

FIGURE 5.- CONTINUED.

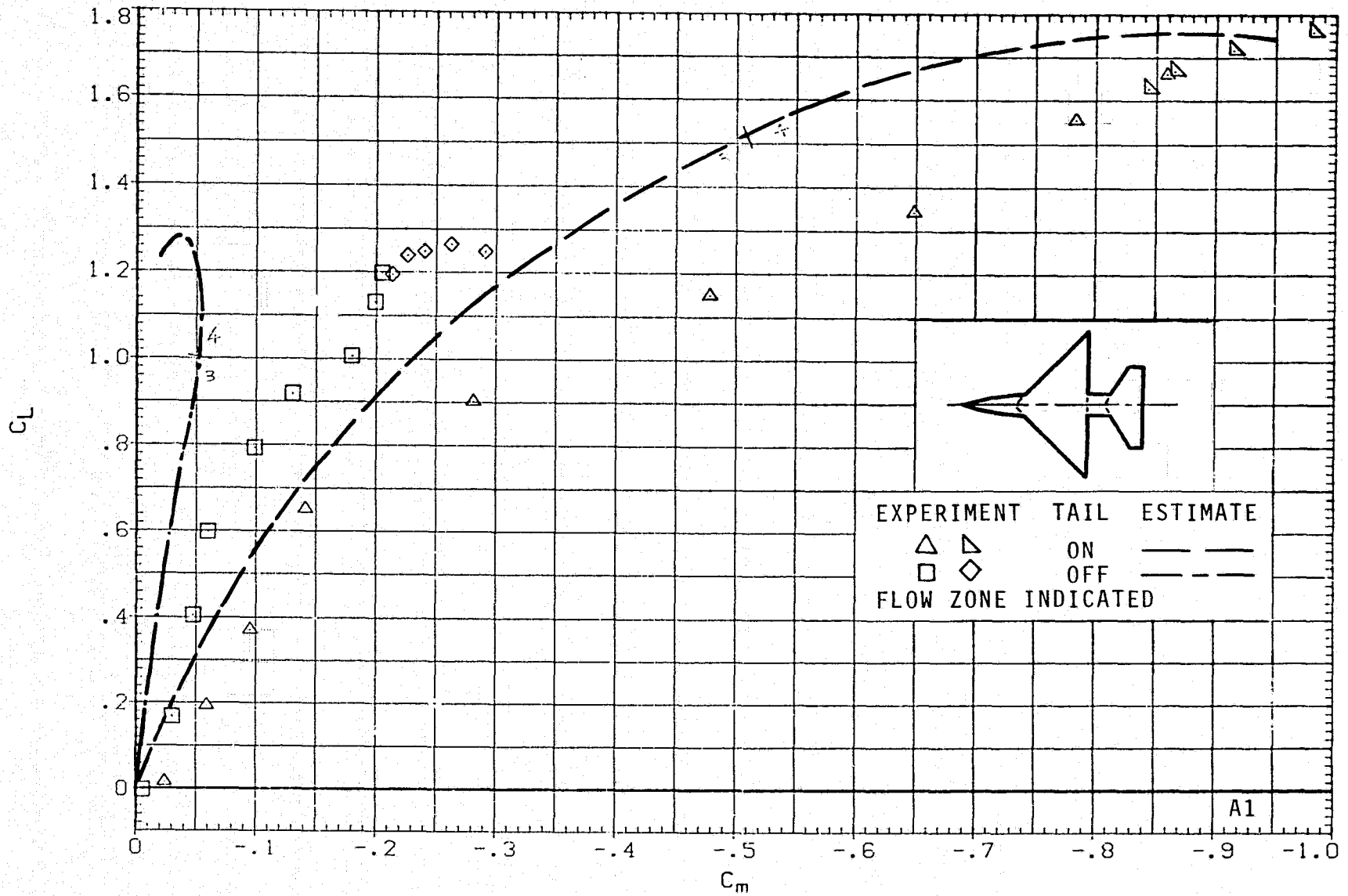
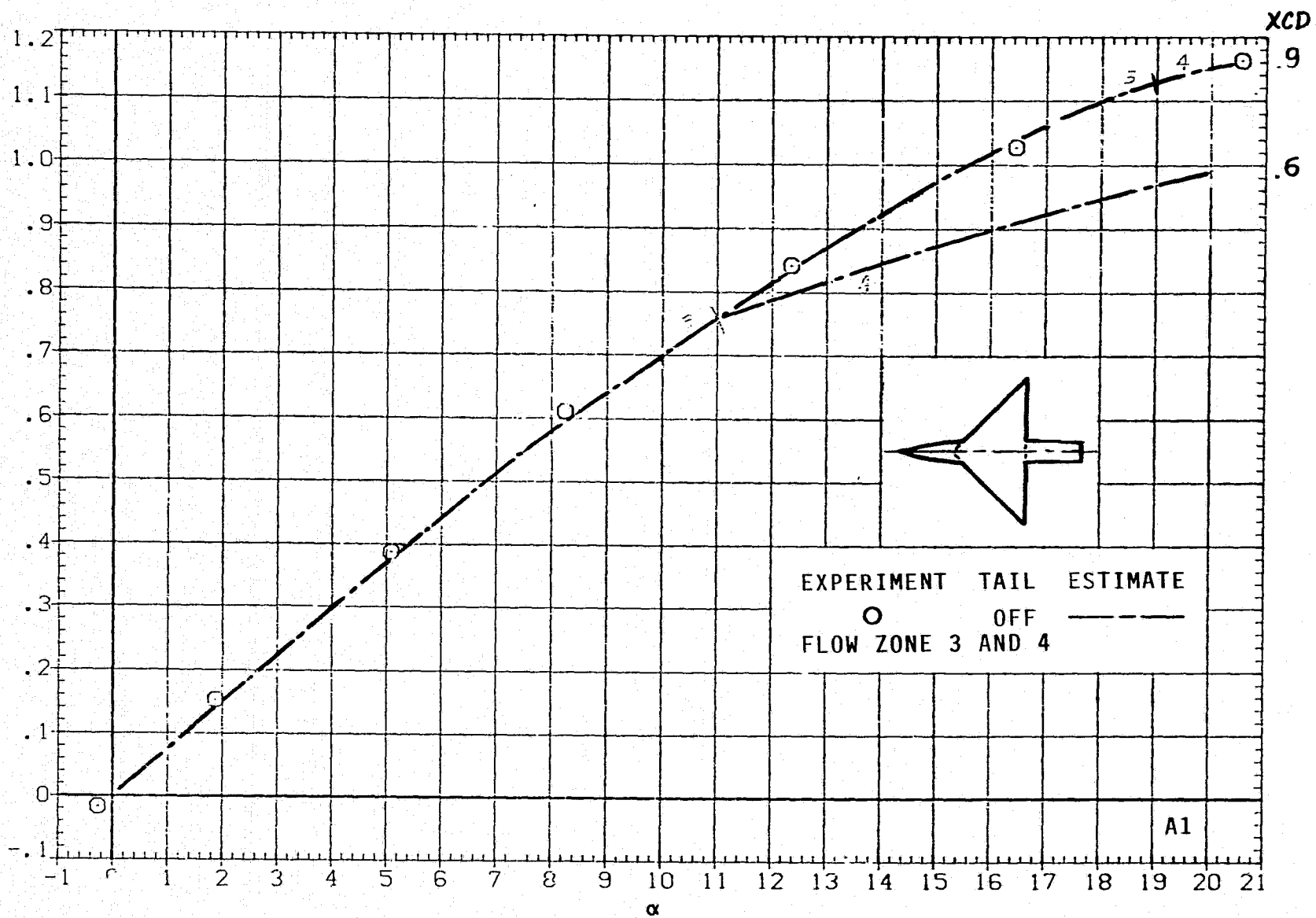
(f)  $C_L$  VERSUS  $C_m$ ;  $M = 0.9$ ,  $J = 1$ .

FIGURE 5.- CONTINUED.

CL

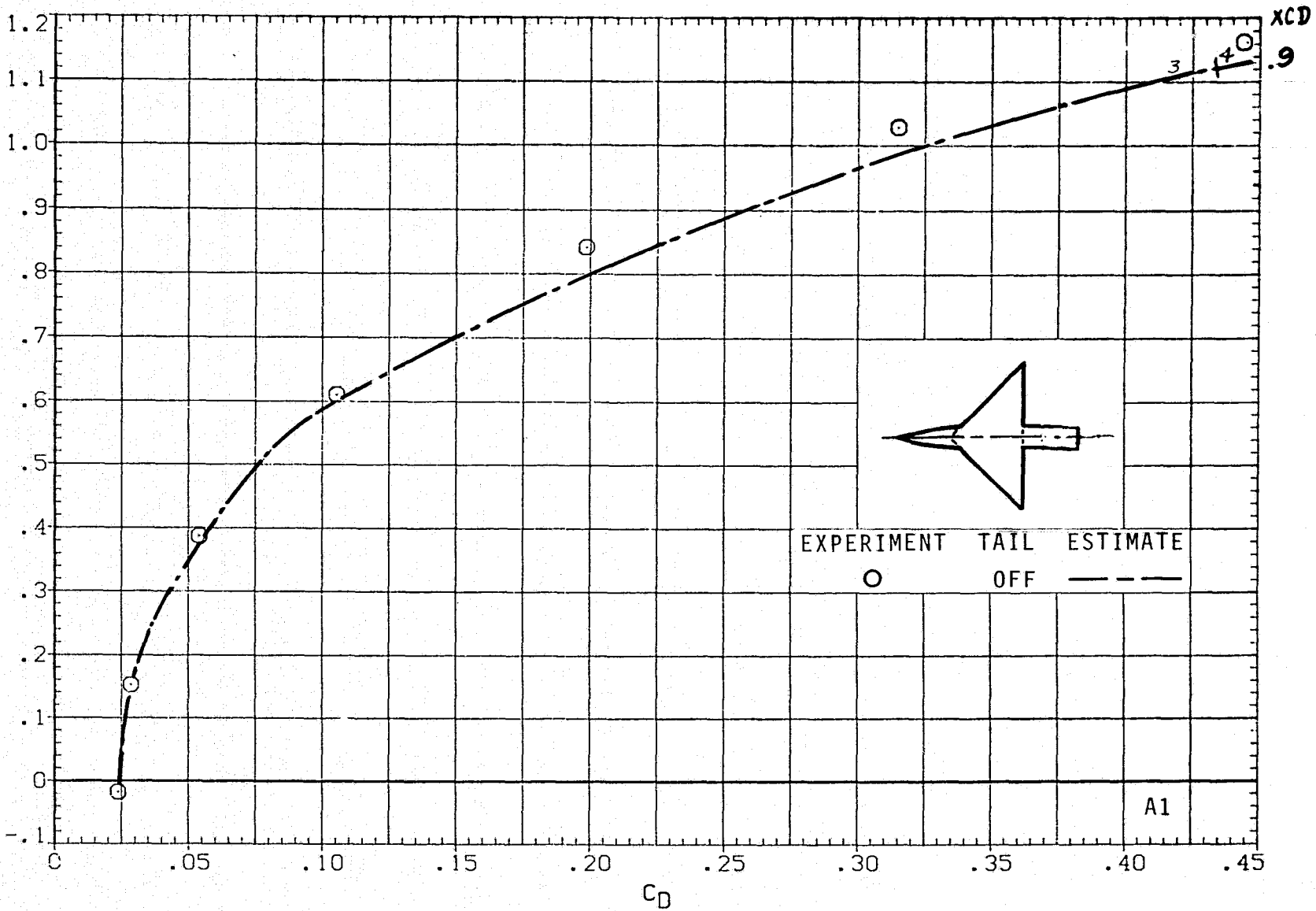


(g)  $C_L$  VERSUS  $\alpha$ ;  $M = 1.2$ ,  $J = 1$ .

FIGURE 5.- CONTINUED.

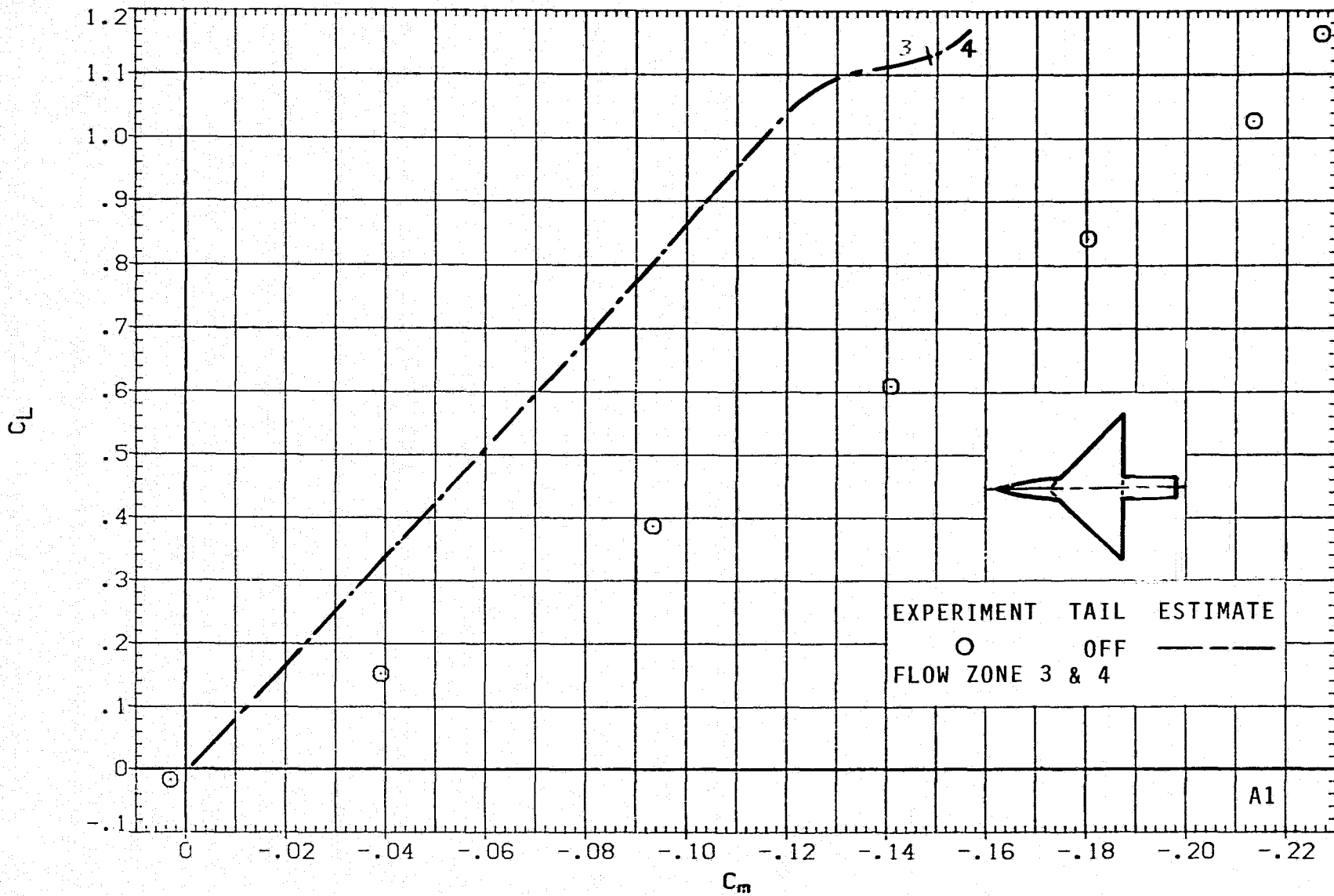
A1





(h)  $C_L$  VERSUS  $C_D$ ;  $M = 1.2$ ,  $J = 1$ .

FIGURE 5.- CONTINUED.



(i)  $C_L$  VERSUS  $C_m$ ;  $M = 1.2$   $J = 1$ .

FIGURE 5.- CONTINUED.

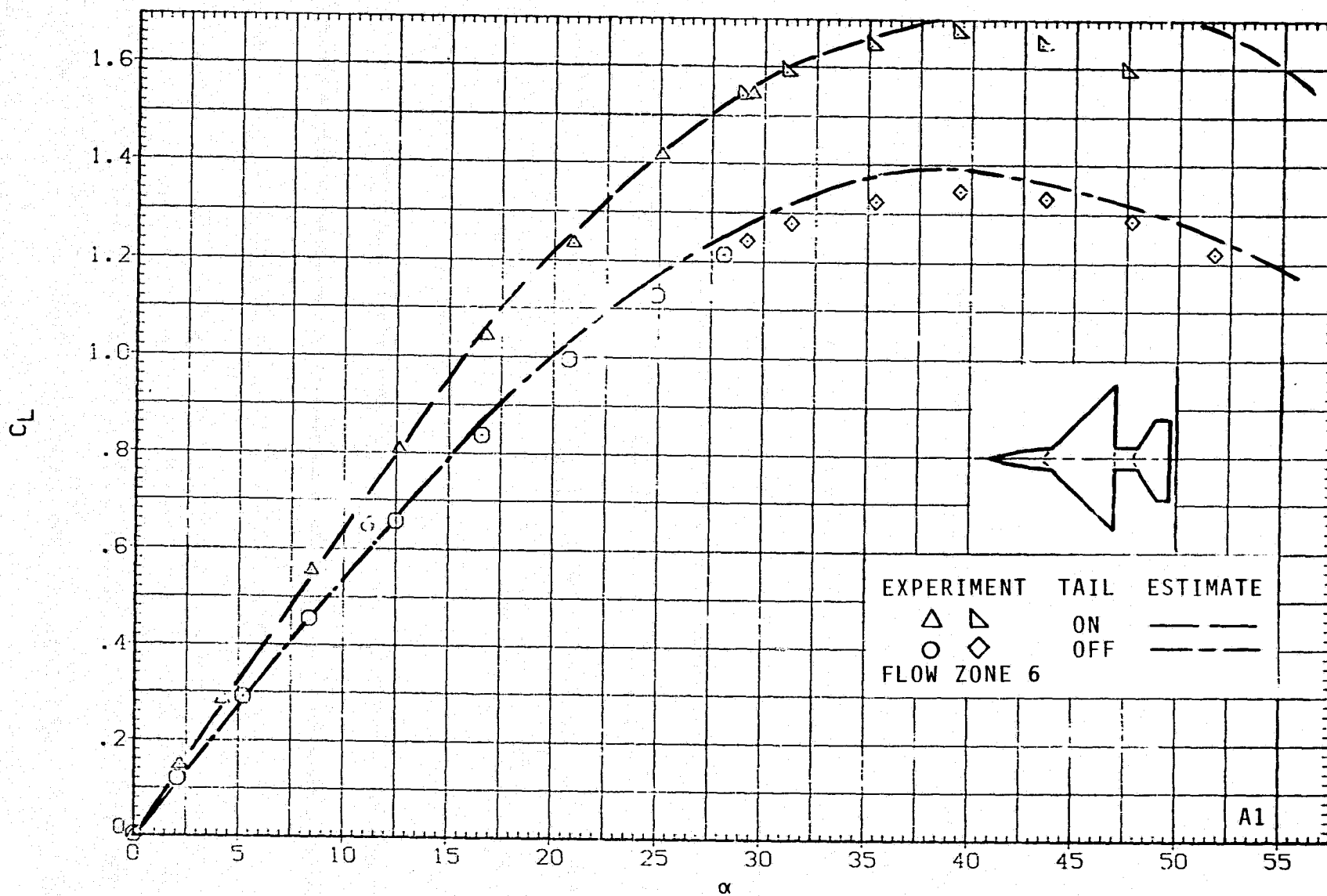
(j)  $C_L$  VERSUS  $\alpha$ ;  $M = 1.5$ ,  $\rho = 5$ .

FIGURE 5.- CONTINUED.

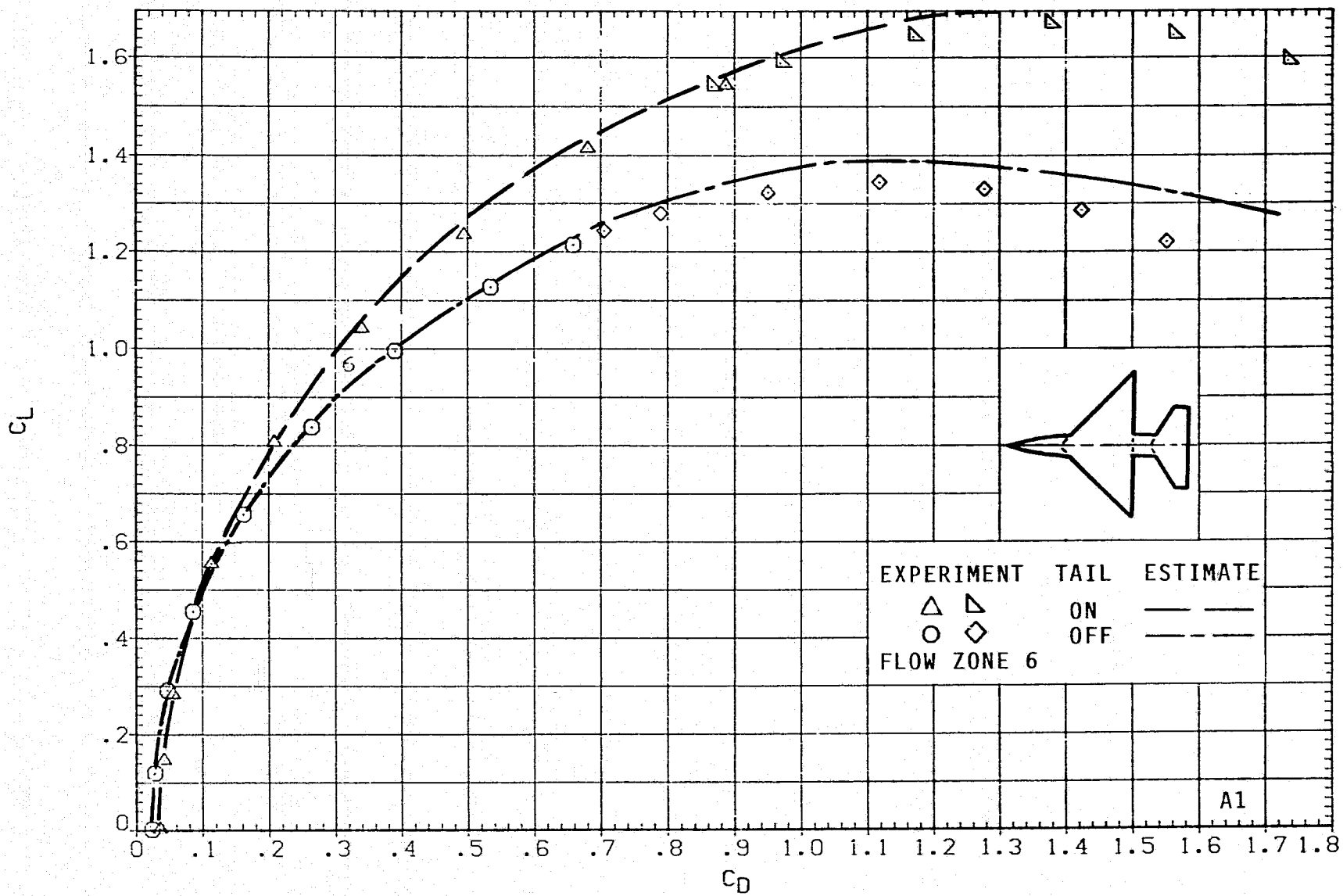
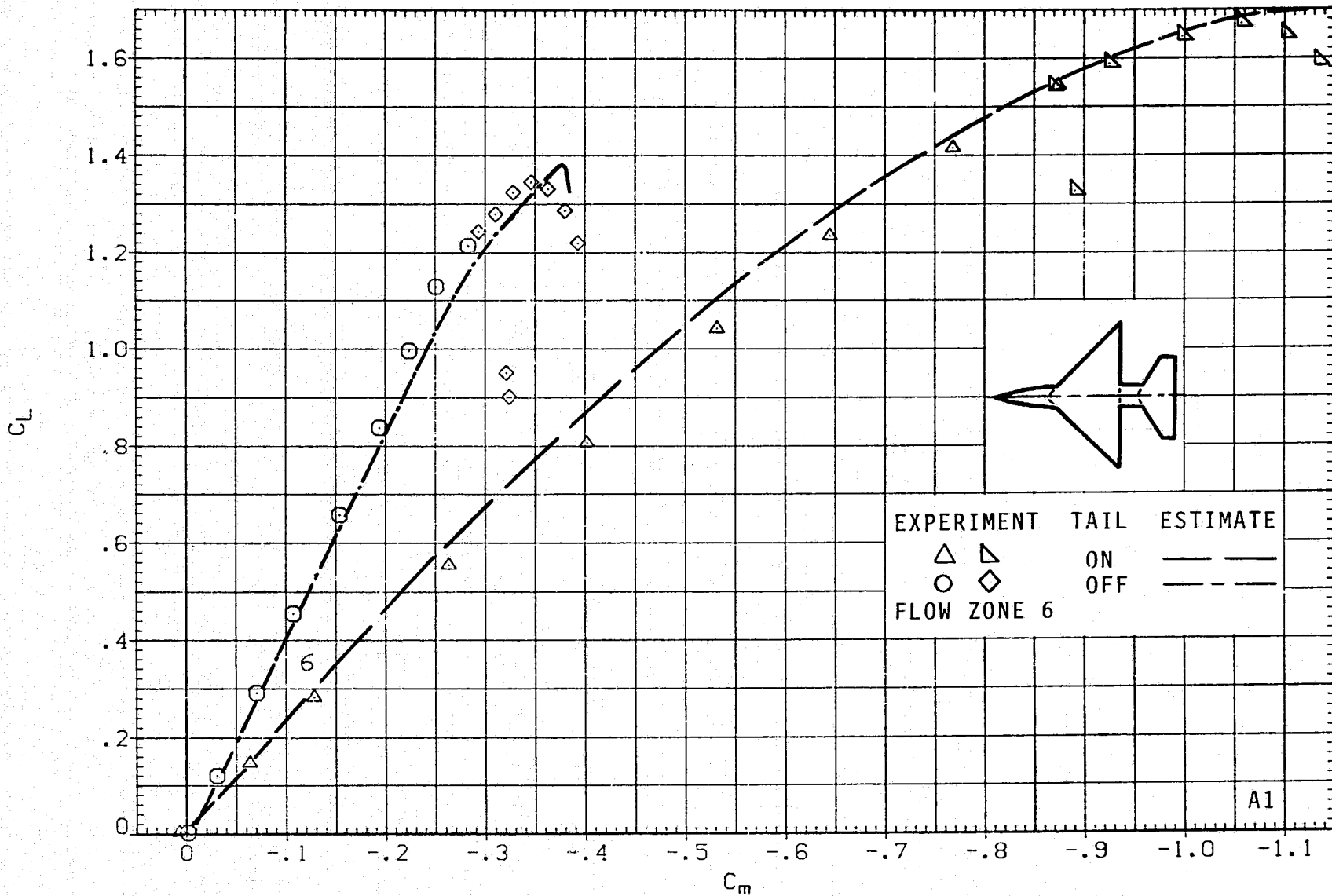
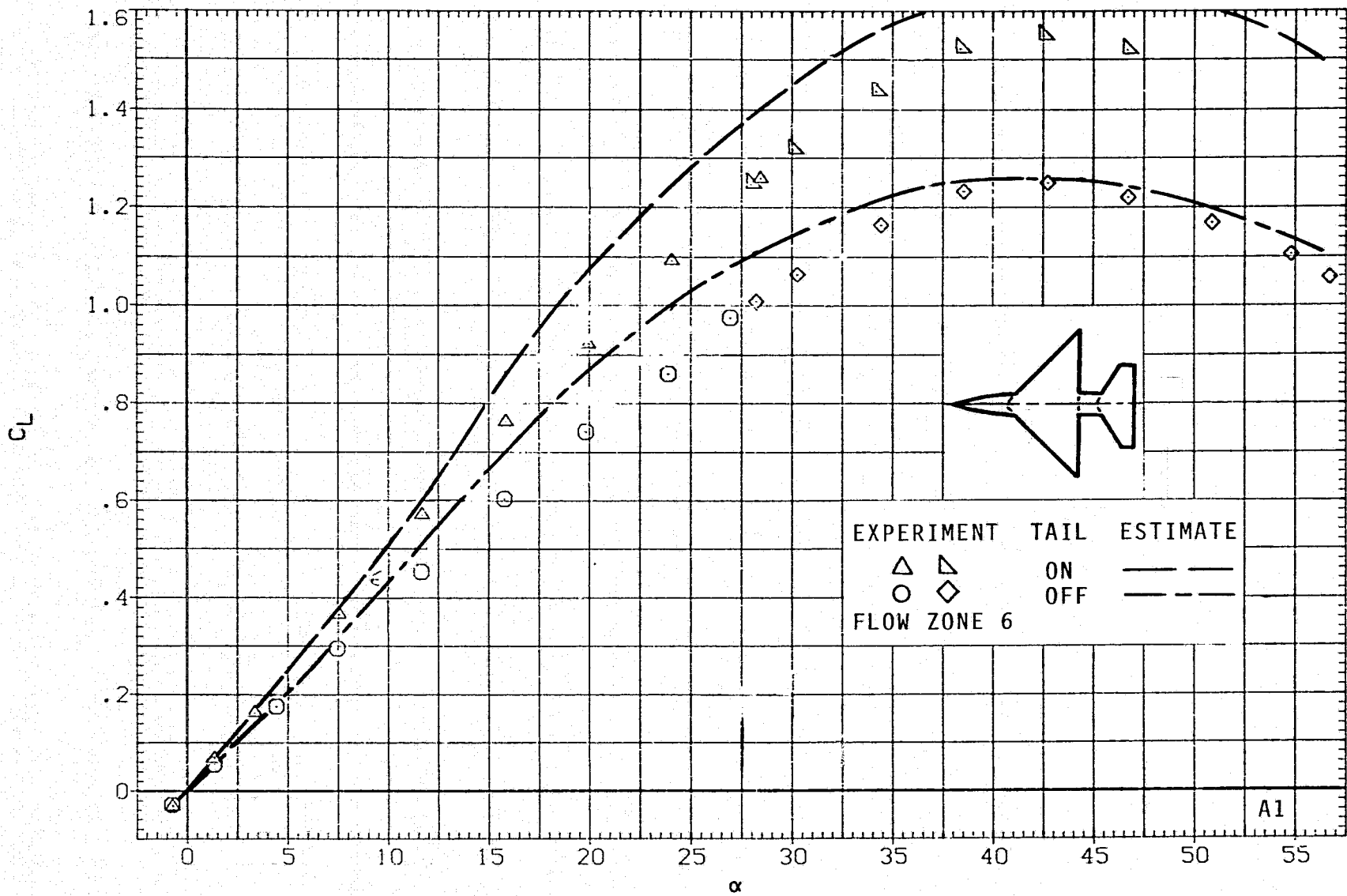
(k)  $C_L$  VERSUS  $C_D$ ;  $M = 1.5$ ,  $J = 5$ .

FIGURE 5.- CONTINUED.



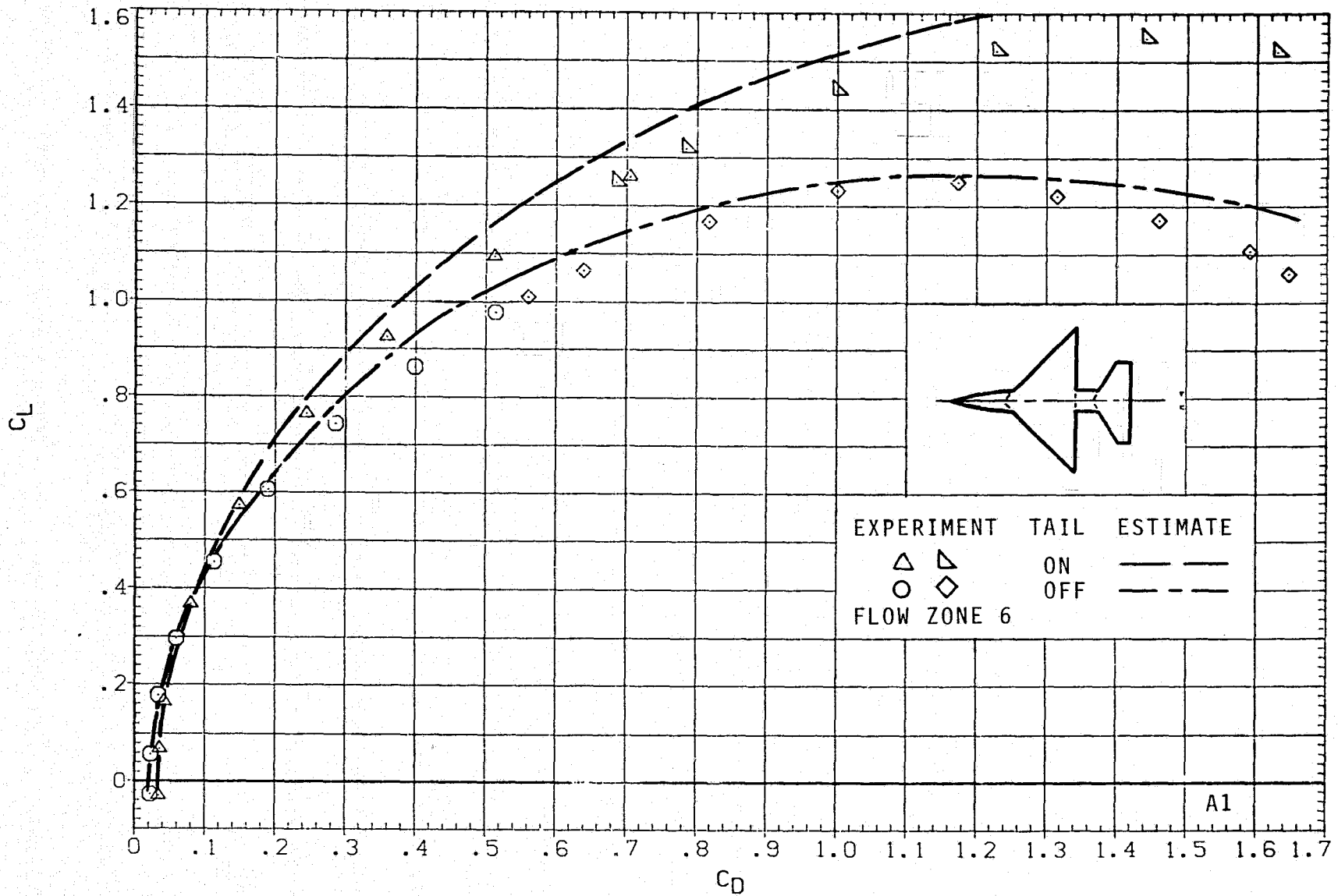
(1)  $C_L$  VERSUS  $C_m$ ;  $M = 1.5$ ,  $J = 5$ .

FIGURE 5.- CONTINUED.



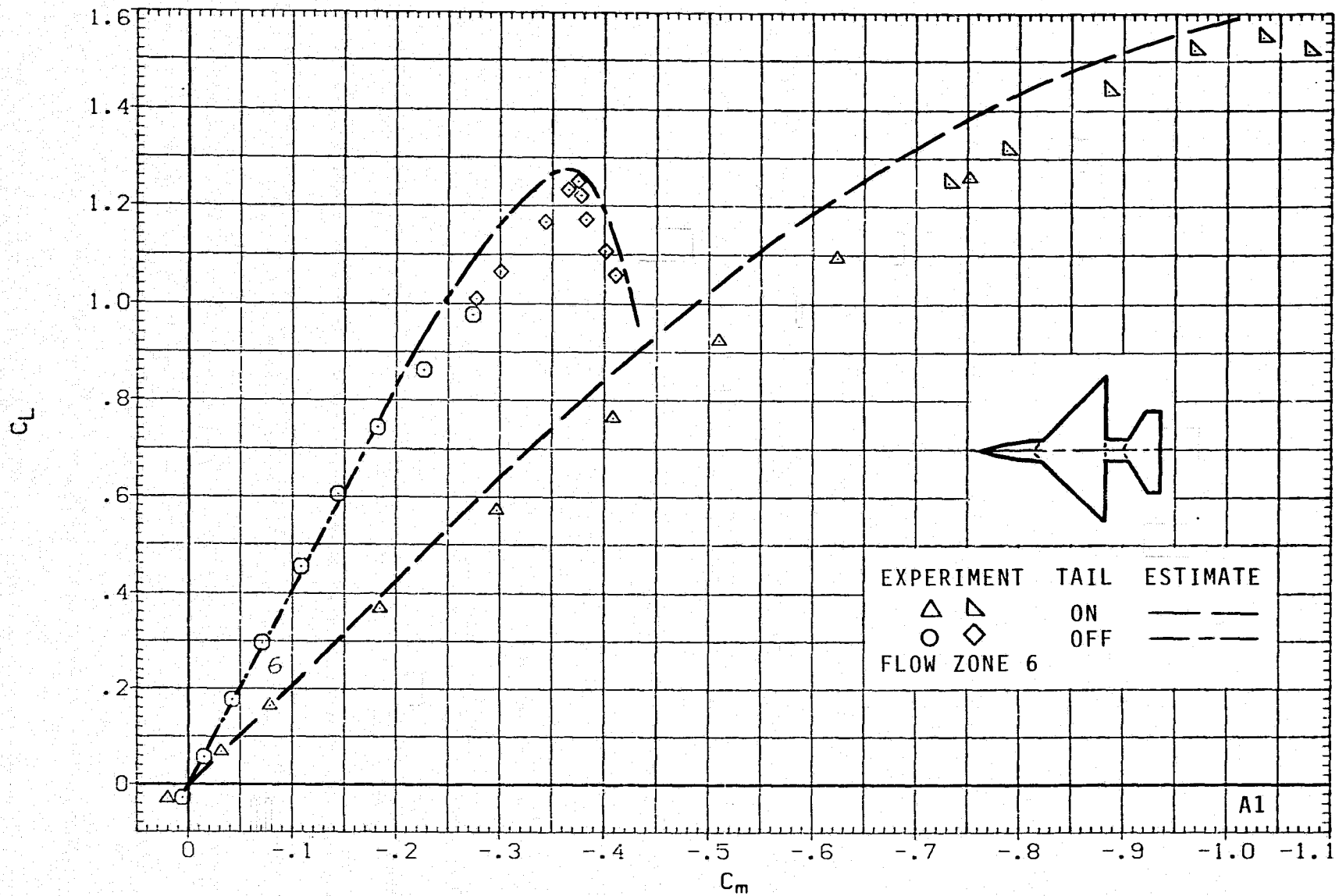
(m)  $C_L$  VERSUS  $\alpha$ ;  $M = 2.0$ ,  $J = 5$ .

FIGURE 5.- CONTINUED.



(n)  $C_L$  VERSUS  $C_D$ ;  $M = 2.0$ ,  $J = 5$ .

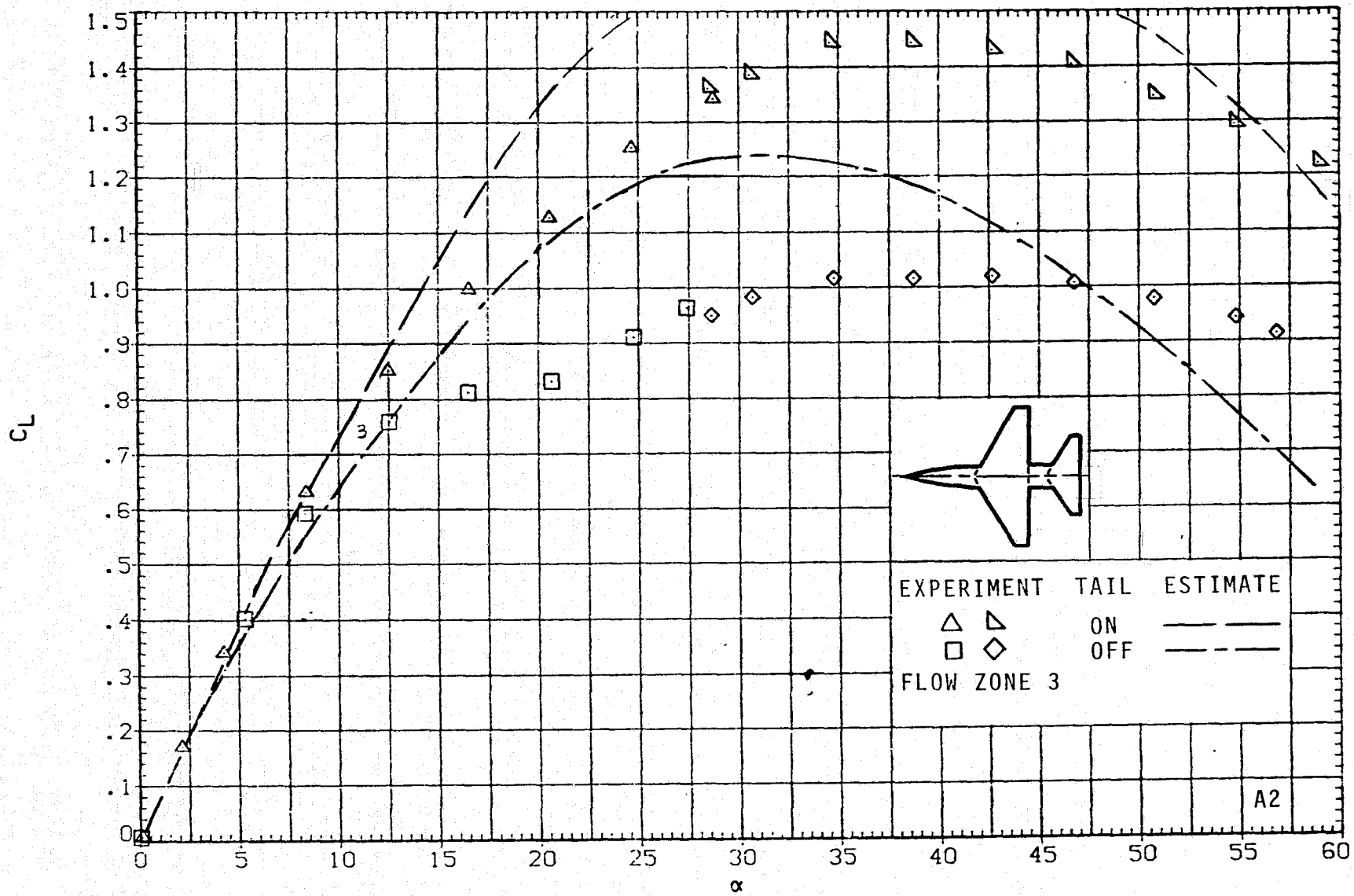
FIGURE 5.- CONTINUED.



(o)  $C_L$  VERSUS  $C_m$ ;  $M = 2.0$ ,  $J = 5$ .

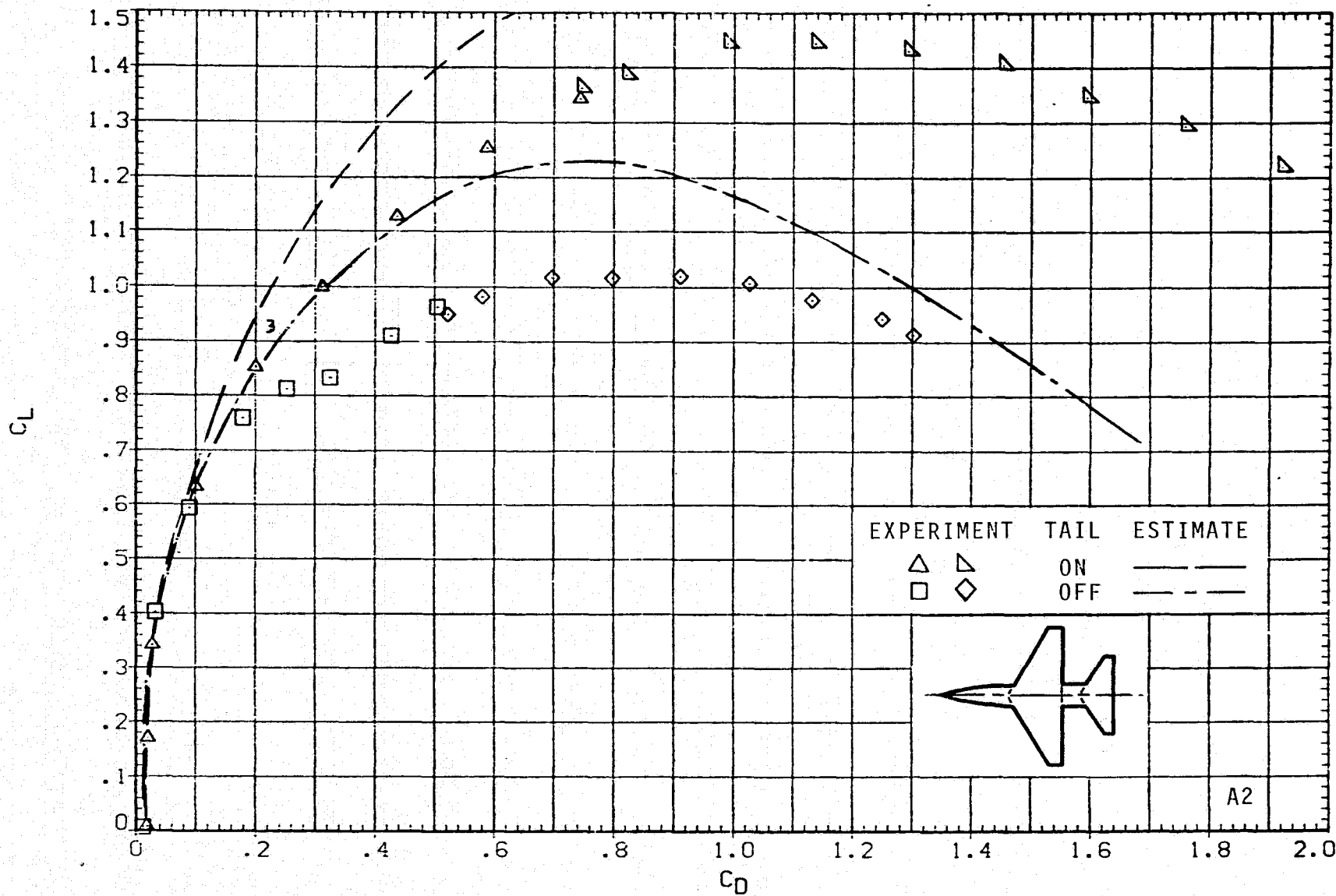
FIGURE 5.- CONCLUDED.





(a)  $C_L$  VERSUS  $\alpha$ ;  $M = 0.6$ ,  $J = 1$ .

FIGURE 6.- AERODYNAMICS FOR MODEL A2;  $ARW = 4$ ,  $TRW = 0.25$ .



(b)  $C_L$  VERSUS  $C_D$ ;  $M = 0.6$ ,  $J = 1$ .

FIGURE 6.- CONTINUED.

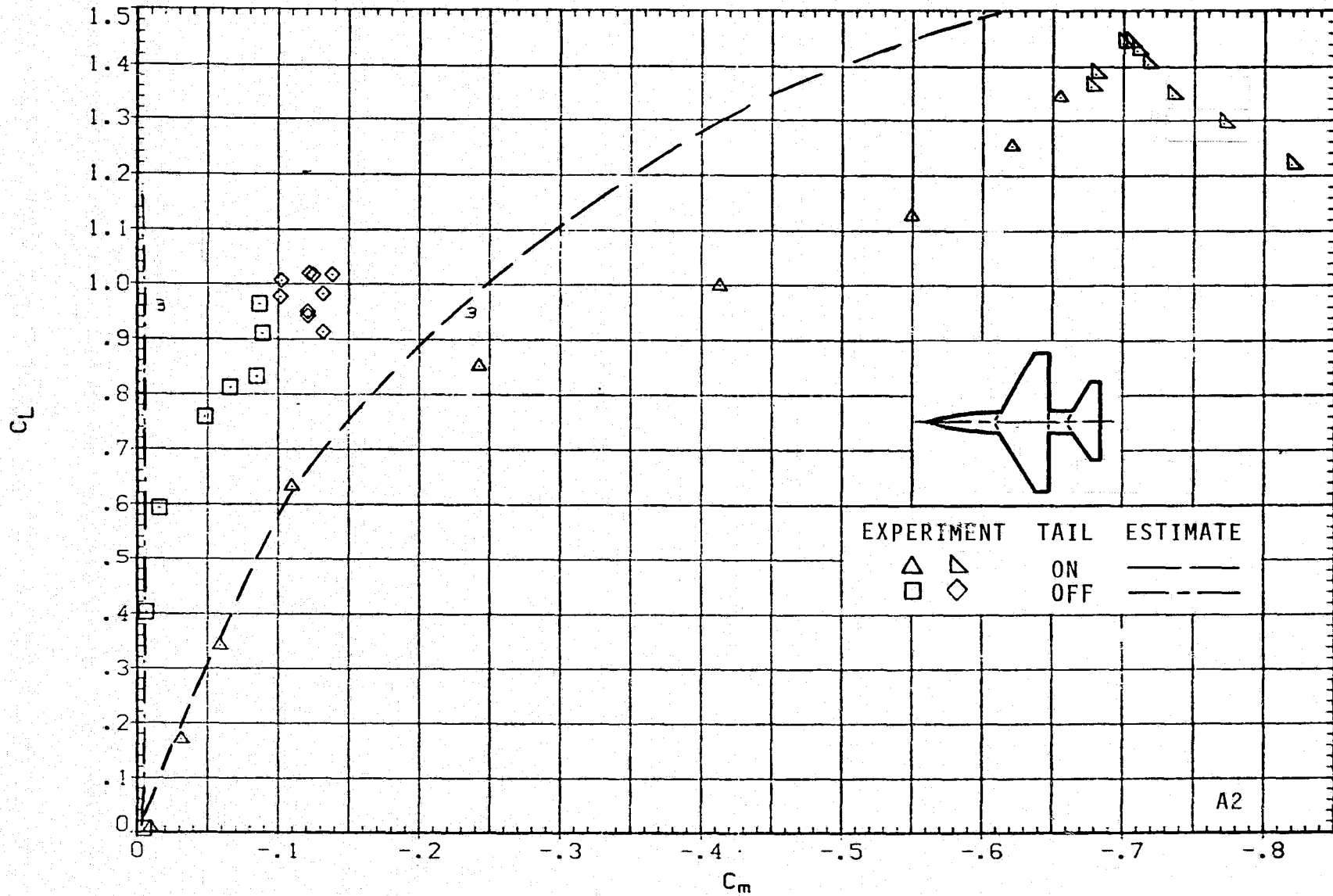
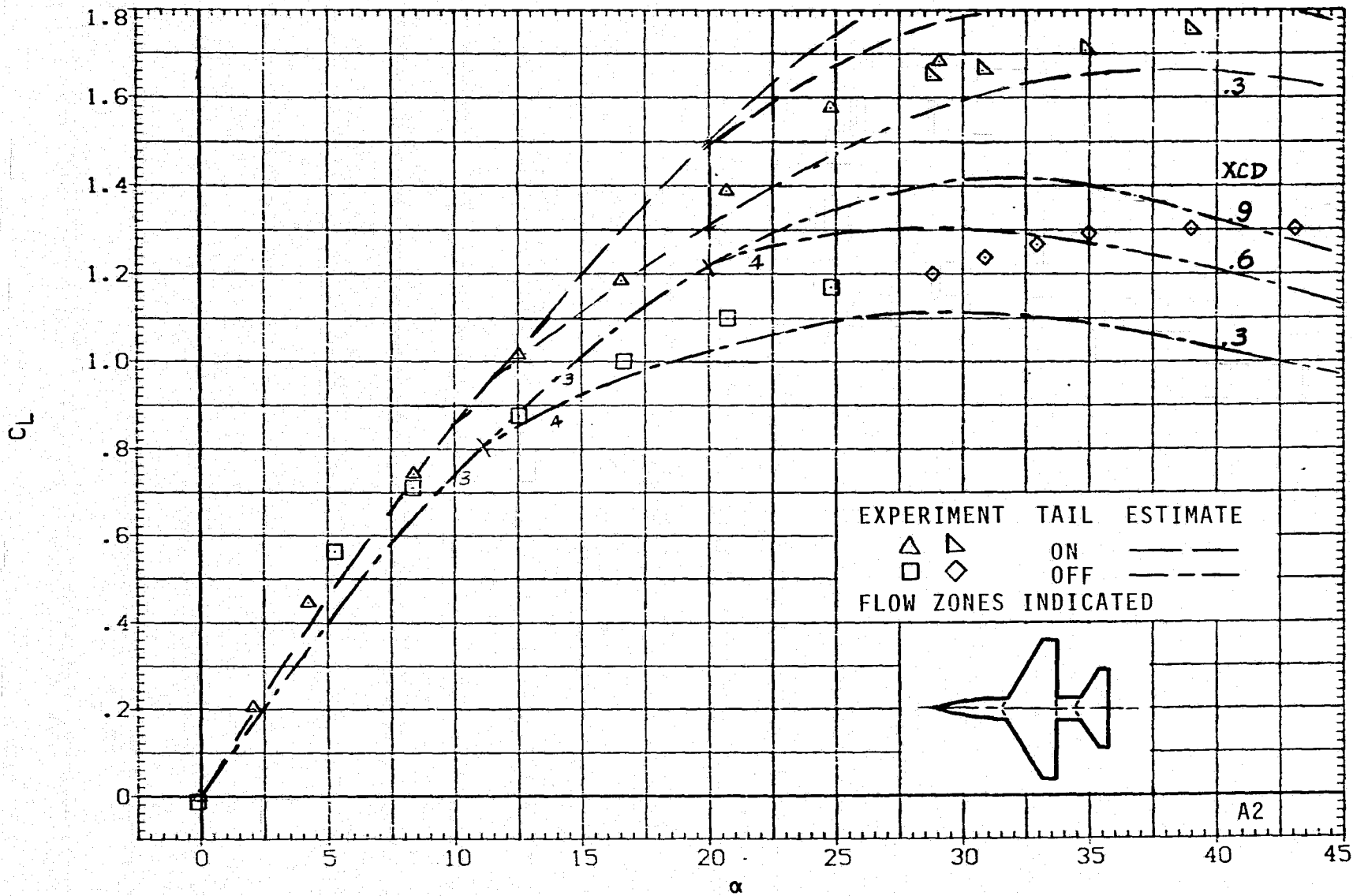
(c)  $C_L$  VERSUS  $C_m$ ;  $M = 0.6$ ,  $J = 1$ .

FIGURE 6.- CONTINUED.



(d)  $C_L$  VERSUS  $\alpha$ ;  $M = 0.9$ ,  $J = 1$ .

FIGURE 6.- CONTINUED.

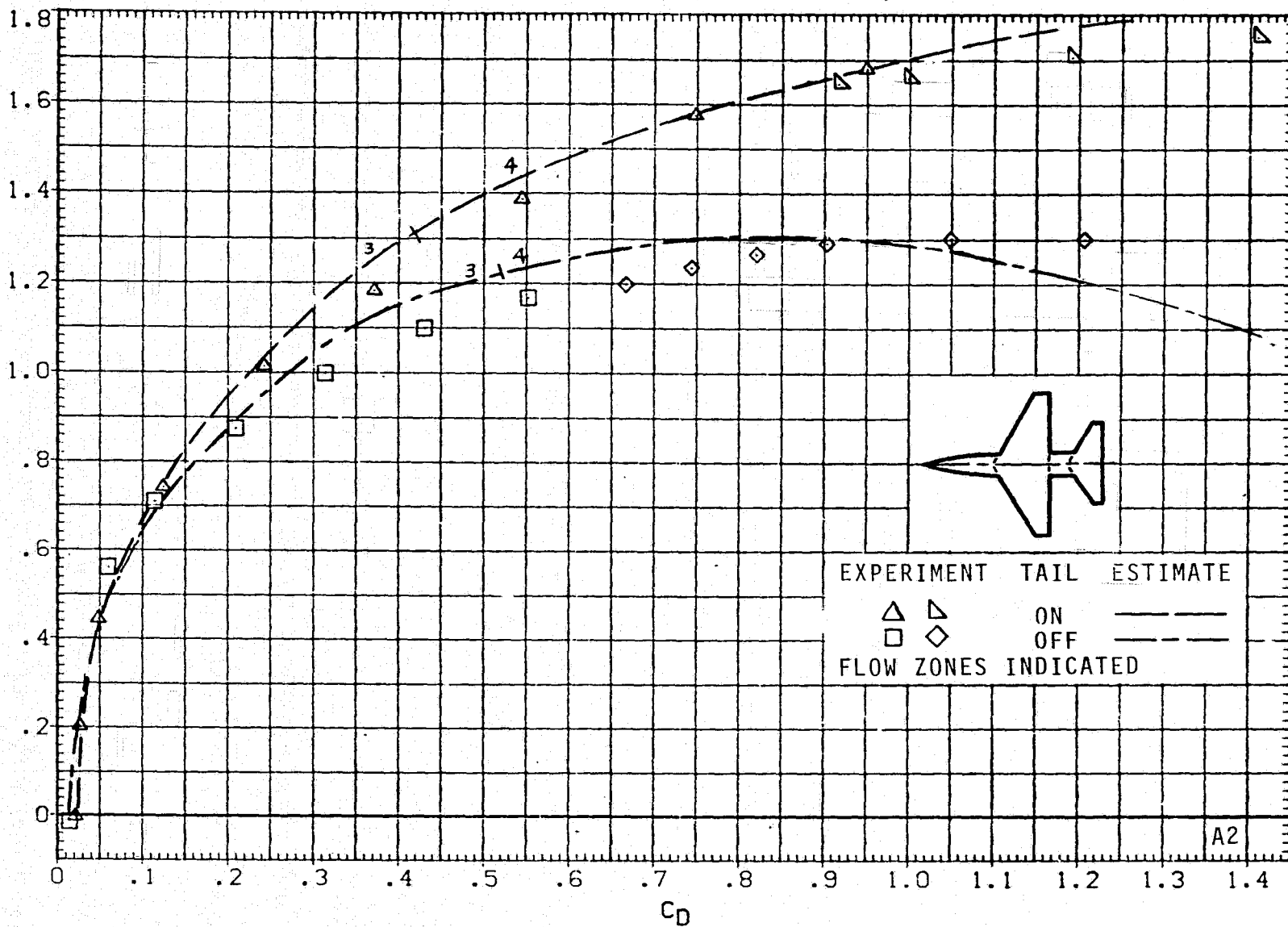
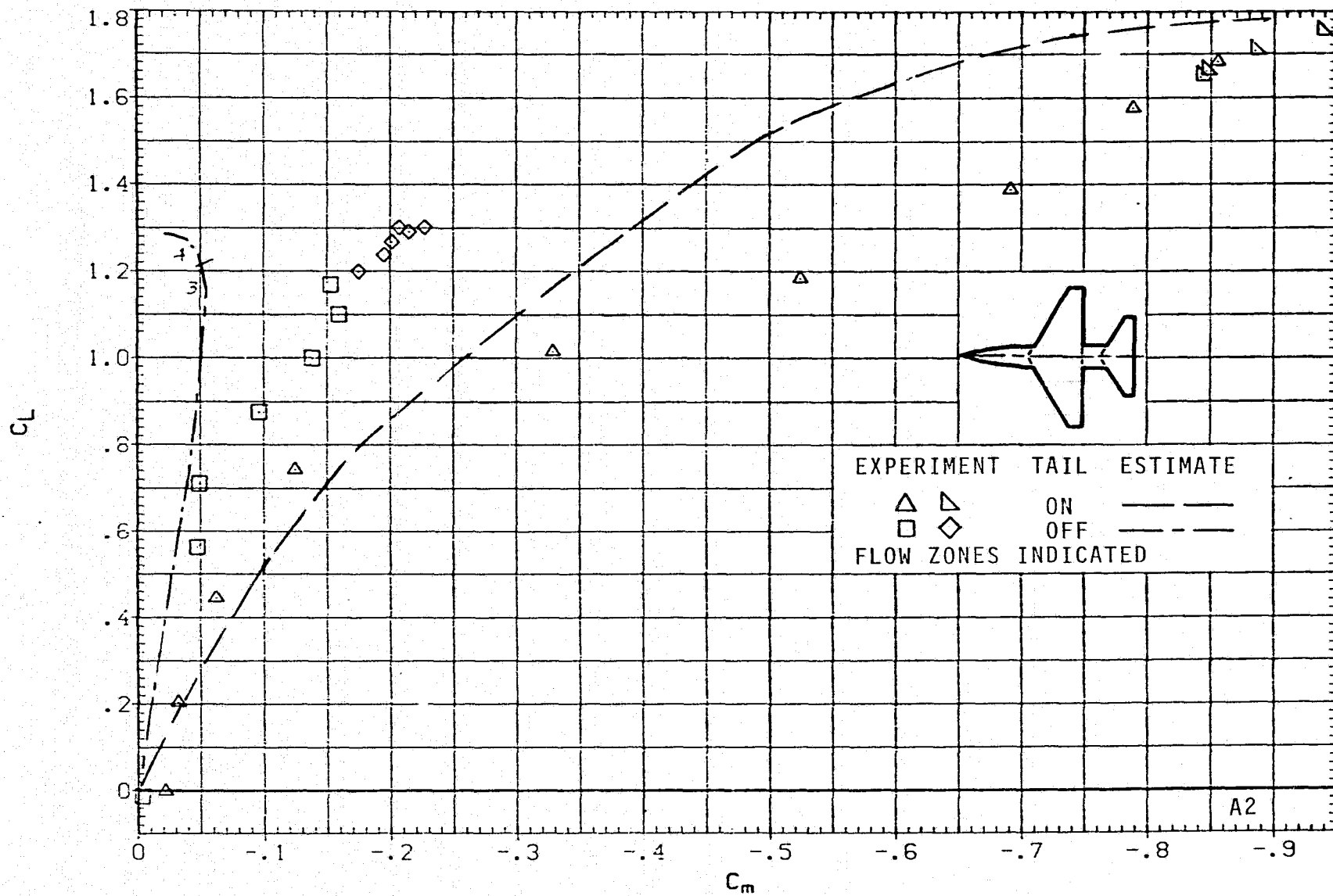
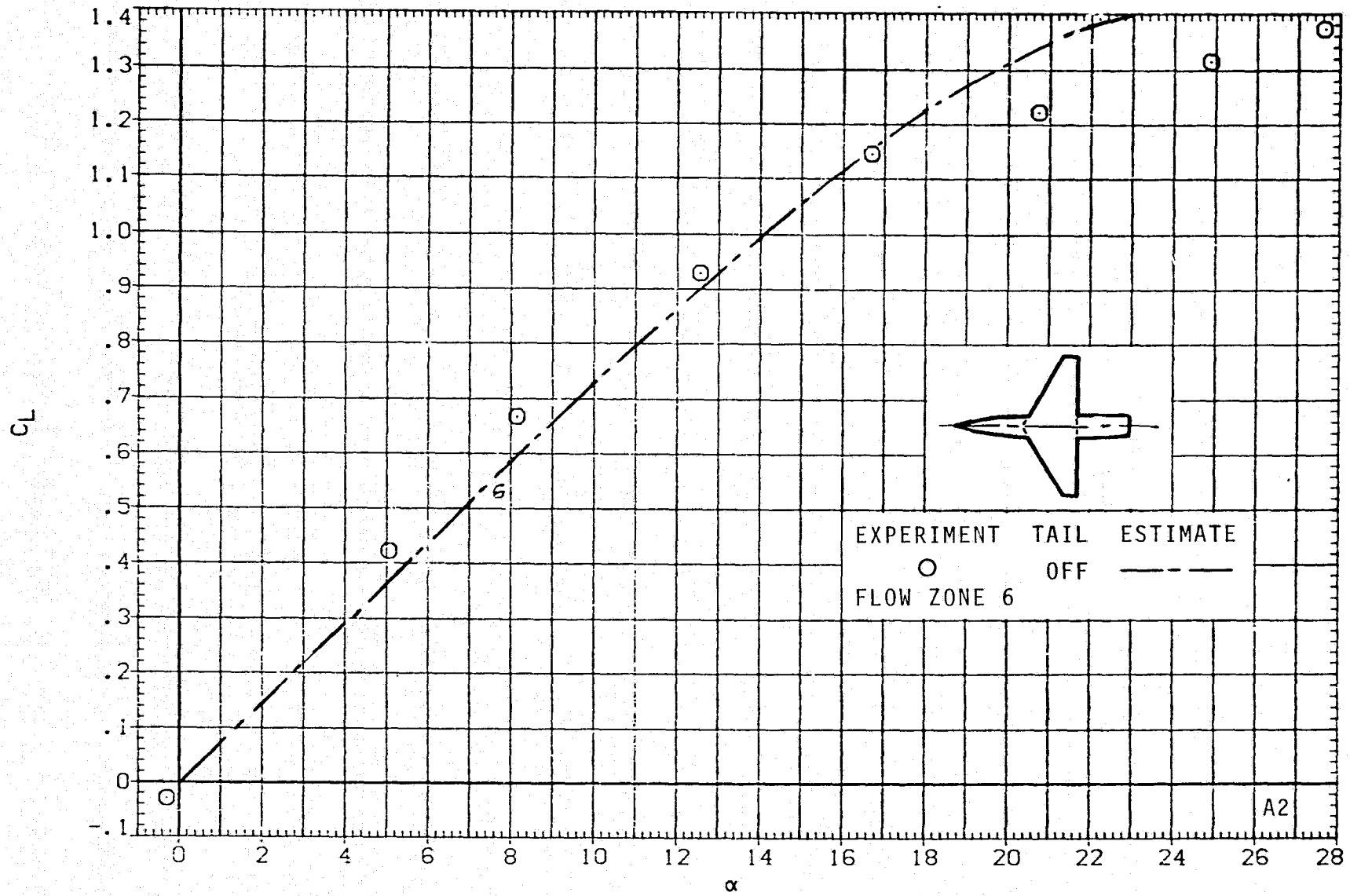
(e)  $C_L$  VERSUS  $C_D$ ;  $M = 0.9$ ,  $J = 1$ .

FIGURE 6.- CONTINUED.



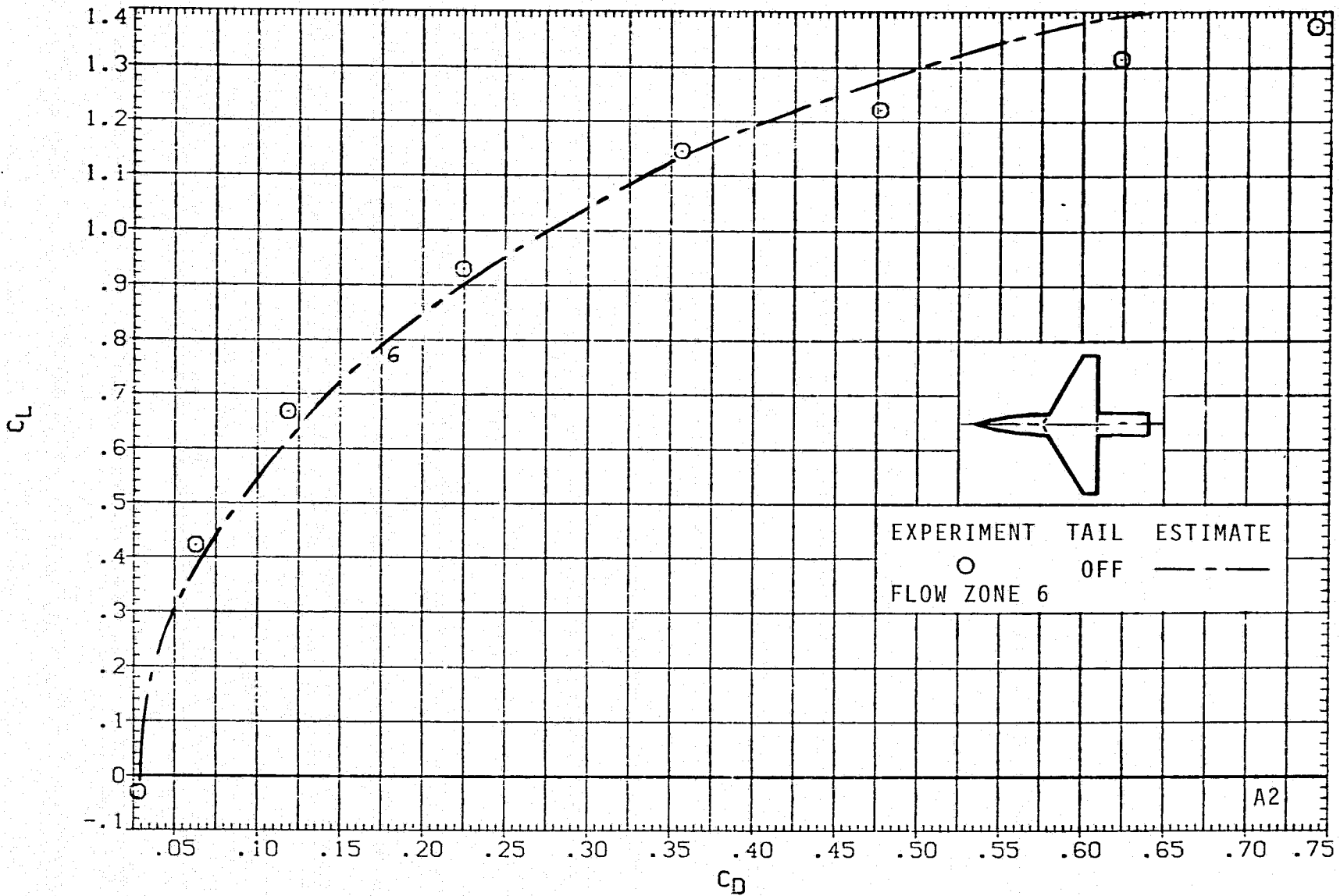
(f)  $C_L$  VERSUS  $C_m$ ;  $M = 0.9$ ,  $J = 1$ .

FIGURE 6.- CONTINUED.



(g)  $C_L$  VERSUS  $\alpha$ ;  $M = 1.2$ ,  $J = 5$ .

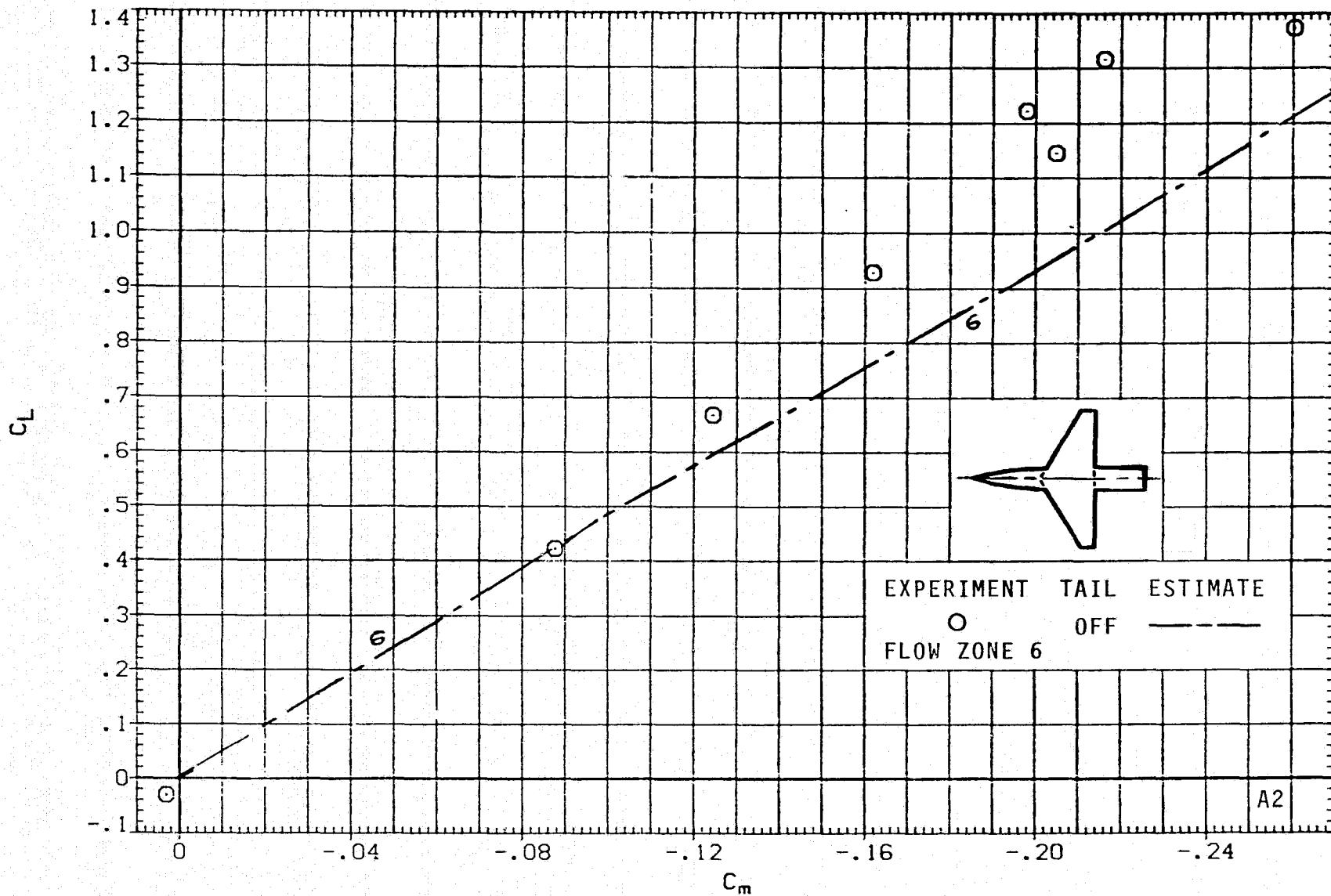
FIGURE 6.- CONTINUED.



(h)  $C_L$  VERSUS  $C_D$ ;  $M = 1.2$ ,  $J = 5$ .

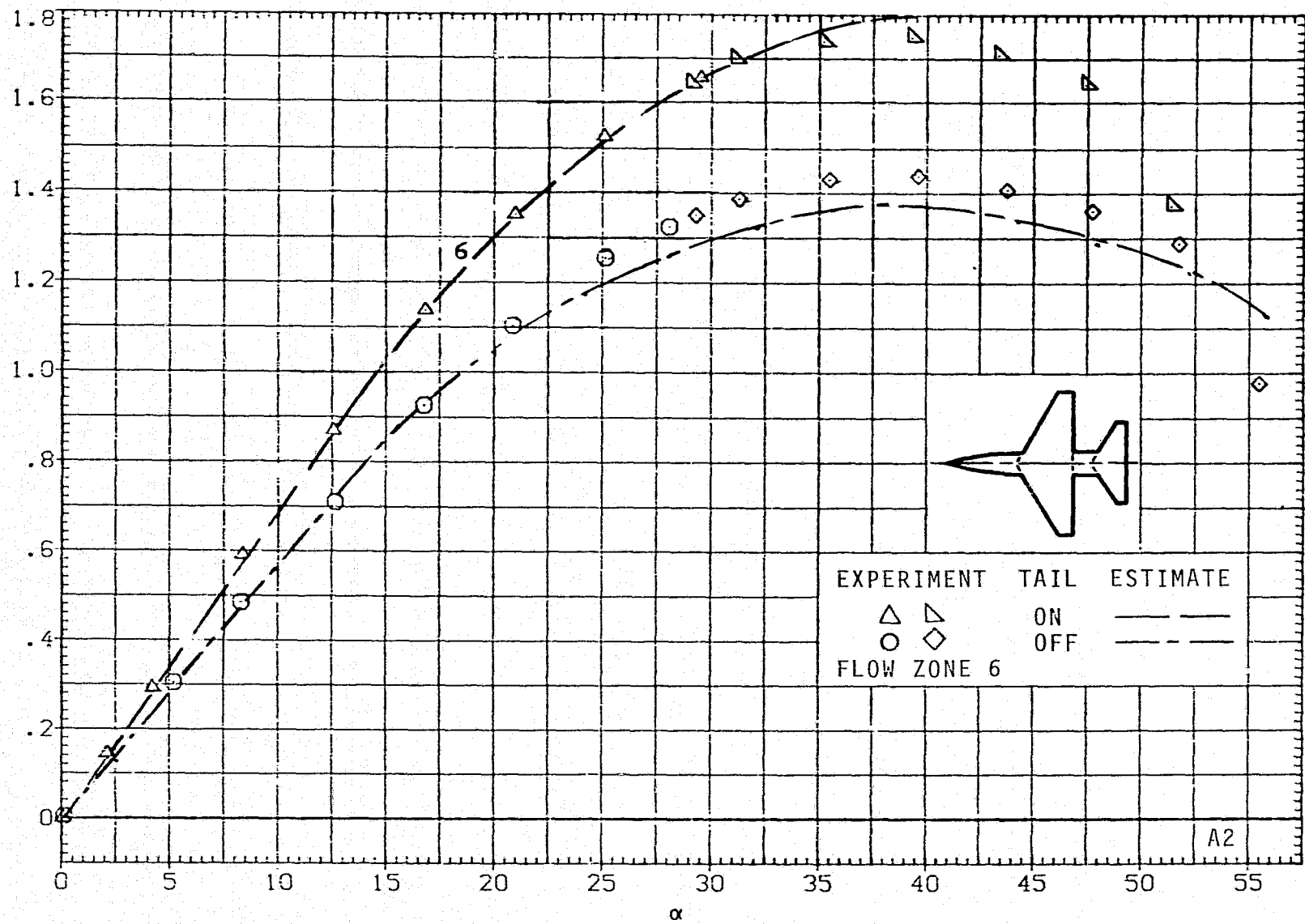
FIGURE 6.- CONTINUED.





(i)  $C_L$  VERSUS  $C_m$ ;  $M = 1.2$ ,  $J = 5$ .

FIGURE 6.- CONTINUED.



(j)  $C_L$  VERSUS  $\alpha$ ;  $M = 1.5$ ,  $J = 5$ .

FIGURE 6.- CONTINUED.

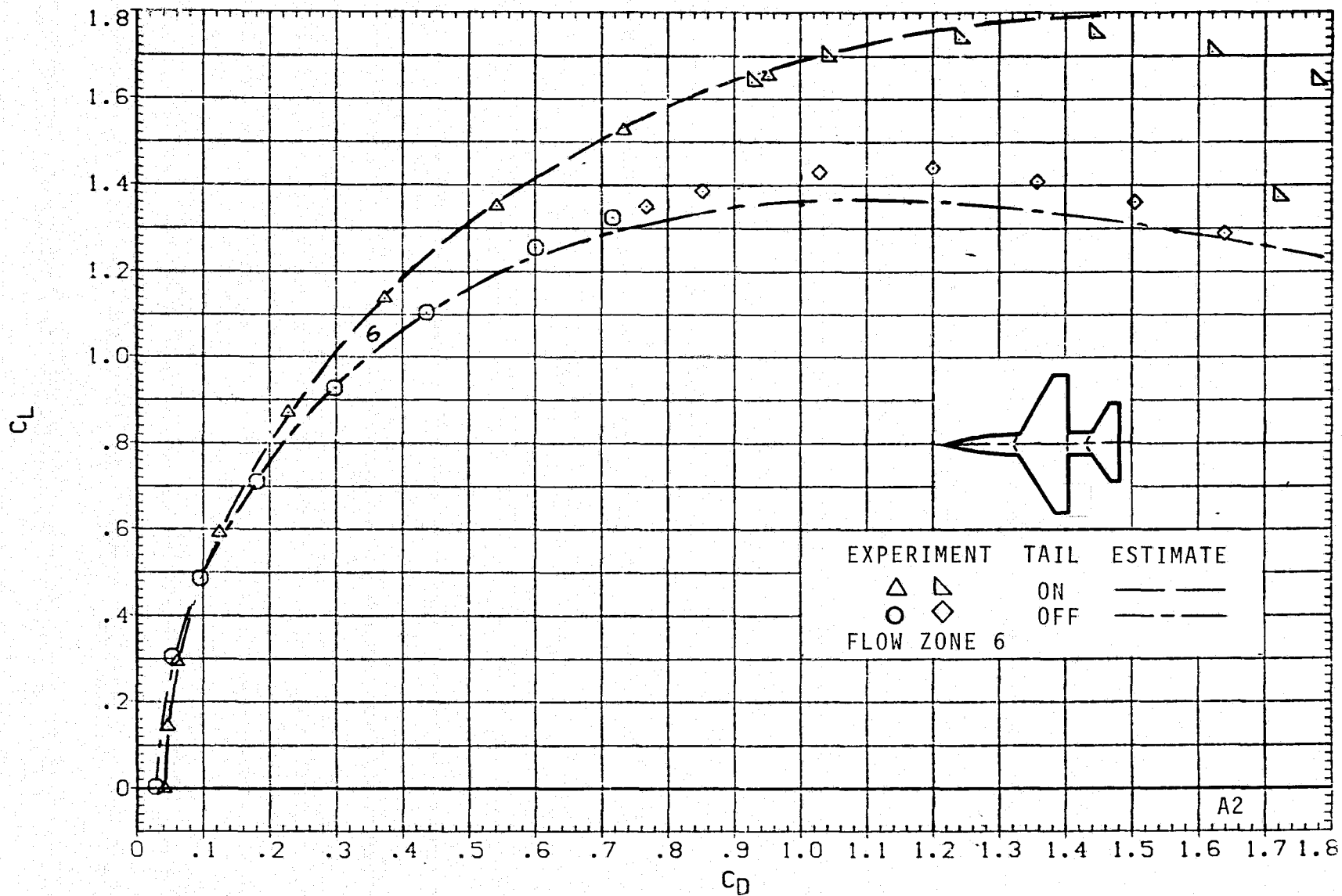
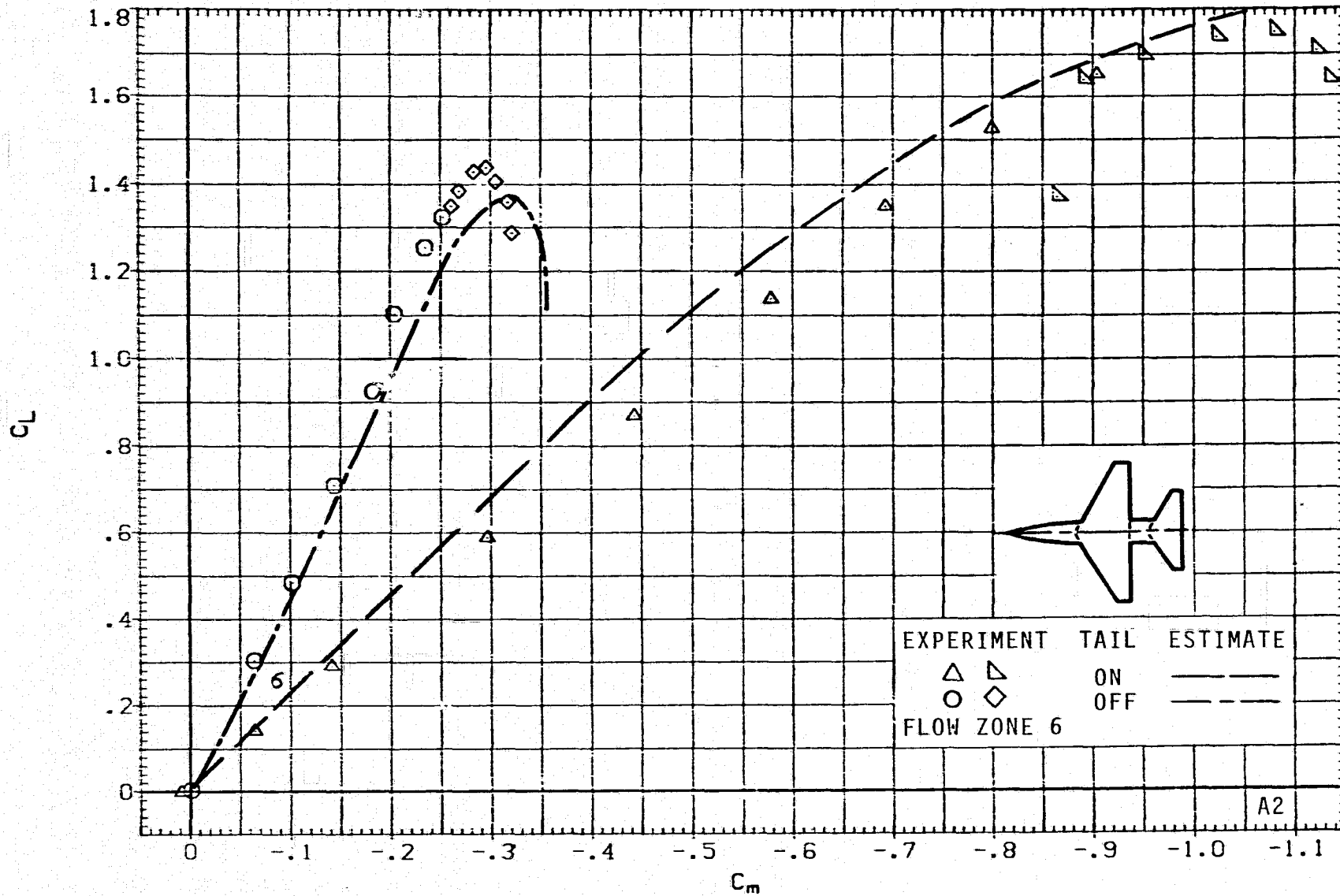
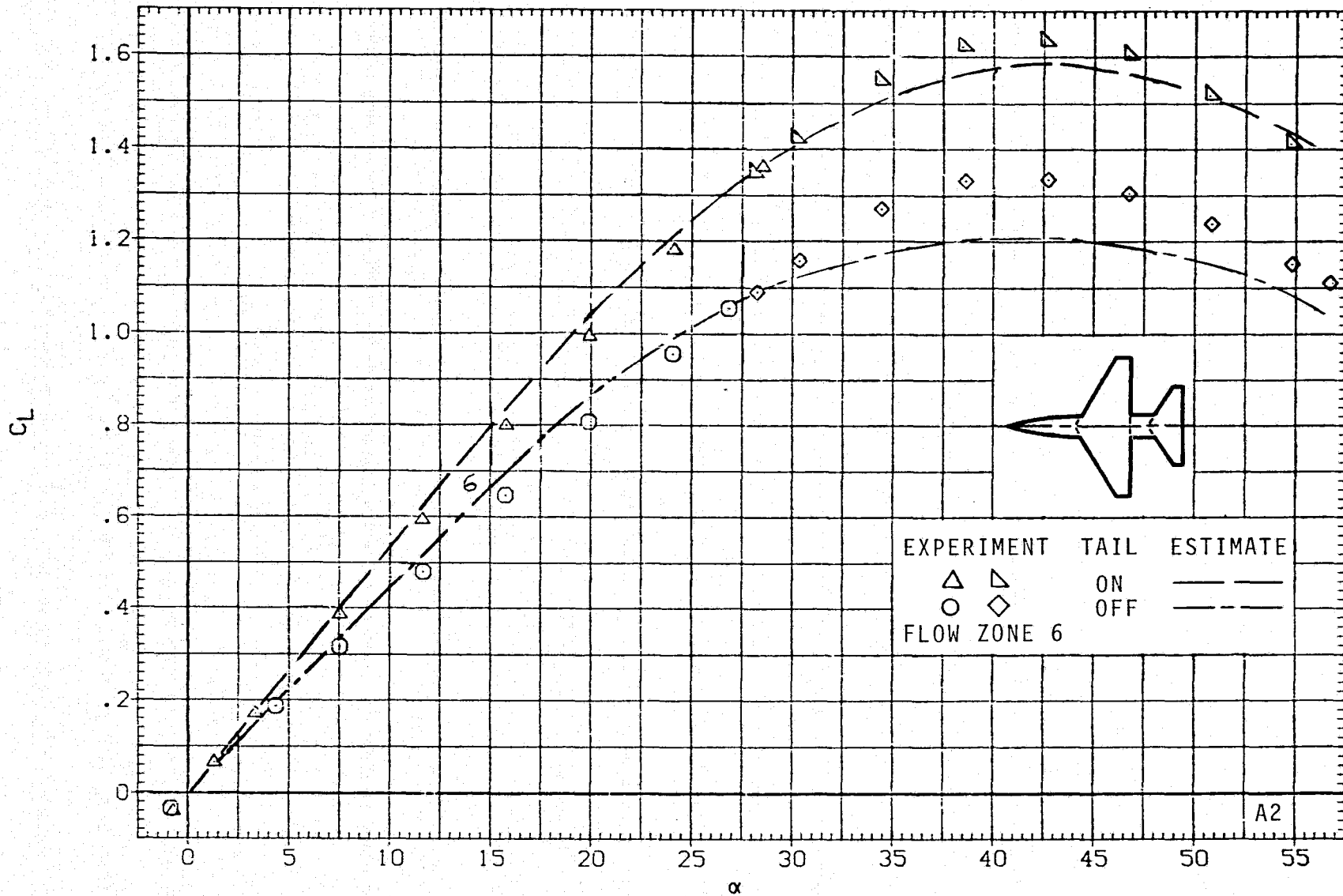
(k)  $C_L$  VERSUS  $C_D$ ;  $M = 1.5$ ,  $J = 5$ .

FIGURE 6.- CONTINUED.



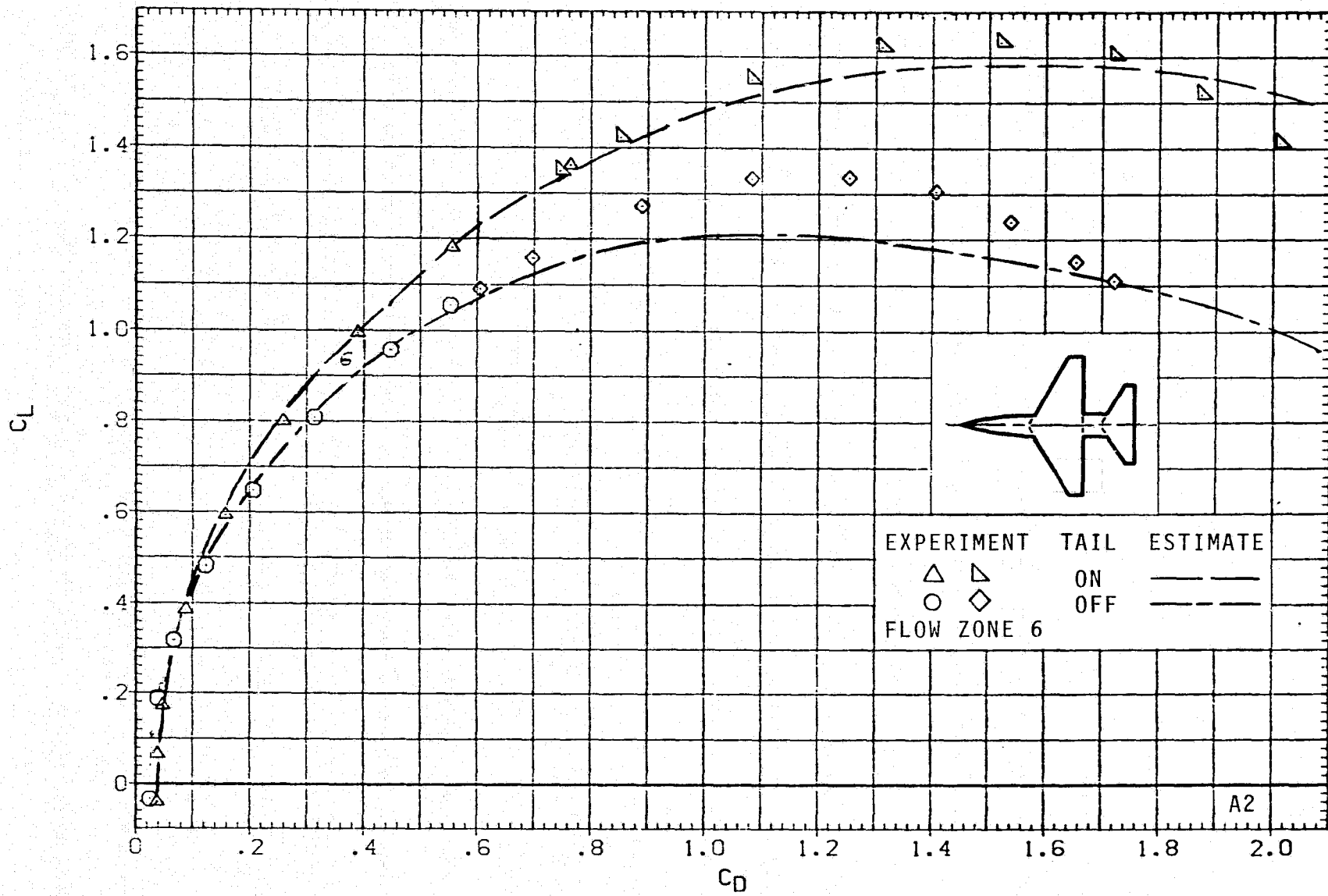
(1)  $C_L$  VERSUS  $C_m$ ;  $M = 1.5$ ,  $J = 5$ .

FIGURE 6.- CONTINUED.



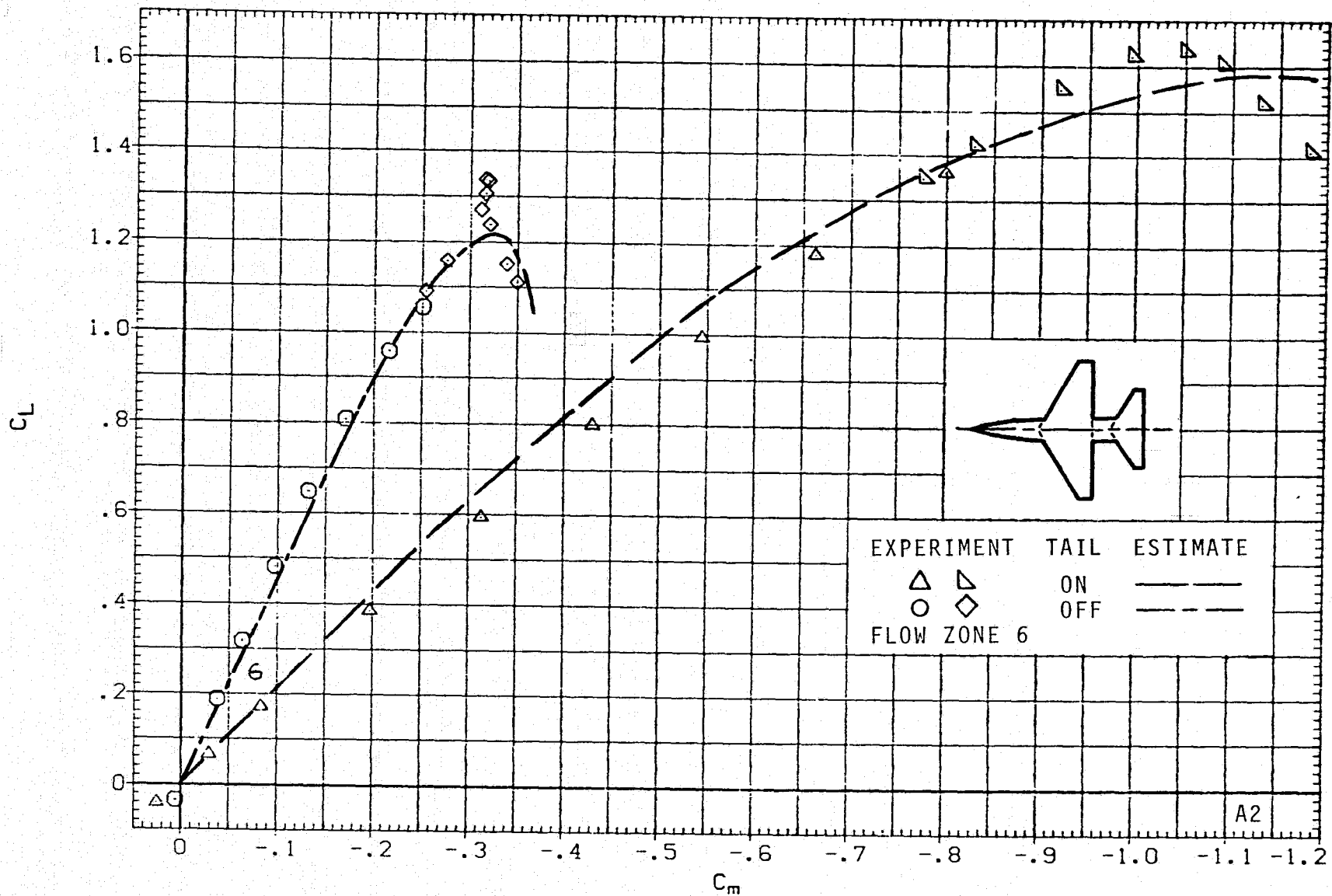
(m)  $C_L$  VERSUS  $\alpha$ ;  $M = 2.0$ ,  $J = 5$ .

FIGURE 6.- CONTINUED.



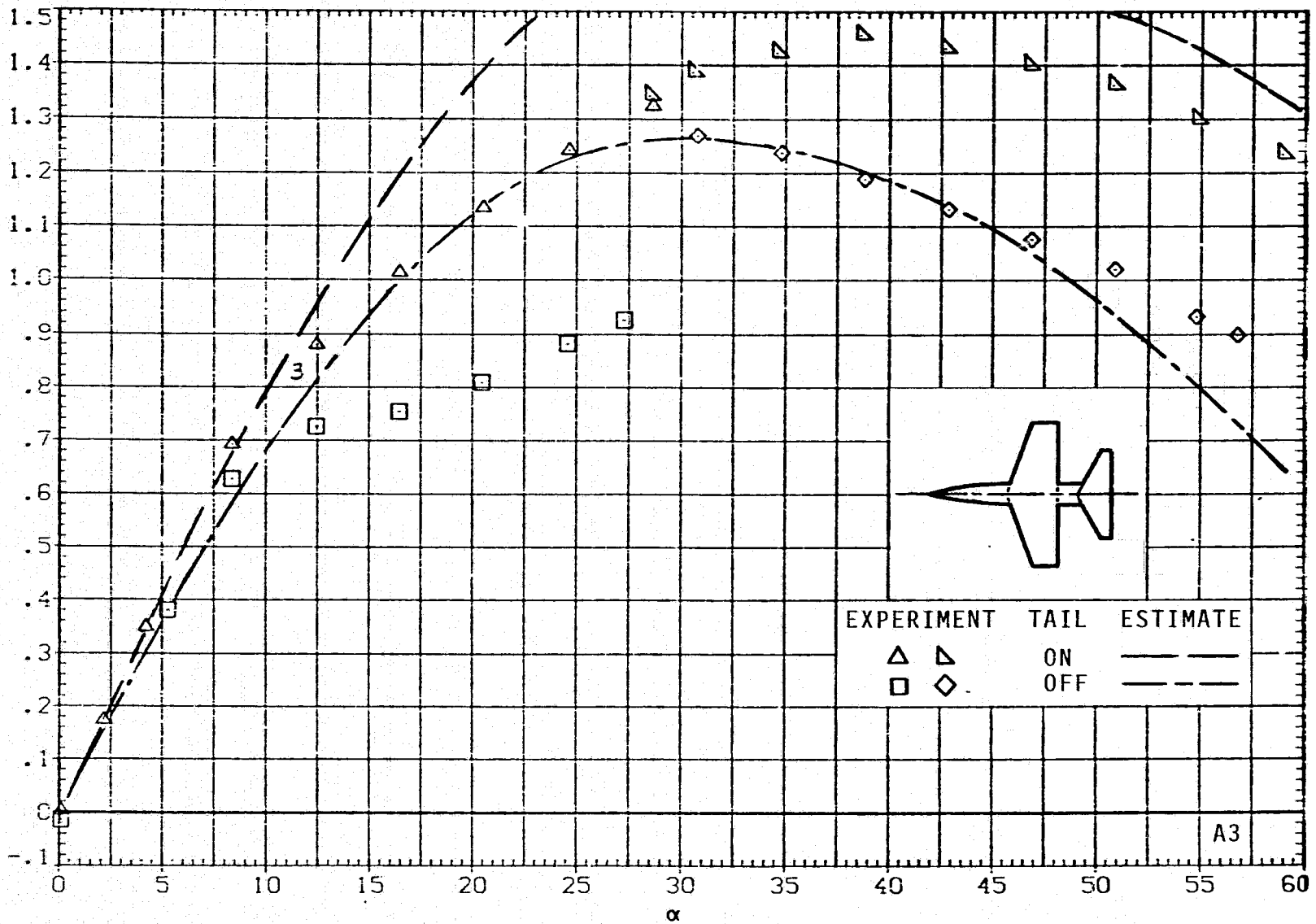
(n)  $C_L$  VERSUS  $C_D$ ;  $M = 2.0$ ,  $J = 5$ .

FIGURE 6.- CONTINUED.



(o)  $C_L$  VERSUS  $C_m$ ;  $M = 2.0$ ,  $J = 5$ .

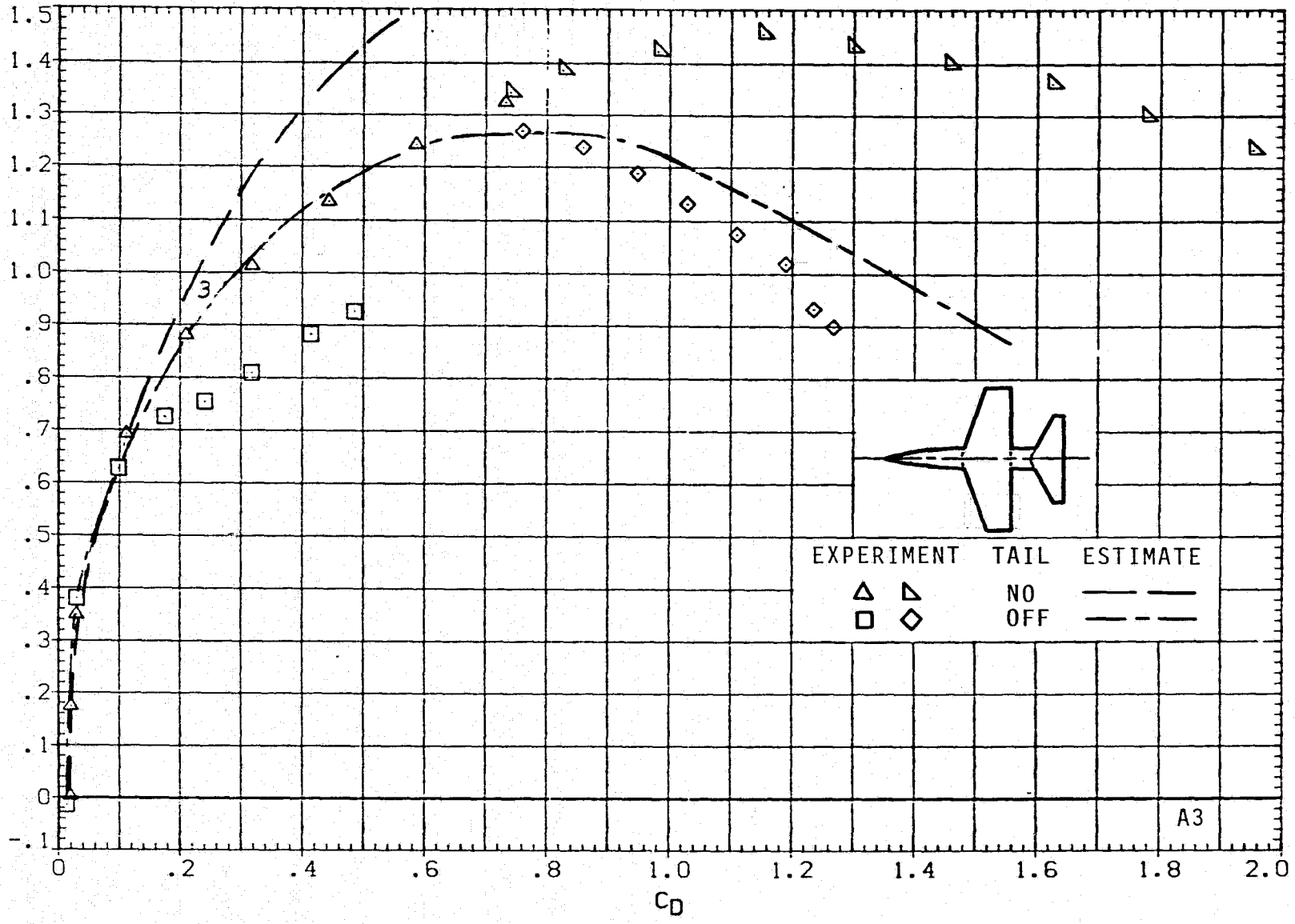
FIGURE 6.- CONCLUDED.



(a)  $C_L$  VERSUS  $\alpha$ ;  $M = 0.6$ ;  $J = 1$ .

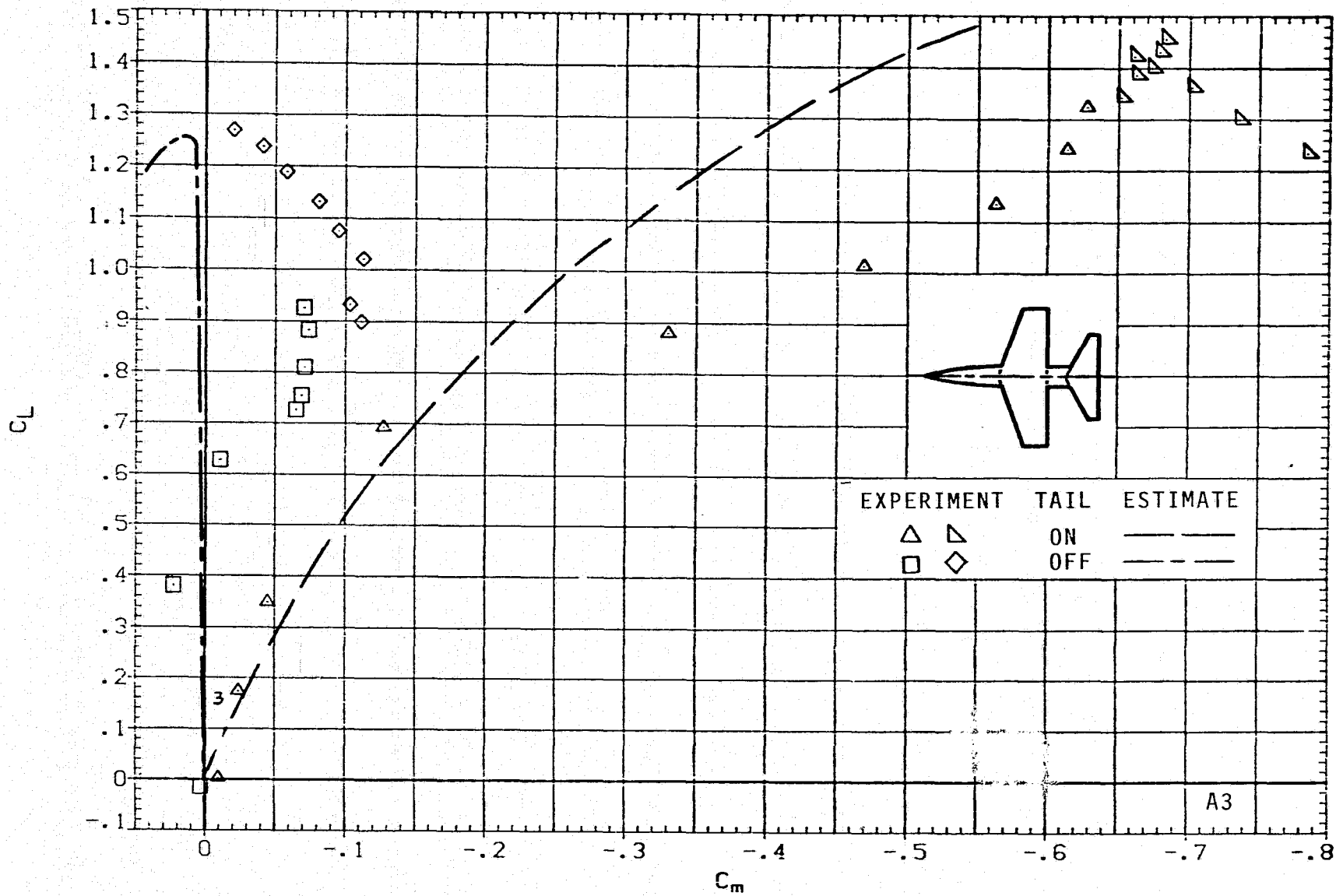
FIGURE 7.- AERODYNAMICS FOR MODEL A3; ARW = 4, TRW = 0.25.





(b)  $C_L$  VERSUS  $C_D$ :  $M = 0.6$ ,  $J = 1$ .

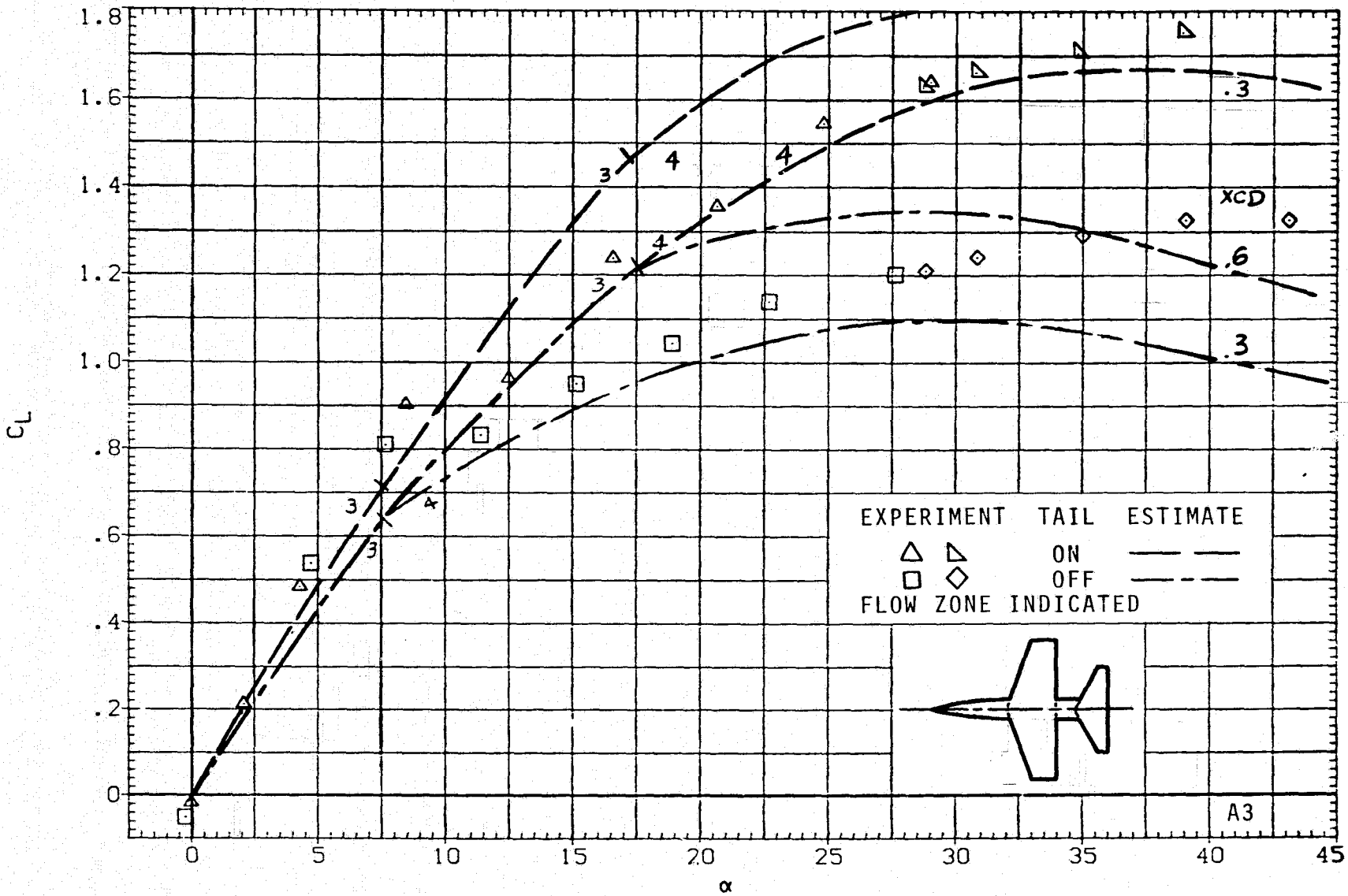
FIGURE 7-. CONTINUED.



(c)  $C_L$  VERSUS  $C_m$ ;  $M = 0.6$ ,  $J = 1$ .

FIGURE 7.- CONTINUED.

75



(d)  $C_L$  VERSUS  $\alpha$ ;  $M = 0.9$ ,  $J = 1$ .

FIGURE 7.- CONTINUED.

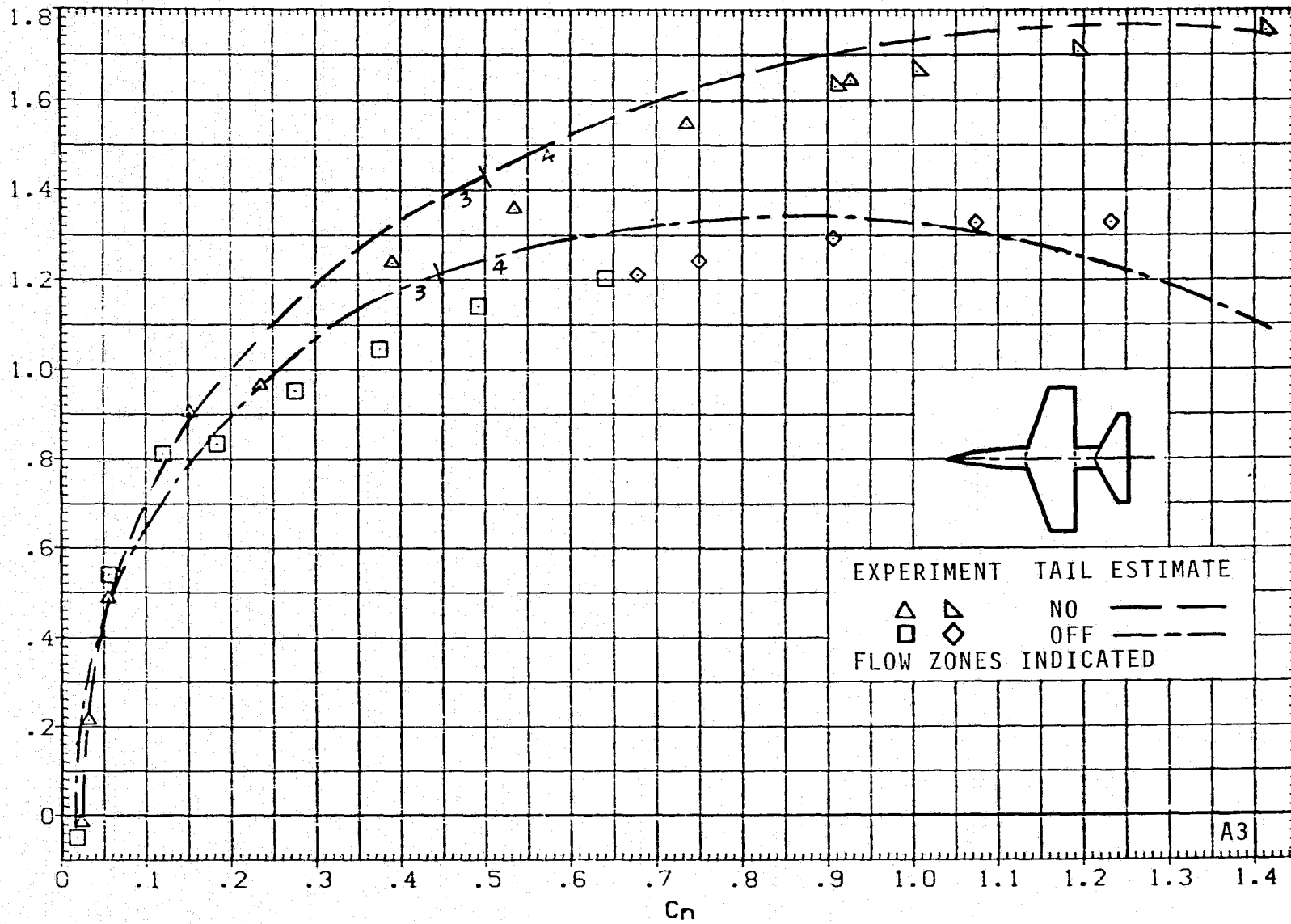
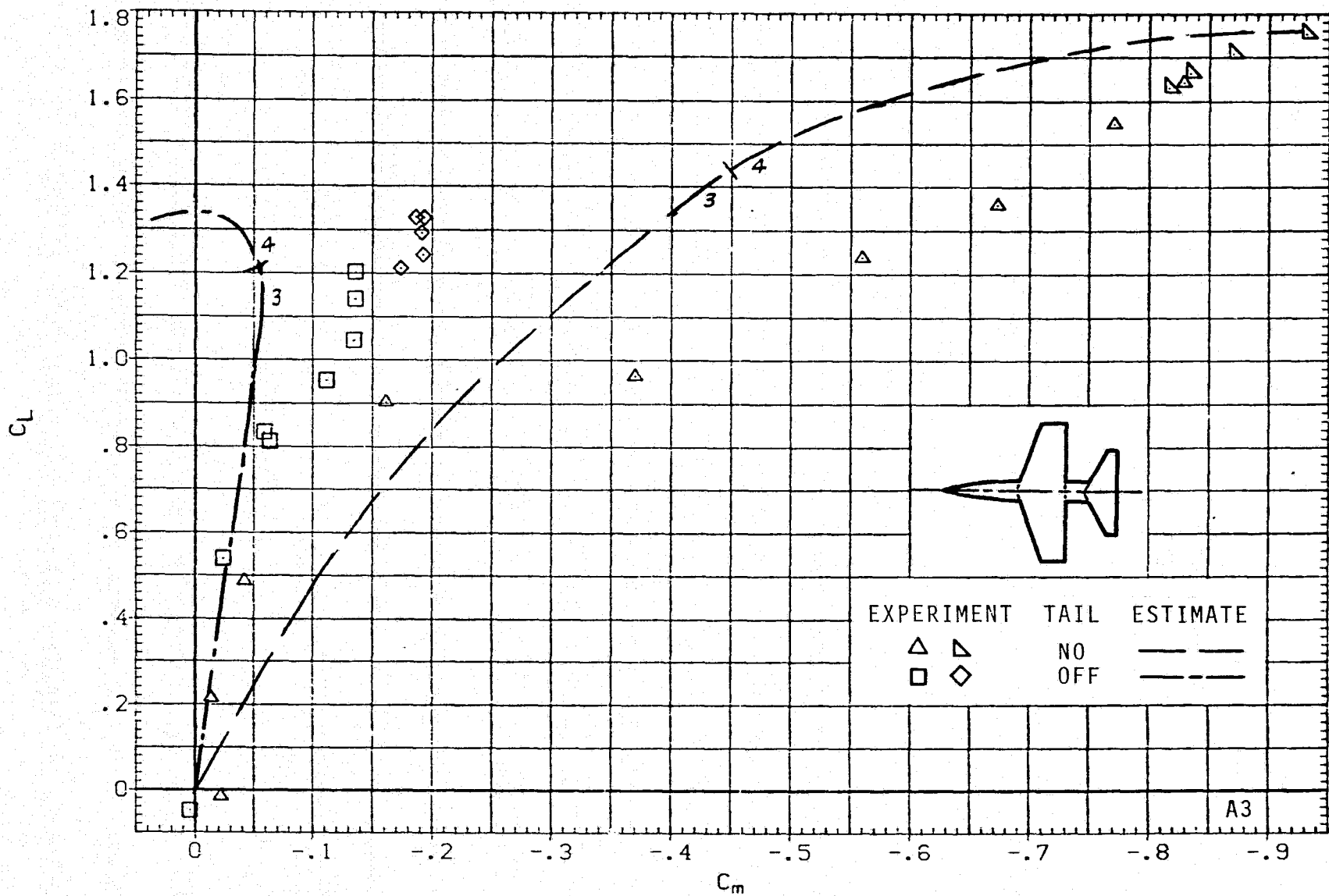
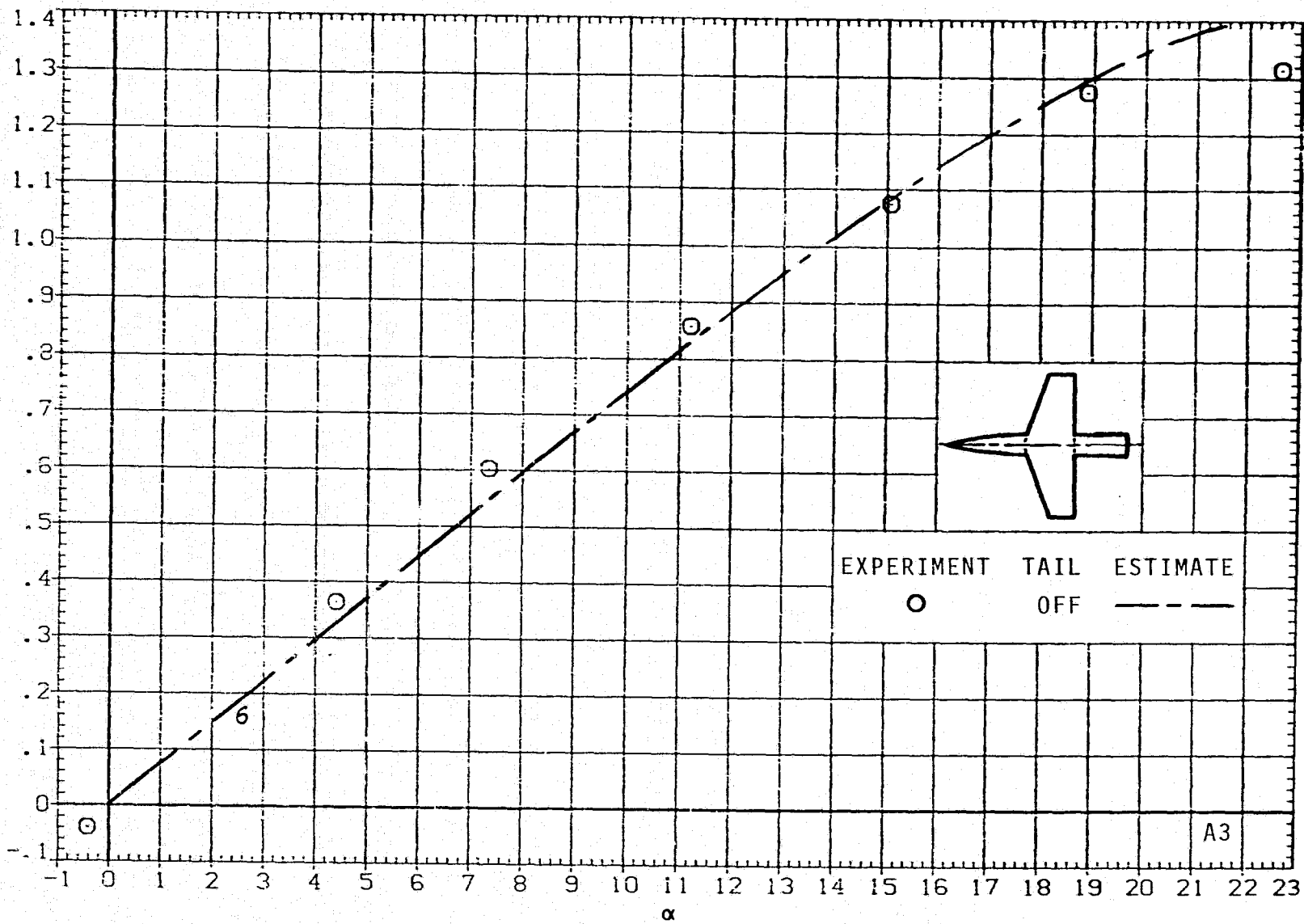
(e)  $C_L$  VERSUS  $C_D$ ;  $M = 0.9$ ,  $J = 1$ .

FIGURE 7.- CONTINUED.



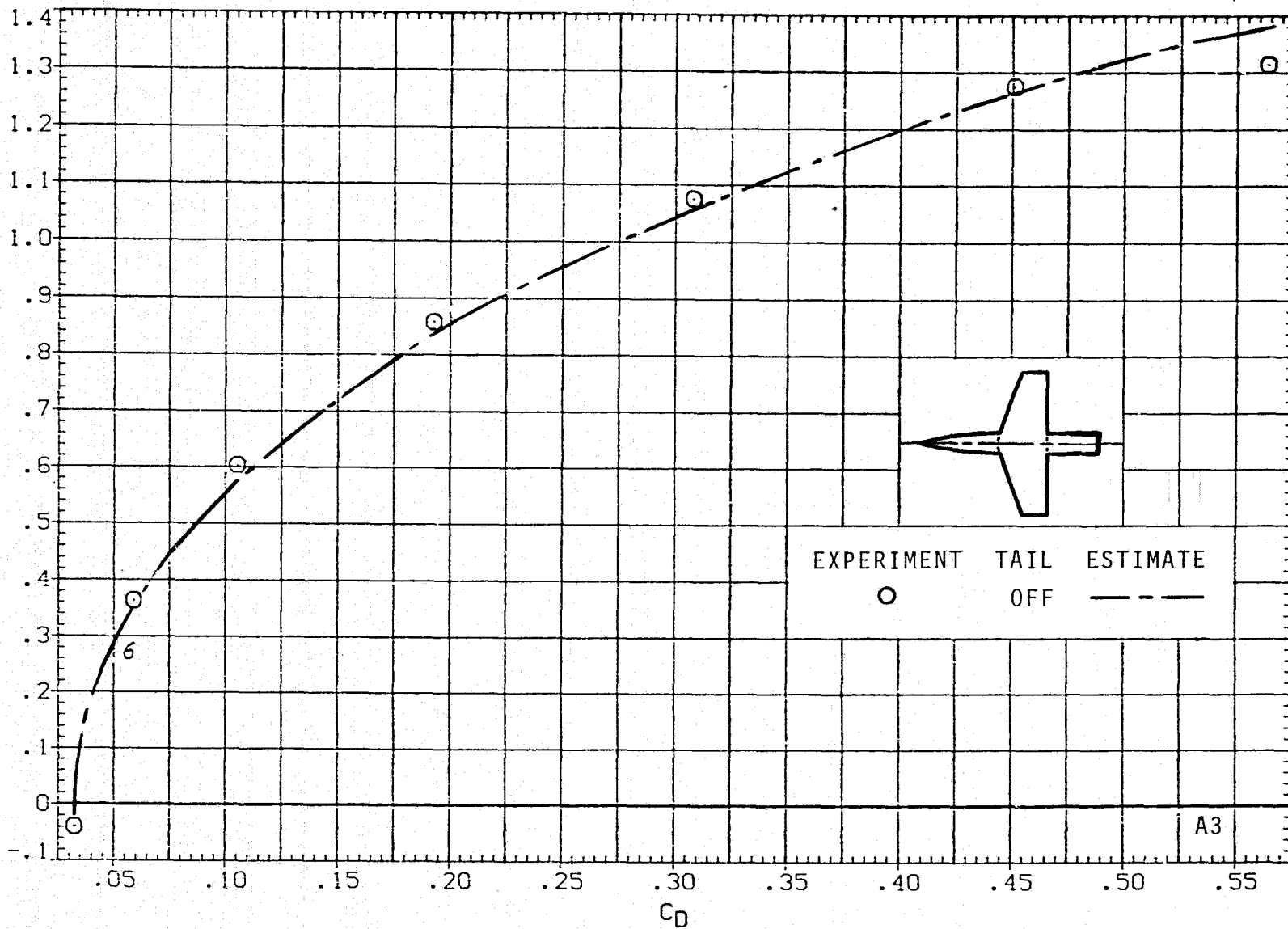
(f)  $C_L$  VERSUS  $C_m$ ;  $M = 0.9$ ,  $J = 1$ .

FIGURE 7.- CONTINUED.



(g)  $C_L$  VERSUS  $\alpha$ ;  $M = 1.2$ ,  $J = 5$ .

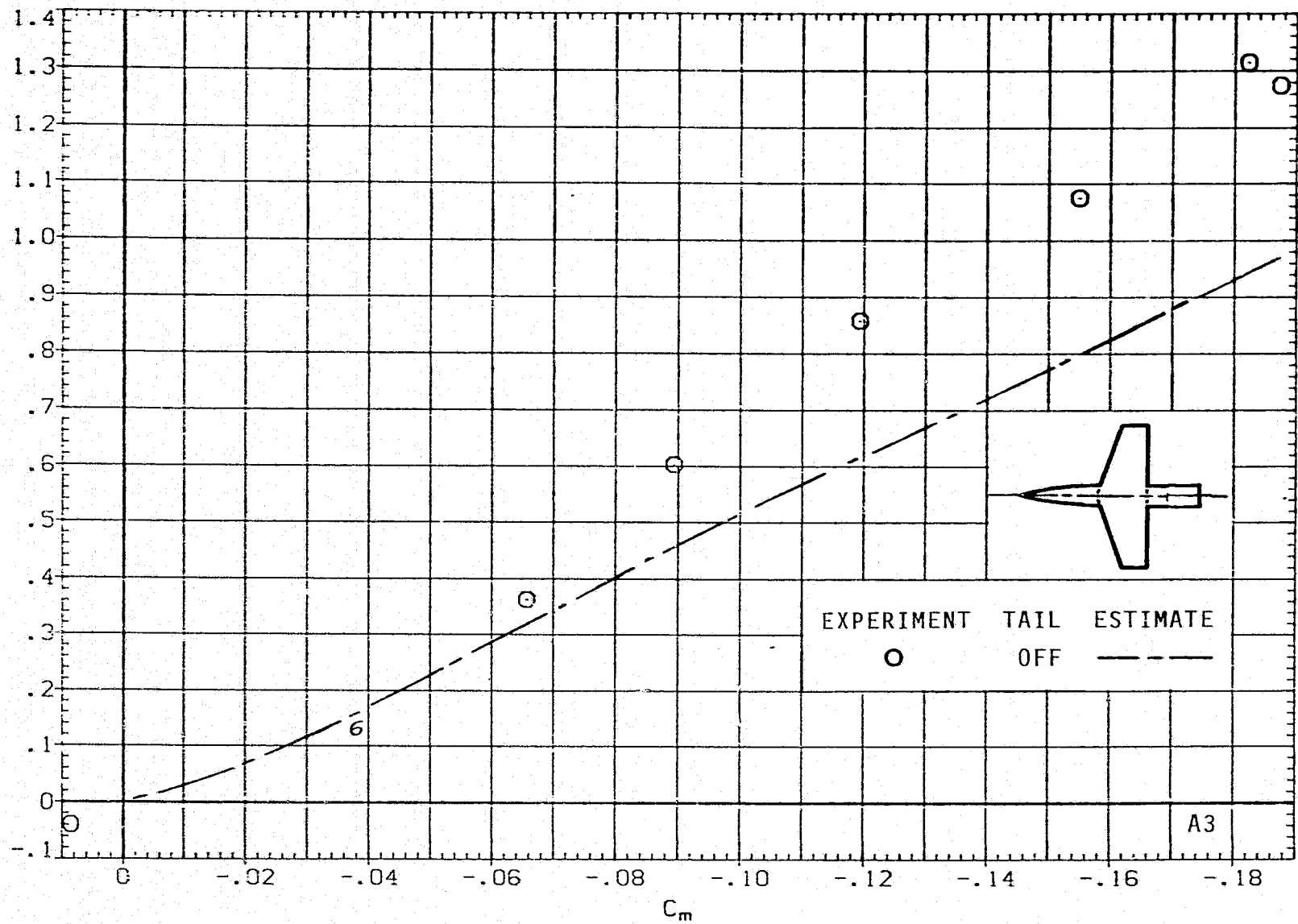
FIGURE 7.- CONTINUED.



(h)  $C_L$  VERSUS  $C_D$ ;  $M = 1.2$ ,  $J = 5$ .

FIGURE 7.- CONTINUED.

08

 $C_L$ 

(i)  $C_L$  VERSUS  $C_m$ ;  $M = 1.2$ ,  $J = 5$ .

FIGURE 7.- CONTINUED.



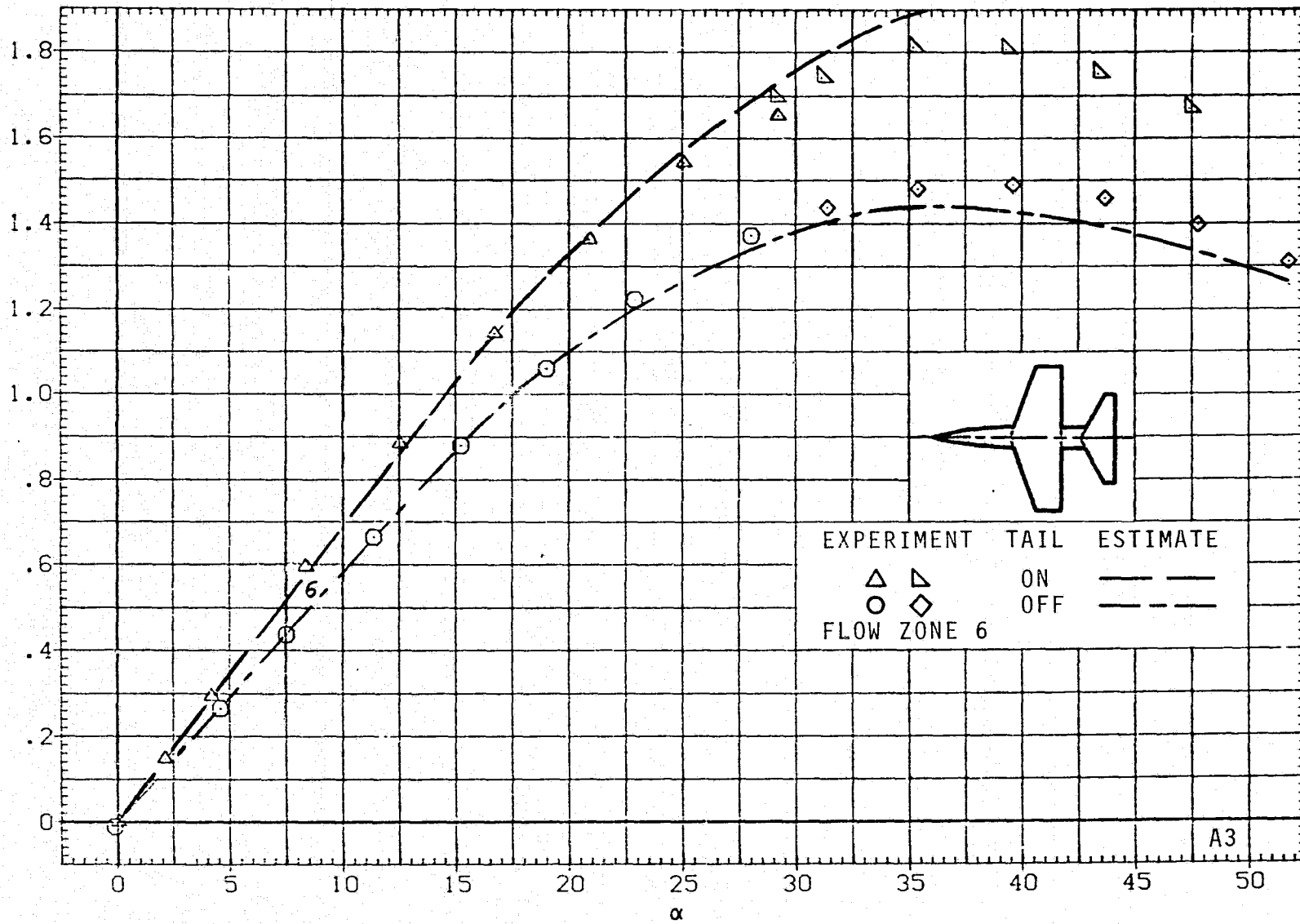
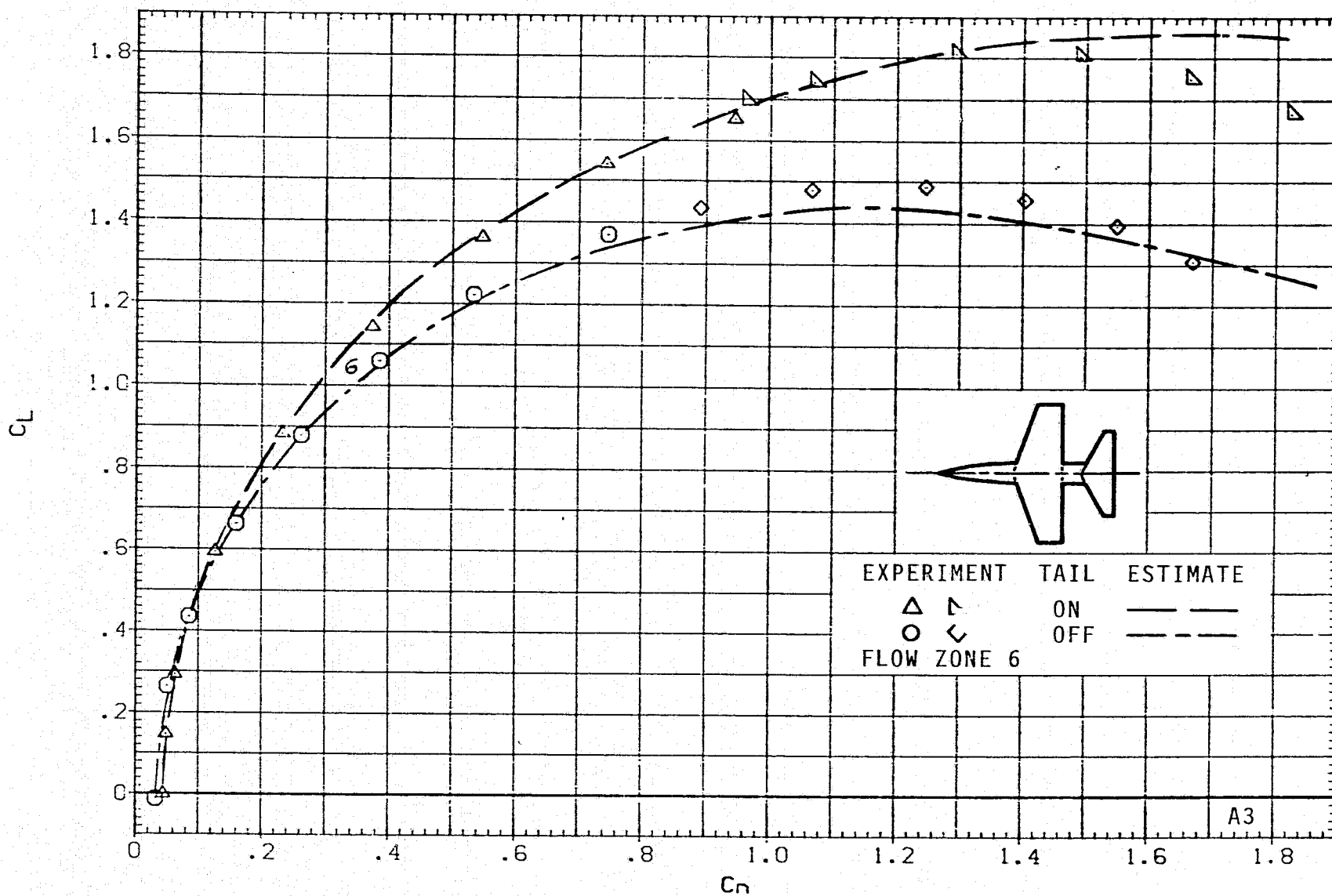
(j)  $C_L$  VERSUS  $\alpha$ ;  $M = 1.5$ ,  $J = 5$ .

FIGURE 7.- CONTINUED.



(k)  $C_L$  VERSUS  $C_D$ ;  $M = 1.5$ ,  $J = 5$ .

FIGURE 7.- CONTINUED.

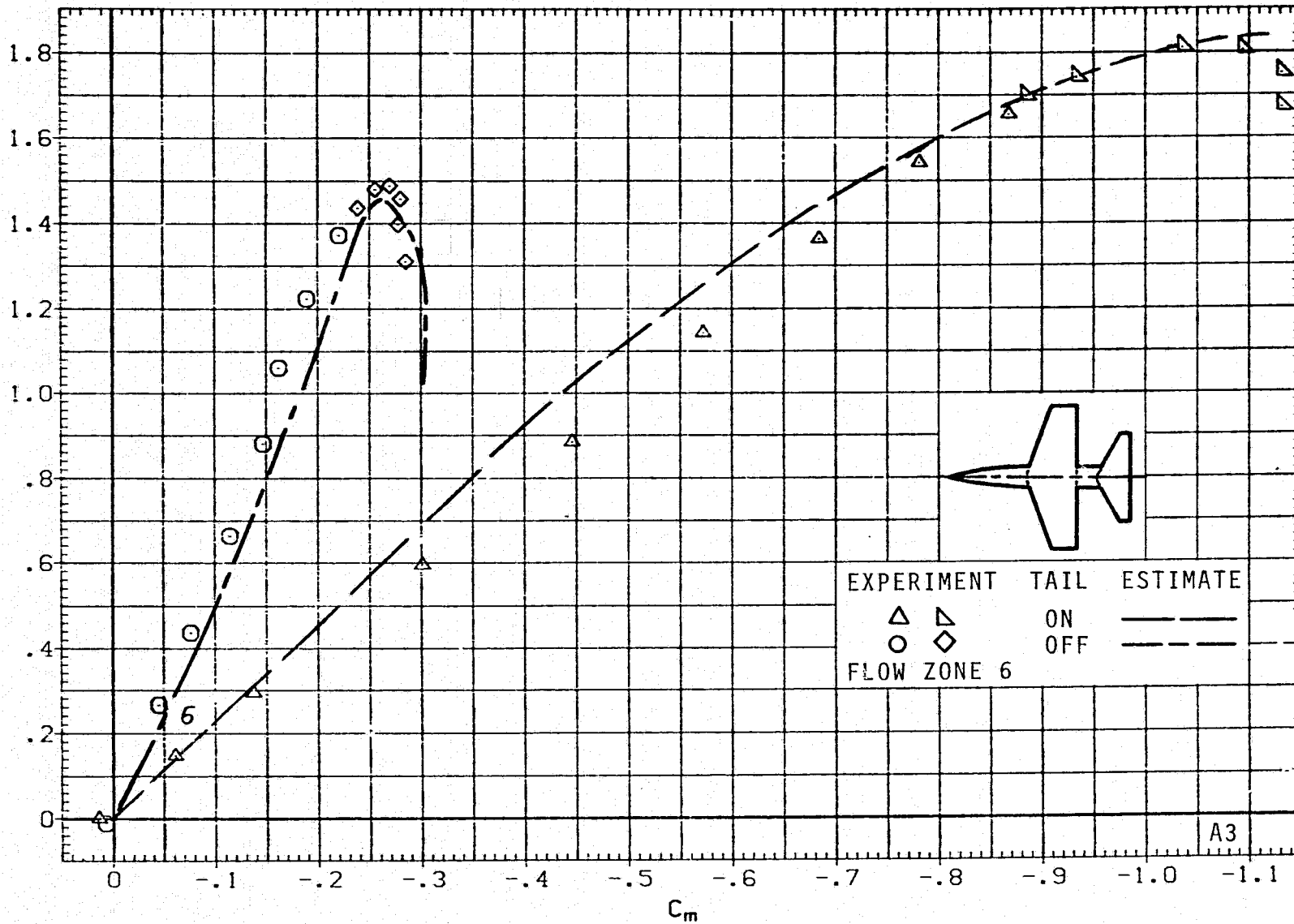
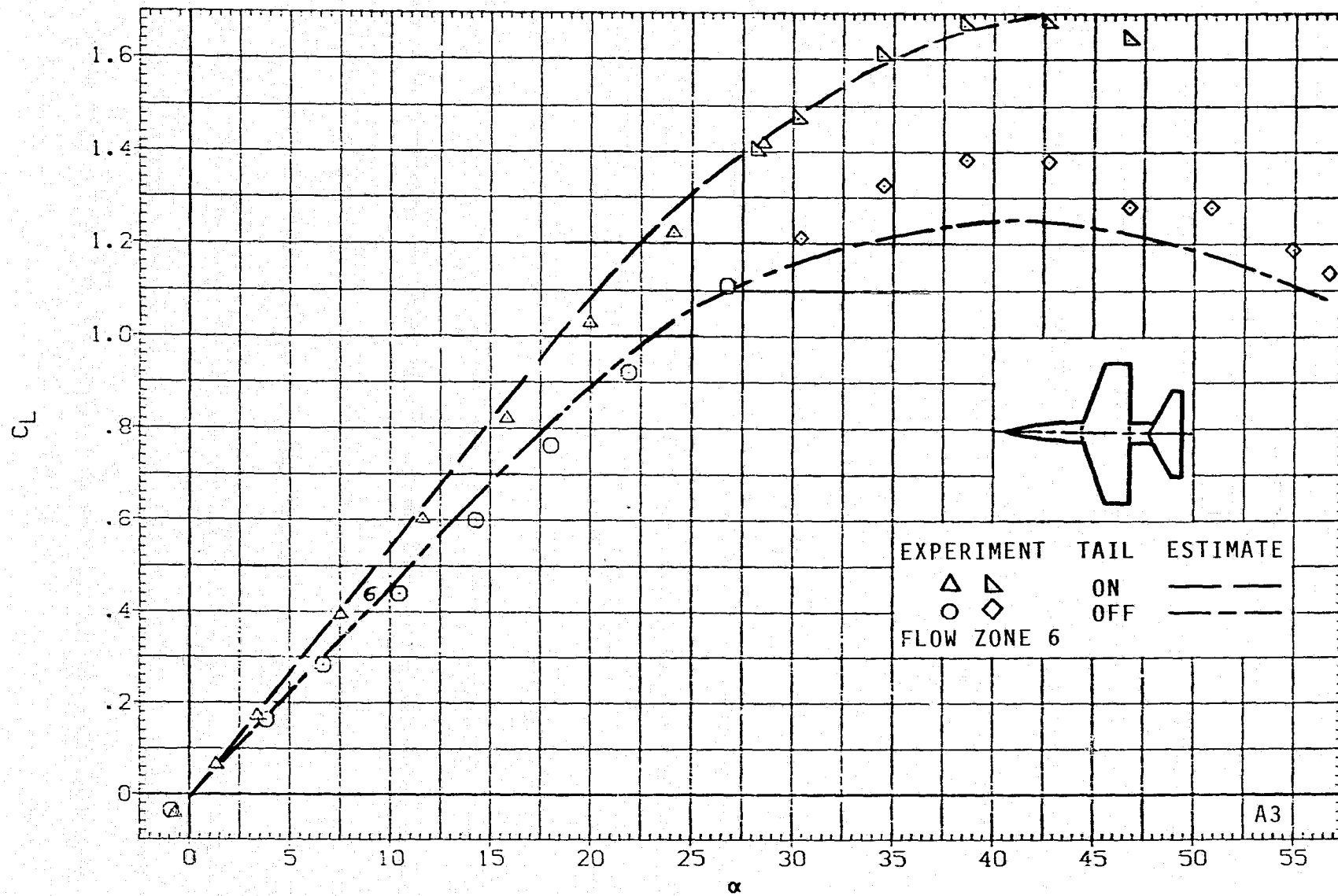
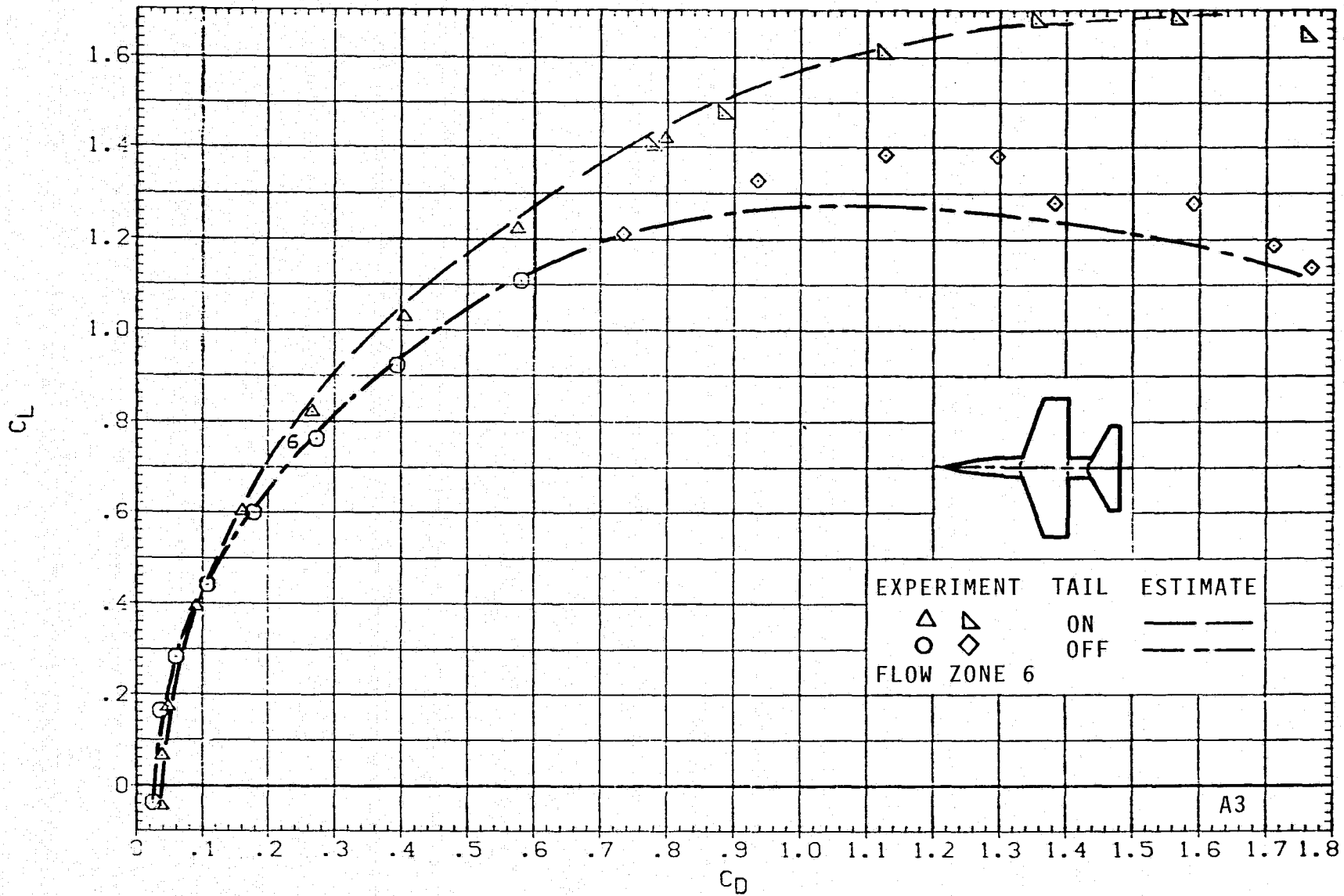
(1)  $C_L$  VERSUS  $C_m$ ;  $M = 1.5$ ,  $J = 5$ .

FIGURE 7.- CONTINUED.



(m)  $C_L$  VERSUS  $\alpha$ ;  $M = 2.0$ ,  $J = 5$ .

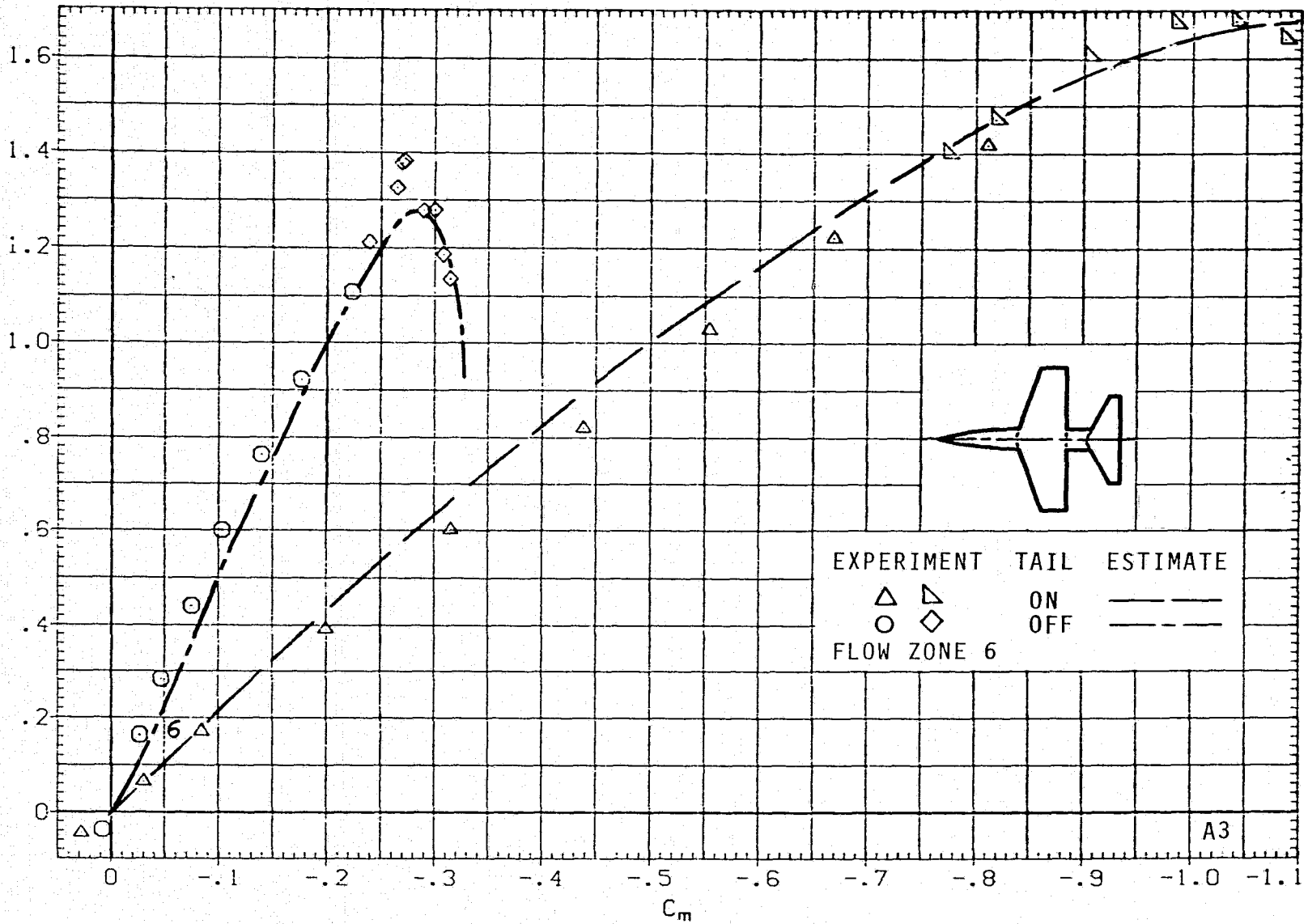
FIGURE 7.- CONTINUED.



(n)  $C_L$  VERSUS  $C_D$ ;  $M = 2.0$ ,  $J = 5$ .

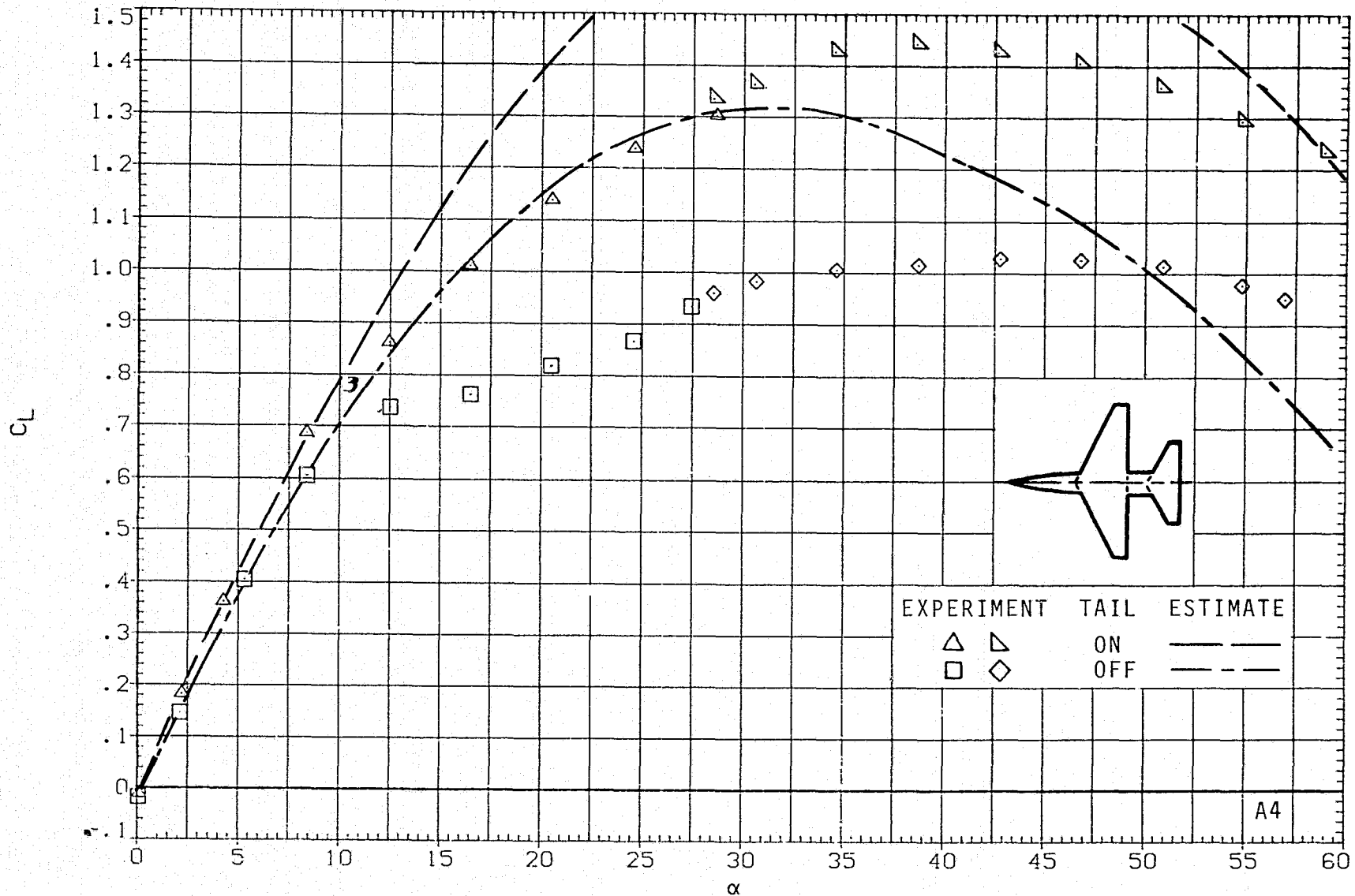
FIGURE 7.- CONTINUED.

$C_L$



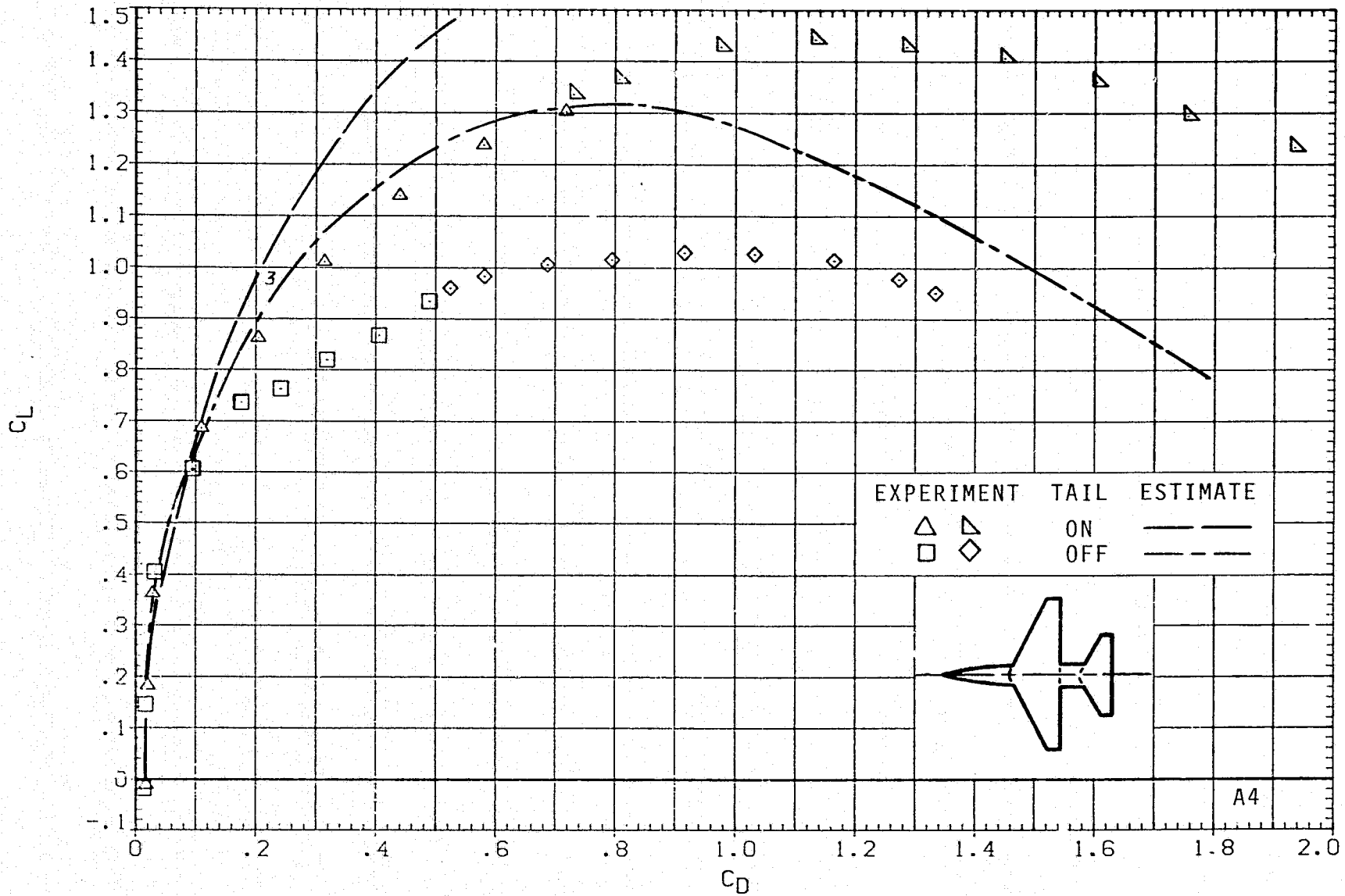
(o)  $C_L$  VERSUS  $C_m$ ;  $M = 2.0$ ,  $J = 5$ .

FIGURE 7.- CONCLUDED.



(a)  $C_L$  VERSUS  $\alpha$ ;  $M = 0.6$ ,  $J = 1$ .

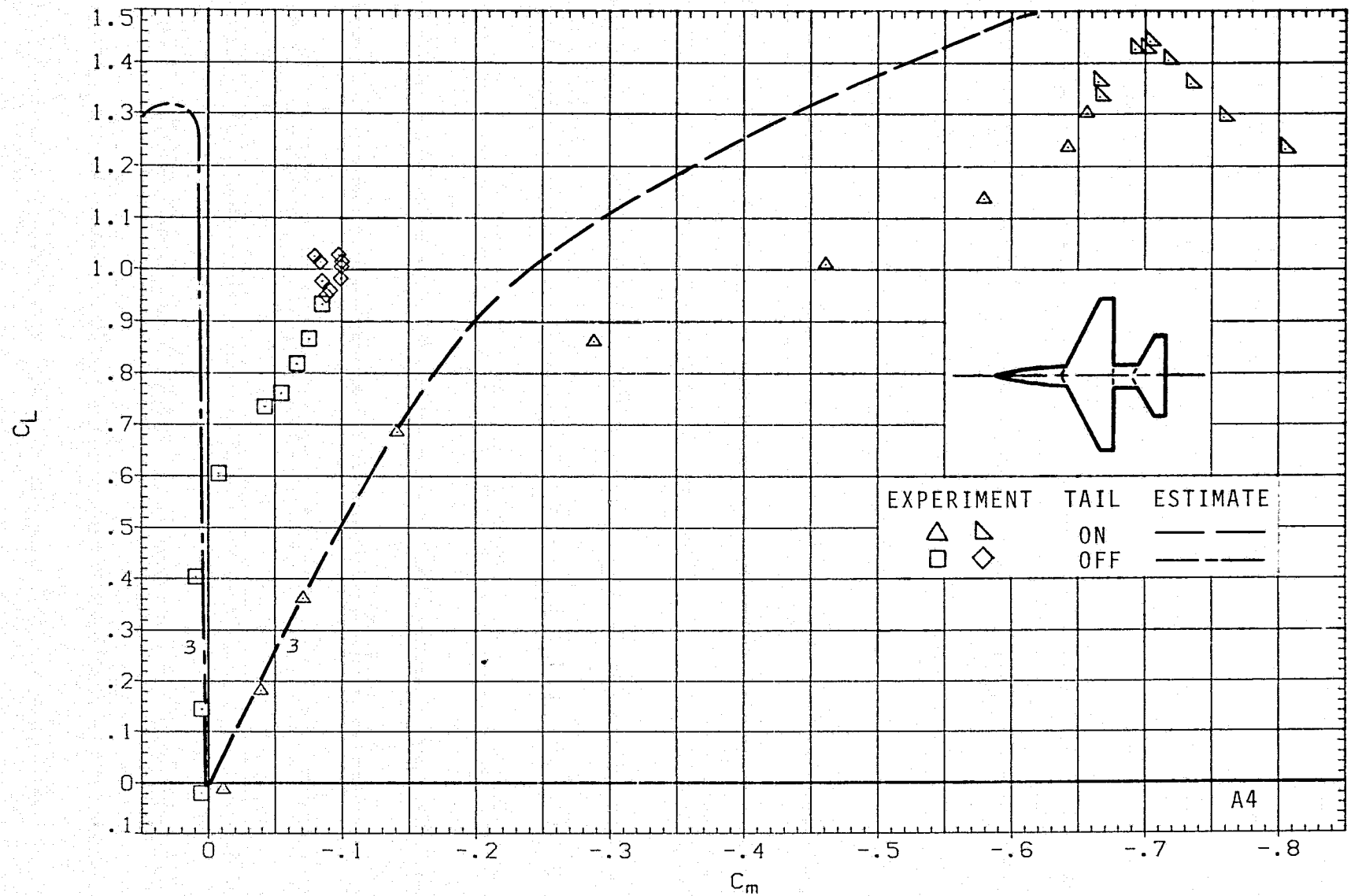
FIGURE 8.- AERODYNAMICS FOR MODEL A4;  $ARW = 5$ ,  $TRW = 0.25$ .



(b)  $C_L$  VERSUS  $C_D$ ;  $M = 0.6$ ,  $J = 1$ .

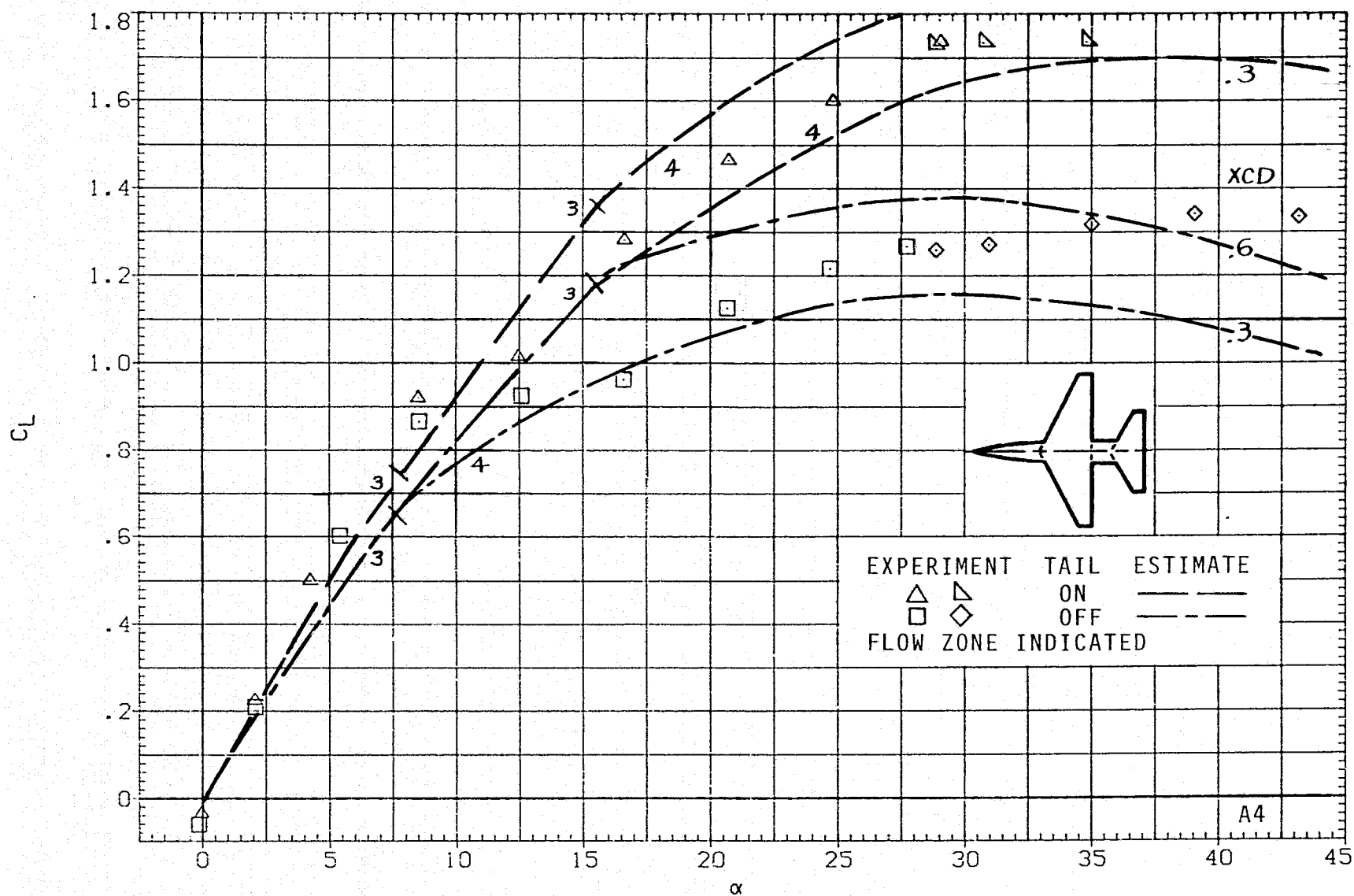
FIGURE 8.- CONTINUED.





(c)  $C_L$  VERSUS  $C_m$ ;  $M = 0.6$ ,  $J = 1$ .

FIGURE 8.- CONTINUED.



(d)  $C_L$  VERSUS  $\alpha$ ;  $M = 0.9$ ,  $J = 1$ .

FIGURE 8.- CONTINUED.

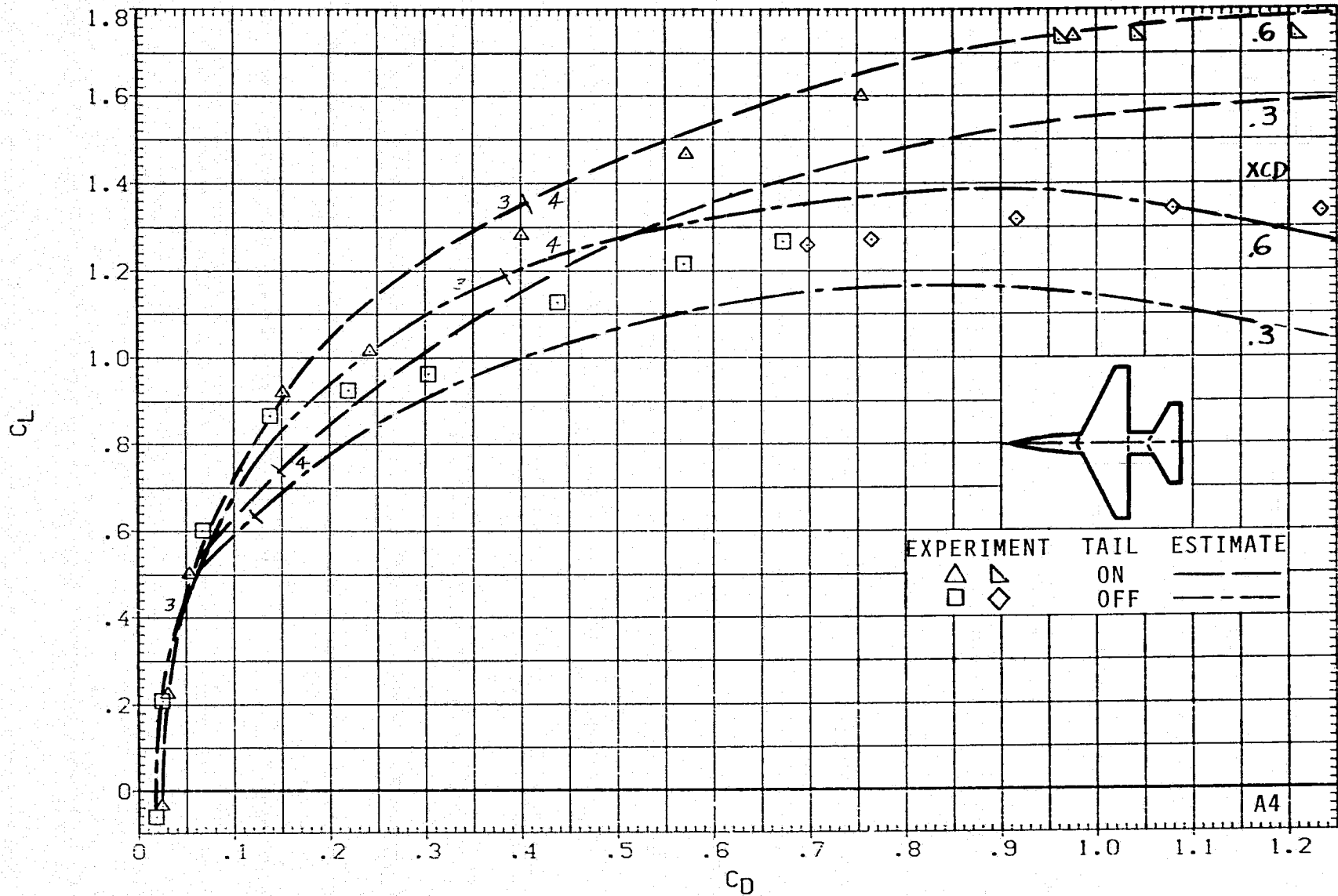
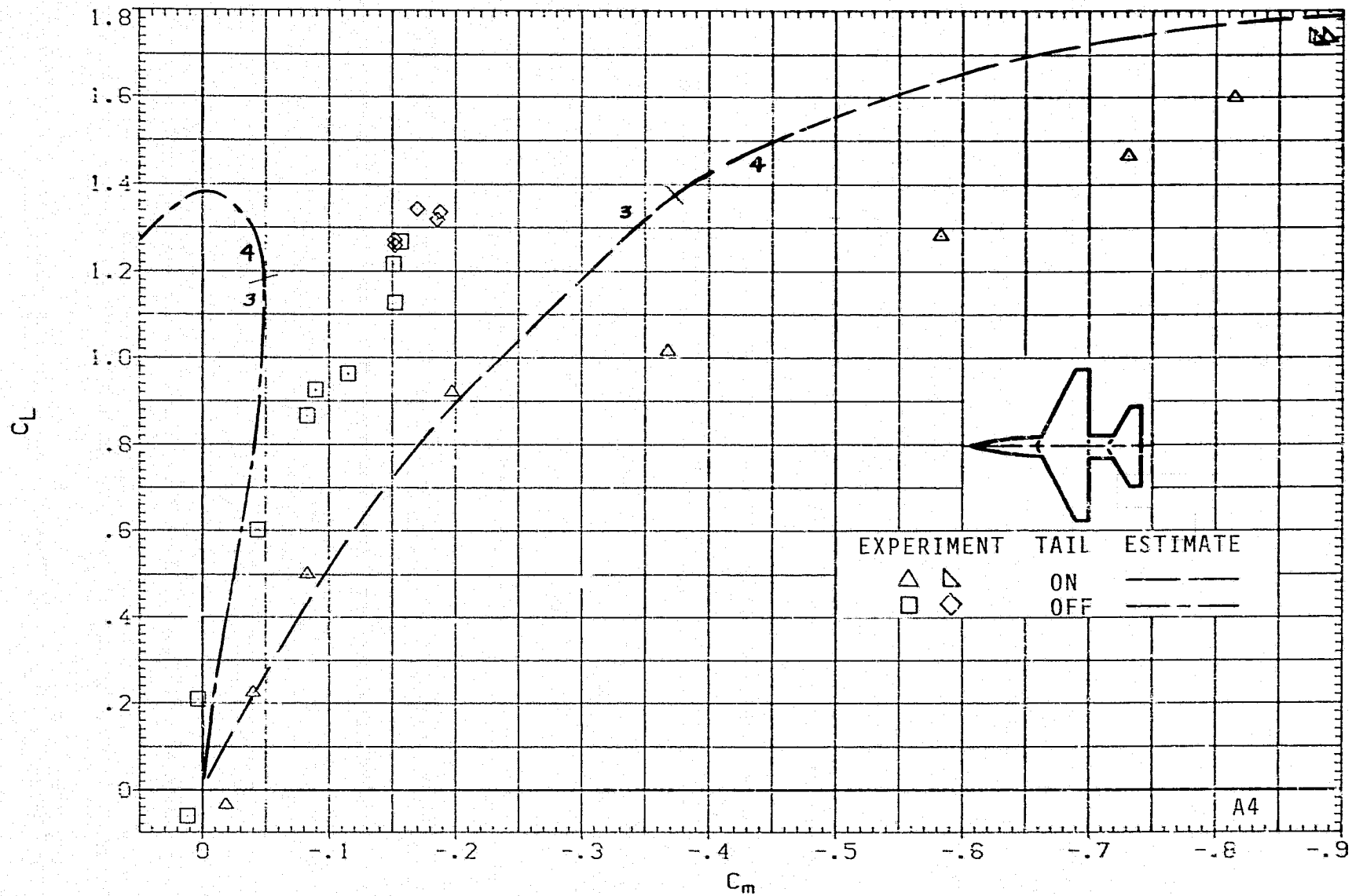
(e)  $C_L$  VERSUS  $C_D$ ;  $M = 0.9$ ,  $J = 1$ .

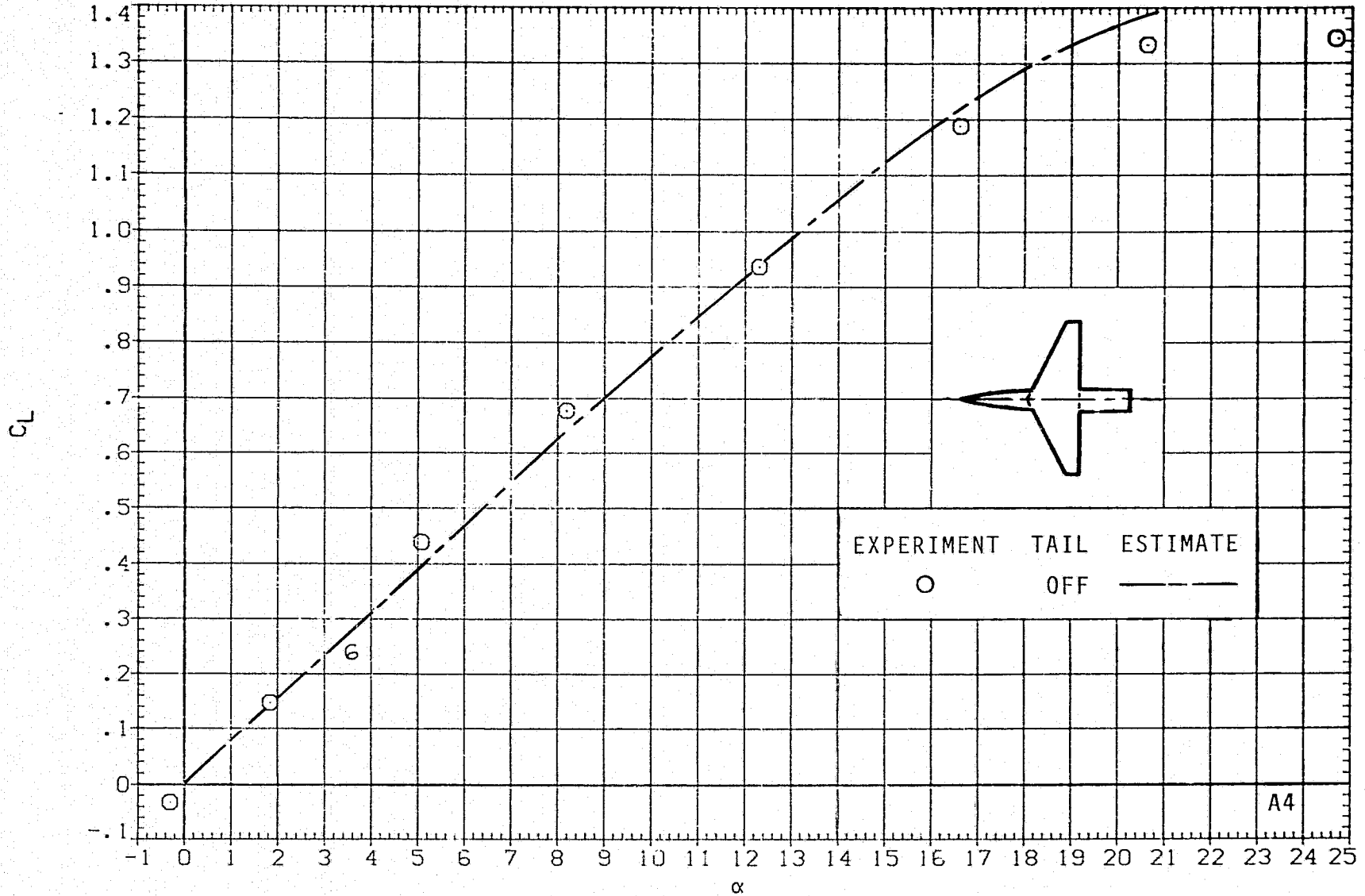
FIGURE 8.- CONTINUED.



(f)  $C_L$  VERSUS  $C_m$ ;  $M = 0.9$ ,  $J = 1$ .

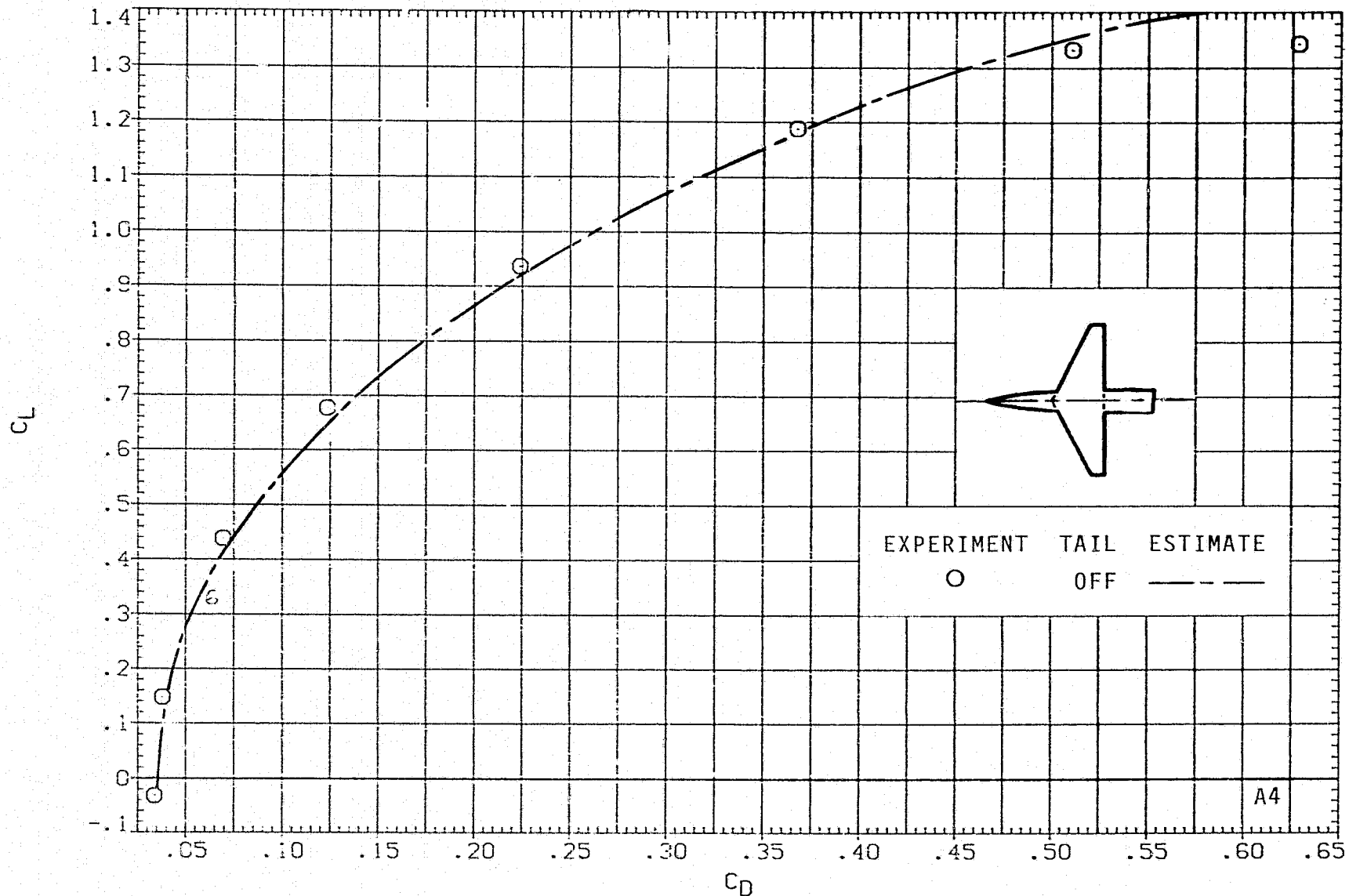
FIGURE 8.- CONTINUED.

A4



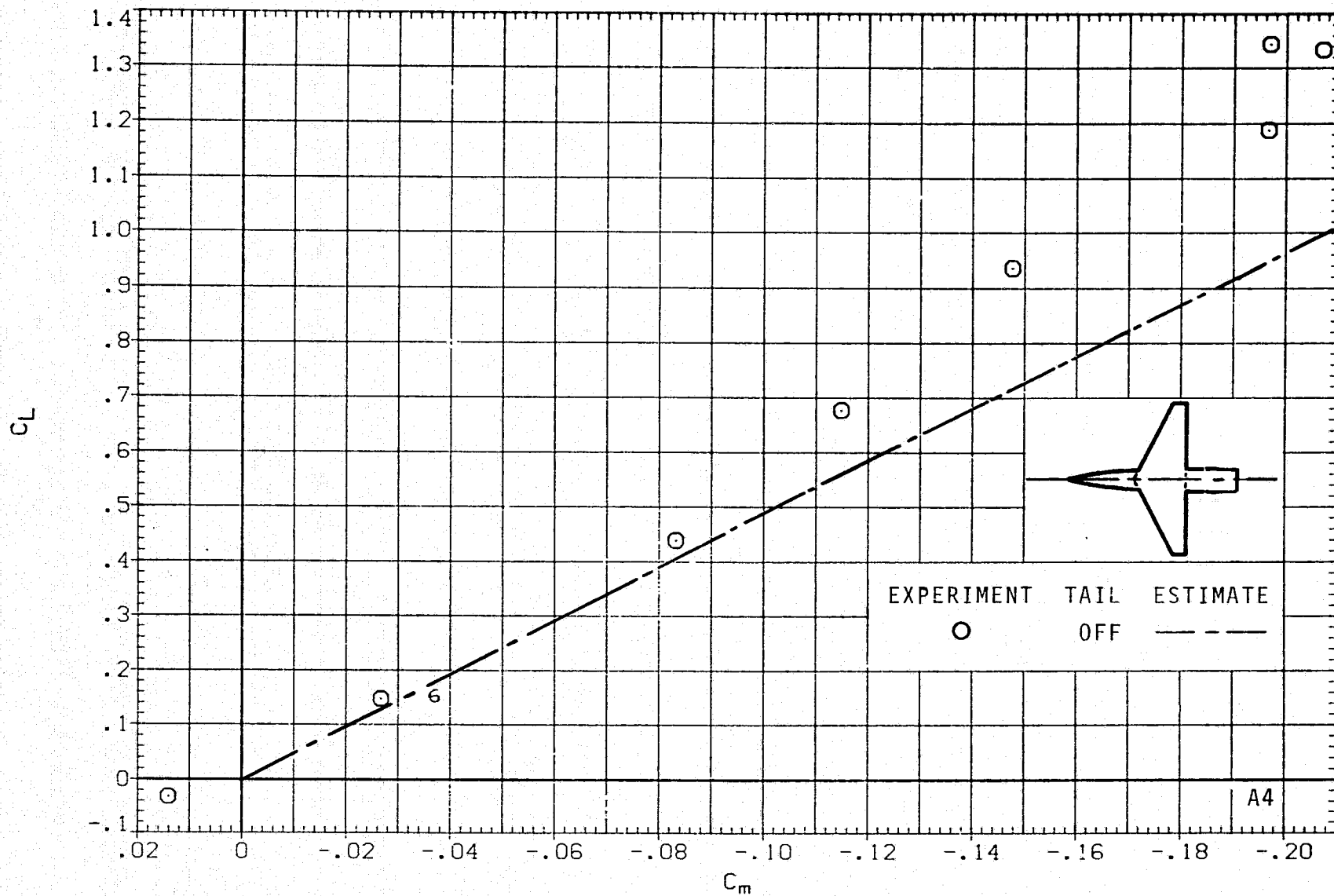
(g)  $C_L$  VERSUS  $\alpha$ ;  $M = 1.2$ ,  $J = 5$ .

FIGURE 8.- CONTINUED.



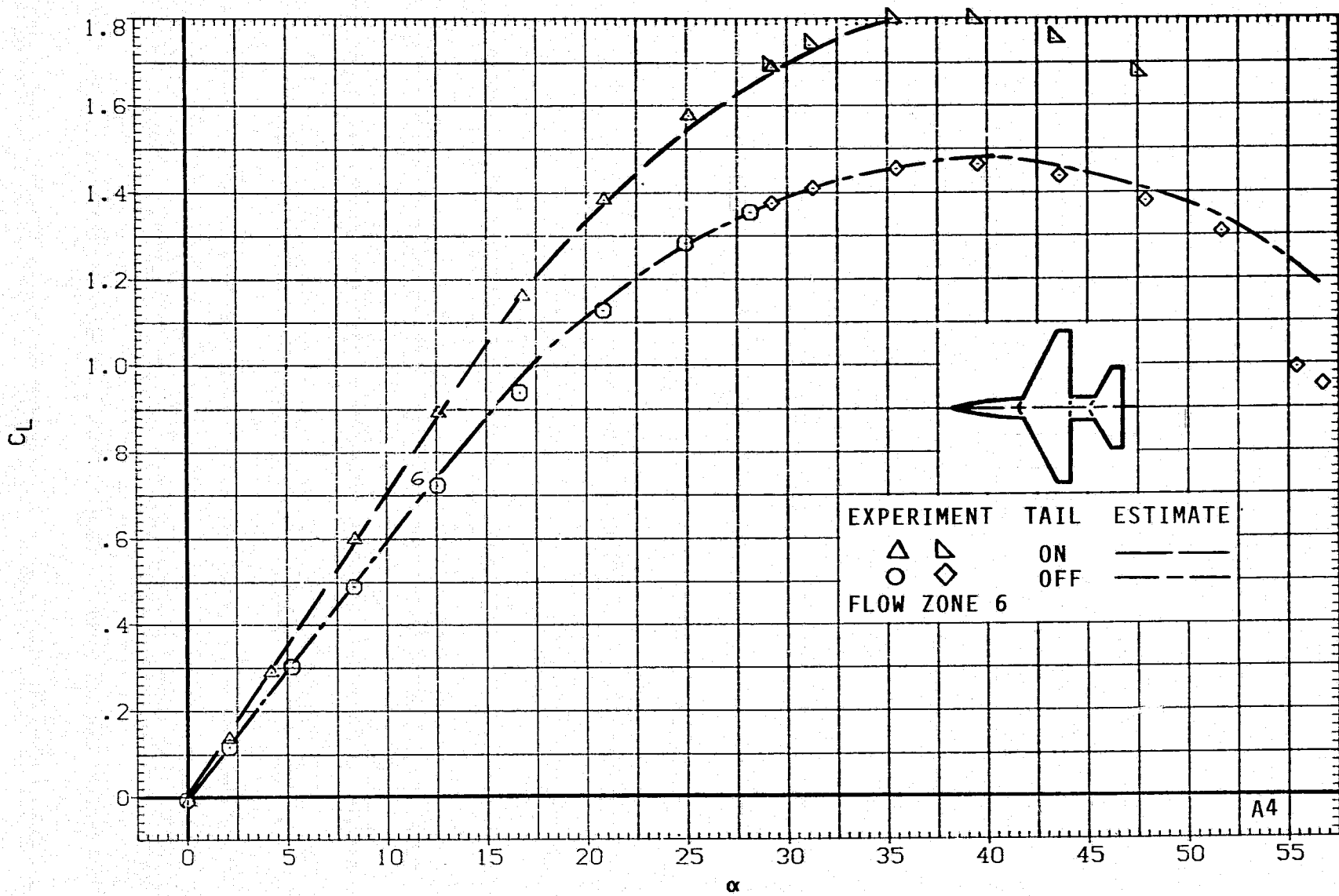
(h)  $C_L$  VERSUS  $C_D$ ;  $M = 1.2$ ,  $J = 5$ .

FIGURE 8.- CONTINUED.



(i)  $C_L$  VERSUS  $C_m$ ;  $M = 1.2$ ,  $J = 5$ .

FIGURE 8.- CONTINUED.

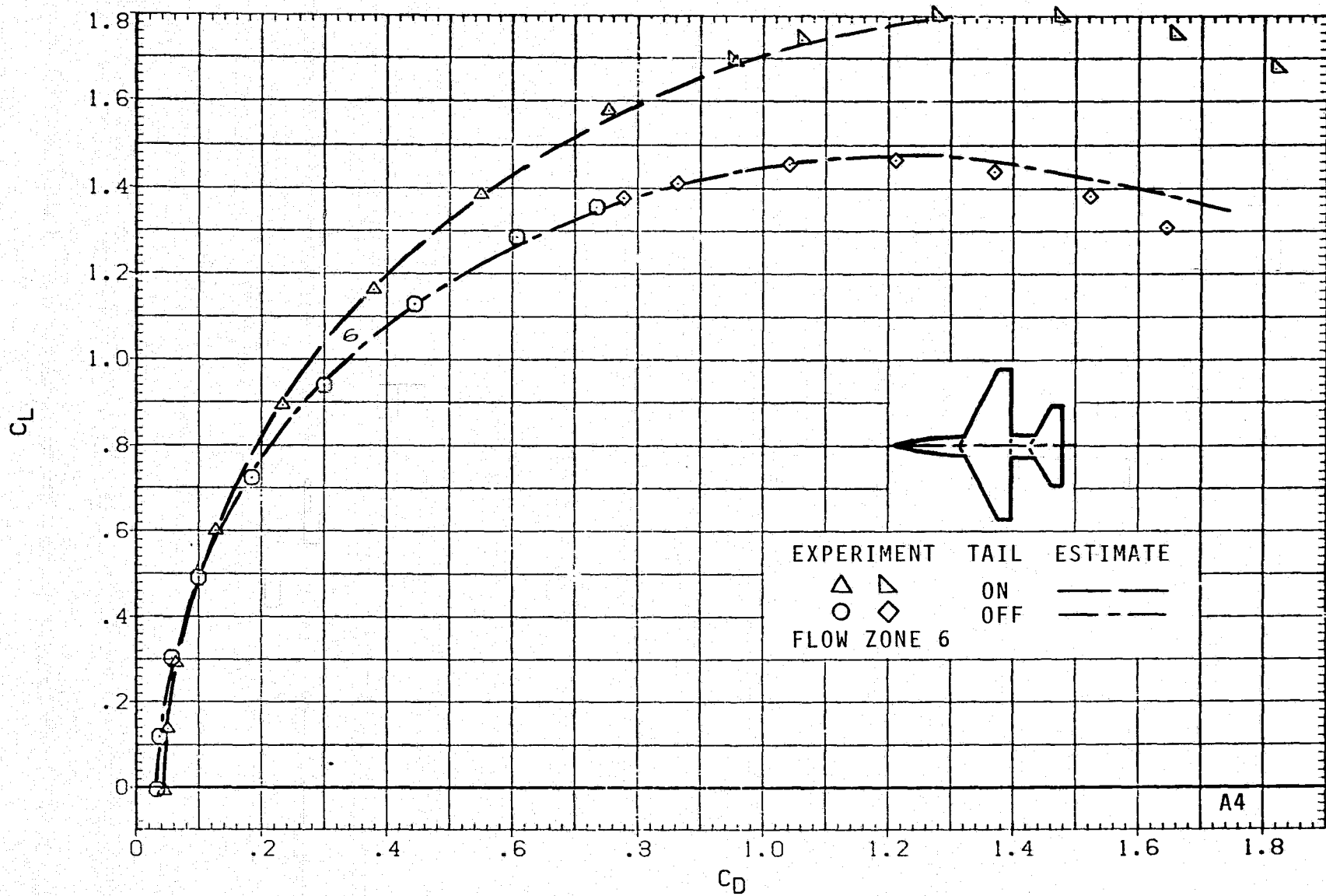


(j)  $C_L$  VERSUS  $\alpha$ ;  $M = 1.5$ ,  $J = 5$ .

FIGURE 8.- CONTINUED.

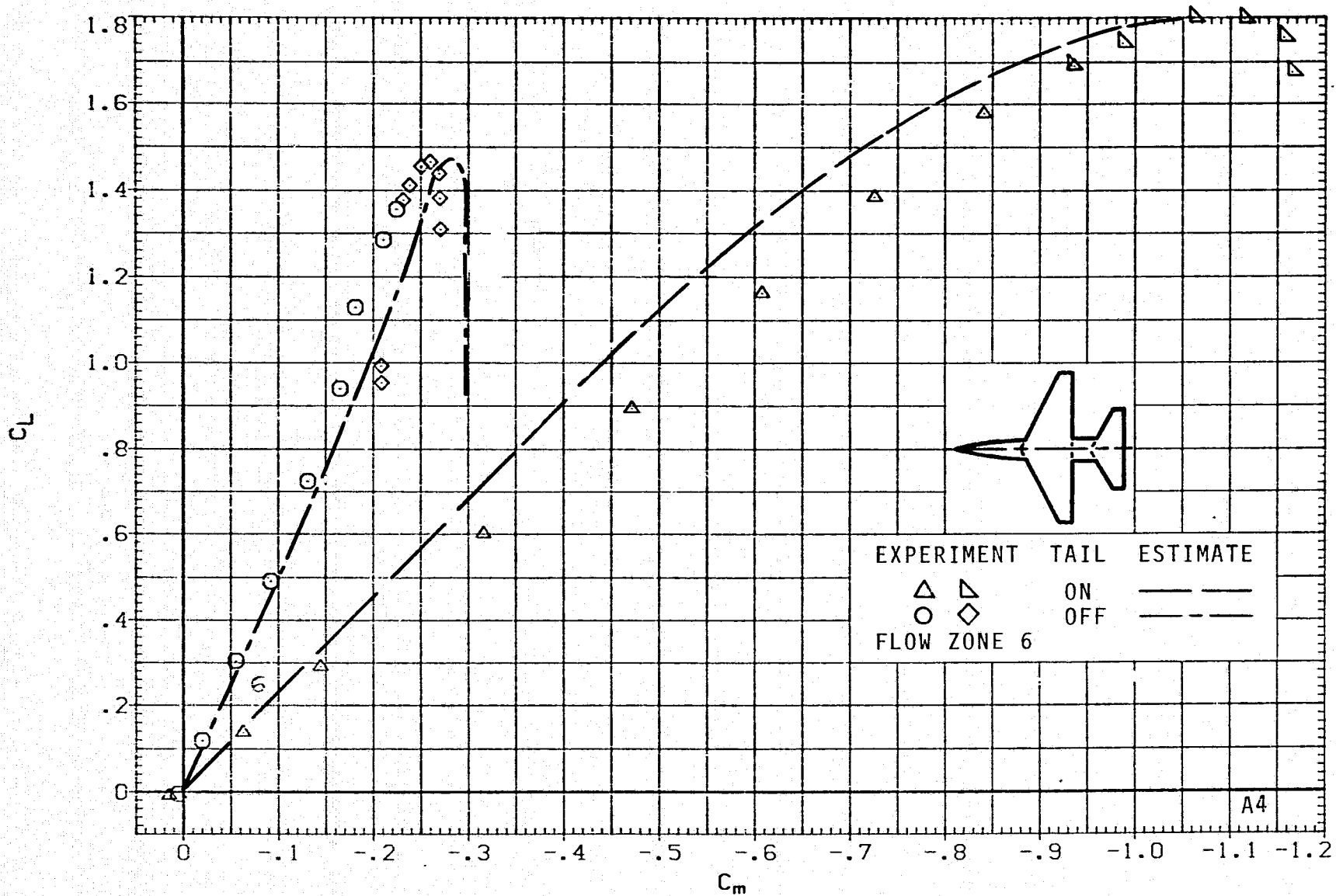
A4





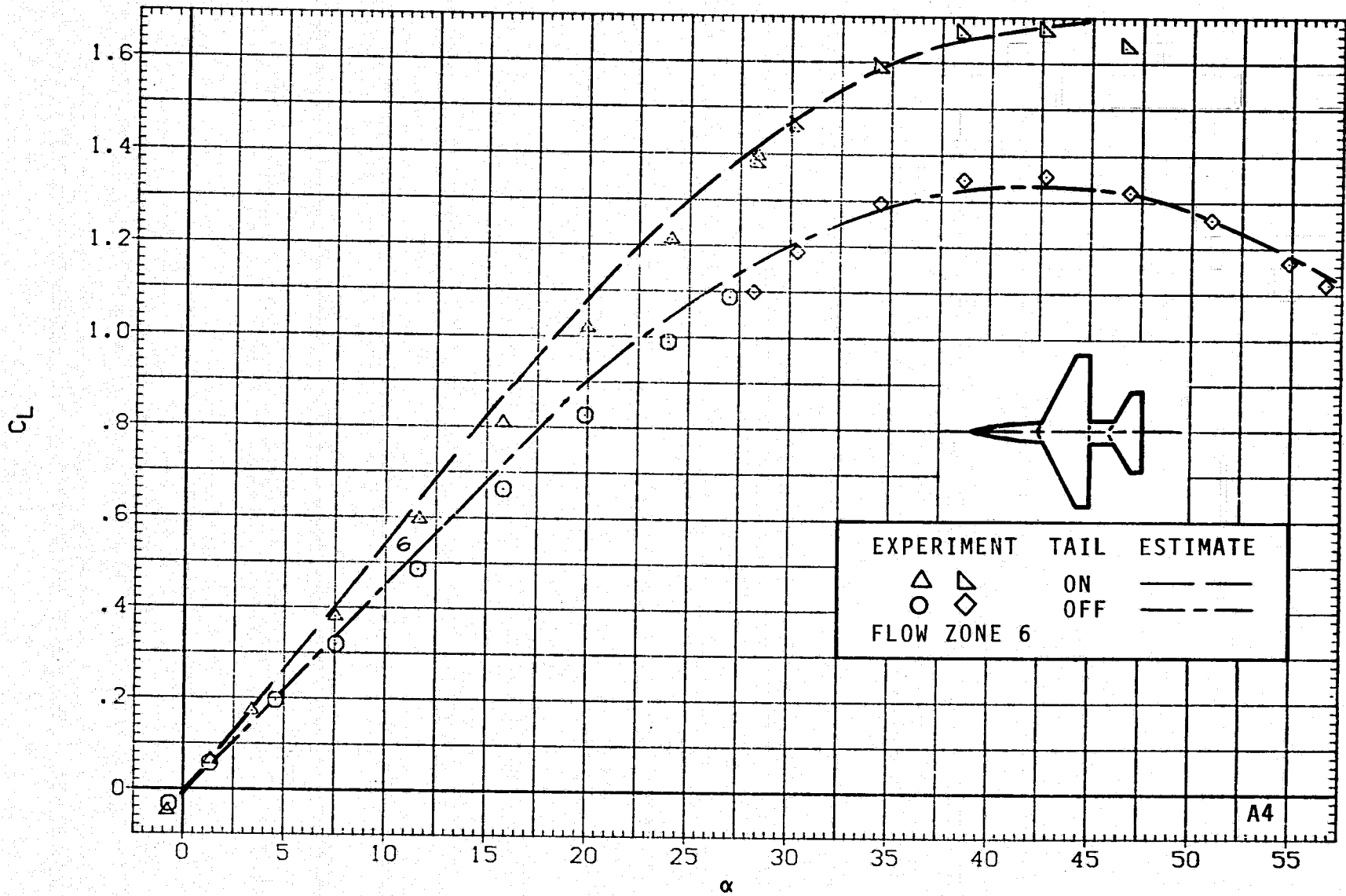
(k)  $C_L$  VERSUS  $C_D$ ;  $M = 1.5$ ,  $J = 5$ .

FIGURE 8.- CONTINUED.



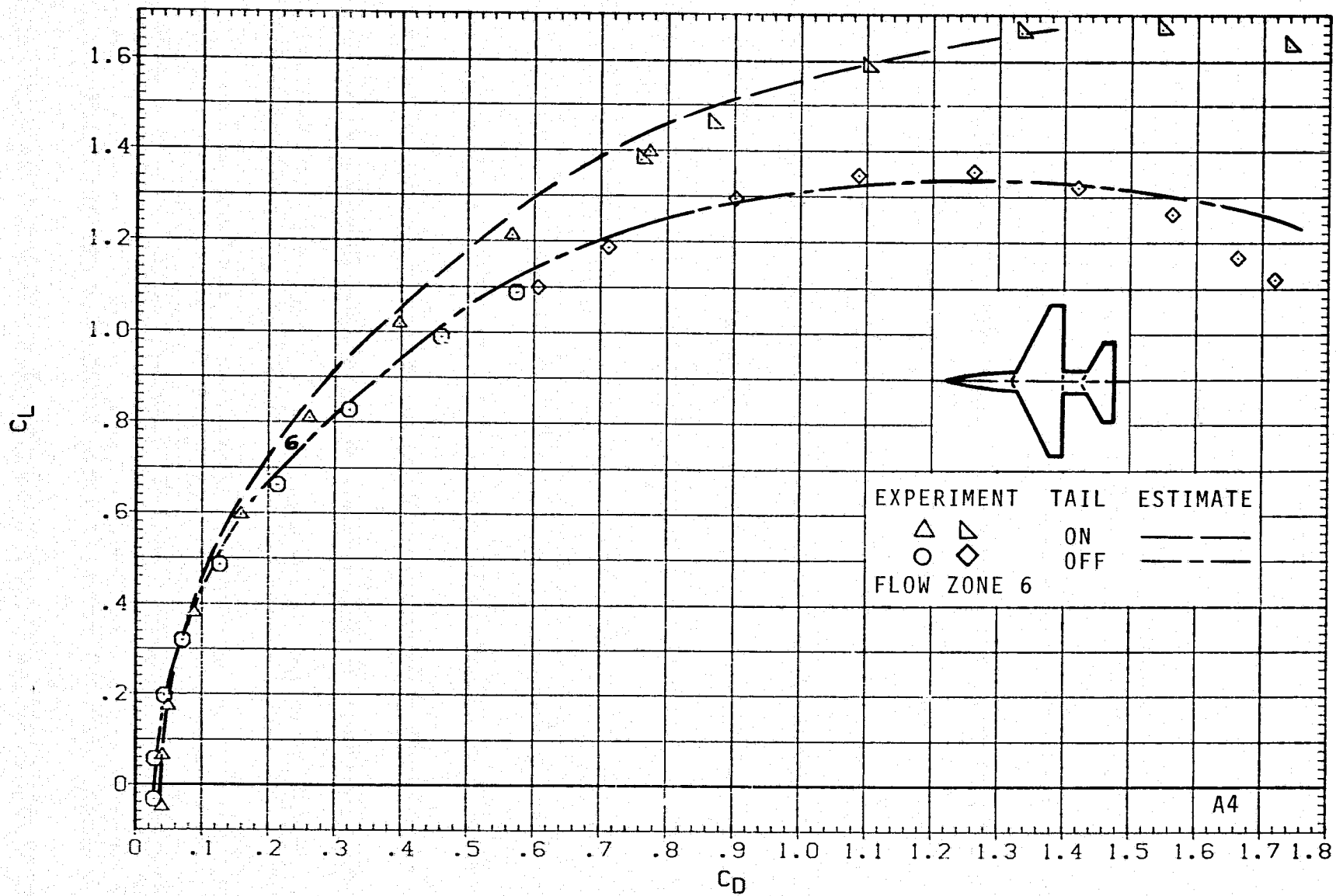
(1)  $C_L$  VERSUS  $C_m$ ;  $M = 1.5$ ,  $J = 5$ .

FIGURE 8.- CONTINUED.



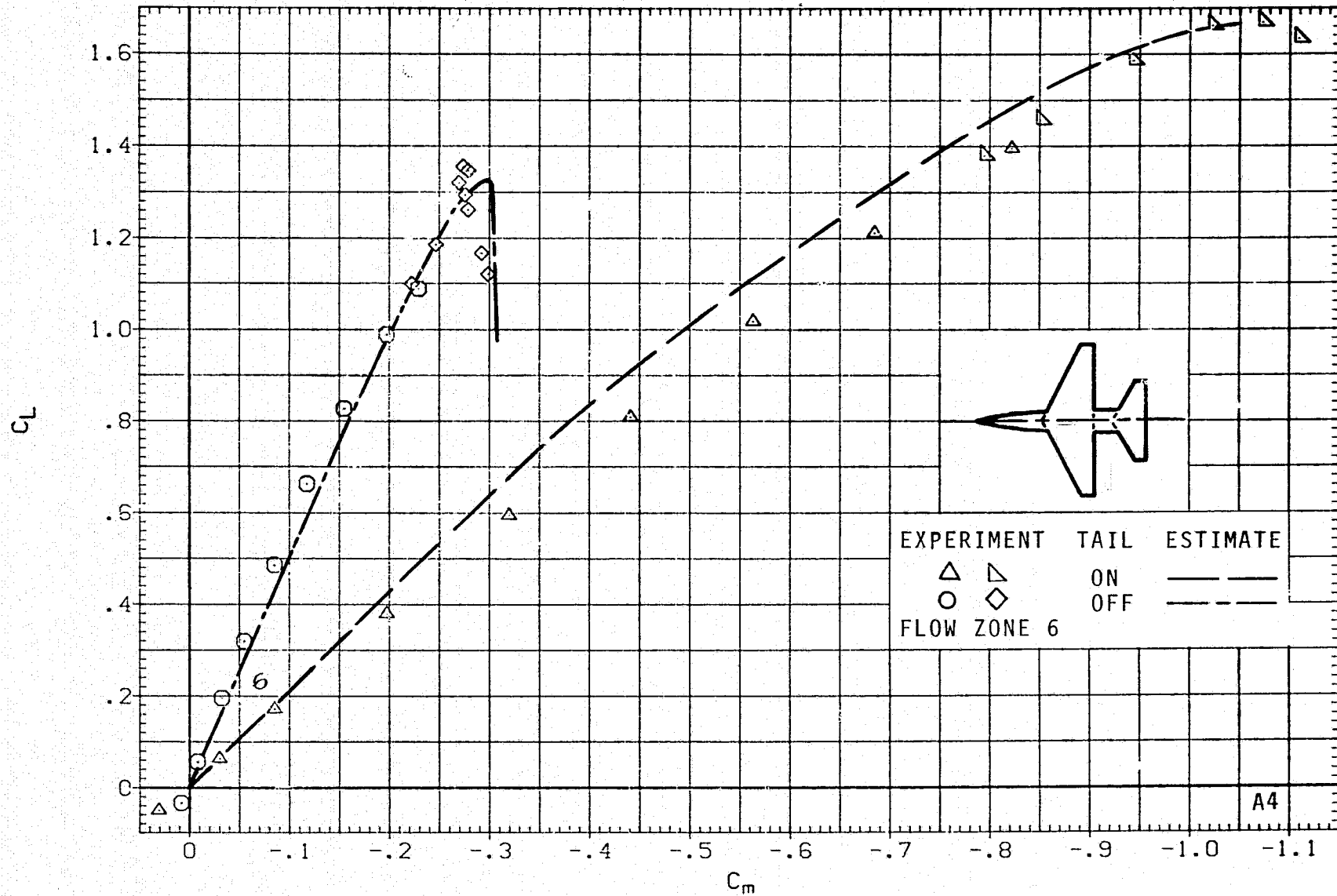
(m)  $C_L$  VERSUS  $\alpha$ ;  $M = 2.0$ ,  $J = 5$ .

FIGURE 8.- CONTINUED.



(n)  $C_L$  VERSUS  $C_D$ ;  $M = 2.0$ ,  $J = 5$ .

FIGURE 8.- CONTINUED.

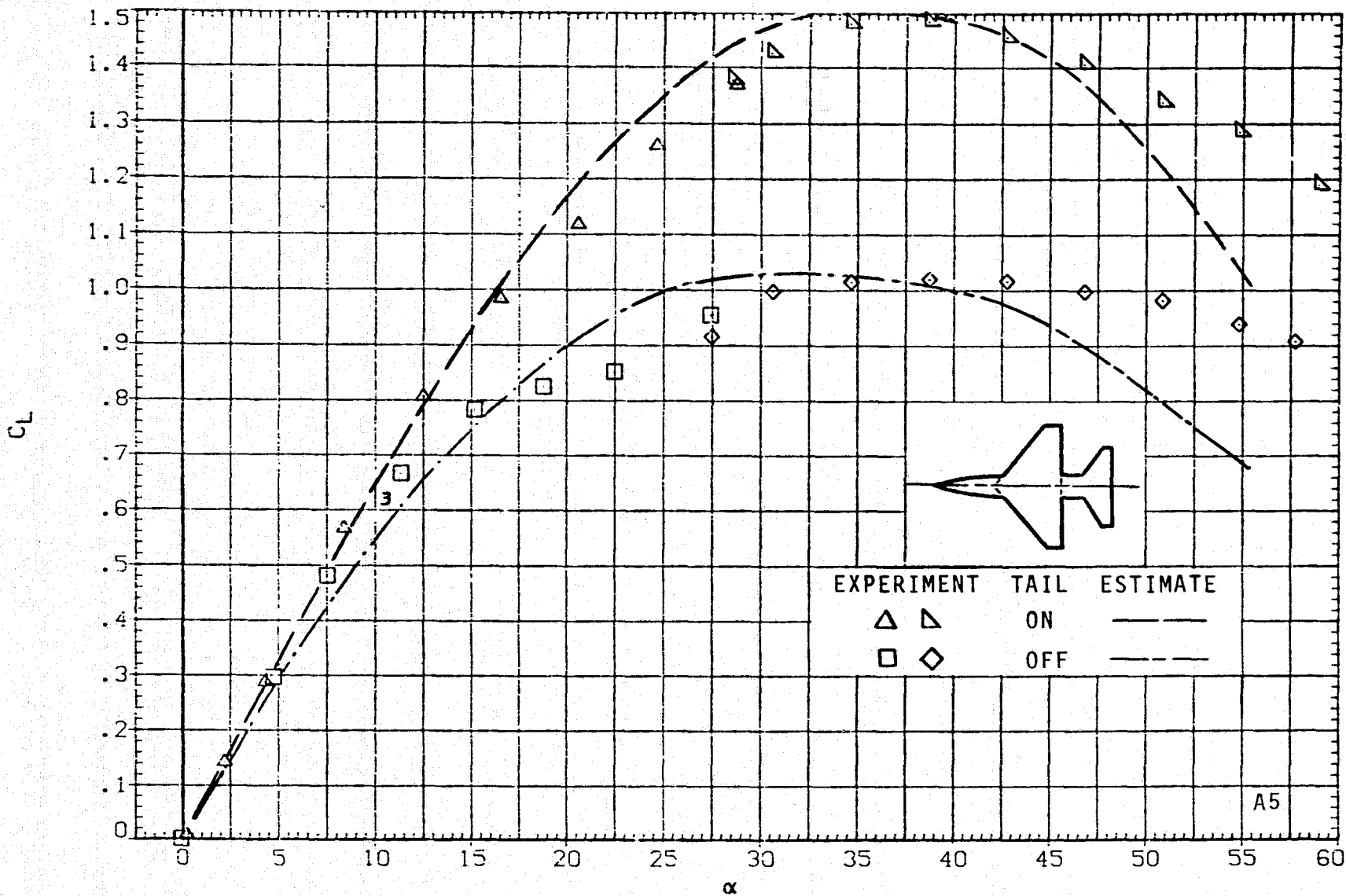


(o)  $C_L$  VERSUS  $C_m$ ;  $M = 2.0$ ,  $J = 5$ .

FIGURE 8.- CONCLUDED.

# RESEARCH MODEL

$M = 0.60$

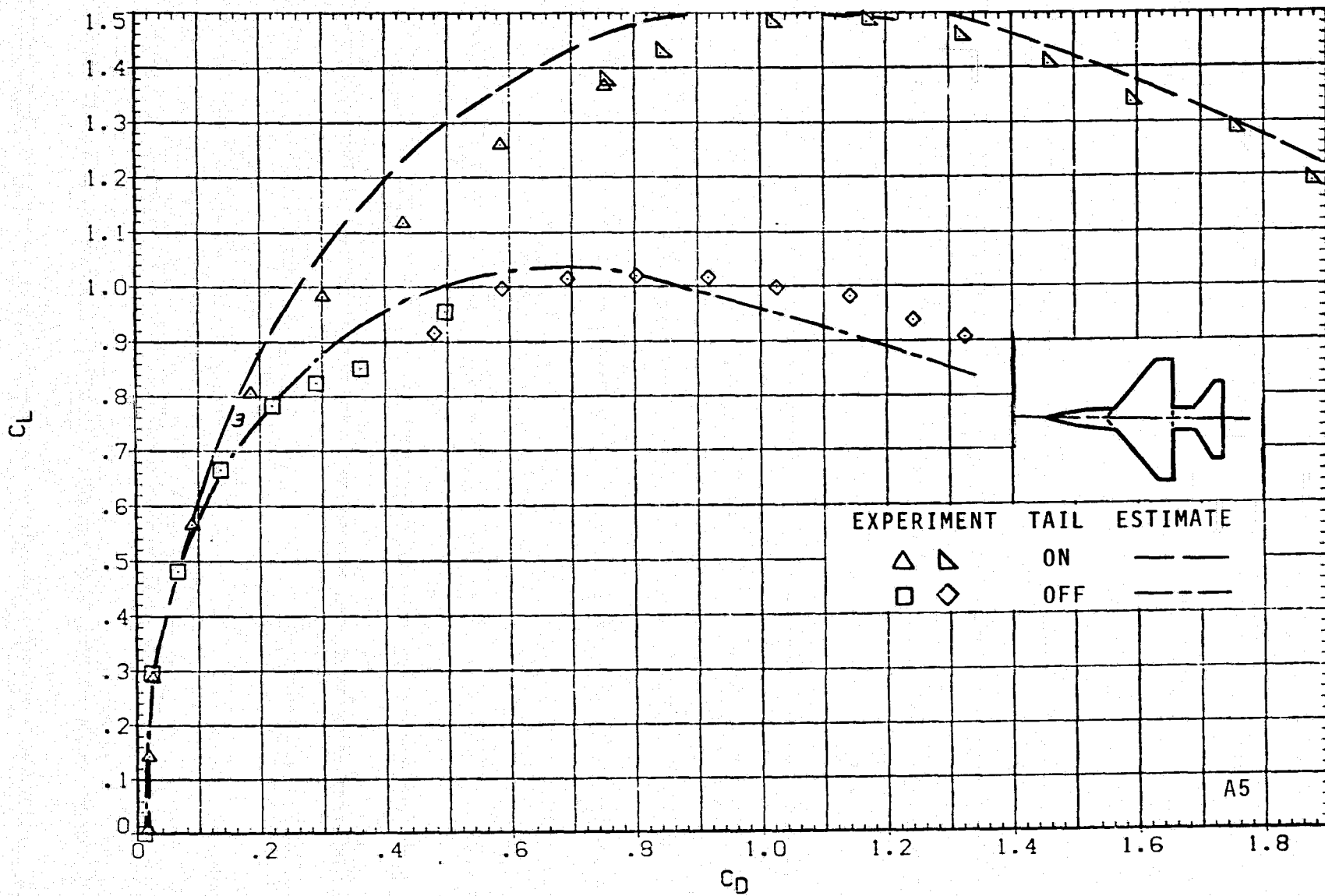


(a)  $C_L$  VERSUS  $\alpha$ ;  $M = 0.6$ ,  $J = 1$ .

FIGURE 9.- AERODYNAMICS FOR MODEL A5; ARW = 3, TRW = 0.25.

RESEARCH MODEL

M = 0.60

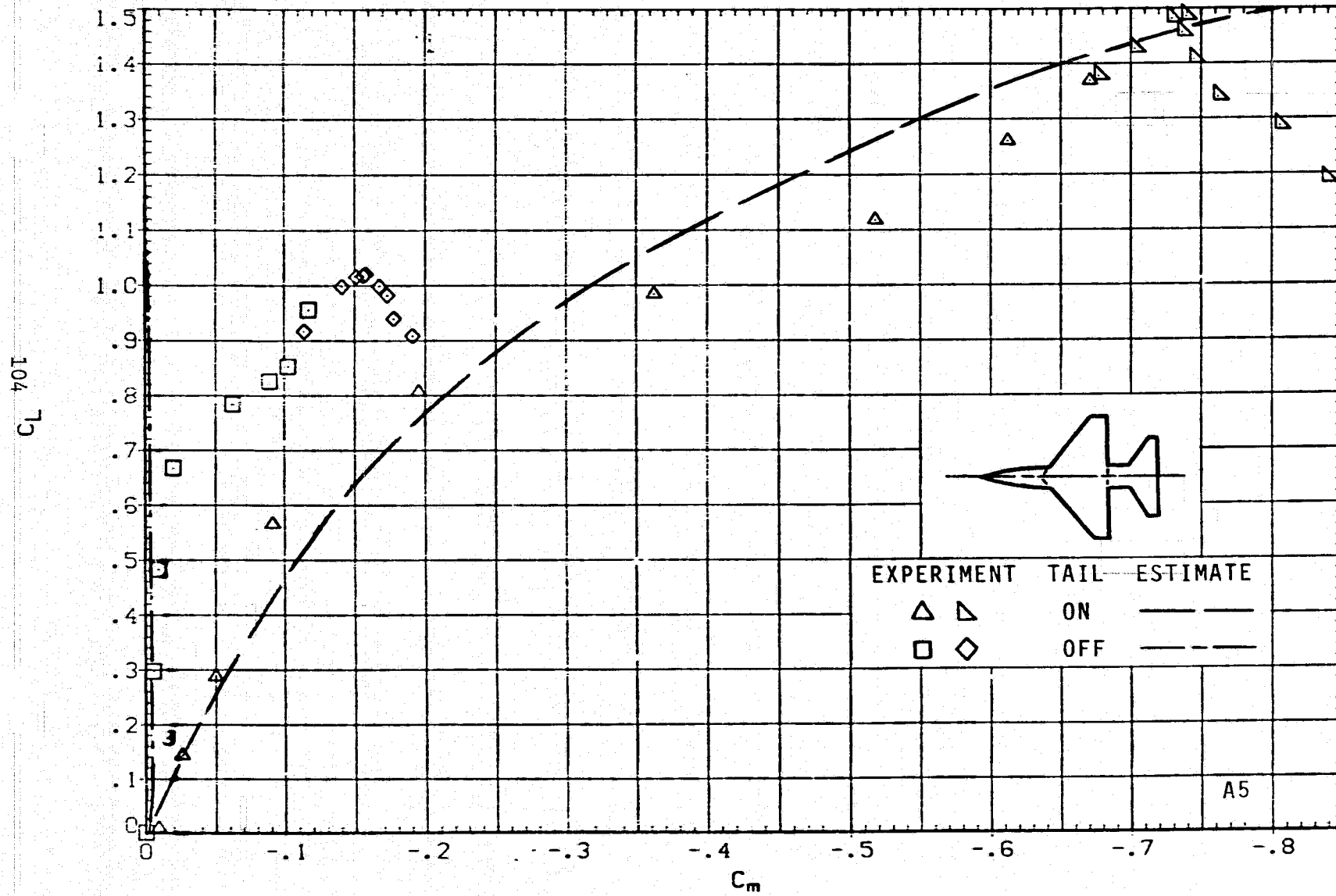


(b)  $C_L$  VERSUS  $C_D$ ; M = 0.6, J = 1.

FIGURE 9.- CONTINUED.

# RESEARCH MODEL

$M = 0.60$



(c)  $C_L$  VERSUS  $C_m$ ;  $M = 0.6$ ,  $J = 1$ .

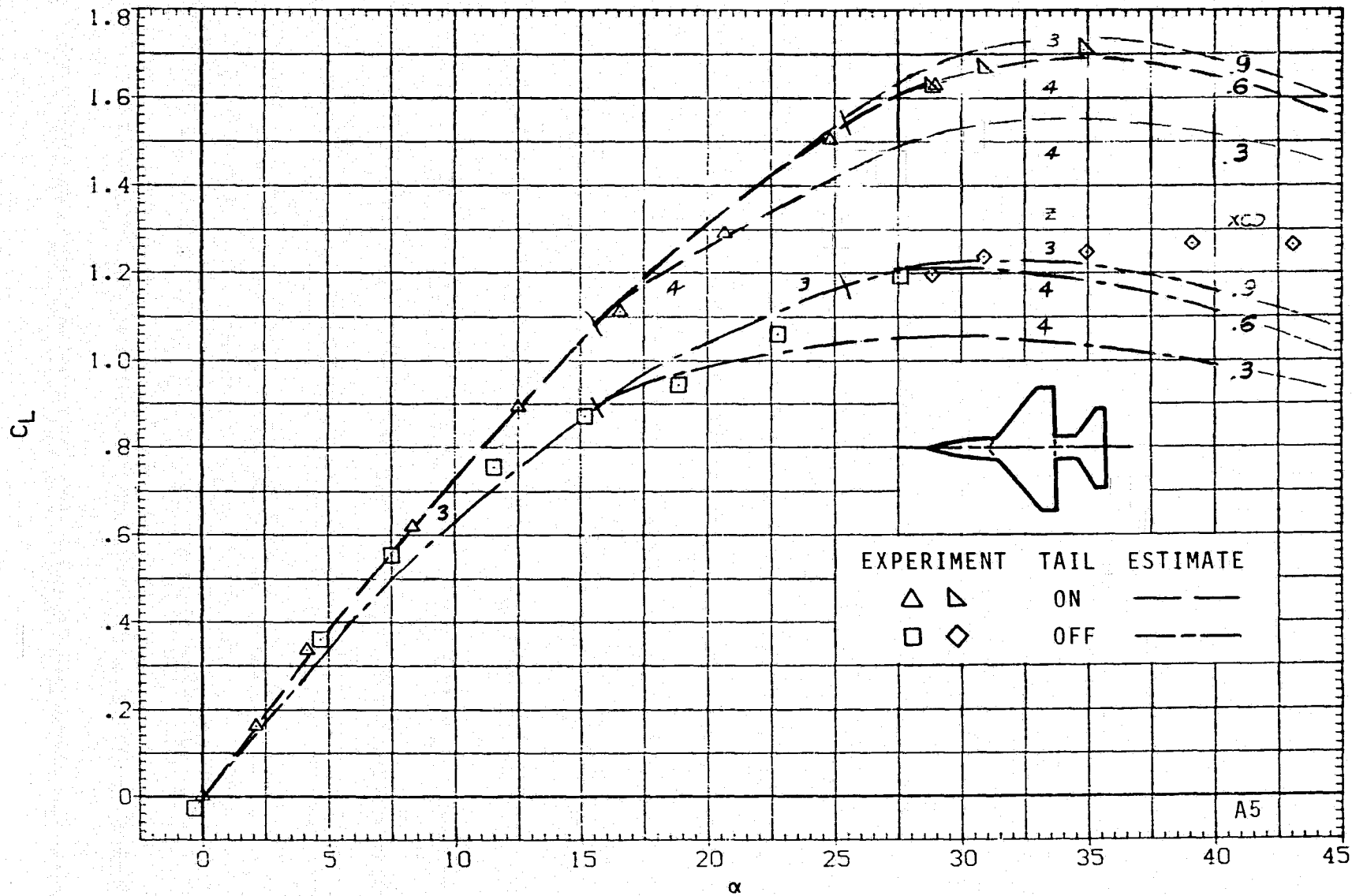
FIGURE 9.- CONTINUED.



# RESEARCH MODEL

$M = 0.90$

105



(d)  $C_L$  VERSUS  $\alpha$ ;  $M = 0.9$ ,  $J = 1$ .

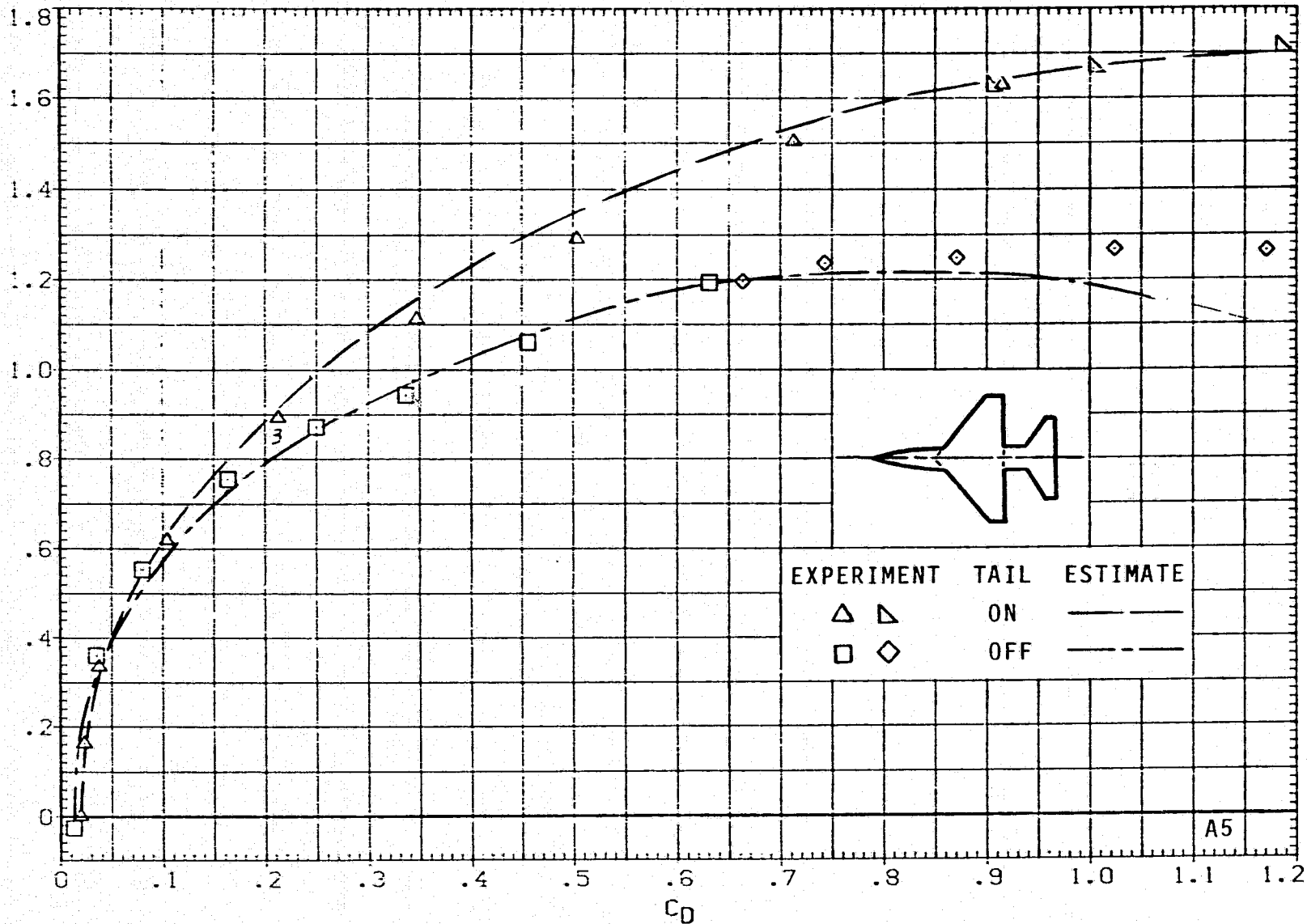
FIGURE 9.- CONTINUED.

A5

# RESEARCH MODEL

M = 0.90

106  
C<sub>L</sub>



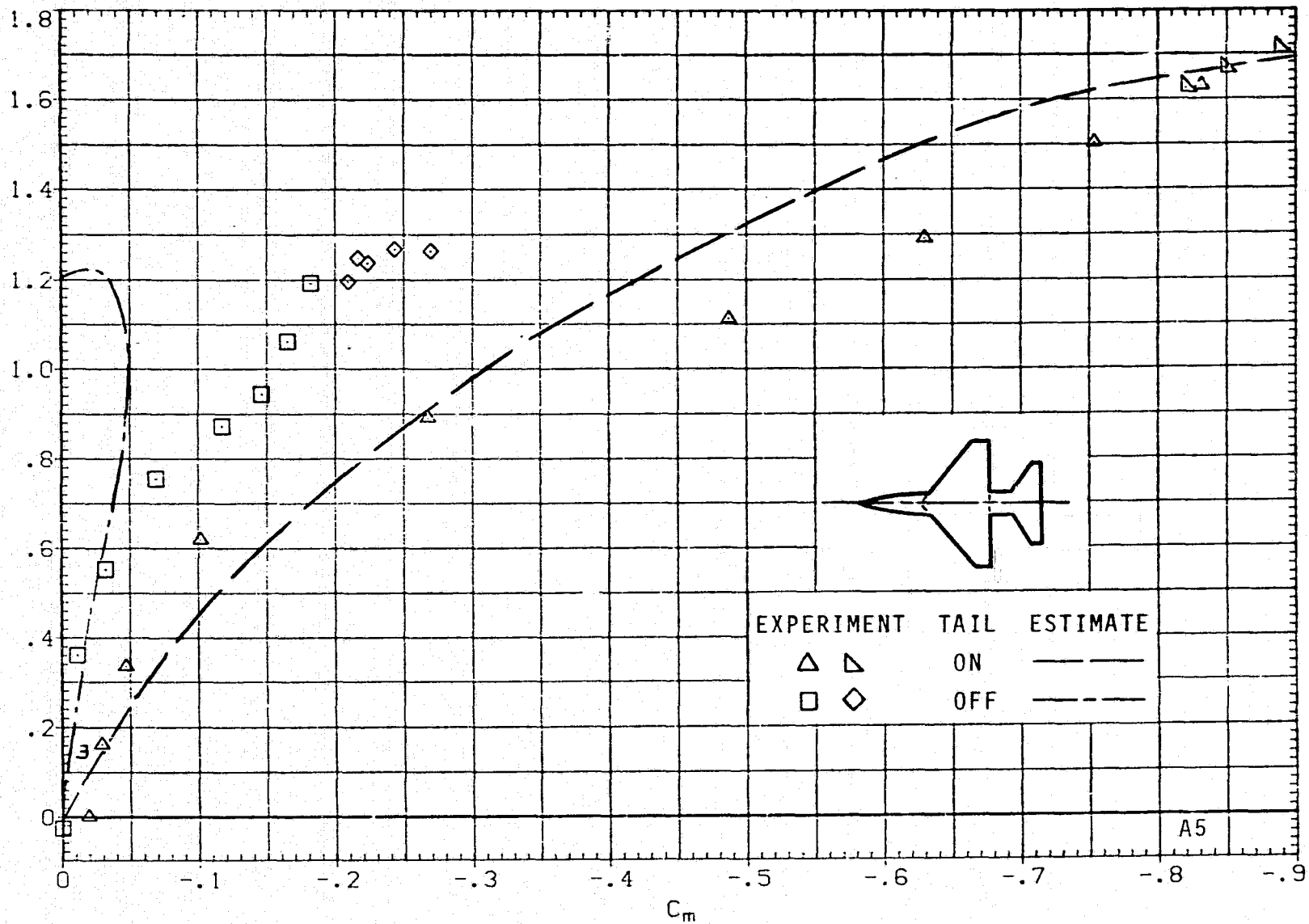
(e) C<sub>L</sub> VERSUS C<sub>D</sub>; M = 0.9, J = 1.

FIGURE 9.- CONTINUED.

A5

# RESEARCH MODEL

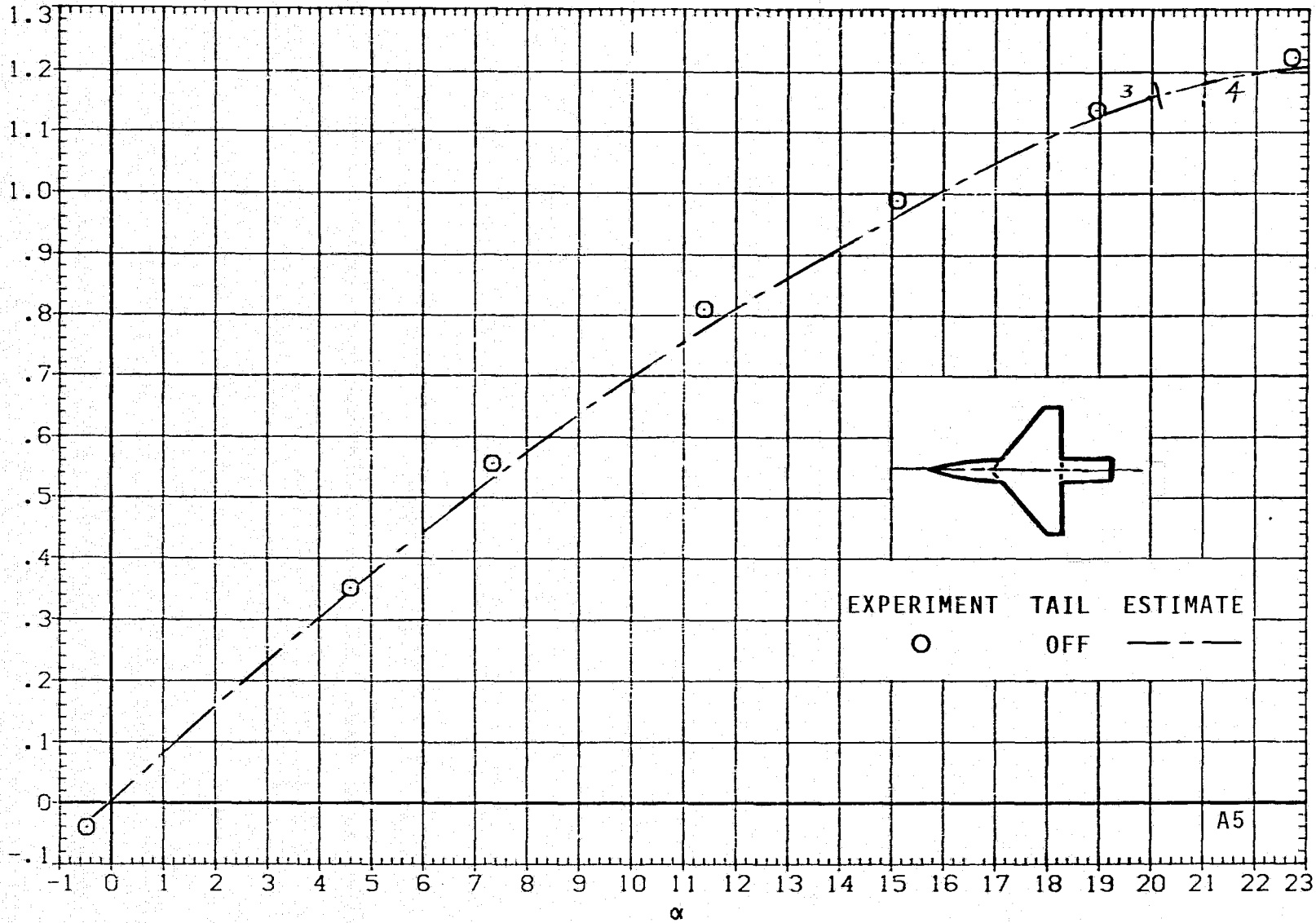
$M = 0.90$



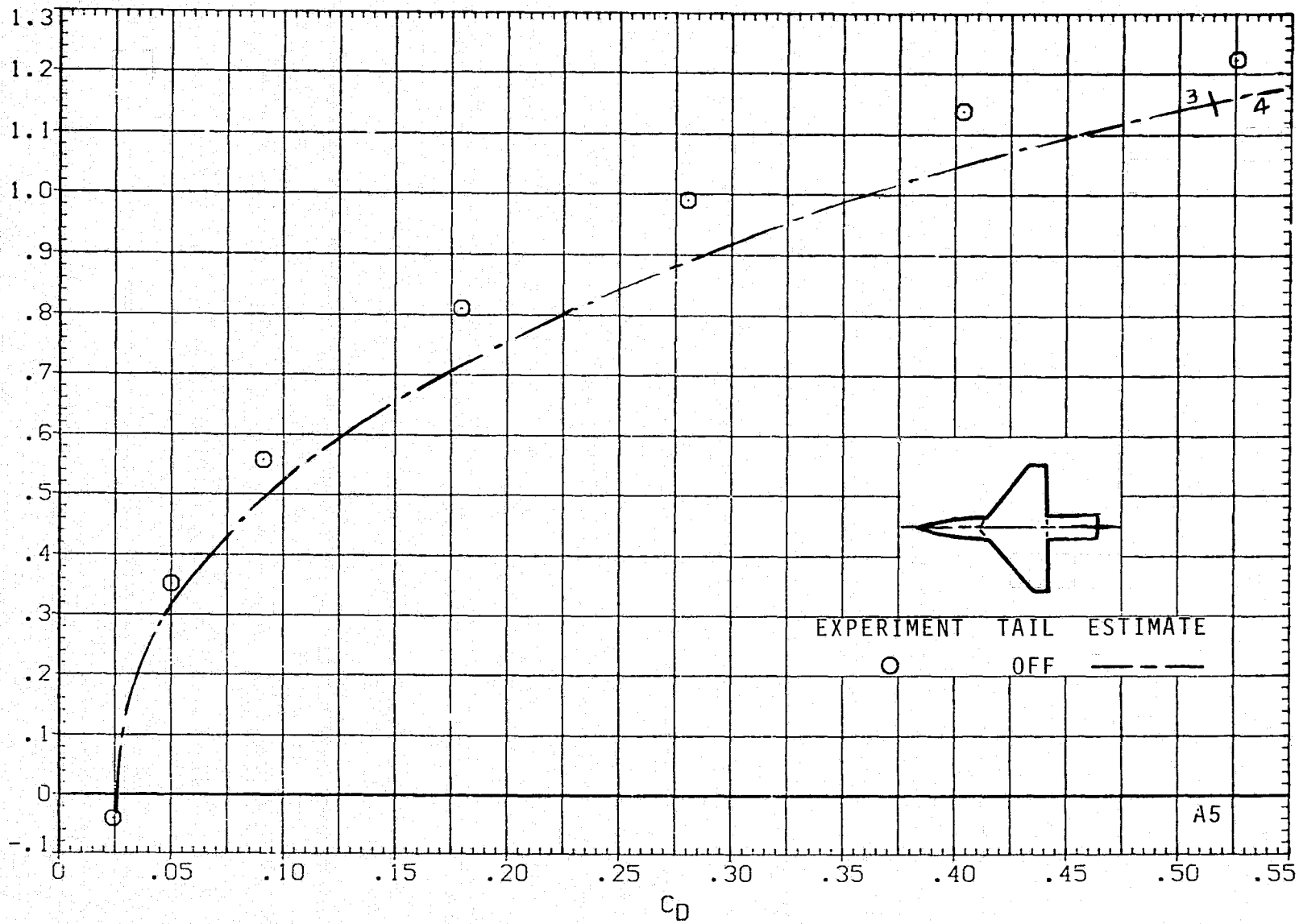
(f)  $C_L$  VERSUS  $C_m$ ,  $M = 0.9$ ,  $J = 1$ .

FIGURE 9.- CONTINUED.

A5



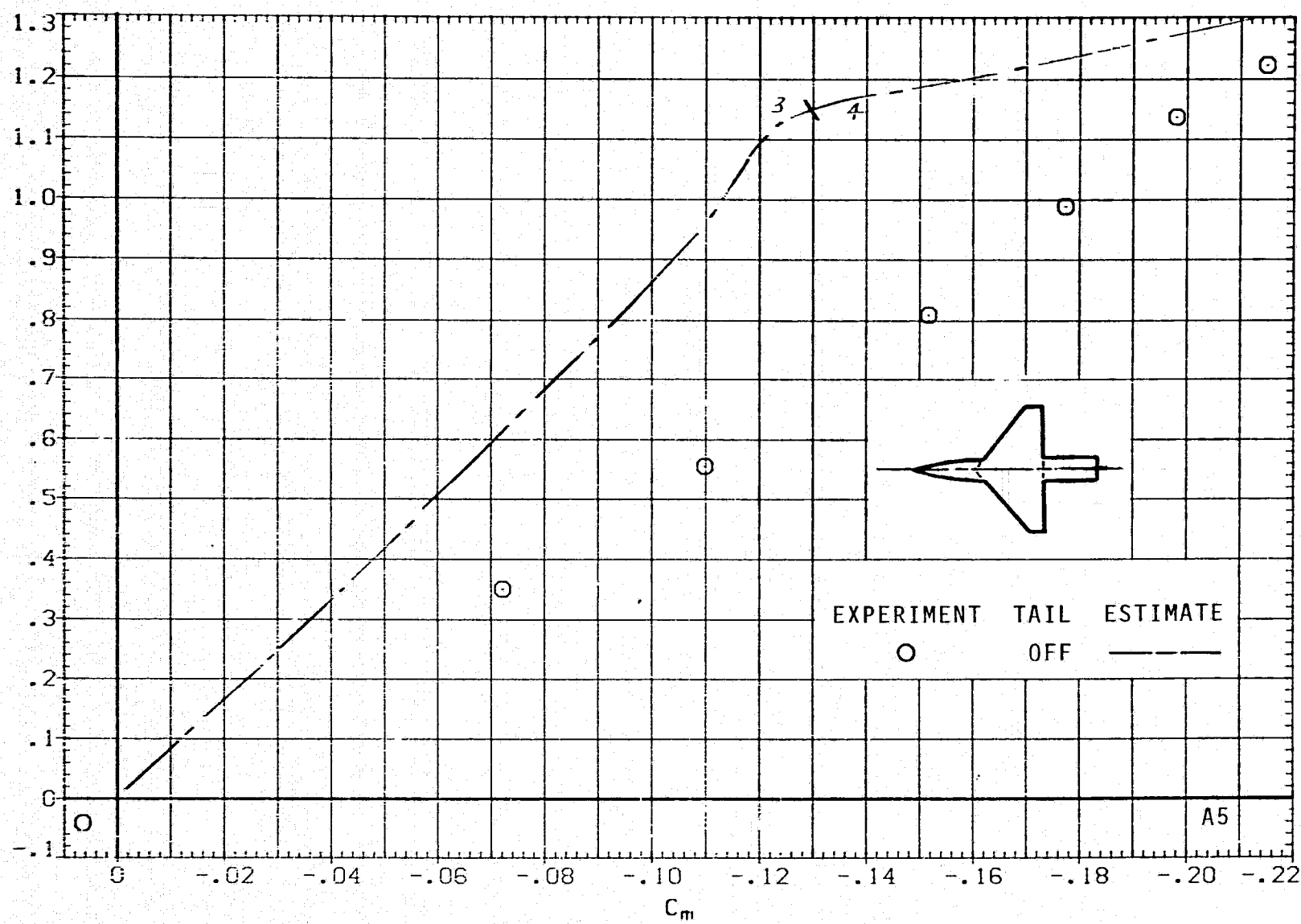
(g)  $C_L$  VERSUS  $\alpha$ ;  $M = 1.2$ ,  $J = 1$ .



(h)  $C_L$  VERSUS  $C_D$ ;  $M = 1.2$ ,  $J = 1$ .

FIGURE 9.- CONTINUED.

$C_L$

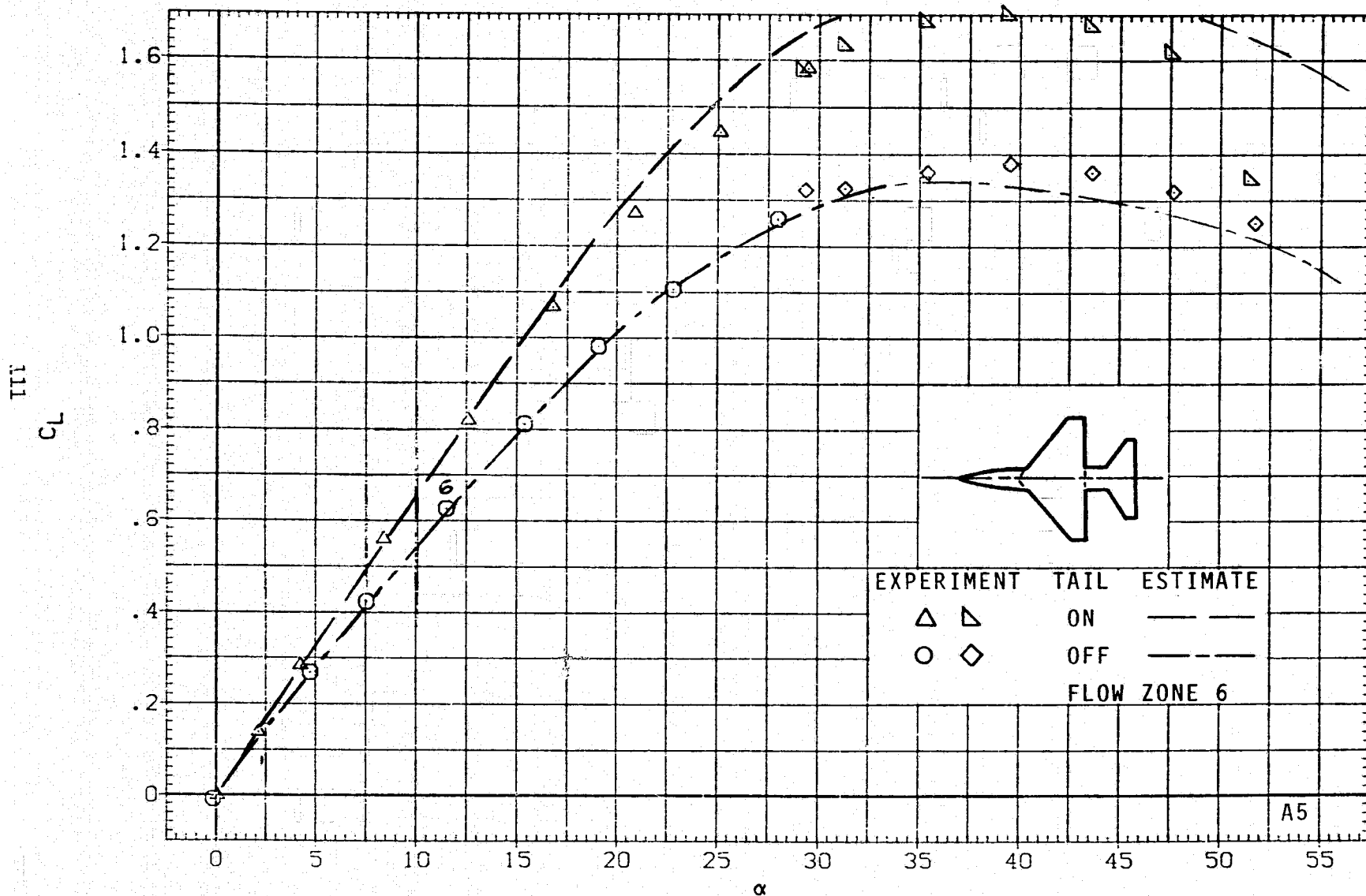


(i)  $C_L$  VERSUS  $C_m$ ;  $M = 1.2$ ,  $J = 1$ .

FIGURE 9.- CONTINUED.

# RESEARCH MODEL

M = 1.50

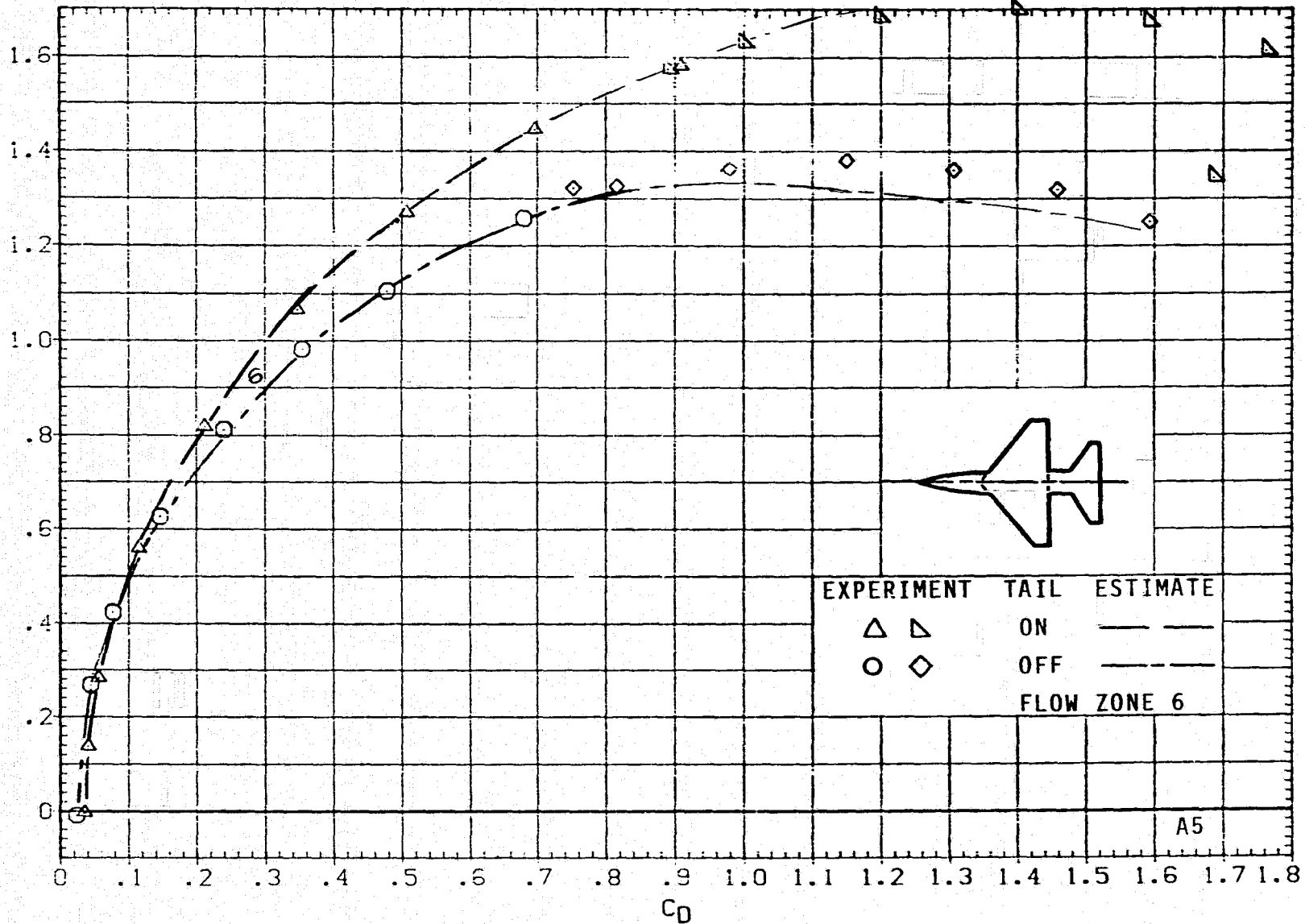


(j) CL VERSUS α; M = 1.5, J = 5.

FIGURE 9.- CONTINUED.

# RESEARCH MODEL

M = 1.50



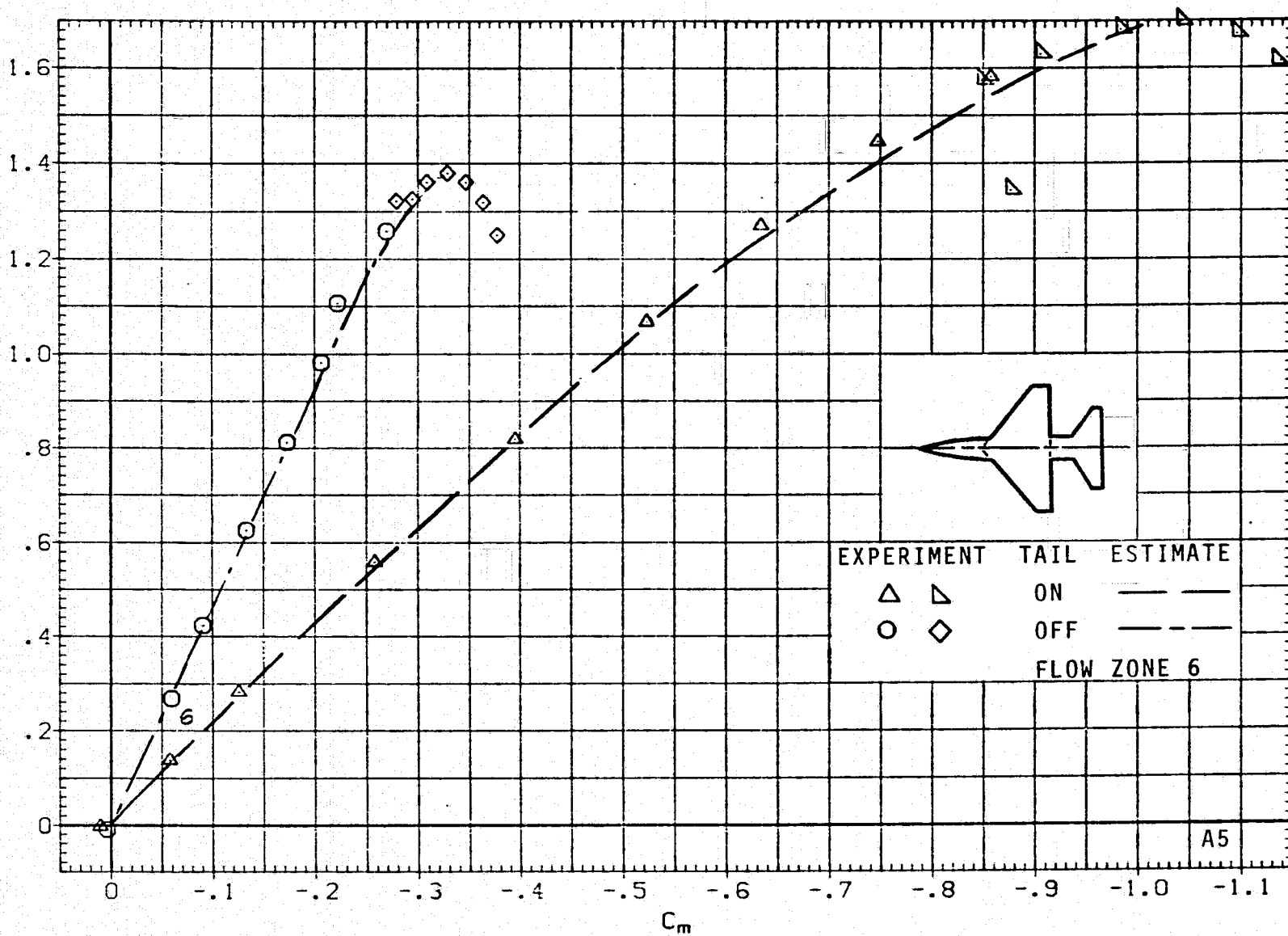
(k)  $C_L$  VERSUS  $C_D$ ; M = 1.5, J = 5.

FIGURE 9.- CONTINUED.



RESEARCH MODEL

M = 1.50



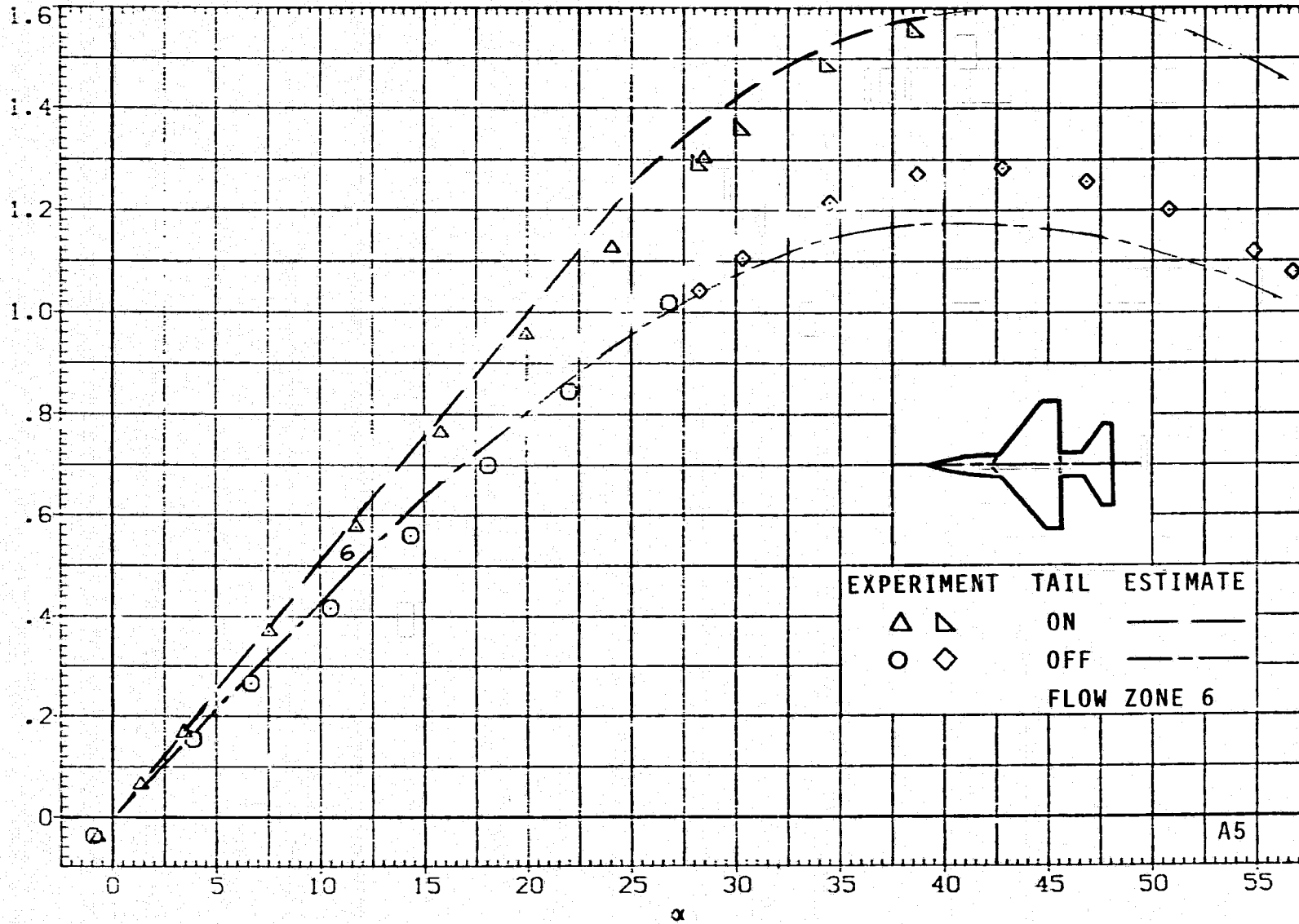
(1)  $C_L$  VERSUS  $C_m$ ;  $M = 1.5$ ,  $\beta = 5$ .

FIGURE 9.- CONTINUED.

# RESEARCH MODEL

$M = 2.0$

114  
CL



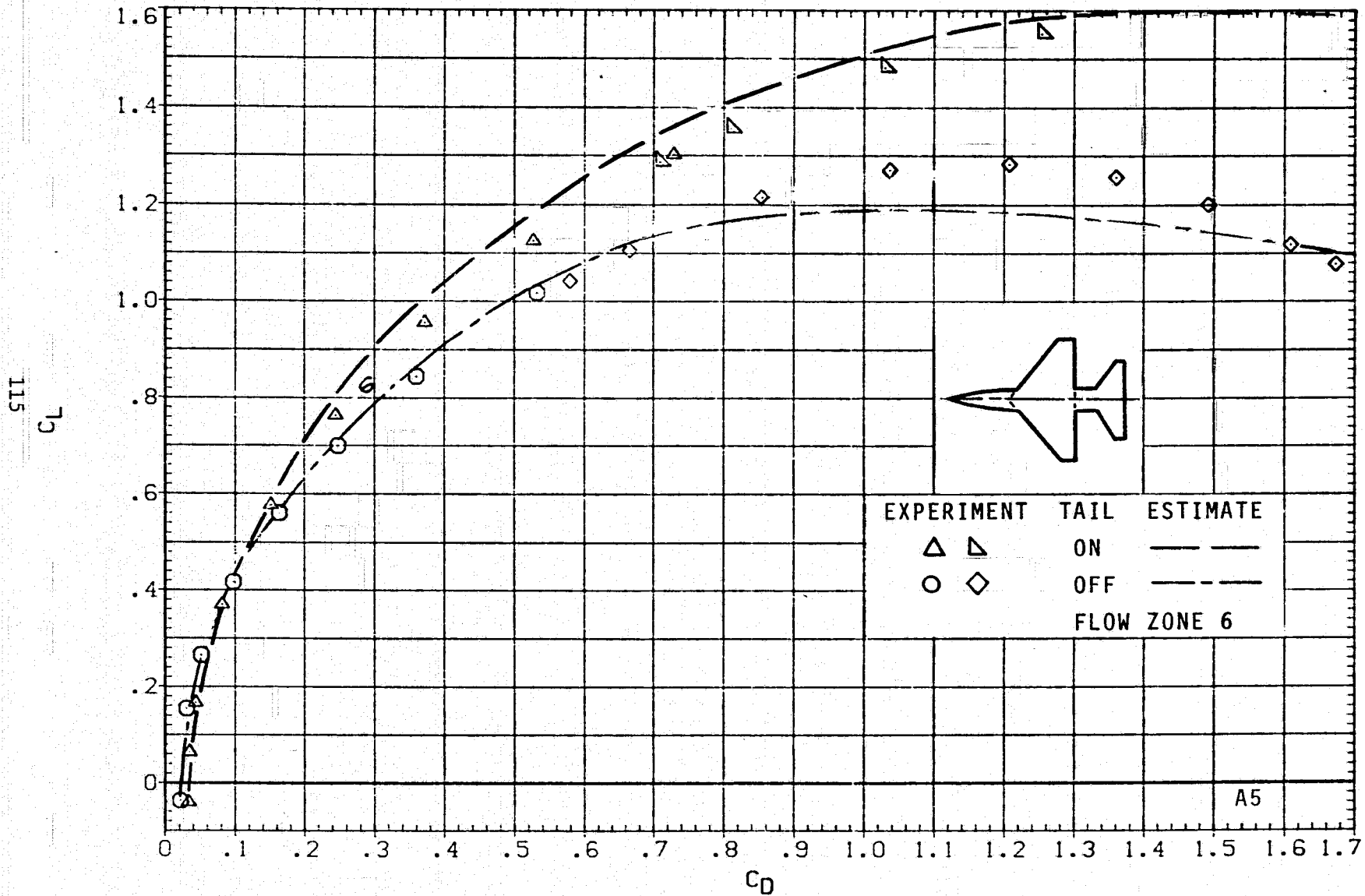
(m)  $C_L$  VERSUS  $\alpha$ ;  $M = 2.0$ ,  $J = 5$ .

FIGURE 9.- CONTINUED.

A5

# RESEARCH MODEL

$M = 2.0$

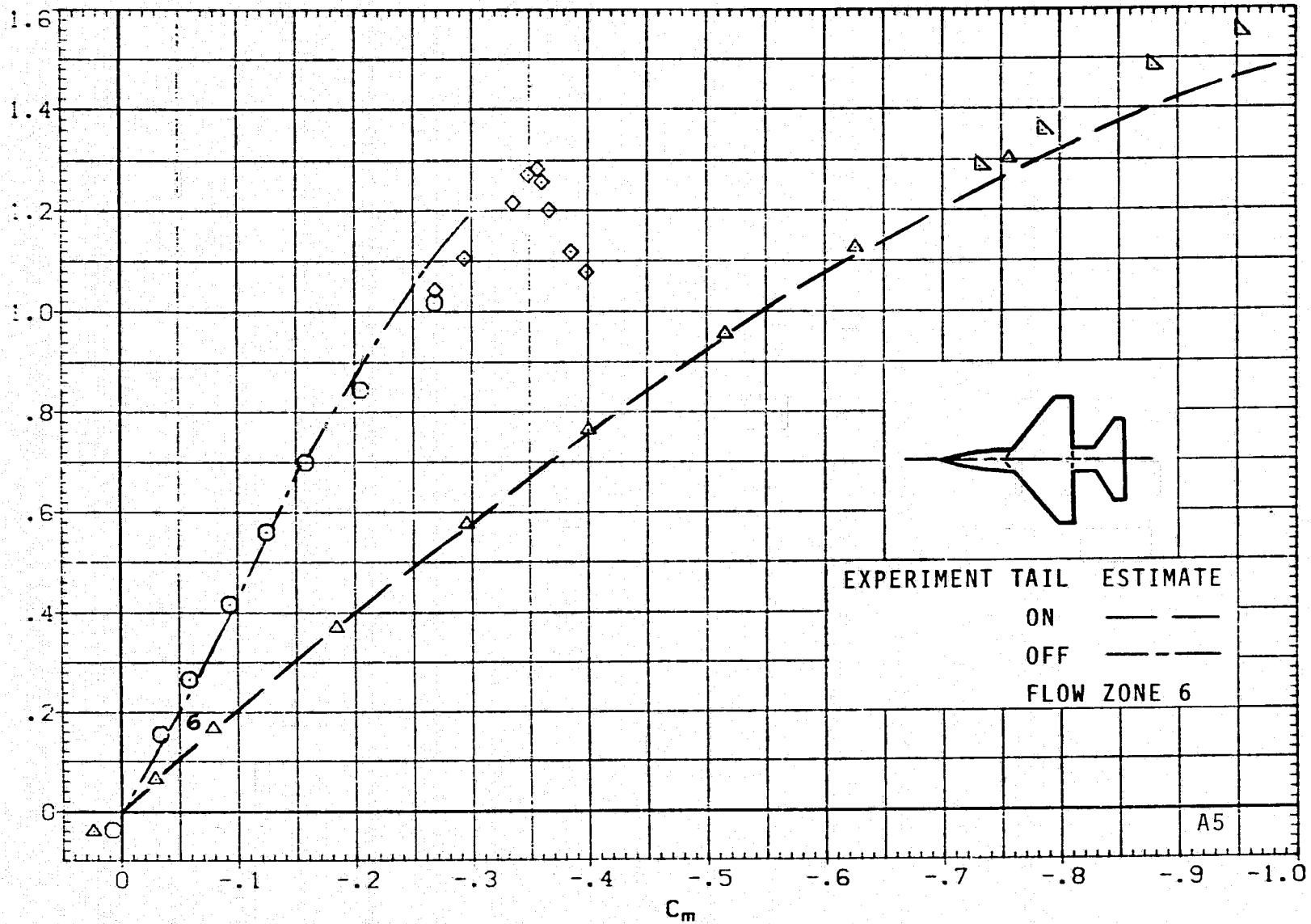


(n)  $C_L$  VERSUS  $C_D$ ;  $M = 2.0$ ,  $J = 5$ .

FIGURE 9.- CONTINUED.

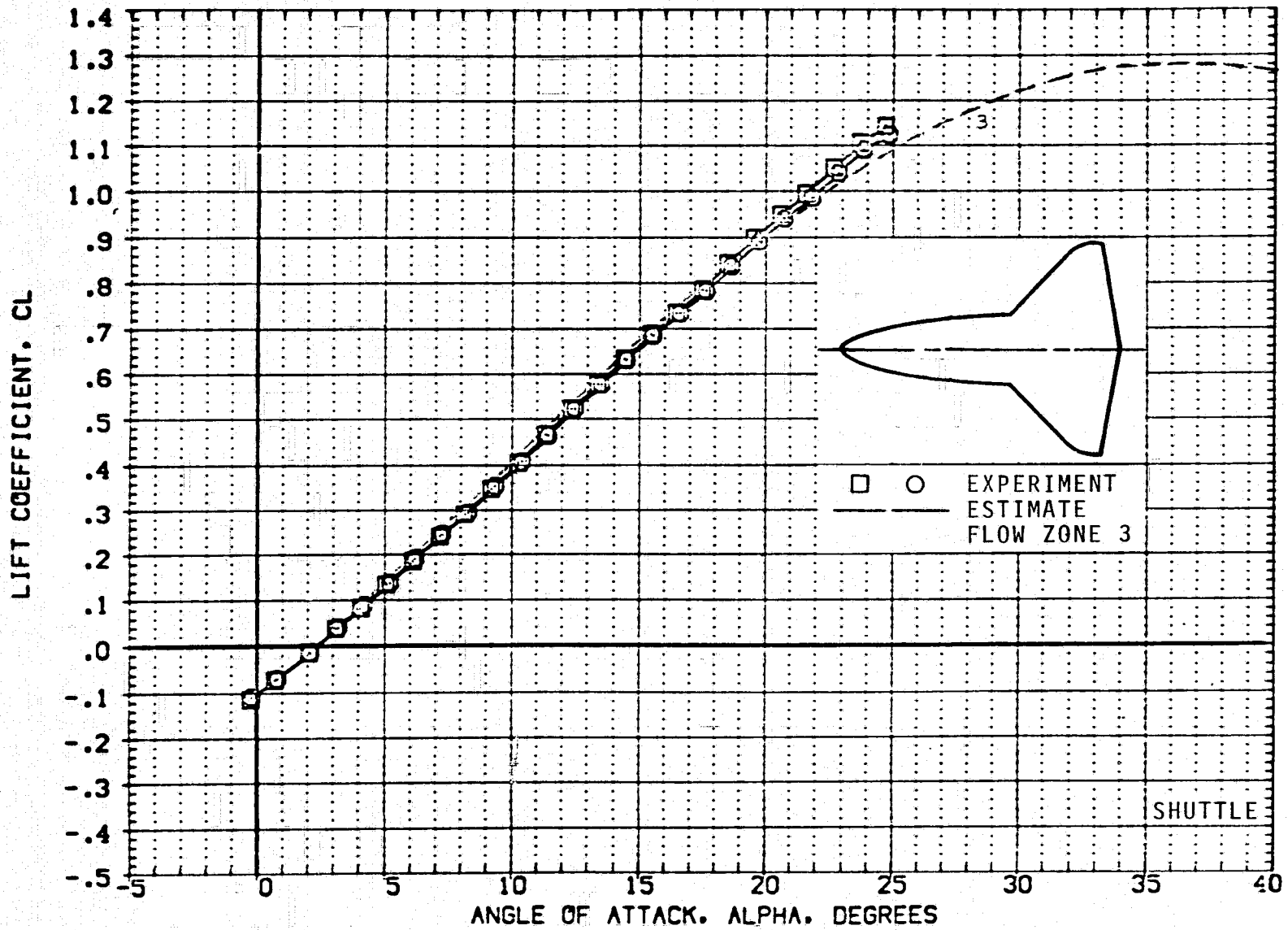
# RESEARCH MODEL

$M = 2.0$



(o)  $C_L$  VERSUS  $C_m$ ;  $M = 2.0$ ,  $J = 5$ .

FIGURE 9.- CONCLUDED.

(a)  $C_L$  VERSUS  $\alpha$ ;  $M = 0.6$ .FIGURE 10.- AERODYNAMICS FOR SHUTTLE ORBITER;  $J = 2$ .

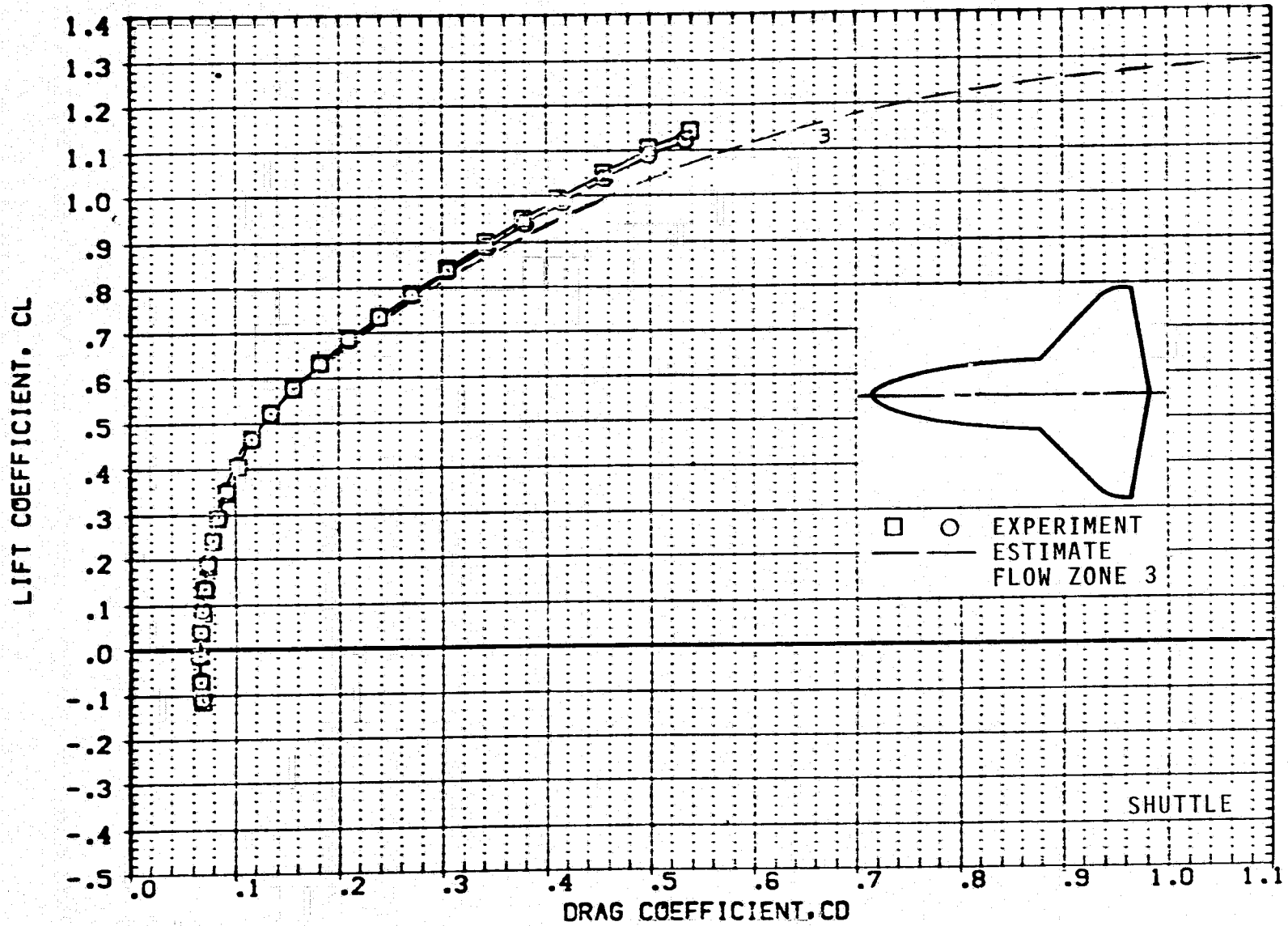
(b)  $C_L$  VERSUS  $C_D$ ;  $M = 0.6$ .

FIGURE 10.- CONTINUED.

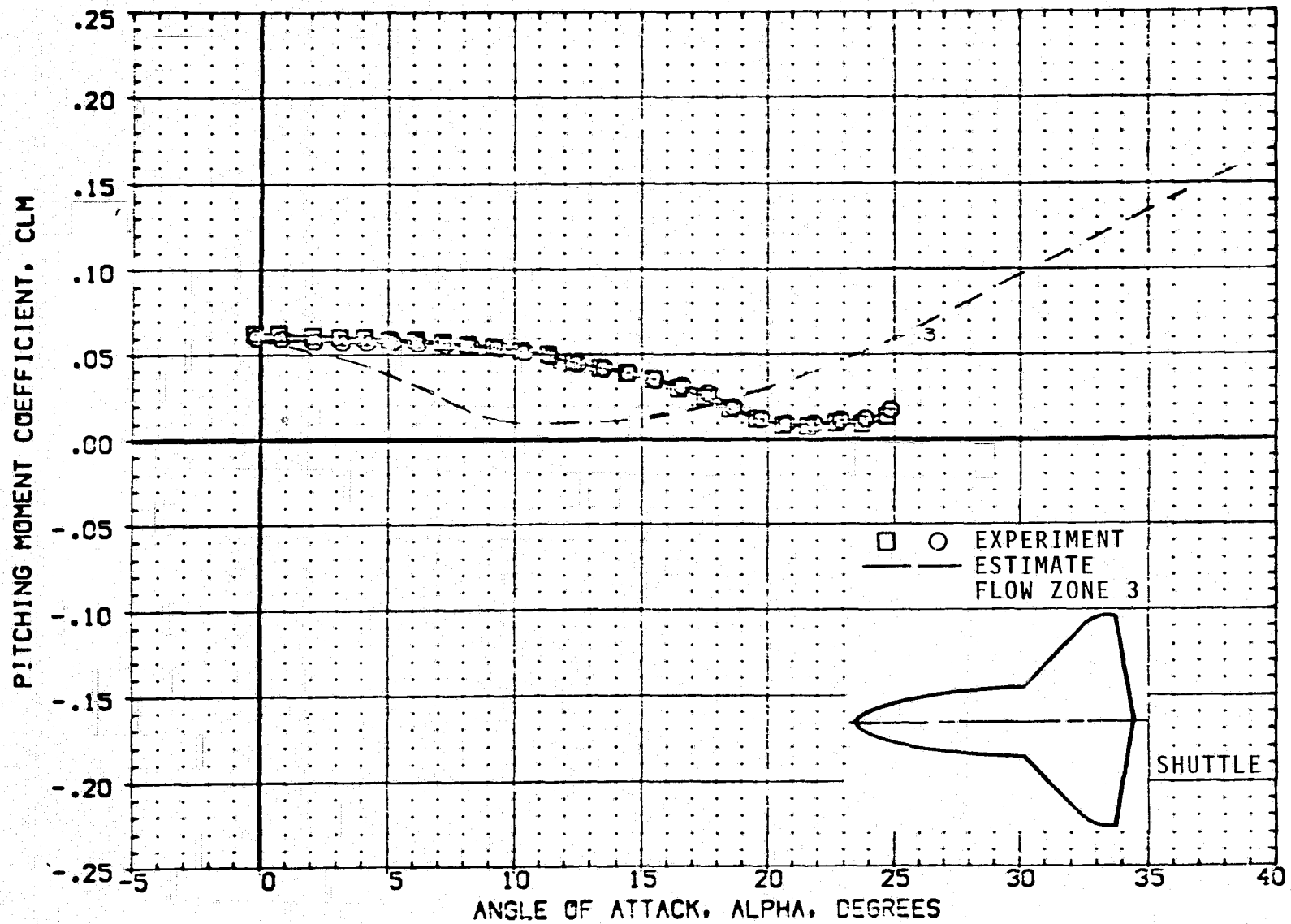
(c)  $C_m$  VERSUS  $\alpha$ ;  $M = 0.6$ .

FIGURE 10.- CONTINUED.

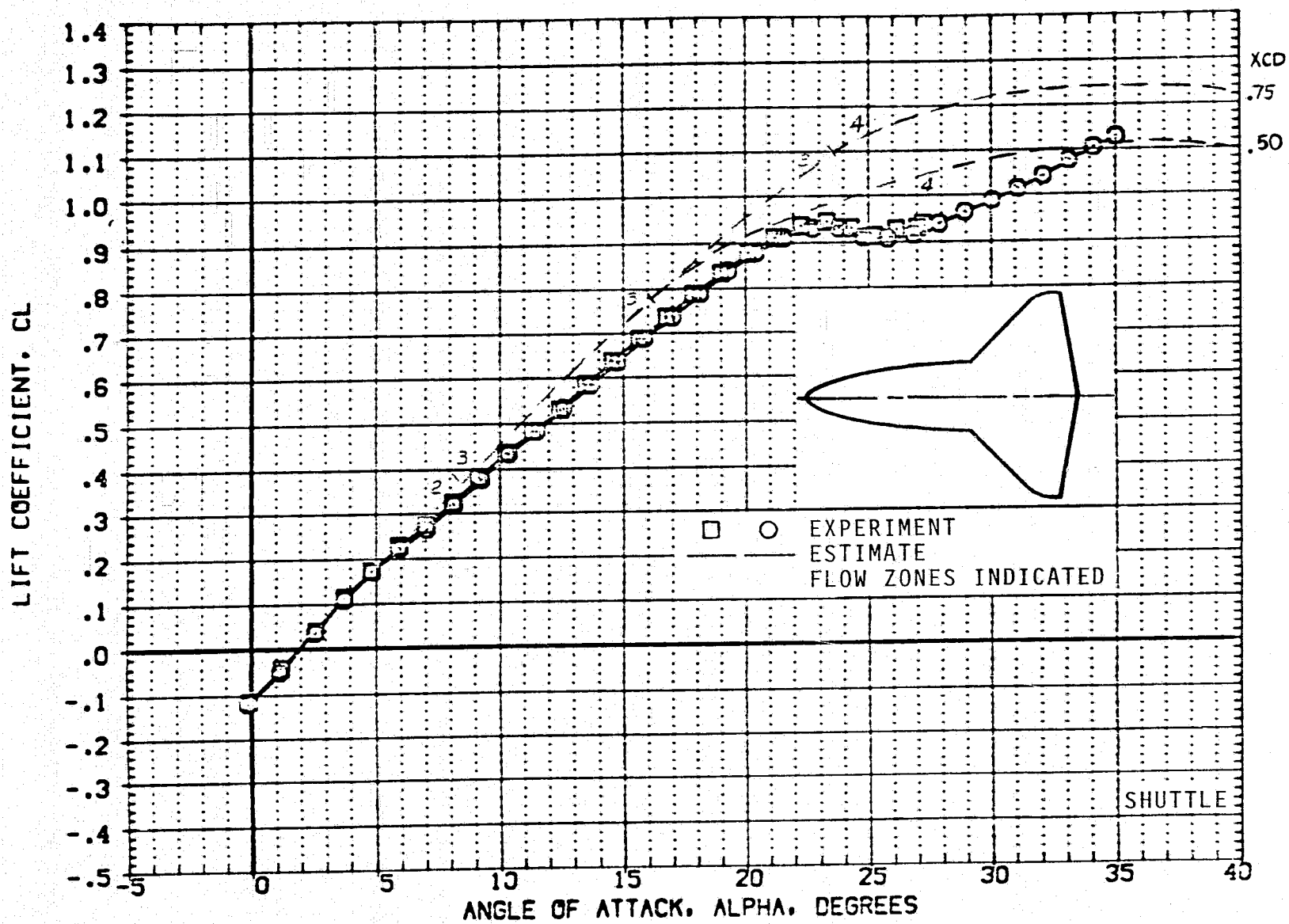
(d)  $C_L$  VERSUS  $\alpha$ ;  $M = 0.9$ .

FIGURE 10.- CONTINUED.



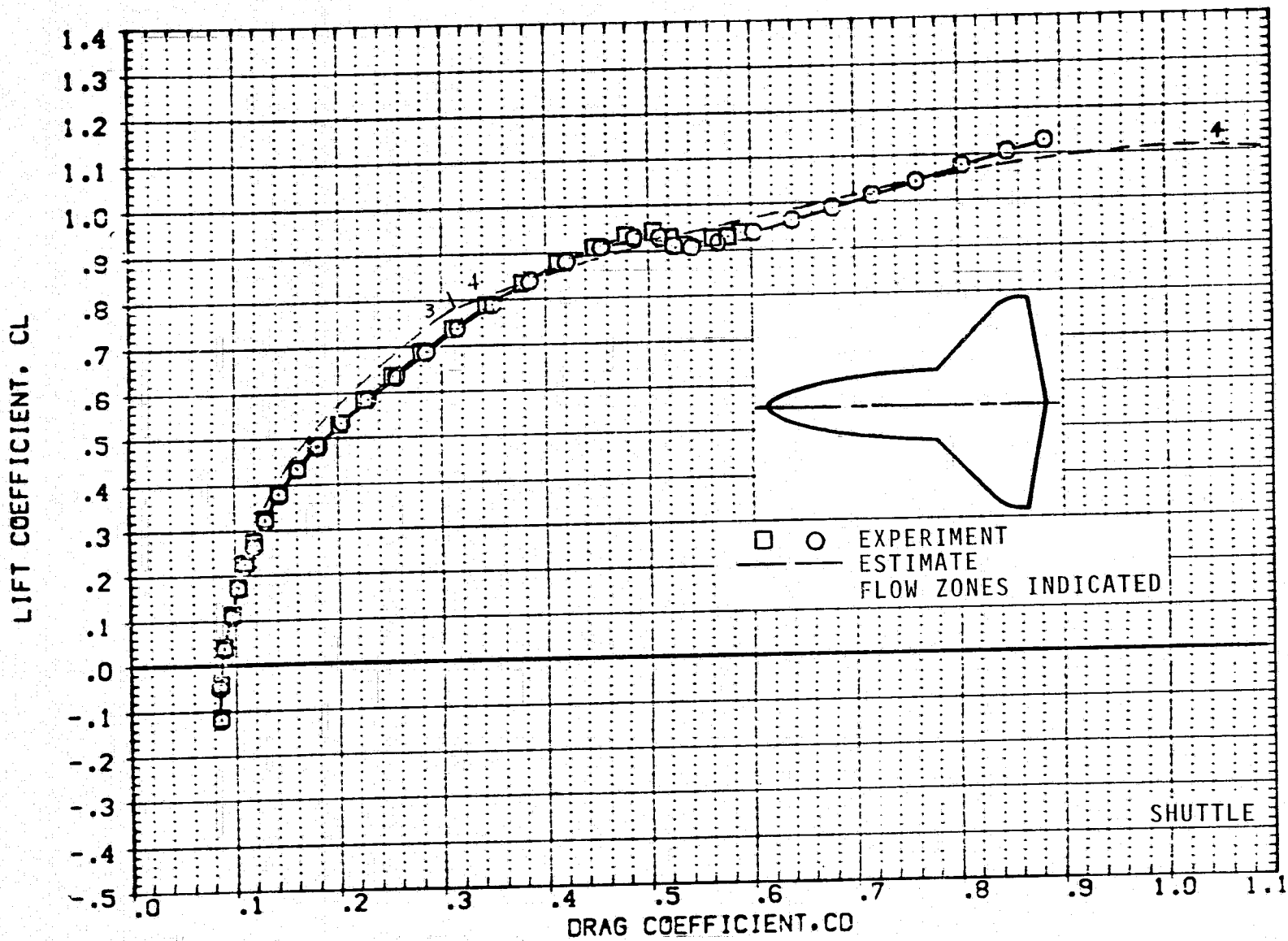
(e)  $C_L$  VERSUS  $C_D$ ;  $M = 0.9$ .

FIGURE 10.- CONTINUED.

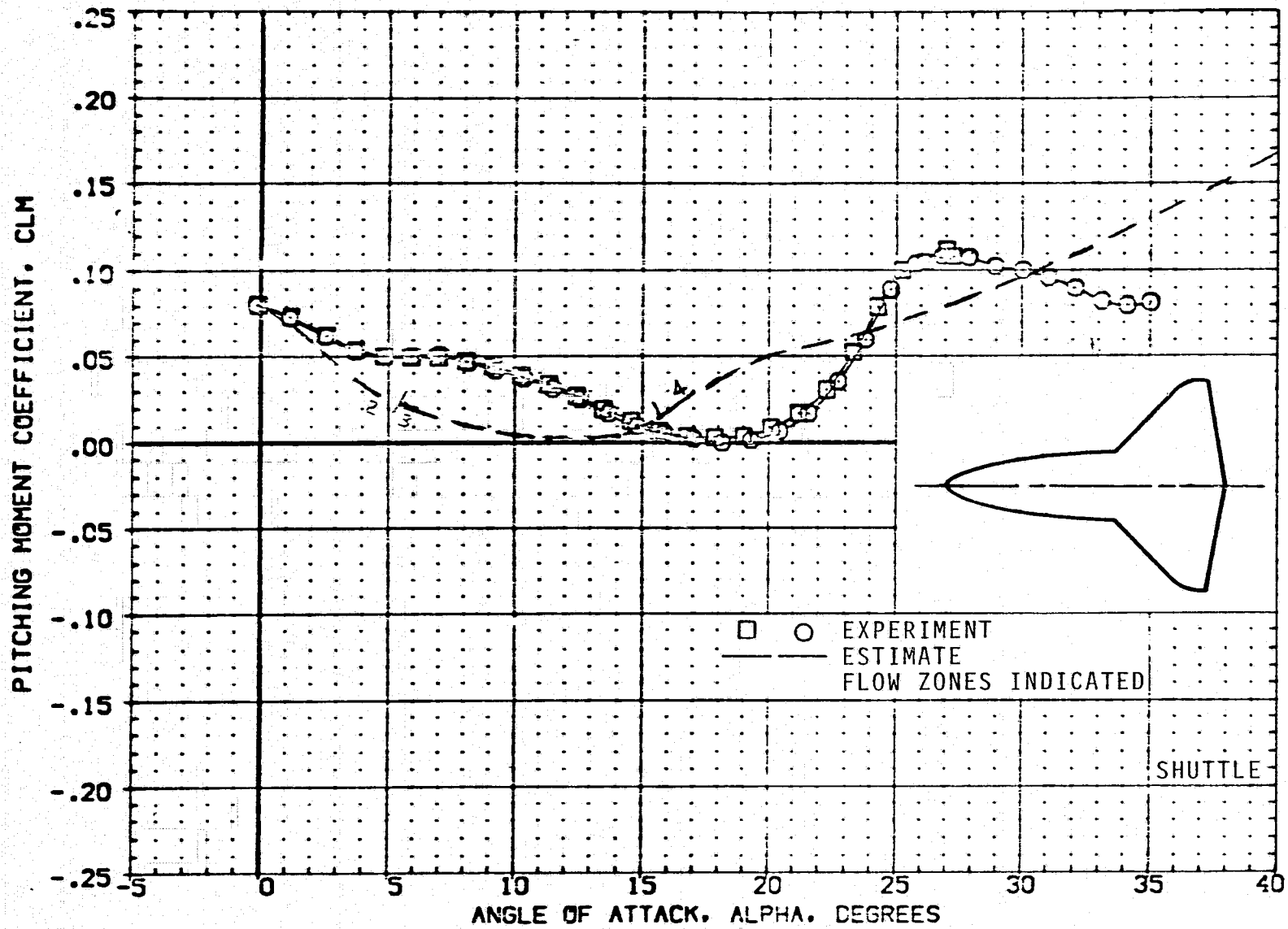
(f)  $C_m$  VERSUS  $\alpha$ ;  $M = 0.9$ .

FIGURE 10.- CONTINUED.

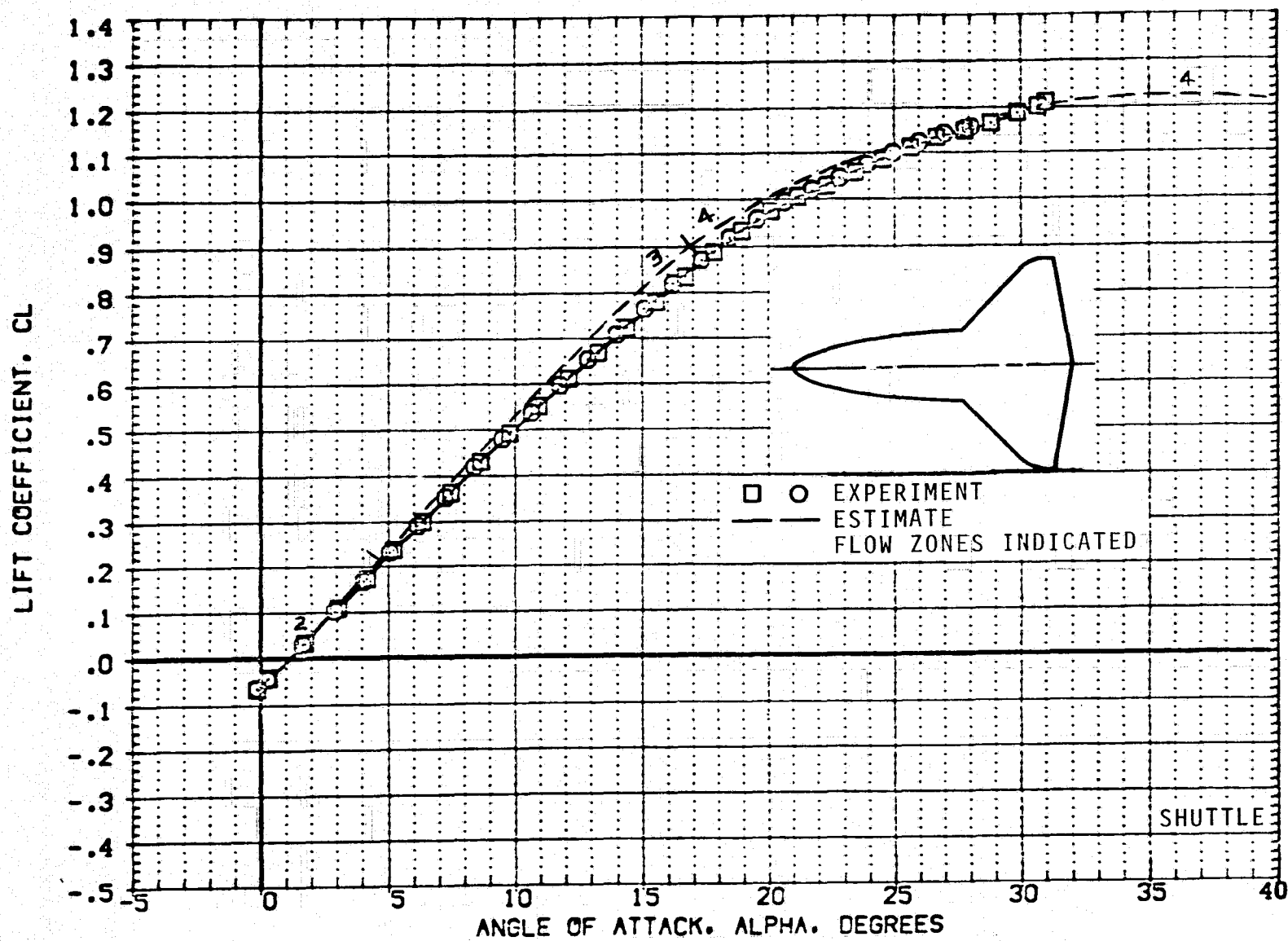
(g)  $C_L$  VERSUS  $\alpha$ ;  $M = 1.2$ .

FIGURE 10.- CONTINUED.

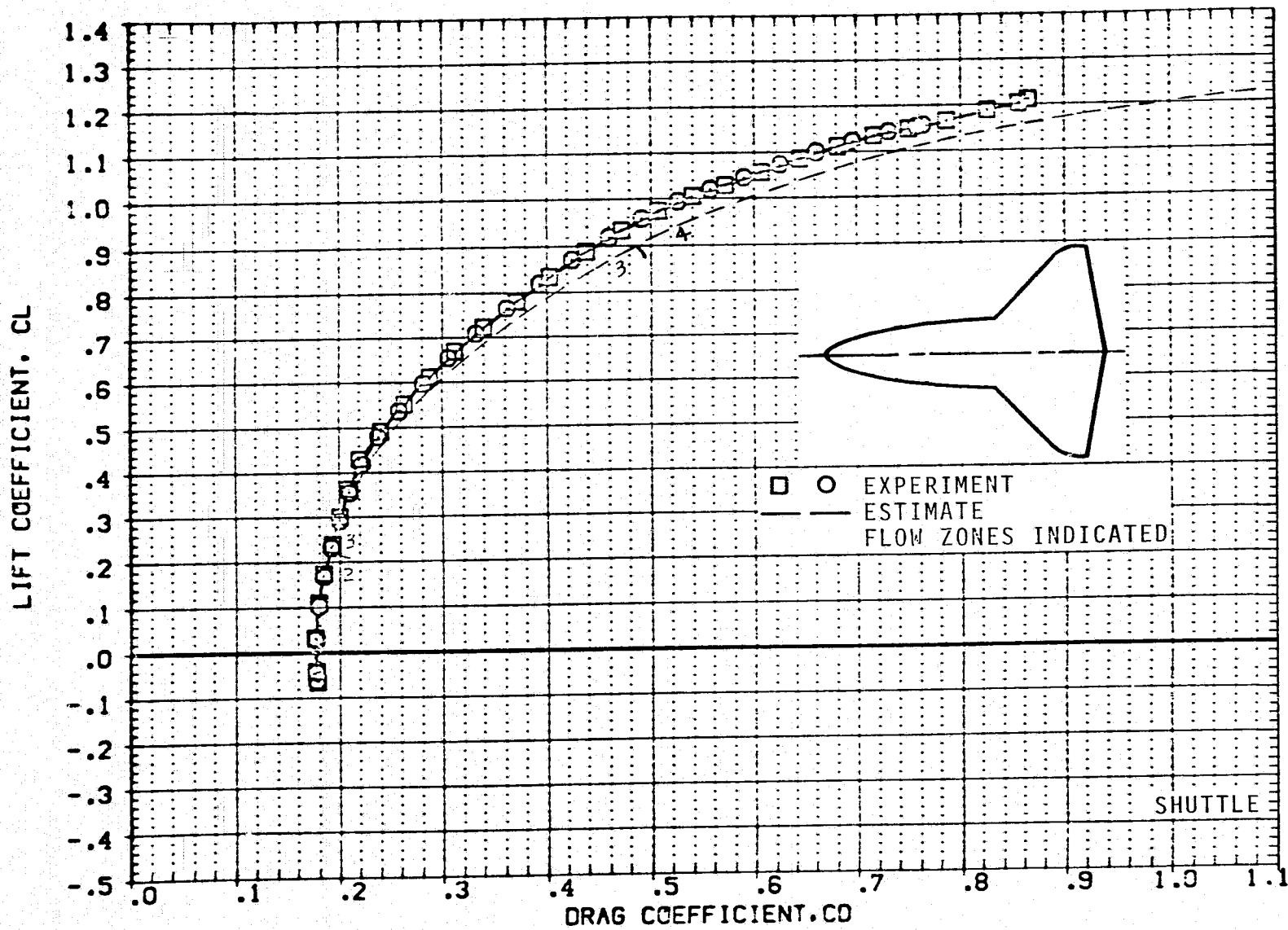
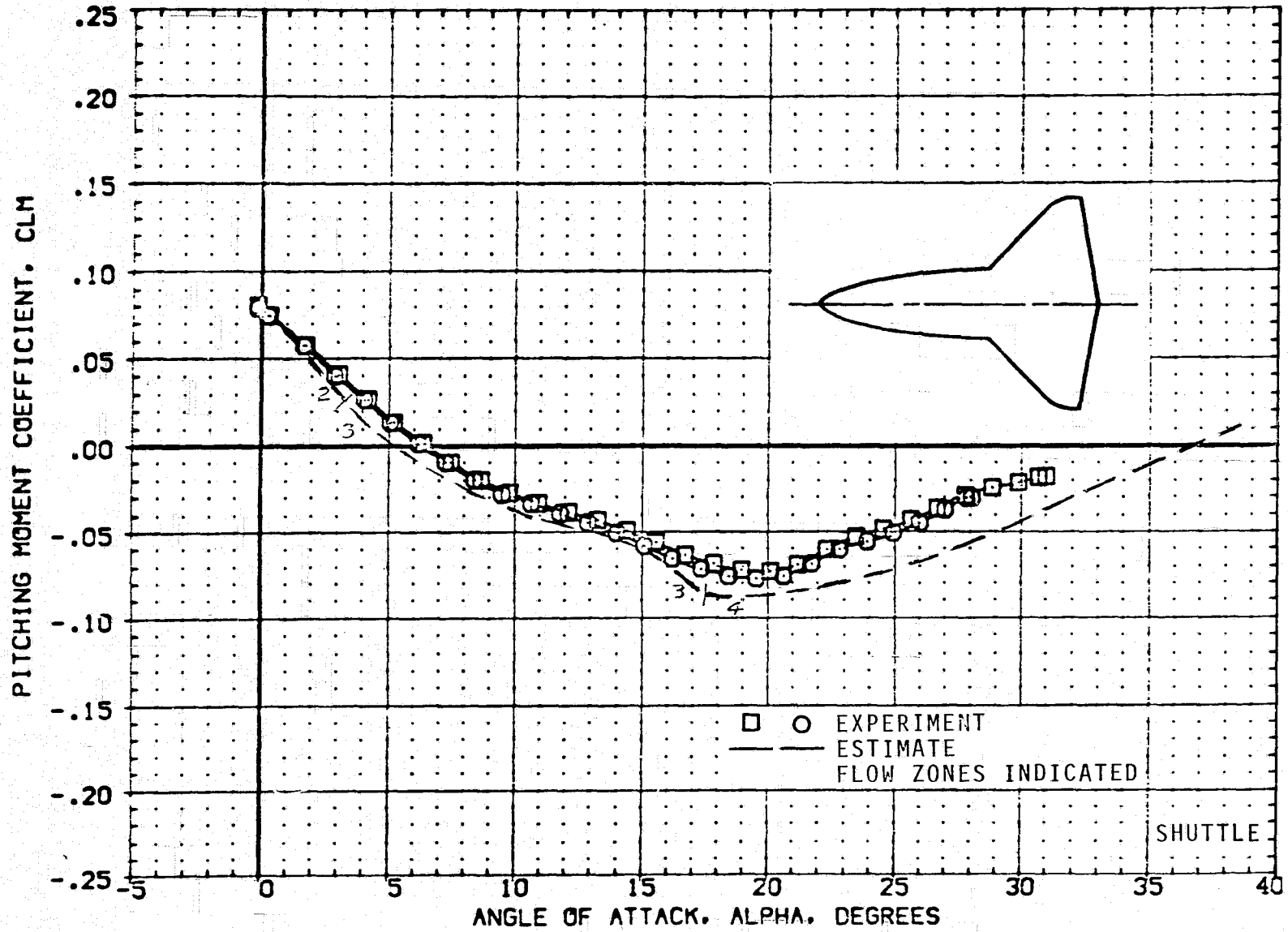
(h)  $C_L$  VERSUS  $C_D$ ;  $M = 1.2$ .

FIGURE 10.- CONTINUED.



(i)  $C_m$  VERSUS  $\alpha$ ;  $M = 1.2$ .

FIGURE 10.- CONTINUED.

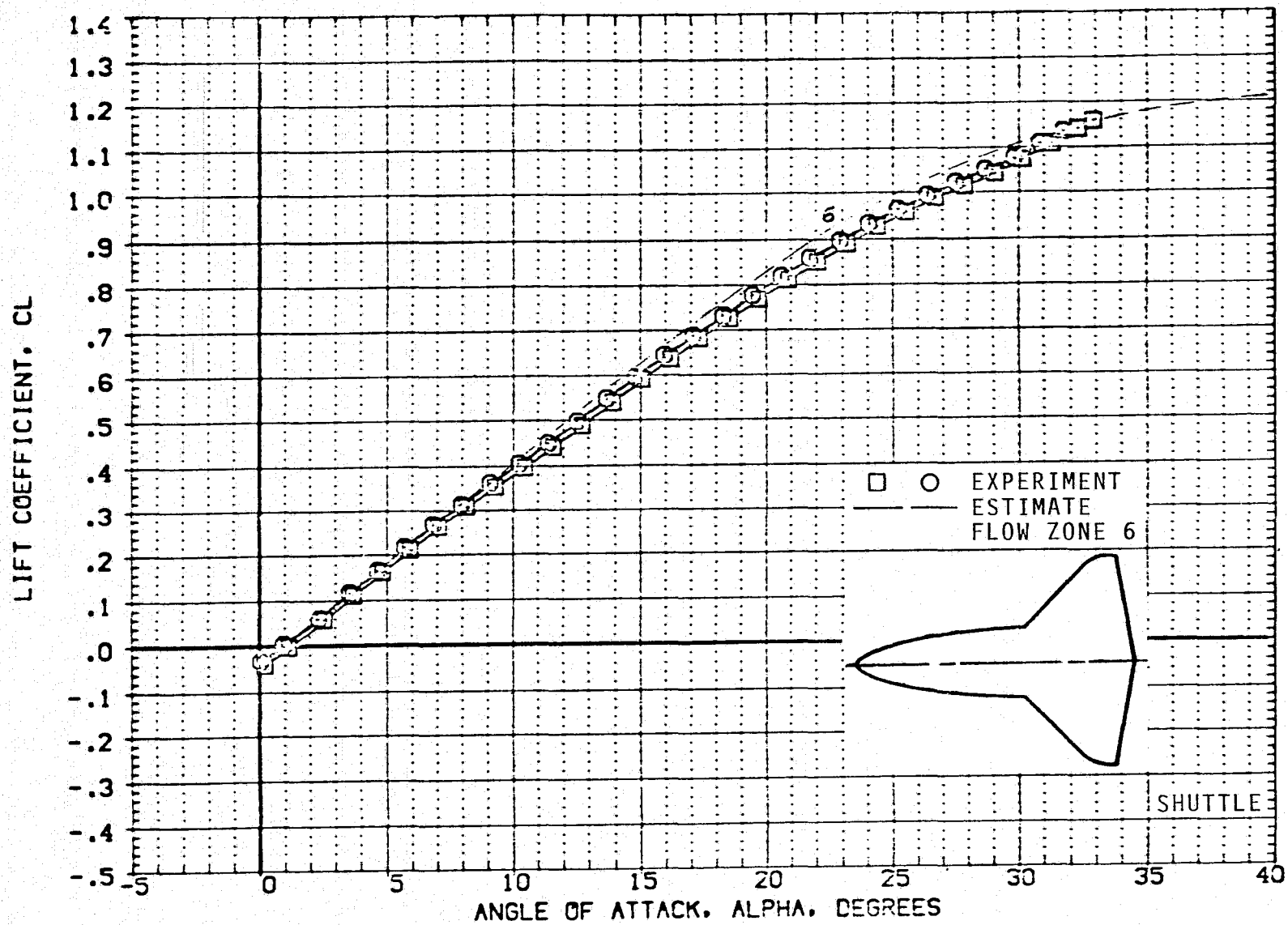
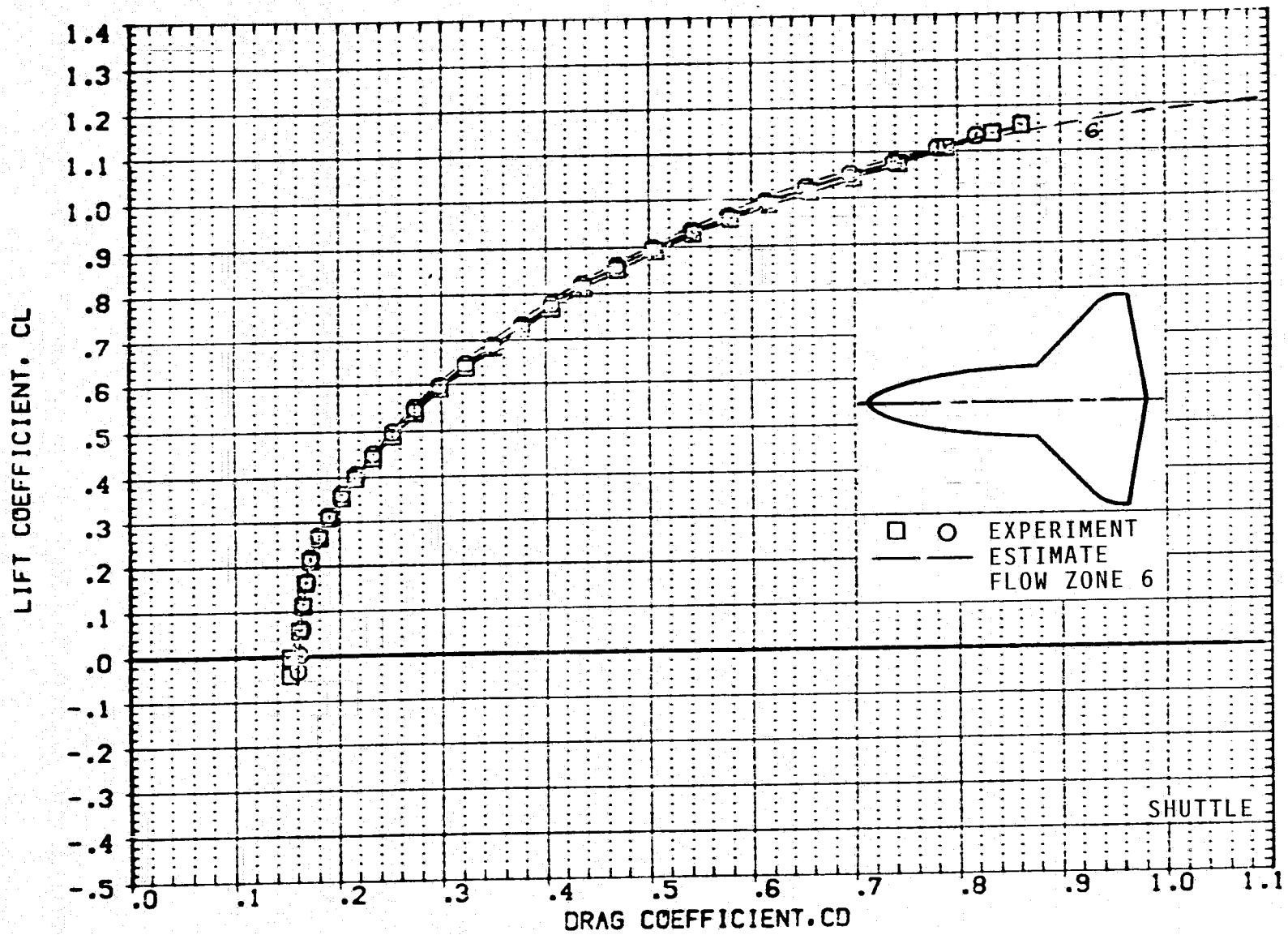
(j)  $C_L$  VERSUS  $\alpha$ ;  $M = 1.6$ .

FIGURE 10.- CONTINUED.



(k)  $C_L$  VERSUS  $C_D$ ;  $M = 1.6$ .

FIGURE 10.- CONTINUED.

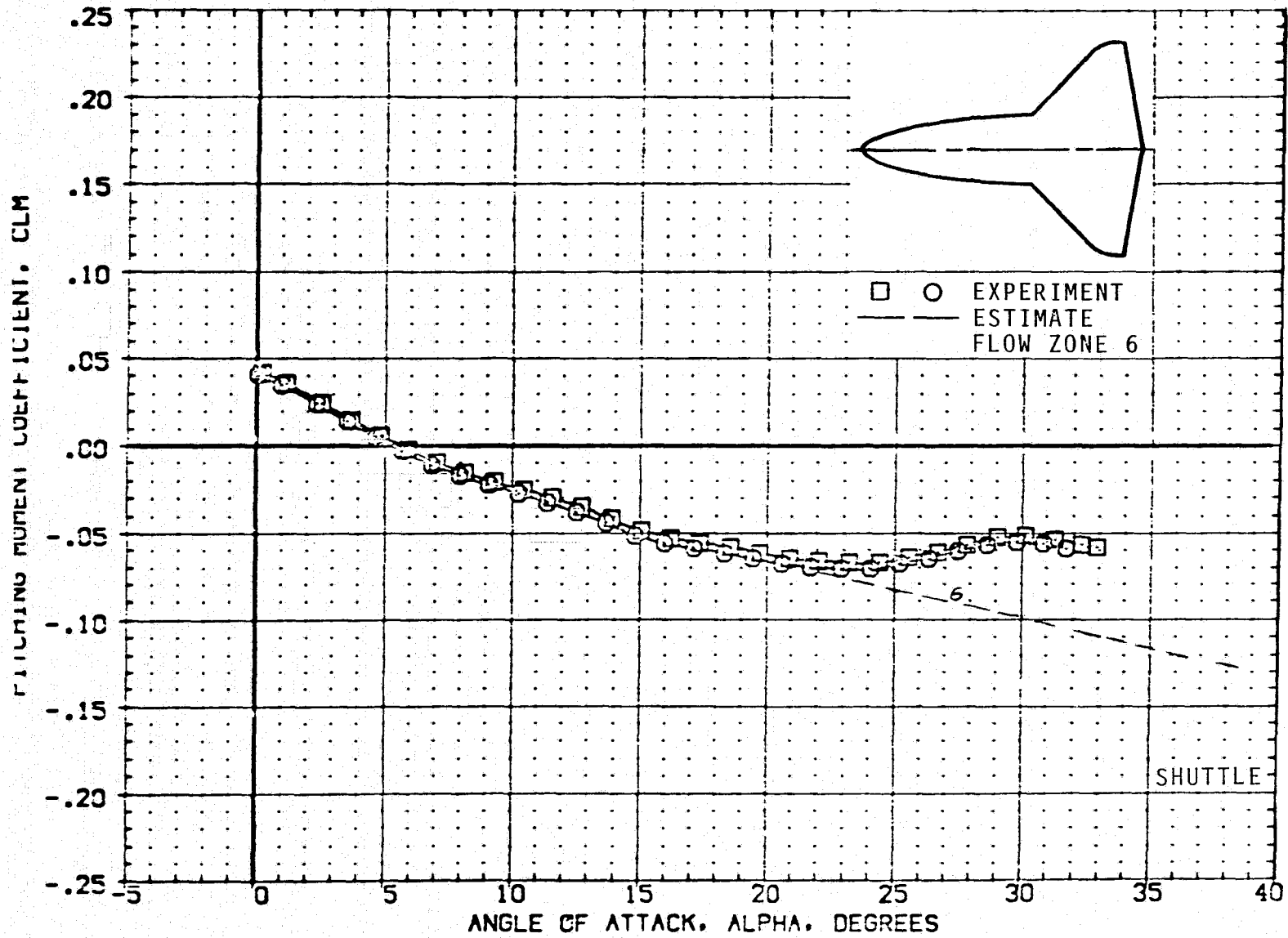
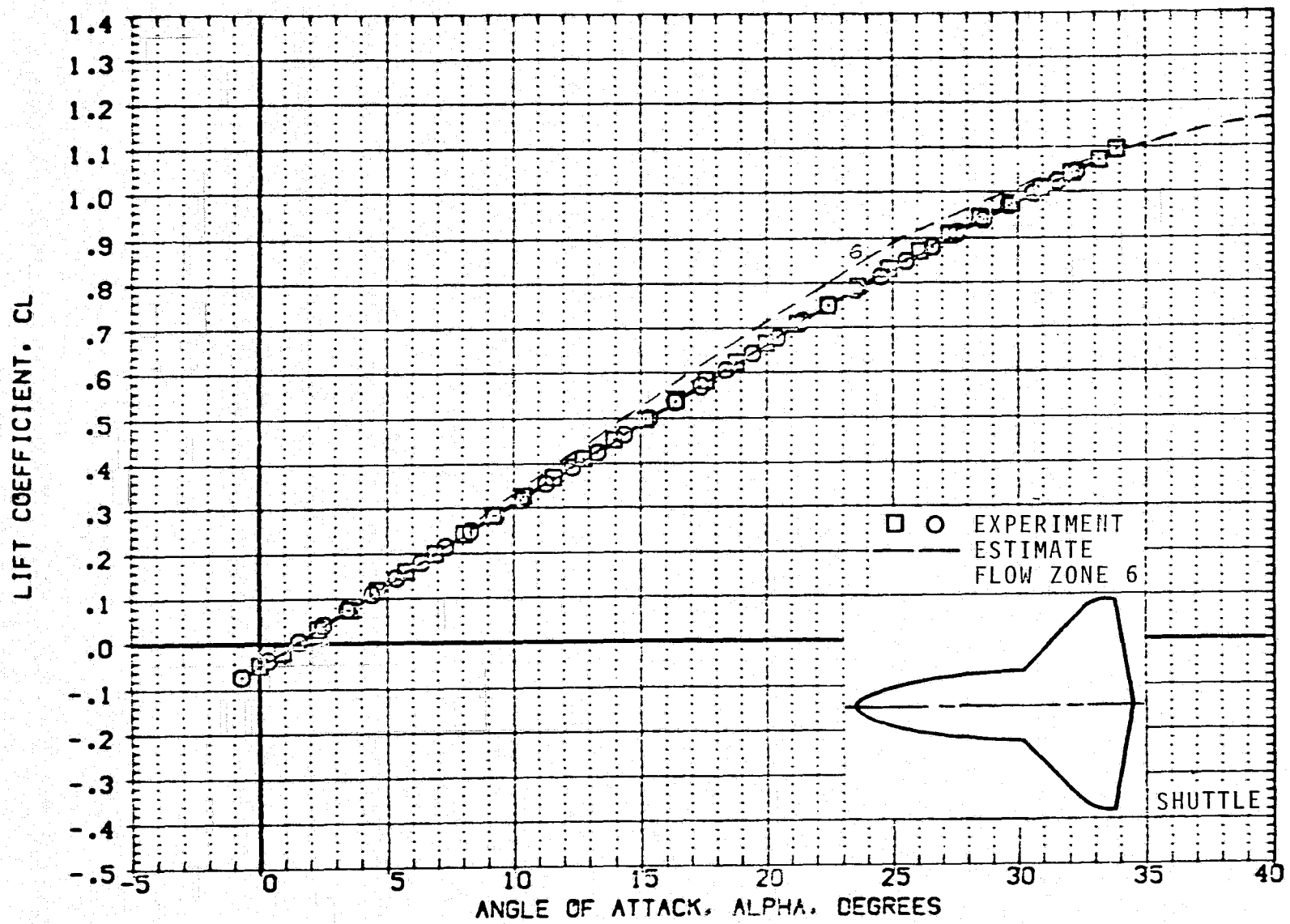
(1)  $C_m$  VERSUS  $\alpha$ ;  $M = 1.6$ .

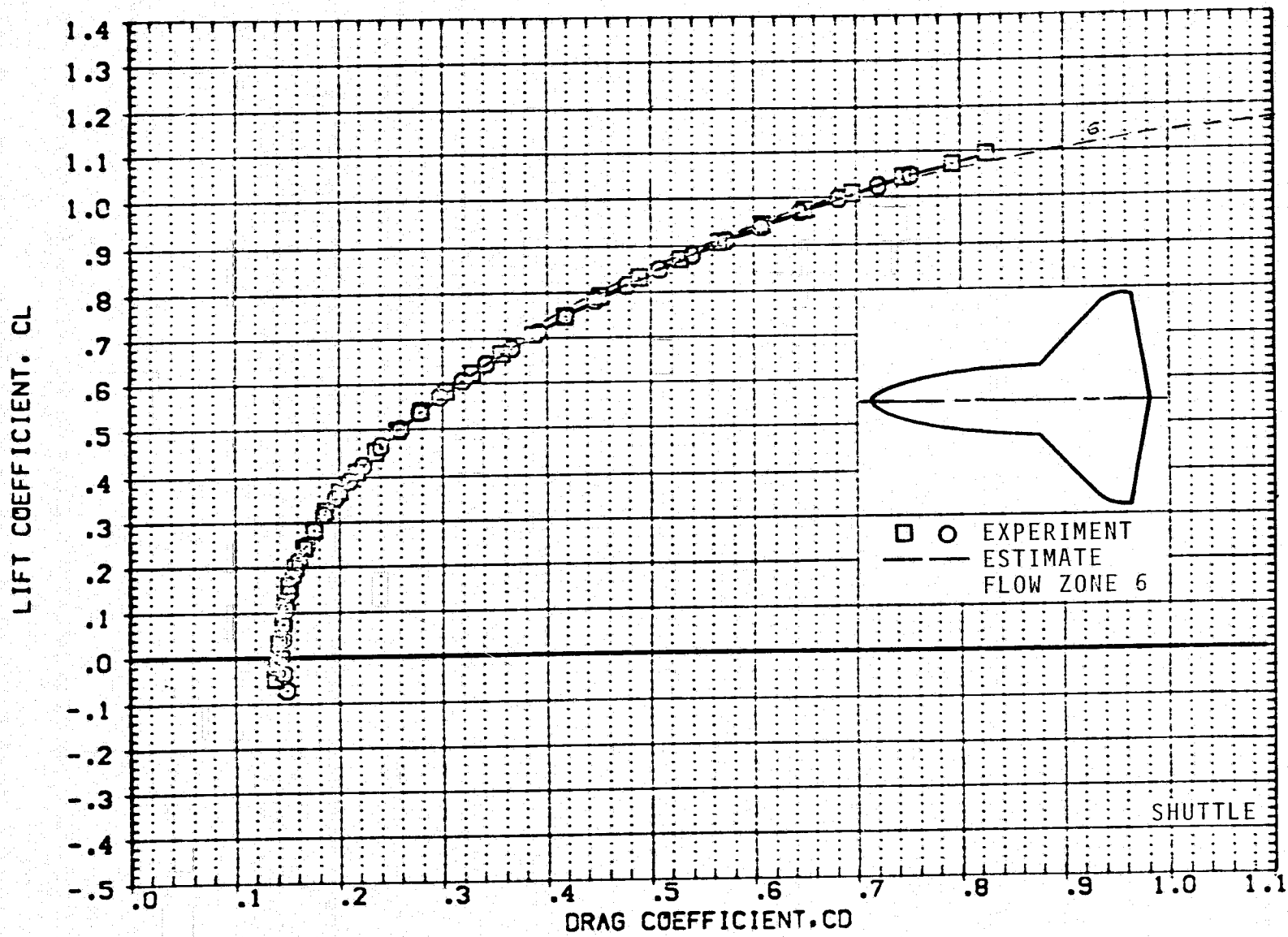
FIGURE 10.- CONTINUED.





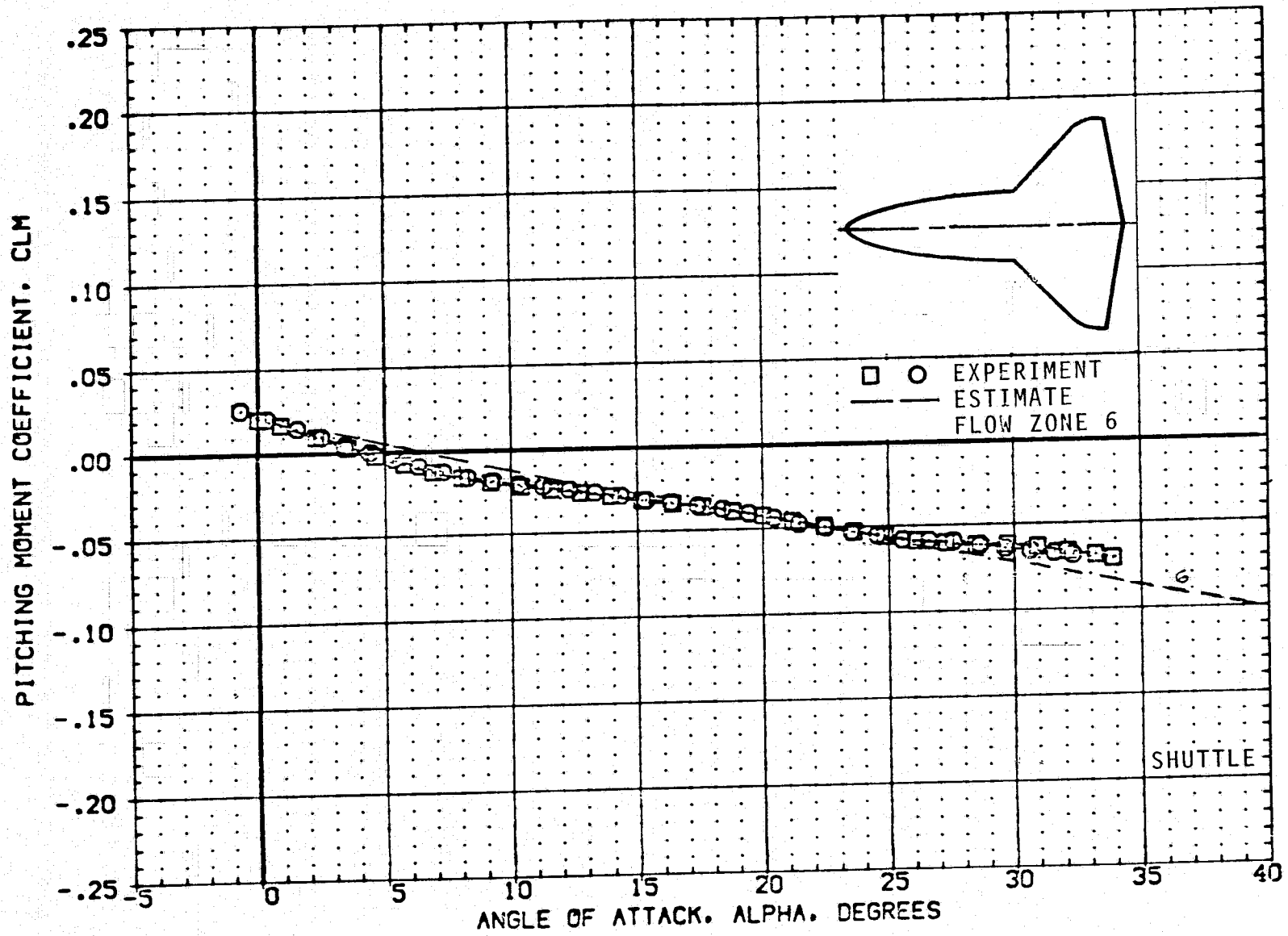
(m)  $C_L$  VERSUS  $\alpha$ ;  $M = 2.0$ .

FIGURE 10.- CONTINUED.



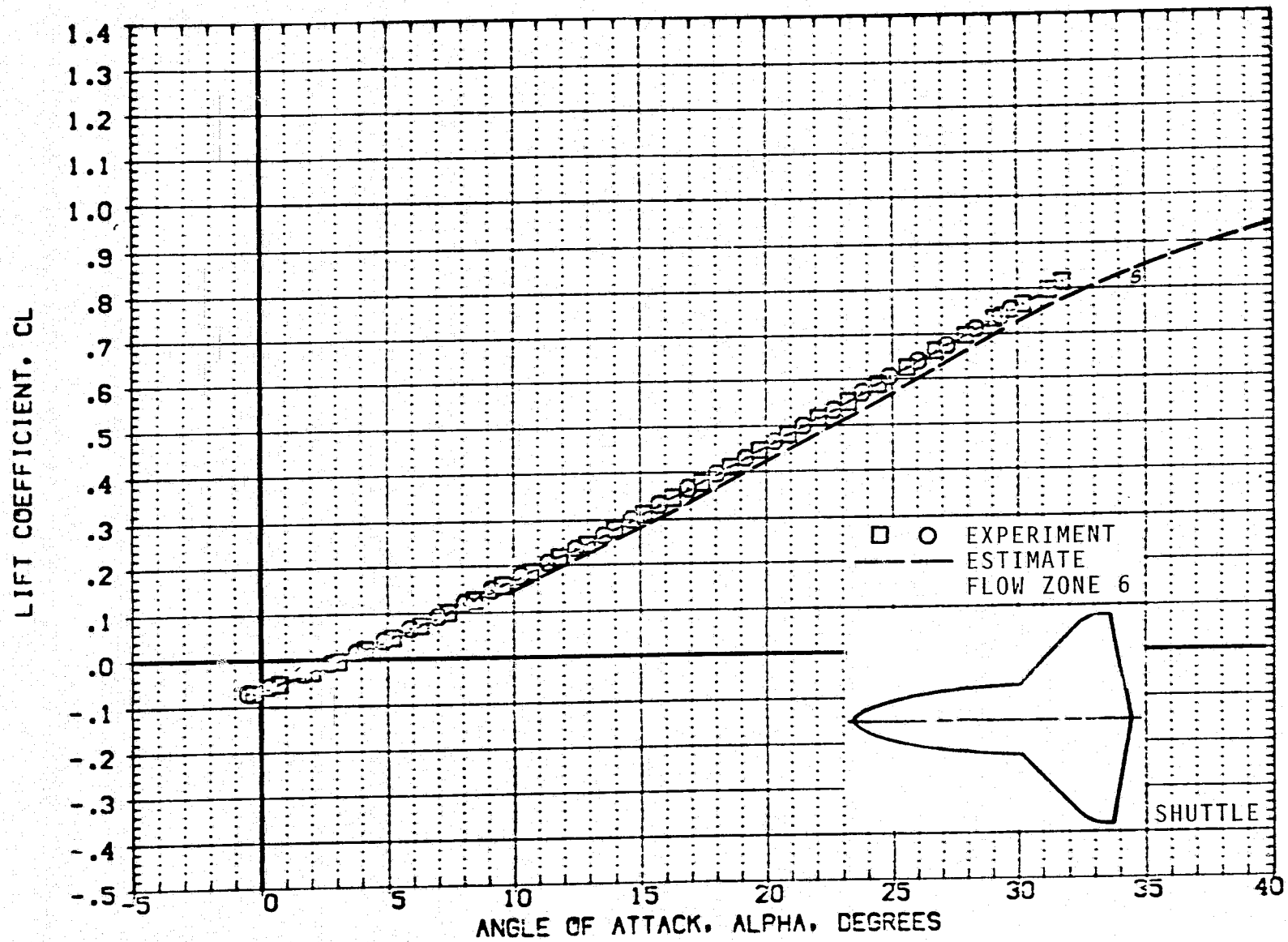
(n)  $C_L$  VERSUS  $C_D$ ;  $M = 2.0$ .

FIGURE 10.- CONTINUED.



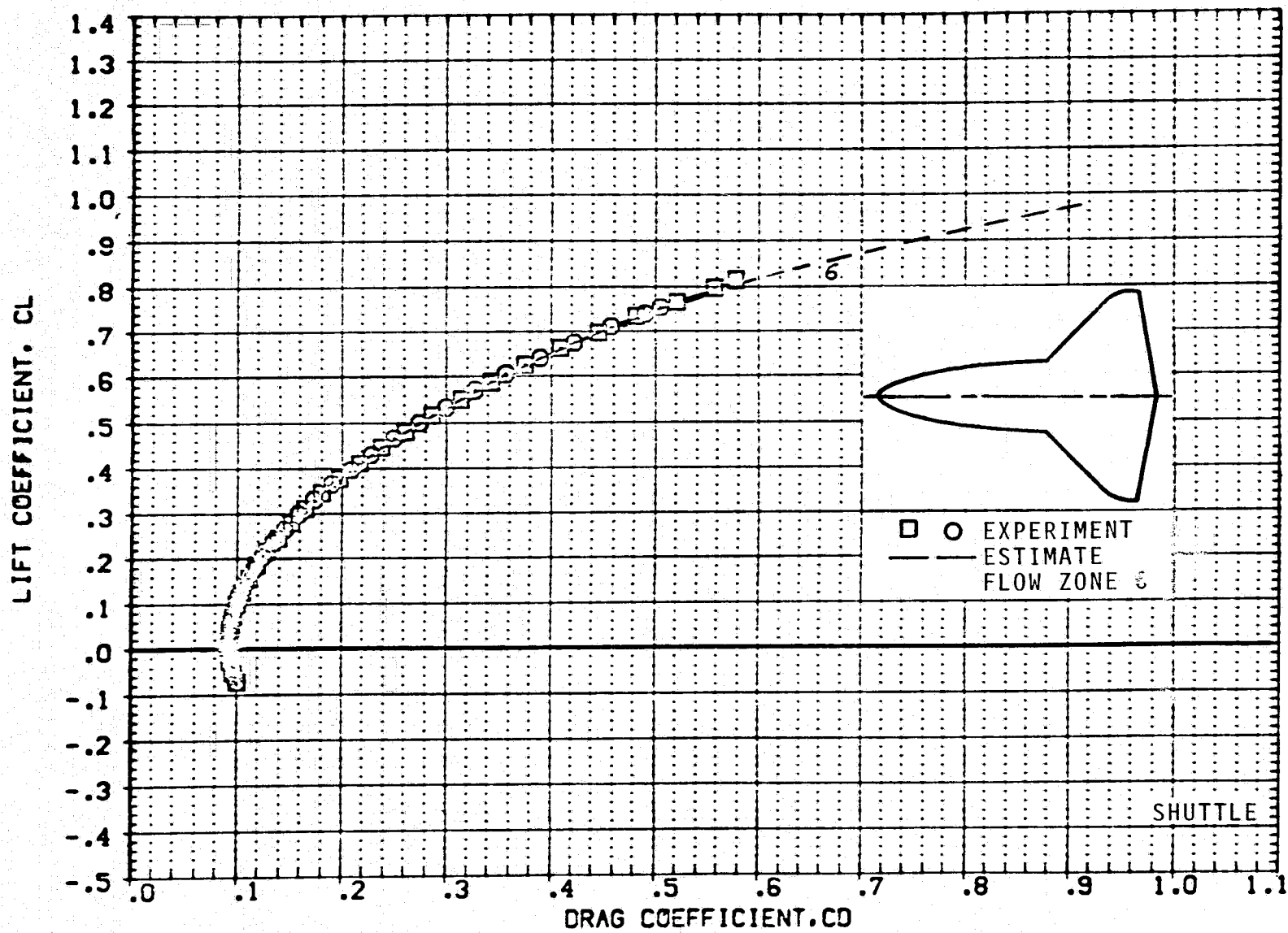
(o)  $C_m$  VERSUS  $\alpha$ ;  $M = 2.0$ .

FIGURE 10.- CONTINUED.



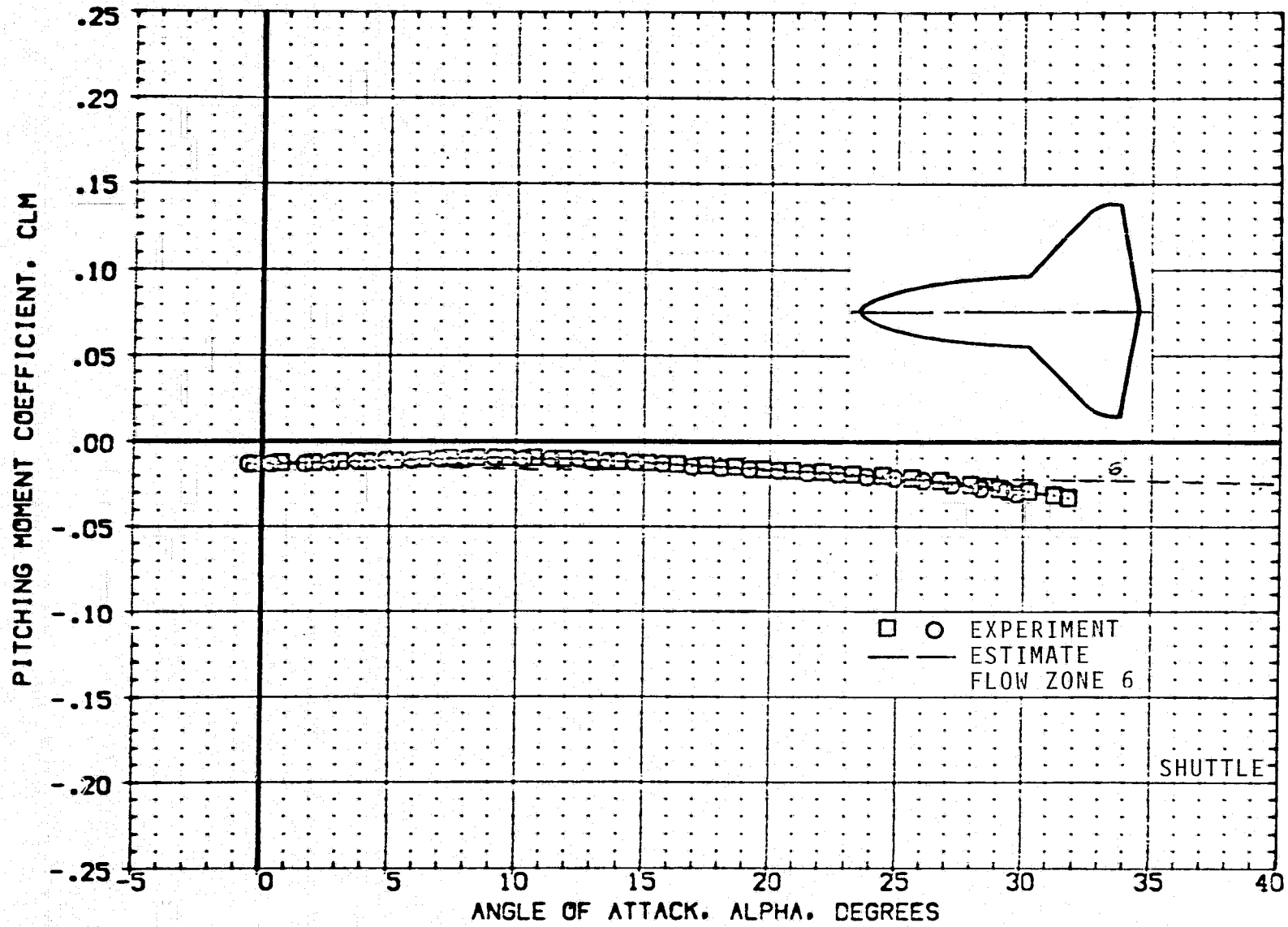
(p)  $C_L$  VERSUS  $\alpha$ ;  $M = 4.0$ .

FIGURE 10.- CONTINUED.



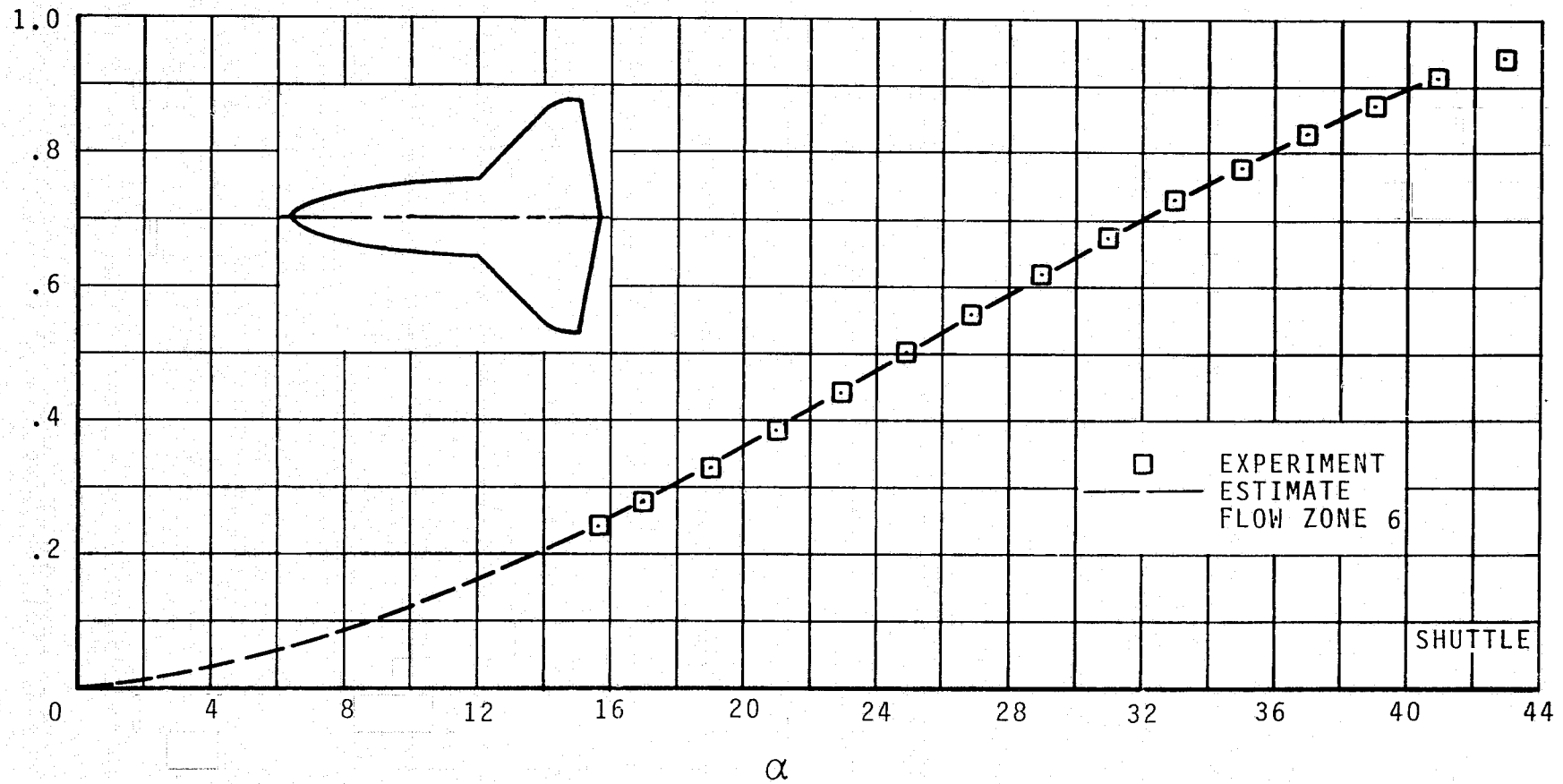
(q)  $C_L$  VERSUS  $C_D$ ;  $M = 4.0$ .

FIGURE 10.- CONTINUED.



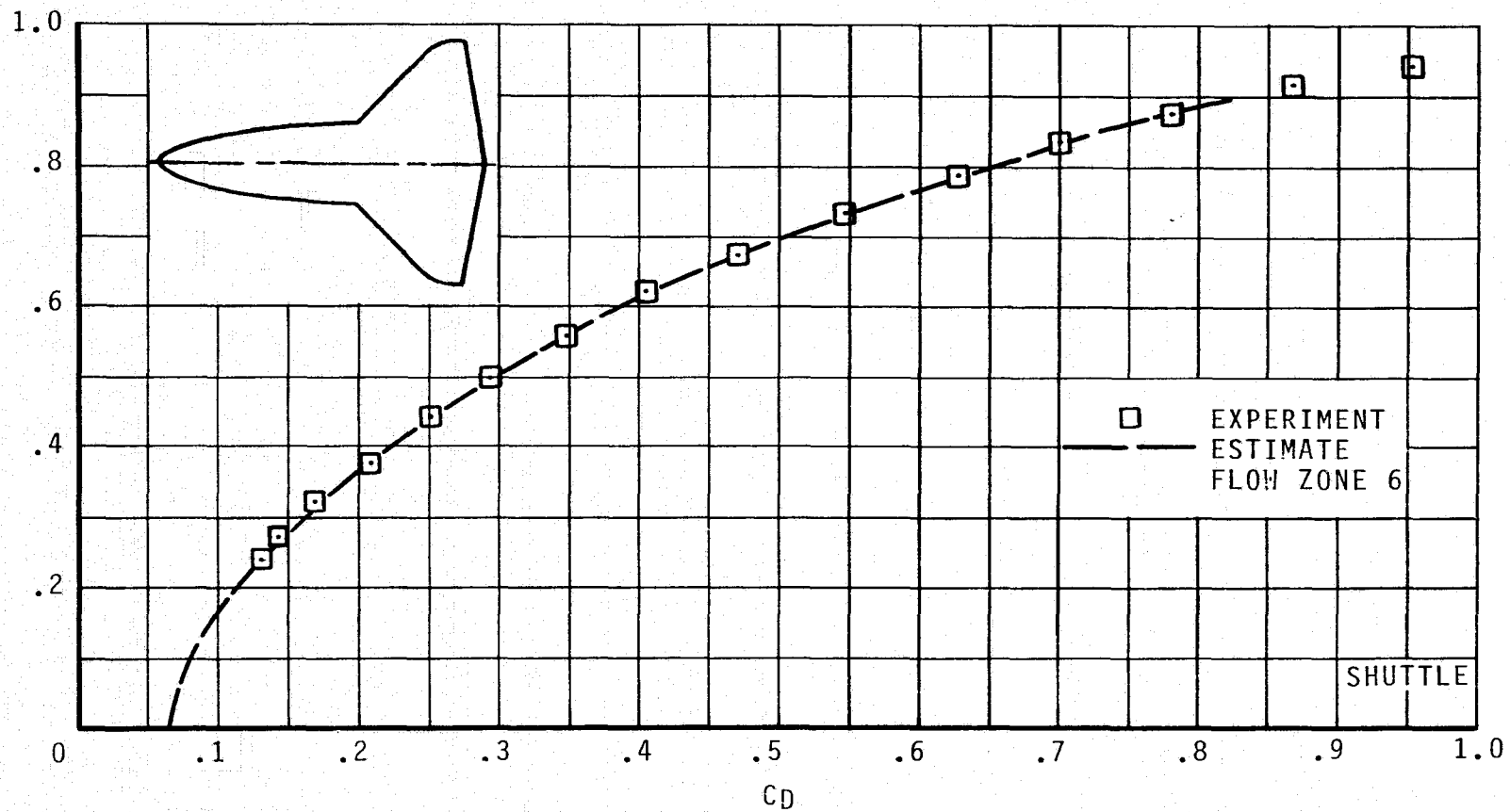
(r)  $C_m$  VERSUS  $\alpha$ ;  $M = 4.0$ .

FIGURE 10.- CONTINUED.



(s)  $C_L$  VERSUS  $\alpha$ ;  $M = 8.0$ .

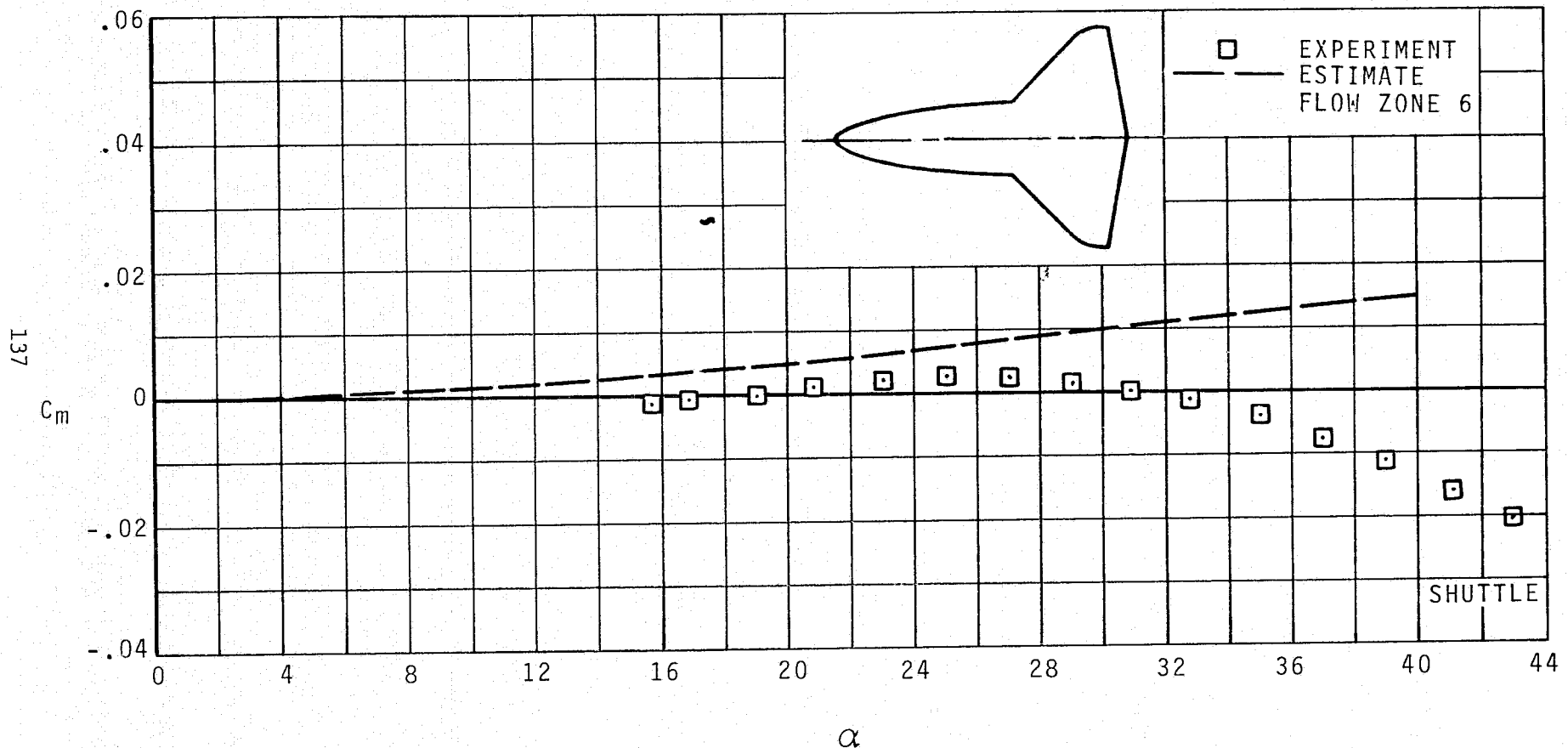
FIGURE 10.- CONTINUED.



(t)  $C_L$  VERSUS  $C_D$ :  $M = 8.0$ .

FIGURE 10.- CONTINUED.





$\alpha$   
 (u)  $C_m$  VERSUS  $\alpha$ ;  $M = 8.0$ .

FIGURE 10.- CONCLUDED.